Theses and Dissertations

5-1-2019

Part I: Design and Synthesis of Novel Drugs to Treat Asthma By Targeting GABAA Receptors in the Lung Part II: Design and Synthesis of Novel **A**2/α3 Subtype Selective GABAAR Ligands for CNS Disorders

Rajwana Jahan
University of Wisconsin-Milwaukee

Follow this and additional works at: https://dc.uwm.edu/etd

Part of the Organic Chemistry Commons

Part I

DESIGN AND SYNTHESIS OF NOVEL DRUGS TO TREAT ASTHMA BY TARGETING GABA$_A$ RECEPTORS IN THE LUNG

Part II

DESIGN AND SYNTHESIS OF NOVEL α$_2$/α$_3$ SUBTYPE SELECTIVE GABA$_A$R LIGANDS FOR CNS DISORDERS

by

Rajwana Jahan

A Dissertation Submitted in

Partial Fulfillment of the

Requirements for the Degree of

Doctor of Philosophy

in Chemistry

at

The University of Wisconsin-Milwaukee

May 2019

ABSTRACT

Part I

DESIGN AND SYNTHESIS OF NOVEL DRUGS TO TREAT ASTHMA BY TARGETING $GABA_A$ RECEPTORS IN THE LUNG

Part II

DESIGN AND SYNTHESIS OF NOVEL α_2/α_3 SUBTYPE SELECTIVE $GABA_A R$ LIGANDS FOR CNS DISORDERS

by

Rajwana Jahan

Abstract-Part I

Asthma is a major healthcare challenge affecting an estimated 300 million people globally. Over $56 billion in asthma-related healthcare expenses occur in the United States annually. Moreover, asthma accounts for the majority of missed school/work days, Doctor and emergency room visits, and patient hospitalizations in young persons. Consequently, asthma continues to be a significant healthcare burden in terms of morbidity, productivity, and medical costs. Beta 2-adrenergic agonists and inhaled corticosteroids (ICs) are the most commonly prescribed treatments for the acute and chronic management of asthma. Both agents present efficacy, compliance, and adverse side effect concerns.

Hence, there is an unmet need for asthma therapies with novel mechanisms of action to better control the disease with decreased adverse side effects. Previously, it was demonstrated that airway smooth muscle (ASM) cells express $GABA_A$ receptors ($GABA_A$R's) of the α_4 and α_5 subunits. Agonists of these $GABA_A$R subtypes can relax ASM acutely. Targeting the limited and overlapping α subunits with subtype selective $GABA_A$R agonists would effect both ASM relaxation and suppression of inflammation in the absence of any off-target CNS activity. Bz/GABAAergic agents have been proven to be safe and have a long clinical safety record. As a result, targeting Bz/$GABA_A$R in the lung and the peripheral nervous system (PNS) would be a novel and effective strategy in a management of asthma in patients. In this vein, novel $GABA_A$R positive allosteric modulators designed specifically for α_4/α_6 subunit selectivity were synthesized using iterative computational analyses. In addition, a series of deuterated analogs at key metabolic sites (C-3 and C-8 of the imidazobenzodiazepine scaffold) were synthesized to increase the drugs stability so that the drug stays in the body for a longer time to permit lower doses and still effect its anti-asthmatic properties for a longer duration, presumably with less side effects. Furthermore, a library of α_4 subtype selective $GABA_A$R ligands which were more hydrophilic to prevent blood brain barrier (BBB) penetration reduced CNS side effects. To obtain better in vitro and in vivo stability, bioisosteric moieties to replace the labile C-3 ester functional groups were designed and synthesized. Preclinical assays such as microsomal stability, cytotoxicity, and sensorimotor impairment have been studied on these novel analogs. Several ligands exhibited the desired properties required for better management of asthma. The results of studies in several models of asthma in vivo reinforces the novel hypothesis, which rests on relaxation of airway smooth muscle (ASM), a decrease in airway hyperresponsiveness (AHR), and a decrease in airway eosinophils,

as well as modulating inflammatory cells. These ligands may be potential treatments for childhood asthma and also for the disease in adults.

Abstract-Part II

Nonselective ligands of the $\alpha_{1-3,5}\beta\gamma_2$ subtypes of GABA$_A$Rs, such as diazepam have been used in the clinic for more than five decades for various central nervous system (CNS) disorders. These drugs exhibit various adverse CNS effects including sedation, ataxia, amnesia, tolerance, and addiction, which are believed to be mediated by α_1 subtypes of GABA$_A$Rs. As a result, these drugs are not applicable to all patients and have limited long-term applications. Despite their adverse CNS effects due to non-selective GABA$_A$R efficacy, novel ligands with better subtype selectivity, efficacy and reduced adverse effects are now emerging to be suitable replacements for these benzos. The GABA$_A$R agonists that possess superior α_2/α_3 subtype selectivity over the α_1 and α_5 subtypes are considered to be a promising avenue for development of novel GABA$_A$R ligands to treat various CNS disorders including inflammatory pain, anxiety, neuropathic pain, and epilepsy, while avoiding side effects such as, ataxia, amnesia, tolerance and dependence.

Previously, it had been shown the α_2/α_3 subtype selective Bz/GABA$_A$R positive allosteric modulator (PAM) HZ-166 exhibited anticonvulsant, antihyperalgesic and anxiolytic properties while being devoid of sedation, ataxia, dependence and tolerance. However, the C-3 ester function in HZ-166 was too labile for studies of ADME toxicity. Consequently, research here was carried out to prepare new ligands with better efficacy and stability, which resulted in several new lead compounds including a 1,3-oxazole (KRM-II-81) and a 1,2,4-oxadiazole (MP-III-80). These

bioisosteres were synthesized to overcome the problems with the metabolically labile ester functions. Among them KRM-II-81 exhibited prominent anxiolytic, anticonvulsant, antihyperalgesia, and antidepressant activity. An improved synthetic route was developed to better access the key ligand (HZ-166) in gram quantities for further optimization of this "privileged" scaffold. Synthesis of several new ester bioisosteres, importantly, those which contained deuterium in the scaffold at key metabolic sites, resulted in d1-MP-III-80, d3-MP-III-80, d5-MP-III-80, as well as a few 3-alkyl-1,2,4-oxadiazole derivatives. The in vitro and in vivo evaluation of these new ligands look promising and further investigations in vivo are underway. It is felt these new α_2/α_3 subtype selective ligands will result in novel compounds for development into effective treatments for anxiety disorders, for depression, for pain syndromes and for treatment of epilepsies with no tolerance nor dependence.

To

my parents,

my husband,

&

my son REON

TABLE OF CONTENTS

Part I

x

Part II

LIST OF FIGURES

Part I

Part II

vehicle; HZ-166: $F_{(4,9)} = 14.47$, $p<0.001$; Bonferroni t-tests, $p<0.05$ vs. vehicle; YT-III-31: $F_{(3,9)} = 120.45$, $p<0.001$; Bonferroni t-tests, $p<0.05$ vs. vehicle]. L-838,417 (functionally selective PAM at α_2GABA$_A$, α_3GABA$_A$, and α_5GABA$_A$ receptors), HZ-166 (functionally selective PAM at α_2GABA$_A$ and α_3GABA$_A$ receptors) as well as YT-III-31 (functionally selective PAM at α_3GABA$_A$ receptors) induced almost exclusive responding on the ethanol-paired lever over the dose ranges tested, generating 97%, 84% and 99% ethanol-lever responding, respectively. None of these compounds significantly altered average rates of responding when compared to average rates following vehicle administration (Figure 7b). Modified from the Figures in Berro *et al*..174

LIST OF TABLES

Part I

Part II

LIST OF ABBREVIATIONS

ASM   airway smooth muscle

AHR   airway hyper-responsiveness

ASP   Anticonvulsant Screening Program

BBB   blood-brain-barrier

BZD   benzodiazepine

BzR   benzodiazepine binding site

β_2AR β_2-adreno receptors (β_2AR)

CMC   carboxymethyl cellulose

CNS   central nervous system

COPD   chronic obstructive pulmonary disease

DI   diazepam-insensitive

DLM   dog liver microsomes

DS   diazepam-sensitive

FLIPR   fluorescence imaging plate reader

FDA   The Food and Drug Administration

GABA   gamma-aminobutyric acid

$GABA_AR$ gamma-aminobutyric acid type A receptors

HLM	human liver microsomes
IBZD	imidazobenzodiazepine
IP	intraperitoneal
IV	intravenously
ICS	inhaled corticosteroids
LABA	long acting beta agonists
MES	maximal electroshock
MLM	mouse liver microsomes
NAM	negative allosteric modulator
NINDS	National Institute for Neurological Disorders and Stroke
PAM	positive allosteric modulator
PHA	phytohemagglutinin
PMA	phorbol myristate acetate
PNS	central nervous system
PPI	prepulse inhibition
PTZ	pentylenetetrazole
PWT	paw withdrawal threshold
PO	oral administration

RLM	rat liver microsomes
SAR	structure-activity relationship
SABA	short acting beta agonists
scMET	subcutaneous pentylenetetrazole
SEM	standard error of the mean
SNL	sciatic nerve ligation
SSRI	selective serotonin reuptake inhibitors
TM	transmembrane domain

LIST OF SCHEMES

Part I

Part II

ACKNOWLEDGEMENTS

PART I

1. Introduction

1.1 Asthma

The term 'asthma' was first used by Homer (800 BC) in his book *The Iliad,* which in Greek (ásthma) means panting and shortness of breath.[20] Hippocrates (400 BC) first defined the disease asthma to the medical community through the Corpus Hippocraticum.[20] As it appears, asthma is not new, and it has been around for many many centuries, but modern asthma that we now know has rapidly evolved over the past several decades. It has become a global health problem affecting people from all ages and ethnic groups, especially children and the elderly.[21] The cause behind the increase in asthma reports is not ethnic nor genetic in nature, rather it is the combined effects of many risk factors which includes genetic, environmental, and lifestyle.

Asthma is a chronic lung disease, which is characterized by recurring inflammation and narrowing of the airways that results in frequent and involuntary wheezing and shortness of breath. Asthma exhibits several major features; inflammation, mucous production, airflow obstruction, and airway hyper-responsiveness.[22] The results of inflammation can range from discomfort in breathing to a life-threatening condition. As a result, asthma accounts for the majority of missed school/work days, doctor and emergency room visits, and patient hospitalizations in young persons.[23,3,24] The severity and rate of recurrence of asthma varies among individuals. The World Health Organization (WHO) identifies asthma as one of the major noncommunicable diseases.[25] Asthma is a life-long condition in the majority of asthmatic individuals and the symptoms can be kept under control but there is no cure for it as yet.[26] It can affect anyone from children to elderly and under-control asthma can flare up at any moment without warning, which can cause severe to morbid acute respiratory inflammation. In many cases the triggers of asthma are not visible and

asthmatic triggers may vary from person to person, which makes it a challenge to predict and control. Another problem with asthma is that the triggers responsible for asthma attacks are in the asthmatics, surroundings (outside in the environment or inside the household) and thus the exposure seems to be inevitable in many cases. Some of the triggers may be seasonal and for those affected by the seasonal triggers (e.g. flower or grass pollen), a certain time of the year may be more dangerous than the remaining time of the year. With rapid development and urbanization, many people who lead strictly urban lifestyles have less and less exposure to the elements of nature and may eventually develop sensitivity towards many common natural substances. In addition, due to urbanization, most of the children grow up in a household or surroundings with a higher level of hygiene and spends less time outside. This results in fewer infections in the early ages. Thus, these children do not develop immunity to many of the germs or triggers that they become exposed to as they get older. This argument is known as "The Hygiene Hypothesis",[27] which has been reported as a possible origin of some asthmatics.

This ill-educated immune system could also lead to sensitivity to various common germs or molecules present in the surroundings. As a result, this type of asthma is more prevalent in western civilization and in the rapidly growing industrialized societies than in rural areas where a pristine environment exists.[28-30]
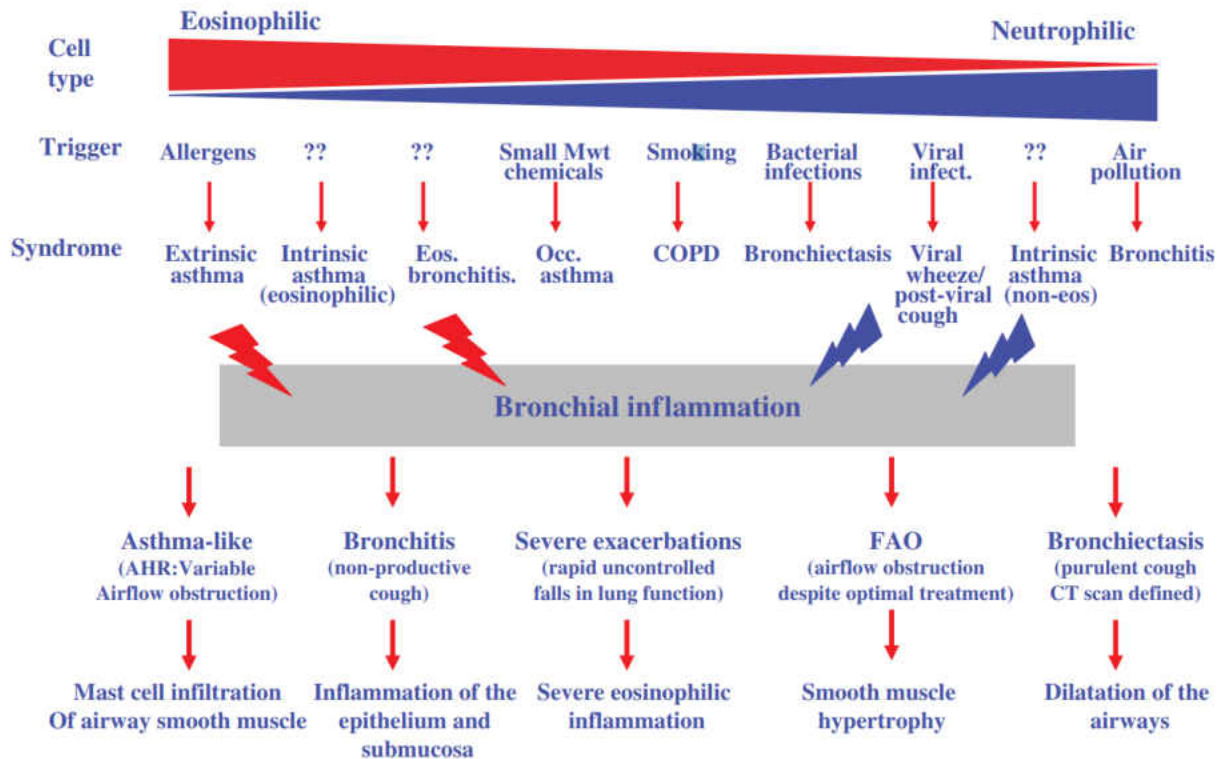
Figure 1. Schematic diagram illustrating the heterogeneity of airway diseases in terms of triggers, pattern of airway inflammation, associated diseases, airway physiology and the specific underlying pathological abnormality (modified from the figures in Wardlaw, *et al.*[5] **and Green,** *et al.*[6]**).**

A proper definition and classification of asthma is troublesome since asthma is a heterogenous disease and there is lack of consensus for such an accurate classification. Recent developments in the recognition of phenotypes and sub-phenotypes of asthma based on the pattern of airway inflammation have facilitated a systematic understanding of the disease.[6] By understanding the link between phenotype and pathology, it would be helpful to comprehend the pathogenesis and aetiology. The first classification of asthma was based on aetiology by Rackemann in 1921,[31] which divided asthma into two subclasses, namely extrinsic and intrinsic asthma. Afterwards, several other causative phenotypes have been identified, for example aspirin-sensitive and occupational asthma.[6] Further subclassification based on the different patterns of airflow obstructions includes 'brittle asthma', 'irreversible asthma', and 'the morning dripper'.[32] Asthma

management guidelines usually classify asthma based on the severity of the disease and amount of required treatments to maintain proper lung function and to control symptoms.[33] More recent classification of asthma is based on the nature of underlying airway inflammation.[34,35] It has also been suggested from experimental evidence that identification of such inflammatory phenotypes might be a useful guide for asthma management for individual patients.[36,37] A schematic diagram, which illustrates the heterogeneity of asthma is illustrated in Figure 1.[5]

Examination of Figure 1 depicts how a number of triggers can result in inflammatory responses that may range from highly eosinophilic to highly neutrophilic in origin. This is, presumably, the relationship between the extent of involvement of the innate (Th1) and adaptive (Th2) immune responses. Certain triggers such as allergens and small molecular weight chemicals cause syndromes such as extrinsic or occupational asthma and are mainly eosinophilic in origin. On the other hand, triggers such as bacterial or viral infections cause syndromes non-eosinophilic (neutrophilic) in origin. The triggers for some syndromes such as eosinophilic intrinsic asthma (and eosinophilic bronchitis) or non-eosinophilic asthma are not known or vary among individuals. To simplify, responses from all the eosinophilic and non-eosinophilic (neutrophilic) triggers can be termed as bronchial inflammation, represented as the grey box in the middle of Figure 1. Out of this grey box originates different physiological responses depending on the subject.[5]

If you take away from the broader picture of airway disease as a whole, there is a considerable extent of heterogeneity within the symptoms of asthma itself.[38] There are many descriptive terms to describe the heterogeneity depending on the clinical presentation or aetiology that is used to describe the disease.[39,40,41,42] Based on clinical patterns, asthma can be categorized into chronic

(mild, moderate or severe), acute severe, brittle, nocturnal, premenstrual, and steroid resistant phenotypes. Similarly, based on the nature of triggers, asthma can be categorized as extrinsic or intrinsic (absence or presence of specific IgE to allergens), occupational (small molecule chemicals), infective (virus, bacteria or fungi), aspirin sensitivity, smoking, exercise etc. phenotypes. The infiltration of airway smooth muscle (ASM) by mast cells is specifically an effect in the asthma phenotype. As a result, to be precise, 'classical asthma' can be defined as a condition wherein the following indications are co-present: variable airflow obstruction, airway hyper-responsiveness (AHP), and mast cell infiltration of the airway smooth muscle (ASM).[5,38,39,41-43]

Asthma affects more than 300 million individuals globally and in the United States as stated above and one in every 12 persons suffers from asthma.[44,21] The number of asthmatic patients is predicted to be over 400 million by the year 2025, globally.[45]

According to the National Health Interview Survey (NHIS) 2011,[46] approximately 39.5 million people (12.9% of the population), which includes 10.5 million children (14.0% of child population), in the United States alone have been diagnosed with asthma. It is a lifelong condition in approximately 40 million individuals in the United States in 2012.[21,47] Over 11.5 million asthmatic individuals, which includes approximately 3 million children have had at least one asthma attack in 2015.[48]

Every year asthma attacks result in approximately 180,000 deaths globally.[49] Consequently, there is a huge impact on society, not only in terms of expenses but from productivity as well. As indicative by these statistics, there is considerable indirect costs (e.g., cost lost from absenteeism

from work, disability, and mortality), as well as direct costs (e.g., emergency room visits, hospitalization, medications, investigative treatments etc.) are associated with asthma incidents. Besides, there are some unquantifiable or intangible costs associated with asthma. It is difficult to get an accurate confirmation of the negative effect on life-styles in this situation. For example, in 2013, approximately 13.8 million missed school days were due to asthma incidents.[50] According to a report published in 2010, the US spent approximately $56 billion for asthma care which was several-fold higher than the expense in 1994 (about $12 billion).[51]

During the last decade (2001-2011) asthma incidents increased by an alarming 28%, which indicates asthma was not under control. As a result, more than half a million hospitalizations, and about 2 million emergency room visits occur each year (some are often fatal) and more than 14 million doctor visits occur each year due to asthma incidents.[52] According to the WHO, in 2004 the worldwide asthma costs may have exceeded the cost associated with TB and HIV/AIDS combined.[53,21]

The current options for short-term (acute) and long-term (chronic) management of asthma are primarily based on short acting beta agonists (SABA) and long acting beta agonists (LABA) along with inhaled corticosteroids (ICS). The β_2-adrenergic agonists such as salbutamol or salmeterol act as bronchodilators by activating the β_2-adreno receptors (β_2AR), while corticosteroids, such as beclomethasone dipropionate, act as anti-inflammatory agents, which reduce inflammation caused during an asthma attack. Both types of treatment have their limitation due to efficacy, compliance and side effect concerns. For example, for long term management of asthma, The Food and Drug Administration (FDA) has recommended avoiding LABA's if possible and suggested the use of

LABA's only in combination with corticosteroids due to the effect that LABA's had on increased asthma related deaths.[54] Furthermore, this drug it is reserved for patients whose asthma cannot be maintained by other available treatments.[54] On the other hand, inhaled glucocorticoids, which are the best available option for asthma treatments have both oropharyngeal and systemic side effects including adrenal suppression, growth suppression, thinning or bruising of the skin, cataract formation, increased mortality, and loss of asthma control effects.[4,55-60] In addition, there is the possibility of osteoporosis and growth problems associated with long-term use of corticosteroids.[61] Furthermore, orally available leukotriene receptor antagonists are commonly used to manage asthma symptoms;[62] however up to 78% of patients do not respond to this alternative therapy.[61,63] In addition, it is very common to encounter an incident wherein improper use of inhalers results in incorrect dosing, oral infections, and poor patient compliance.[4]

As a result, it can be inferred that the global asthma problem has been exacerbated over the last several decades. The current asthma management and/or treatment options are not good enough for the necessary treatment of clinical long-term treatment of asthma. There are certainly unmet demands for new asthma management programs. The medical community needs strategies to treat and/or control asthma to overcome imprecise dosing, as well as reduce adverse CNS side effects.

1.2 GABA$_A$ Receptors

Gamma-aminobutyric acid (GABA; Figure 2) is a neurotransmitter that plays an inhibitory role in the central nervous system (CNS). In addition, GABA is also involved in several other physiological functions in the peripheral nervous system including the mediation of the paracrine signaling. The overall involvement and mechanism of the role of GABA in neurotransmission is

rather complex. However, it has been investigated in detail and as a result its role as a central neurotransmitter has been fully established, which employed extensive electrophysiological, neurochemical, pharmacological, and molecular biology techniques. GABA is known to be involved in many CNS disorders and degenerative diseases including anxiety disorders, sleep disorders, schizophrenia, major depressive disorder, bipolar depression and PTSD.[64-68] The combination of excitatory and inhibitory transmission regulates the overall activity of the brain. Excitatory transmitters, such as glutamic acid (Glu) depolarize neurons via a large number of receptor subtypes, while the inhibitory transmitter effects of $GABA_A$ receptors hyperpolarizes neurons also via several receptors.[69,70]
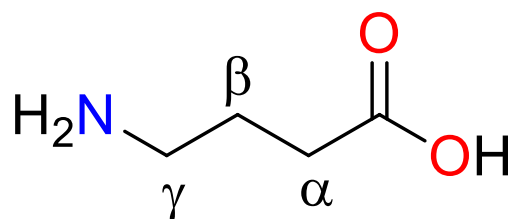
Figure 2. γ-Aminobutyric acid (GABA)

Beside the central nervous system (CNS), GABA also regulates a wide range of physiologically important functions in the peripheral nervous system (PNS),[71,72] as suggested by an increasing number of studies. GABA receptors have been found in a large number of peripheral tissues including the endocrine glands, smooth muscles, and the female reproductive system, which are all parts of the peripheral nervous system (PNS).[73]Although, the peripheral GABA receptors and GABAergic synaptic mechanisms are interesting drug targets, the majority of the GABA based drug discovery programs at UWM, target the central GABA-regulated synapses.[73] It has also been

suggested that GABA plays a crucial role in the hearing mechanism, as indicated by an age-related significant reduction in GABA in the central nucleus of the inferior colliculus (CIC) in rats.[73,74]

Since GABA receptors are the most abundant inhibitory neurotransmitters in the CNS, they control 17-20% of all neurons in the brain.[75] The physiological actions of GABA under study here are implemented via GABA$_A$ receptors, which are contained in chloride ion channels, whose properties are mediated by GABA. The action of GABA$_A$ receptors can be modulated by many drug molecules that bind to distinct allosteric binding sites on GABA$_A$ receptor in channels.[76] Inferred from the pharmacological effects of such drug molecules, it can be concluded that GABA$_A$ receptors are involved in multifunctional roles including but not limited to controlling inhibition of neurons in the CNS,[77,78] which control anxiety.[79,80] They also help to monitor feeding and drinking behavior,[81,82] cognition, the internal body clock, memory and learning, neuropathic pain, epilepsy and others.[83-87]

GABA$_A$ receptors are heteropentameric in nature, which consists of a large N-terminal extracellular domain and four transmembrane (TM) domains.[88-90] The extra cellular region contains sites for potential glycosylation, and a 'Cys-loop' connecting two conserved cysteine residues via a covalent disulfide bond. In addition, there is one intracellular loop connecting TM3 to TM4 (Figure 3). Five individual subunits combine to form a chloride ion channel (Figure 4). Each GABA$_A$R protein is a polypeptide of approximately 50 kD in size and each subunit is structurally related with a high degree of protein homology between subunits.[7,9,91]
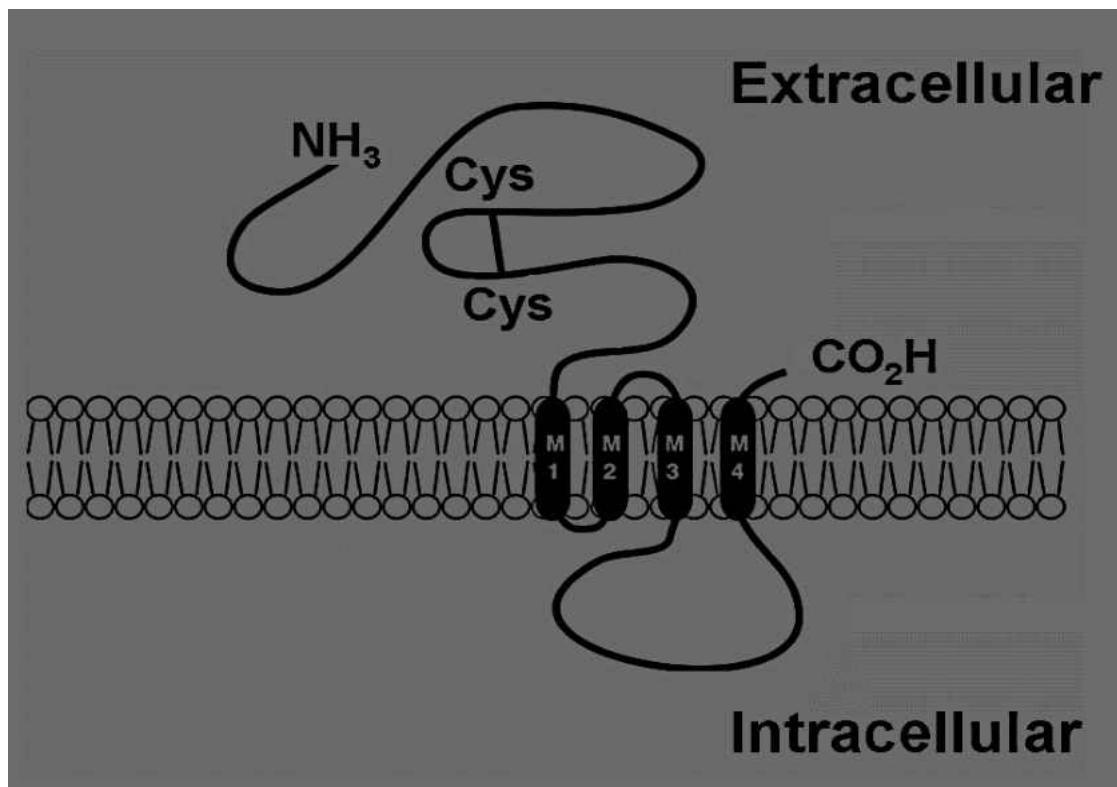
Figure 3. Proposed topology of a GABA$_A$ receptor subunit. The extracellular domain begins with the N-terminus and M1-M4 represents the four transmembrane domains (modified from the figures in Burt, *et al*.[91] and Clayton, *et al*.).[7,9]
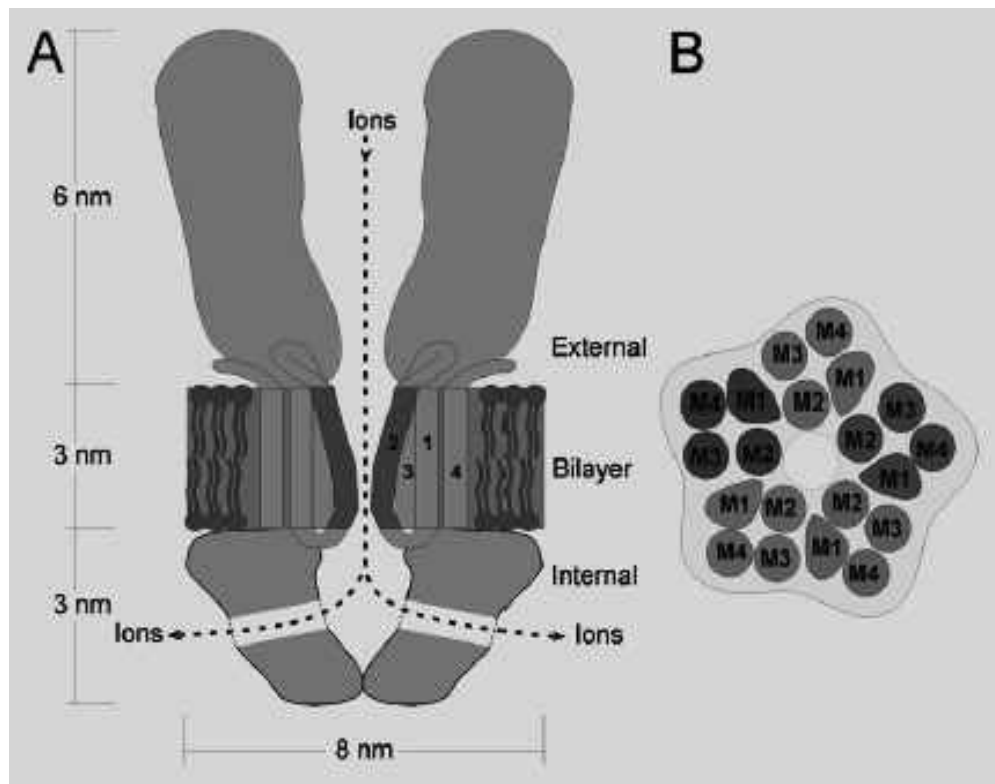
Figure 4. Longitudinal (A) and cross-sectional (B) Schematic representations of the ligand-gated ion channel. The number 1-4 refer to the M1-M4 segments. The M2 segment contributes to the majority of the pore lining within the membrane lipid bilayer (modified from the figures in Keramidas, *et al*[92]. and Clayton *et al.*).[7,9] However, much of this ion channel topography was developed by Werner Sieghart.

In the mammalian nervous system a total of six major alpha, three beta, three gamma, three ro, as well as one of delta, epsilon, pi, and theta each have been sequenced, which results in a set of 19 (i.e., α_{1-6}, β_{1-3}, γ_{1-3}, δ, ε, θ, π, ρ_{1-3}) different subunits. This collection of different subunits of GABA$_A$ receptors is the largest among ion channel receptors.[93,94] It is inferred from experimental evidence that this set of 19 subunits might be the complete set of subunits in the human since no new receptor subunit genes were found in the human genome.[95] On the other hand, additional subunit types have been identified in nonmammalian species.[93,96,97]

Theoretically, if all the subunits could co-assemble with each other, randomly, more than 150,000 GABA$_A$ receptor subtypes with different compositions and arrangements could be formed.[98] Due to restrictions during the assembly of GABA$_A$ receptors, not all theoretically possible subtypes can actually form. It is probable that around 500 different subunits actually exist in the brain.[94] In addition, only a few subunits are abundant in number. The majority of the subunits are comprised of alpha, beta, and gamma subunits. Occasionally, the gamma unit is replaced by either of delta, epsilon, or pi subunits.[94] It is known that the GABA$_A$ receptors, which are modulated by benzodiazepine allosteric binding sites are located in the alpha, beta, and gamma ion channels, which contain two alpha, two beta and a gamma-units forming a hetero-pentameric receptor. In these receptors the four alternating alpha and beta (2 alpha + 2 beta) subunits are connected by a gamma unit in a ratio depicted here (α:β:γ = 2:2:1).[90,99-103] Nonetheless, GABA$_A$ receptors are highly heterogeneous and are widely distributed throughout the brain. Despite its ubiquitous nature in the brain, each subunit has a distinct regional and cellular distribution. Often a special class of cells or tissues express a small sub-set of GABA$_A$ receptor subunits, preferentially.[104] For example, $\alpha_5\beta_3\gamma_2$ subtypes are located primarily in the hippocampus of the CNS and a small amount in the spinal cord.

In the synaptic cleft and within the pore of a GABA$_A$R there are numerous binding sites. A number of ligands of various classes can bind to these sites and activate the GABA$_A$R complex. These compounds include β-carbolines, barbiturates, ethanol, benzodiazepines, picrotoxin, as well as endogenous molecules such as neurosteroids.[105,106] The synaptic cleft of the $\alpha_{1-6}\beta_{1-3}\gamma_2$ subunit, viewed from an extracellular region is depicted in Figure 5. The $\alpha\beta\alpha\beta\gamma$ subunits are arranged in a clockwise manner from such view point (Figure 5). GABA binding sites are located at the two α^- β^+ interfaces while benzodiazepines bind to the $\gamma^-\alpha^+$ interface.[107,108] Recent studies by Sieghart have

located a CGS 9895 binding site (termed PQ) at the $\beta^-\alpha^+$ interface.[109,110] In addition to these known ligands, a number of pyrroloquinolines also have been found to bind and activate this GABA$_A$R site.[105,111] Additionally, neurosteroids and ethanol may also bind in the interior of the ion pore.[9,112-114,115,116]
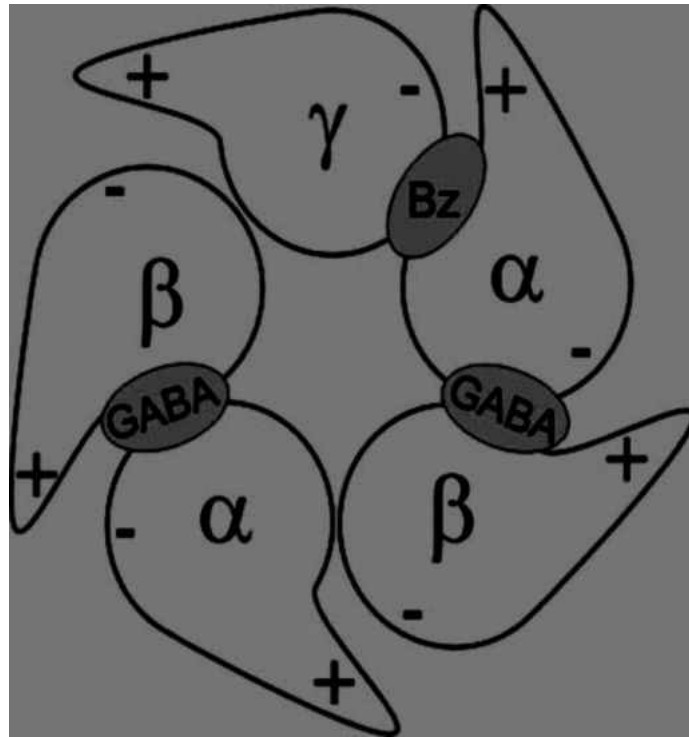
Figure 5. Absolute subunit arrangement of the α1β2γ2 GABAA receptor when viewed from the synaptic cleft. The GABA binding sites are located at the β+α- subunit interfaces and the Bz modulatory binding site is located at the α+γ- subunit interface. The part of the schematically drawn subunits marked by the + indicates loop C of the respective subunits (modified from the figures in Clayton, *et al.*[7] and Ernst, *et al.*).[8,9]
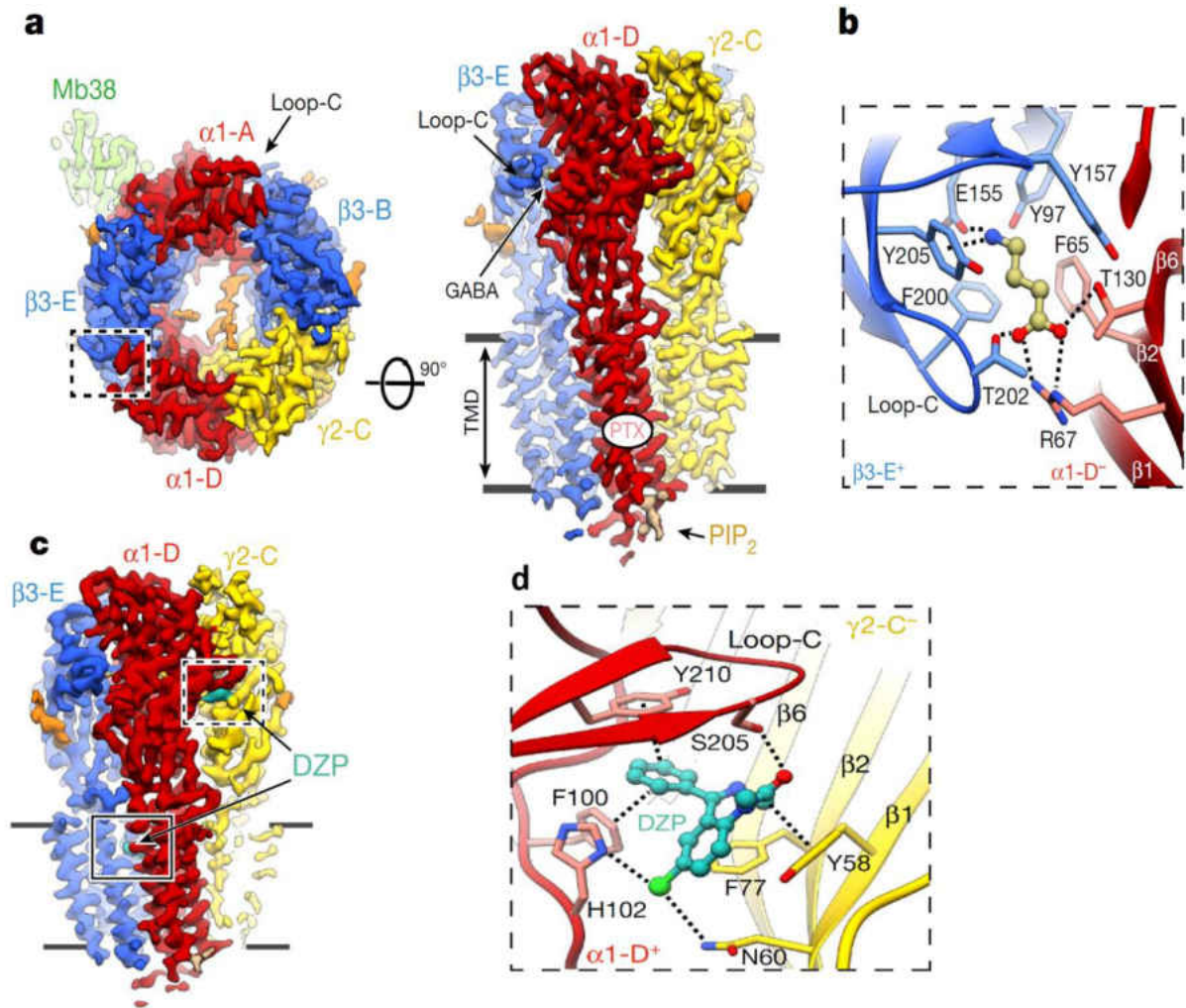
Figure 6. Conformational impact of GABA binding to the α₁β₃γ₂L GABA$_A$ receptor. a) Cryo-EM map of the PTX/GABA-bound α₁β₃γ₂L receptor viewed from the extracellular space (left) and parallel to the membrane plane (right). b) One GABA-binding pocket viewed from the extracellular space. GABA is shown in ball-and-stick representation with the atoms colored as follows: carbon, khaki; oxygen, red; nitrogen, blue. c) The cryo-EM map of the α₁β₃γ₂ GABA receptor in complex with diazepam (DZP, teal) viewed parallel to the membrane plane. d) Views of the benzodiazepine binding site at the α₁₊/γ₂₋ interface showing DZP binding mode (modified from the figure in Masiulis, *et al*.).[10] PTX is picrotoxin, a channel blocker.
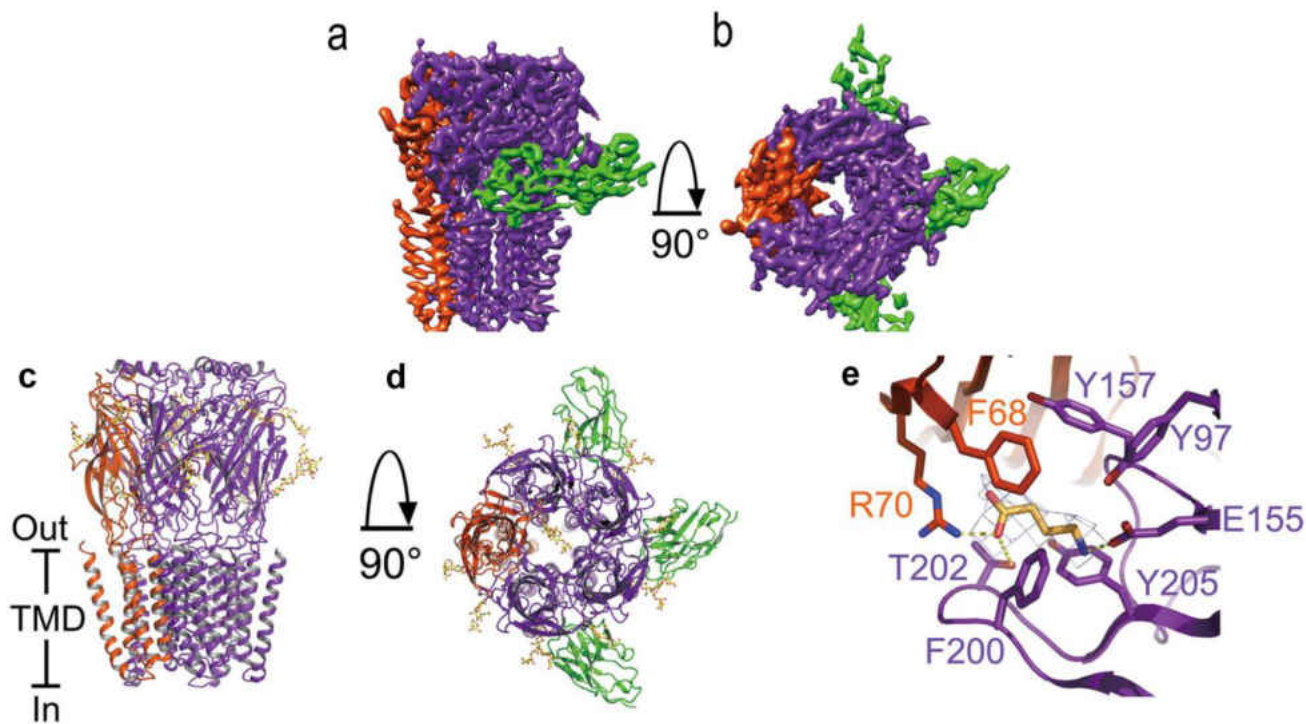
Figure 7. The cryo-EM structure of the human α₅β₃ GABAₐ receptor. a, b Surface views parallel to the plasma membrane (a) or from the extracellular space down the five-fold pseudo-symmetry axis (b) of the cryo-EM density map of the human α5β3 GABAA receptor in complex with Nb25 reveals a distinct assembly of one α (red) and four β subunits (purple), and three bound Nb25s (green). c, d The α₅β₃ GABAₐ receptor viewed parallel to the plasma membrane (c) or from the extracellular space down the five-fold pseudo-symmetry axis (d) with three Nb25s bound (d). N-linked glycans are shown in ball and stick representation. e GABA-binding site at β(+)/α(−) interface with density at 3σ contour level. Dashed links indicate salt bridges or hydrogen bond. The residues in β(+), α(−) and GABA are depicted in sticks. (modified from the figure in Liu, *et al.*)[11]

In the present work ligands that bind to this α₁β₃γ₂ site are not wanted, since this receptor site is known to mediate sedation, amnesia, ataxia, and anticonvulsant activity, as well as addiction, and/or dependence. The cryo-EM map of the α₁β₃γ₂ receptor with the binding site of diazepam is illustrated in Figure 6.[10] Depicted in Figure 7 is the cryo-EM map of the α₅β₃ receptor bound to Nb25s.[11] However, there is no structure of diazepam in this binding site so that the Bz receptor is not illustrated here.

16

1.3 Benzodiazepines

Diazepam (Valium), which is a traditional benzodiazepine (BZD), contains the pendent phenyl ring and binds non-selectively to the $\alpha_{1\text{-}3,5}\beta_{1\text{-}3}\gamma_2$ GABA$_A$ receptors[7,107,108] at the BzR site. They (BZDs) bind at the interface between the α and γ_2 subunits of the ion channel.[104] Benzodiazepines (BZDs, see Figure 6) have been prescribed for various CNS disorders including anxiety, convulsions, and muscle relaxation[117,118] for over 45 years. The BZDs allosterically enhance the action of GABA on the GABA$_A$ ion channel by increasing the frequency of channel opening. This means, BZDs do not cause any effect on their own and can only modulate an ongoing GABA$_A$ergic process.[104] Thus, BZDs exhibit much less toxicity than other drugs. This class of compounds has several advantages including the ready absorption through the GI tract and they reach a maximum blood concentration within a short period of time after oral ingestion.[119] In addition, BZDs can cross the blood brain barrier (BBB) within 20 to 30 minutes of administration and readily distributes throughout the brain. Some BZDs can reach high enough concentration in the brain within five minutes after iv administration which has made them suitable for treatment of status epilepticus.[120-122] Unfortunately, the development of tolerance in humans after 3 – 5 days limits their use in emergency rooms, as a treatment for epilepsy. BZDs also cause a number of adverse effects, as mentioned, such as drowsiness, sedation, ataxia, dependence, withdrawal issues and tolerance to the anticonvulsant effects, which further limits their clinical use.[104,106,123,124] These adverse effects are principally due to the positive modulation (PAM) of $\alpha_1\beta_3\gamma_2$ GABA$_A$-subunits, but some side effects can also be mediated by other Bz receptors including (in the CNS) the $\alpha_4\beta_3\gamma_2$ receptors; certainly high doses of $\alpha_3\beta_3\gamma_2$ subtypes can also lead to some muscle relaxation.
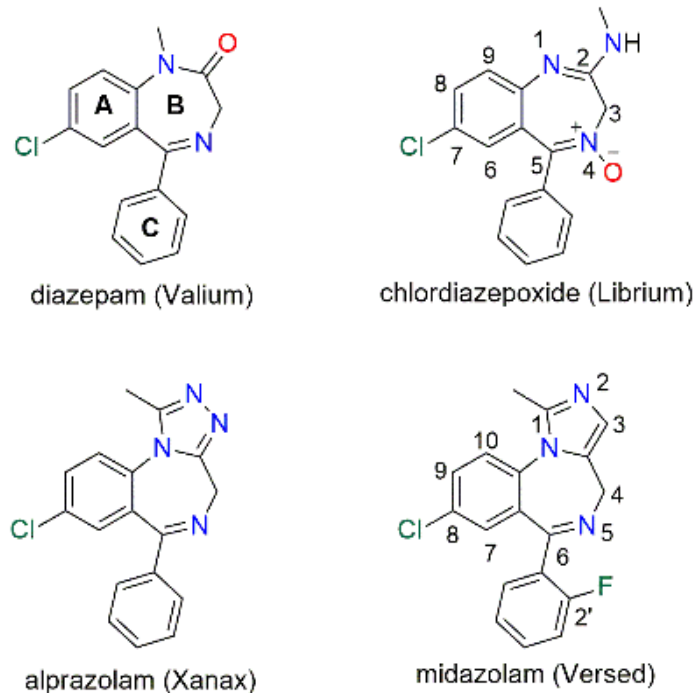
Figure 8. Structures of some representative examples of BZDs: diazepam, chlordiazepoxide, the triazolobenzodiazepine alprazolam and imidazobenzodiazepine (IBZD) midazolam.

The BZDs such as diazepam or flunitrazepam exhibit high affinity at $\alpha_1\beta_{2/3}\gamma_2$, $\alpha_2\beta_{2/3}\gamma_2$, $\alpha_3\beta_{2/3}\gamma_2$, and $\alpha_5\beta_{2/3}\gamma_2$ subtypes. These sites are termed diazepam sensitive (DS) sites. Other BZDs can also interact with $\alpha_4\beta_{2/3}\gamma_2$ or $\alpha_6\beta_{2/3}\gamma_2$ receptors, which are termed "diazepam insensitive" (DI) sites. The receptors containing γ_1 or γ_3 are present in very low abundance and their respective in vivo effects on benzodiazepine binding sites and on GABA processes is still unclear.[13]

The α_4 and α_6 benzodiazepine binding sites are insensitive to benzodiazepines because in the binding site the lipophilic pocket (L_3) is too small or nonexistent, consequently, the pendant phenyl ring will not fit in the pocket. This is due to the histidine (DS) to arginine switch (DI) in the Bz/GABA ion channel subunit.[125]

It is known that compounds of various classes can bind to the BZD binding site of the GABA$_A$R.[104] When a ligand binds to the BZ site, it can influence the action of GABA to its receptor site and hence can alter the chloride ion flow through the pore.[126] A ligand can act as an agonist, antagonist, or inverse agonist. The binding of an agonist ligand results in an increase in the frequency of the opening of the chloride channel, which results in a net hyperpolarization of the neuron and a decrease in neuronal firing. This type of ligand is called a 'Positive Allosteric Modulator (PAM) and illicits anxiolysis, sedation, and anticonvulsant effects. The opposite effect occurs when an inverse agonist binds to the BZD site, which decreases the flow of Cl$^-$ ions. These are called negative allosteric modulators (NAM) or inverse agonists. The NAMs exert an opposite action on GABA neurotransmitter actions on the GABA$_A$R, i.e., they exhibit effects that include: anxiogenic, proconvulsant, convulsant, enhanced vigilance, as well as increased cognition and learning. There is one more type of allosteric modulator that, presumably, stabilizes the BZD antagonist conformational state, which does not have a major effect on the chloride ion-flux. As a result, these antagonists are nearly functionally silent on their own but can antagonize the effects of agonists or inverse agonists at BZD receptors. This type of ligand is termed an 'antagonists'.[104]

The efficacy of these allosteric modulators can be different. Full agonists or full inverse agonists exhibit maximum effects on their respective processes. Between these two efficacy extremes, there are partial agonists and partial inverse agonists, which elicit the same type of effects as their full versions but to a lesser extent. The allosteric efficacy of modulators are distinct at different receptor subtypes and as a result, a full agonist or inverse agonist at one receptor may be a partial agonist or partial inverse agonist at another. It is also possible for compounds to show efficacy in the opposite direction at different receptor subtypes; i.e., a partial agonist at one receptor can be an antagonist or inverse agonist (NAM) at another subtype. This illustrates the different spectrum of

efficacy of clinically used BZDs. In addition, a number of compounds may have similar affinity

for an $\alpha_x\beta_{2/3}\gamma_2$ subtype but their efficacy is usually different at these receptors, which can affect

the spectrum of specific anxiolytic, antinociceptive, antidepressant, anticonvulsant, sedative, or

muscle relaxant activity.[104] Illustrated in Figure 6 is a schematic diagram of subunits and ligands

that mediate effects via the of the GABA-BzR channel complex.
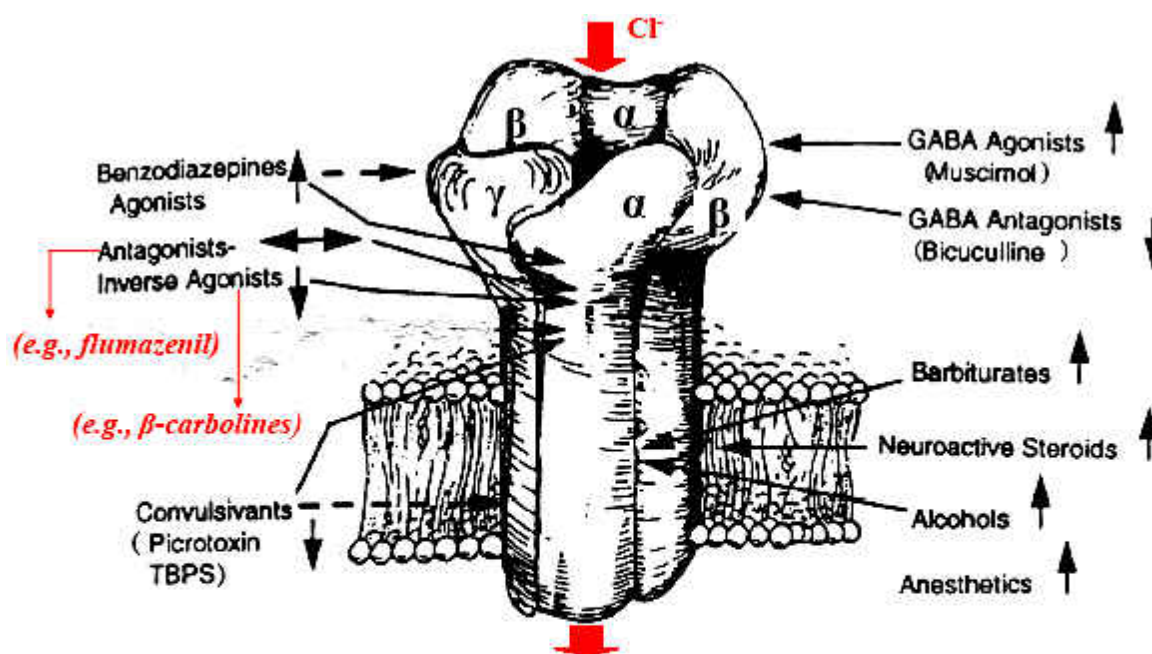
The five subunits of the GABAA receptor complex:
- 2 α subunits (comprising of at least six peptides designated α1–α6)
- 2 β subunits (comprising of at least 4 peptides designated β1- β4)
- 1 γ gamma subunit (comprising of at least 3 peptides designated γ1 – γ3)
Subunits other than α, β, and γ exist.

Figure 9. Diagram of the benzodiazepine-GABA receptor-chloride channel complex (modified from the figure in Rallapalli, S.)[12]

The pharmacological responses vary with the composition of the activated $\alpha_{1-6}\beta_{1-3}\gamma_2$-GABA$_A$R.

As mentioned above, benzodiazepines bind to the interface between the α and the γ subtypes. In

the mammalian nervous system there are 6 different α and 3 different γ subunits, which would result in 18 such possible sites for BZD binding. It is known that most BZDs are inactive or show very weak efficacy at receptors containing γ_1 subunits.[127] Furthermore, although BZDs show some activity at γ_3, the very low abundance of γ_3 containing receptors in the mammalian nervous system render the contribution from these receptors as insignificant in the overall efficacy of BZDs. Consequently, BZDs that are used currently for clinical practice, interact with $GABA_ARs$ containing (DS) $\alpha_1\beta_{2/3}\gamma_2$, $\alpha_2\beta_{2/3}\gamma_2$, $\alpha_3\beta_{2/3}\gamma_2$, and $\alpha_5\beta_{2/3}\gamma_2$ subunits. The α_4 and α_6 subunits exhibit completely different pharmacology than most of the clinically used BZDs (e.g., diazepam, clonazepam, flunitrazepam etc.) because they do not bind or interact at these (DS) BZD receptor subtypes.

The presence of different α subunits plays a major role. Single-point-knock-in mice have been used to identify the role of different α subunits located in the brain pioneered by Seeburg, Möhler, McKeinan, and Rudolph.[128,129] The α_1 containing $GABA_AR$ receptors have been associated with amnesia, motor impairment, sedation, ataxia, addiction, muscle relaxation and dependence, as well as anticonvulsant effects.[130,131] The positive activation of α_2 subunits mediates anxiolytic effects and anticonvulsant effects.[132,133] On the other hand, activation of α_3 subunit effects anxiolysis and muscle relaxation at higher concentrations.[134,135] The α_5 subunits influences cognition and spatial memory as well as schizophrenia, depression and asthma.[136] The α_4 and α_6 subunits are diazepam insensitive (DI) sites. In the brain the α_1 subtype of the $GABA_AR$ is the most abundant (40-50%)[135,137,138] followed by α_2 and α_3 (up to 35% and 14%, respectively)[107]. These are mainly located in the limbic region. The α_5 receptors are the least abundant (~5%) and are present principally in the hippocampus[139,140] and some in the spinal cord as mentioned.[141]

The two diazepam insensitive subtypes (α_4 and α_6 subtypes) correspond to a much smaller percentage of functional GABA$_A$R than the diazepam sensitive (DS) subtypes. Some known imidazobenzodiazepines such as Ro15-4513, and Ro15-1788 (flumazenil) are known to interact with $\alpha_4\beta2$ and $\alpha_6\beta2$ subtypes but they also interact with $\alpha_1\beta\gamma_2$, $\alpha_2\beta\gamma_2$, $\alpha_3\beta\gamma_2$, and $\alpha_5\beta\gamma_2$ subtypes, making them non-selective BZD compounds. The α_4 ion channels make up 6% of all subtypes[142] GABA$_A$ receptors are also expressed in the peripheral nervous system (PNS).[143,144] There are both α_4 and α_6 subtypes in the CNS and periphery. Although GABA$_A$ergic drugs readily cross the BBB, the major quantity of administered BDZ drug is found in the periphery where they can cause side effects.[73] But very very significant amounts of BZDs go through the BBB in 5-30 minutes. This makes them terrific anxiolytics. There is potential for using BZDs targeting the GABA$_A$Rs (especially, the DI sites) expressed in the peripheral nervous system especially within the lungs (Emala *et al.*)[145-147] and spleen.[148,149] The $\alpha_6\beta_3\gamma_2$ subtypes are found largely in the cerebellum.[150]

Although GABA$_A$ receptors are ubiquitously present in the CNS, limited studies have been done to find their distribution in the nonneuronal cells. The GABA$_A$ channels in the central part of the brain control the cholinergic outflow to the lung. Functional GABA$_A$ and GABA$_B$ receptors inhibit cholinergic activity and have been detected in the presynaptic sites of lung prostaglandin parasympathetic nerves. The presence of functional GABA$_B$ and GABA$_A$ receptors in the ASM of human and guinea pig was confirmed recently by Emala.[151] Emala and Cook et al. also illustrated the relaxation of precontracted ASM (substance P or histamine) by selective agonism at the $\alpha_5\beta_3\gamma_2$ receptor subtype. The overall outcome of their study was the finding that GABA$_A$ receptor subtypes especially α_4 and $\alpha_5\beta_3\gamma_2$ subtypes relax the contraction of airway smooth muscle (ASM) by the selective GABA$_A$ agonist (gabazine) as well as α_4 and α_5 subtype selective ligands.[151]

Table 1. Action of benzodiazepines at CNS GABA$_A$ $\alpha_{1-6}\beta_{1-3}\gamma_2$ receptor subtypes. Presented at ASPET Annual Meeting at EB 2019[152]

Subtype	Associated Effect
α_1	Sedation, anterograde amnesia, some anticonvulsant action, ataxia, involved in development of tolerance, addiction
α_2	Anxiolytic, some anticonvulsant action, **antihyperalgesia**
α_3	Anxiolytic, antihyperalgesia action, may be some muscle relaxation at higher doses
α_4	Diazepam-insensitive site; **asthma**
α_5	Cognition, temporal and spatial memory, **depression**, **schizophrenia**, **asthma**
α_6	Diazepam-insensitive site; **migraine**, **trigeminal orofacial pain**, **active in a model of Tourettes syndrome**, **PPI model**

Note: Effects in bold are effects found by pharmacologists using ligands from Milwaukee

As found by Emala, Cook *et al.,* airway smooth muscle (ASM) contains a restricted and conserved repertoire of α_4 and α_5-GABA$_A$ receptors and allosteric modulators of GABA$_A$ receptors enhanced the efficacy of GABA, which resulted in electrophysiological changes (effected by these ligands) in these two subtypes. Selective GABA agonists also augmented ASM relaxation by isoproterenol, as well as spontaneous relaxation of precontracted ASM by various contractile agents due to α_4-GABA$_A$ receptor activation.[153]

The α_4 and α_5 receptor subunits have been identified in airway smooth muscle, airway epithelium, and inflammatory cells, and their ligand-mediated activation has been shown to reduce immune

response measures and reduce airway hyperresponsiveness (ex vivo and in vivo).[151,154-158] In these studies, GABA dose-dependently reduced IL-12 and IL-6 production in LPS stimulated macrophages.[157] GABA and muscimol also inhibited anti-CD_3 and antigen specific T cell proliferation.[159] Honokiol, a $GABA_AR$ agonist, reduced cardinal features of the asthma-like phenotype including inflammation (reduced airway eosinophilia), mucous cell metaplasia, collagen deposition, and airway hyperresponsiveness in acute and chronic ovalbumin-induced murine asthma models.[160] However, nonselective $GABA_AR$ activation is associated with unwanted CNS effects[161] and increased mucous production.[158,162,163]

As mentioned earlier, the classical $GABA_A$ receptors with $\beta_3\gamma_2$ and one subunit of α_1, α_2, α_3, or α_5 represent the diazepam sensitive (DS) sites where benzodiazepines usually bind. On the contrary, diazepam does not bind to the receptors corresponding to α_4, and α_6 subtypes, making these diazepam-insensitive (DI) sites of potential use with clinical significance since the sedation, ataxia, amnesia and dependence cannot be mediated by these two subunits.

While, the functions of DS $GABA_AR$ are well understood in terms of the effects of classical benzodiazepines (Table 1 details) and certain properties can be directly linked to specific receptor subtypes such as sedation (α_1), anxiolysis (α_2), cognition (α_5); the functions of the diazepam insensitive (DI) sites are still largely not understood. Previous studies in rodents reported, α_6-containing receptors were found in the cerebral membranes and granule cell cultures in a distinct anatomical distribution; around 25-30% of brain $GABA_A$ receptors in these brain regions. On the other hand, $\alpha4$ containing receptors were less abundant (approximately 5% of the total $GABA_A$ population) and were primarily located in the hippocampus and thalamus.[16]

Several classes of ligands which include imidazobenzodiazepines are known to bind to DI sites with moderate to high affinities (see Figure 10 for several examples). But these ligands do not

exhibit sufficient selectivity for DI over DS which explains some of their in vivo functions ascribed to DI sites. This represents a complexity in clear characterization of their physiological and pharmacological functions apart from DS receptors.[16]
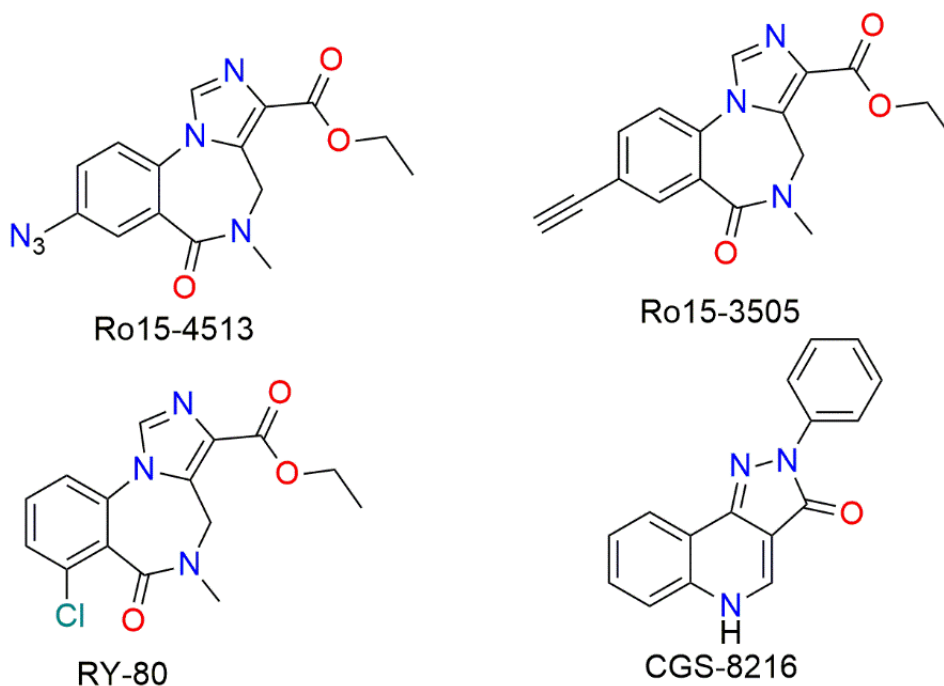
Figure 10. Some benzodiazepine receptor ligands for DI GABA$_A$ receptors

Among the numerous ligands that have been investigated to date, imidazo [1,5-a][1,4] benzo-diazepines are the most extensively studied and exhibited the highest selectivity towards the DI sites, as well. It was shown that alteration at the C-3 and C-8 positions of 6-oxo- imidazo [1,5-a][1,4] benzodiazepines have profound effects on their DI-site selectivity, as compared to DS-sites.[16]

2. Aims of this Research

It is evident from the above discussion that there is a huge unmet demand for better treatments for asthma. The current options for treatment of asthma are neither sufficient nor up to the desired clinical level in regard to safety and convenience. The adverse CNS side effects, poor patient compliance and inconsistent dosage is due to several individual factors; frequent dosage as well as expense, improper use of inhalers, ineffective long term treatment, and unavailability of better medications are among the shortcomings of the current management of asthma. The aim of the current study was to develop a novel strategy for treatment of asthma by targeting the diazepam insensitive α_4 GABA$_A$ receptor sites in the periphery, but to avoid untoward side effects that usually occur with some drugs in the CNS. It has been found that receptors in the lung, which is a part of peripheral nervous system (PNS), express functional GABA$_A$ receptors including the DI subtypes (i.e., α_4). In addition, it was illustrated that an α_4 GABA$_A$R agonist effected relaxation in pre-contracted airway smooth muscle (ASM) by different contractile agents both in human and in guinea pig tissues.[153] Expression of functional α_4-GABA$_A$R subunits was also confirmed in mouse lungs. The reduction of airway-hyperresponsiveness by α_4-selective GABA$_A$ agonists or positive allosteric modulators (PAM) of the GABA$_A$ receptor was reported in mouse model, as well.[15]

Furthermore, part of the immune system plays a key role in airway inflammation during asthmatic periods. Interestingly, immune and inflammatory cells (CD$_4$ and T-helper cells) also express functional GABA$_A$ receptors including those of the $\alpha_4\beta_{2/3}\gamma_2$ subtype. The α_4-subtype selective GABA$_A$R modulators have been shown to reduce both AHR and inflammation in a murine asthma model.[15]

To summarize, the useful effects of $\alpha_4\beta_{2/3}\gamma_2$ receptor subtypes as selective GABA$_A$R allosteric modulators, which can mediate the efficacy of the functional GABA$_A$Rs expressed in airway smooth muscle, as well as immune/inflammatory cells by removing contraction, reducing hyperresponsiveness or reducing and/or preventing inflammation by reducing eosinophilia count or mucous hypersecretion is important in regard to treatment strategies. These previously found important results provided important insight for a novel treatment of asthma by targeting the α_4 GABA$_A$R receptors in the lung and in the immune cells. By avoiding the central part of the nervous system (CNS), this would provide asthma drugs, which would be ideal to avoid any off-target CNS side-effects. Since, α_4-sites are diazepam insensitive sites activation (PAM) of α_4-GABA$_A$R subtypes would avoid effects corresponding to diazepam or other benzodiazepine adverse effects. By controlling the lipophilicity of the ligands, it should be possible to prevent them from travelling across the BBB, while maintaining optimal GABA$_A$R efficacy in the peripheral target organ GABA$_A$ receptors. The ultimate goal of this research was to optimize the development of an α_4-subtype selective drug for treatment of asthma, using the imidazodiazepine lead ligand (XHE-III-74), which has elicited α_4-subtype selective GABA$_A$R efficacy and showed promising results both in ASM and inflammatory cells. These results also indicated further improvement in terms of desired drug properties was required. In addition, increasing the in vivo stability (by fortifying metabolic sites) for a longer duration of action was needed. By incorporating the following properties into a drug candidate for treatment of asthma by targeting α_4 (DI) subtype selective ligands in the PNS.

i. Avoid CNS activity by retarding drug molecules from penetrating the BBB and avoid any sensorimotor effects

ii. Develop drugs with appropriate lipophilicity which will retard BBB-penetrability, as well as will be orally bioavailable

iii. Develop ligands with a longer duration of action by improving metabolic stability to decrease frequency of dosage by the incorporation of deuterium at metabolically labile sites or by employing bioisosteric equivalents at the C-3 position to optimize drug properties.

iv. Develop a drug capable of administration as an aerosol or as the alternative oral tablets.

3. Chemistry and Results

3.1 Background

Earlier in the search of a diazepam insensitive (DI) GABA$_A$ receptor ligands ($\alpha_4\beta_3\gamma_2$ and $\alpha_6\beta_3\gamma_2$), a series of 3- and 8- substituted 6-oxo-imidazo [1,5a] [1,4]-diazepines were prepared. After a study of their SAR and receptor binding, it was found that CMD-45 and XHE-III-74 (Figure 11) exhibited potent binding affinity (with K$_i$ values less than 1nM) and selectivity at DI subtypes (Table 2).[16] The difference between these two ligands is in the ring size of the D ring. The outcome of this study with Emala et al.[2] suggested that CMD-45 and XHE-III-74 were potential leads for further development in cases where DI ligands might exhibit unique biological activity.
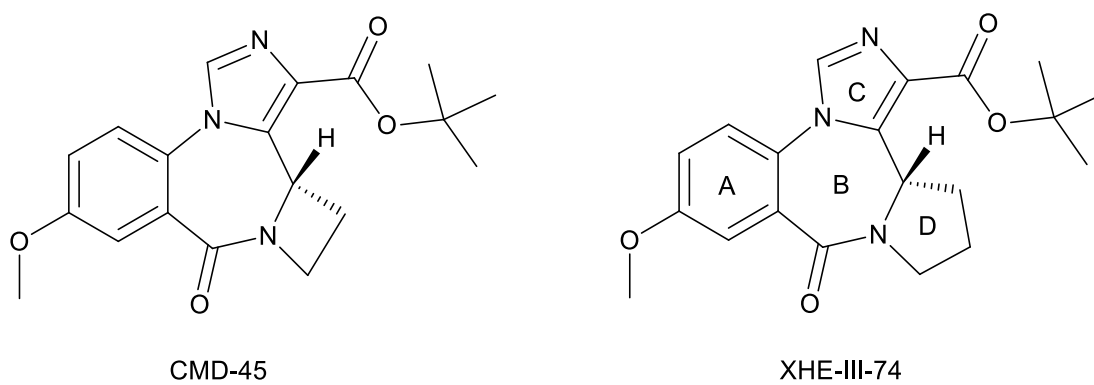
CMD-45   XHE-III-74

Figure 11. Structures of XHe-III-74 and CMD-45

Table 2. *In vitro* **binding affinity at $\alpha_x\beta_3\gamma_2$ (values in nM)[16]**

Comp.	α1	α2	α3	α4	α5	α6
XHe-III-74	77	105.5	38.5	0.42	22	5.8
CMD-45	90.5	65.5	30.3	0.15	1.65	0.23

3.2 The Synthesis of CMD-45 and XHE-III-74

Based on the earlier route of Fryer and Gu,[3,16,17] the synthesis of XHE-III-74 **7** began with the preparation of 5-methoxyanthranilic acid **2** (Scheme 1) from 5-methoxy-2-nitrobenzoic acid **1** by catalytic hydrogenation. The resulting anthranilic acid **2** was converted into isatoic anhydride **3** with triphosgene. (**Be very careful in working with triphosgene**. **After the completion of the reaction, be careful to remove and quench the remaining triphosgene or phosgene. To this end air or a gas was passed through the reaction flask into a scrubber flask which contained a solution of NaOH in water**). The anhydride **3** was heated with L-proline in DMSO to generate the corresponding benzodiazepine **4**. This compound was converted into the imidazodiazepine, XHE-III-74 ethyl ester **5**. This ester was converted into the tert-butyl analog XHE-III-74 (**7**) with Li rod (small pieces) in ^{t}BuOH on multi-gram scale. CMD-45 was synthesized in Dr. Cook's lab by Michael Stephen by using the same synthetic route with replacement of L-azetidine-2-carboxylic acid for the L-proline in high overall yield.

The last step of the synthesis of XHE-III-74 (**7**), i.e. the conversion from ethyl ester to tert-butyl ester was deemed problematic for several reasons. The reaction was extremely moisture sensitive and as a result a significant amount of the starting ethyl ester became saponified, which resulted in yield loss. In addition, reactions often fail to go to completion and the unreacted ethyl ester (if any) poses a hindrance to purification of the desired tert-butyl ester. This is because the polarity of these two esters are quite similar and often co-elute on chromatography or requires long, tenuous separations, which retard the pace of derivatization of XHE-III-74 (**7**). As an alternative, the carboxylic acid of XHE-III-74, which was also an important target ligand, was treated with DMF-di-tertbutyl acetal in toluene at reflux.[18] This resulted in a cleaner reaction to execute in which it was easy to isolate the desired product even if the reaction failed to go to completion. This

accelerated the process of making novel analogs of XHE-III-74 (7) which are potential drug candidates under the current hypothesis.

Scheme 1. Synthesis of XHE-III-74 (7) and XHE-III-74 ethyl ester (5)[3,16,17]
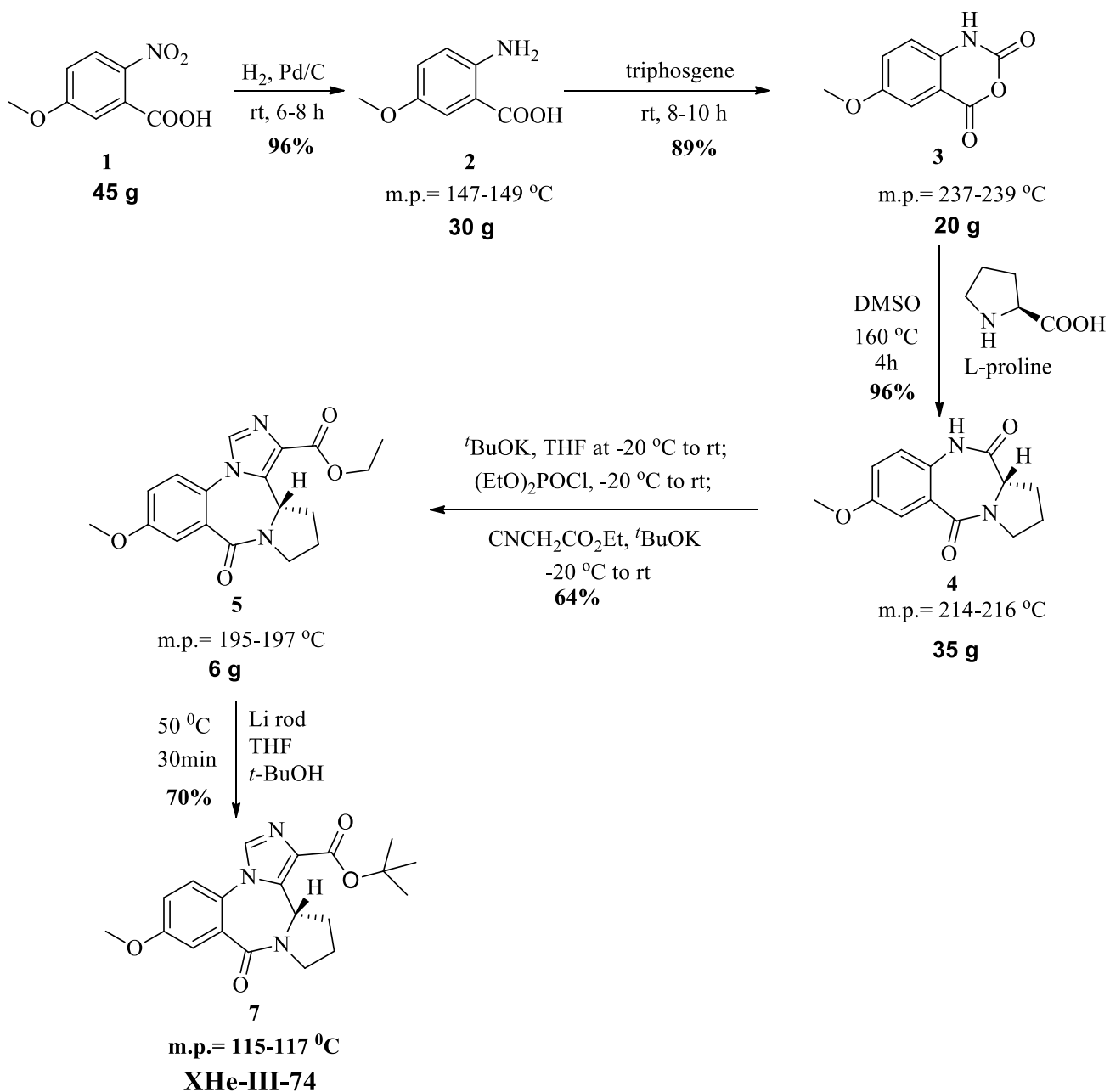
Scheme 2. Alternative access to XHe-III-74 (7) on multigram scale[18]
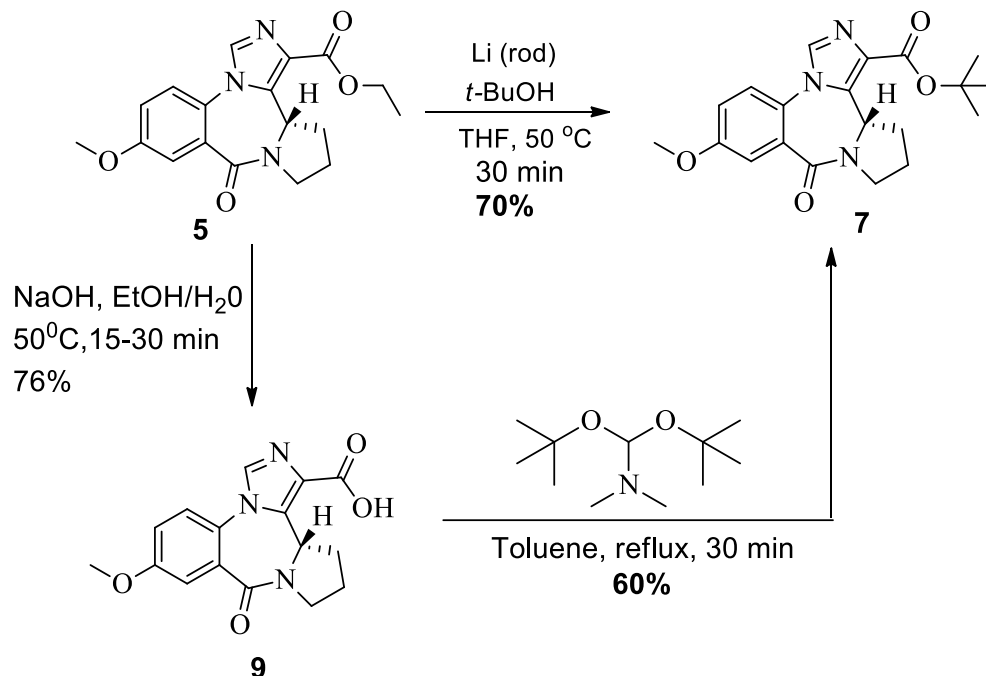
3.3 Comparative Biological Evaluation of CMD-45 and XHE-III-74

To evaluate the effectiveness of these two ligands, their corresponding therapeutic potential, and to find out the best one of the two for further development, it was decided to compare their effectiveness in relaxing airway smooth muscle (ASM) in the laboratory of Dr. Charles Emala at Columbia University. Dr. Emala had recently discovered that $\alpha_4\beta_3\gamma_2$ and $\alpha_5\beta_3\gamma_2$ Bz/GABA(A)ergic subtypes were found in tissue from healthy transplantation donor lungs. His results were on the healthy part of the lung tissue. The same phenomenon was discovered in rodents including guinea pigs.[151,153] This was an important breakthrough.

3.3.1 Oocyte Efficacy Study of XHE-III-74 and CMD-45[2]

In oocytes, which expressed each α subunit individually (along with β_3 and γ_2 subunits; $\alpha_{1\text{-}6}\beta_3\gamma_2$), both CMD-45 and XHe-III-74 produced a greater augmentation of GABA [EC_3]-induced currents in oocytes which contained α_4 or α_6 subunits compared with the other α subunits at multiple concentrations (Figure 2; $P < 0.01$, n = 3–4). A higher value of the current at EC_3 (Y-axis) implies better efficacy at that subunit at a particular concentration (X-axis). Illustrated in Figure 12 are both CMD-45 and XHE-III-74, which produced better augmentation of GABA-EC_3 induced currents at α_4 and α_6 subtypes than others. Ligand XHE-III-74 induced more current at the α_4 subtype than at the α_6 receptor up to the highest concentration of 30 μM and induced higher current (up to ~300% of the control), as compared to CMD-45. On the other hand, CMD-45 induced higher EC_3 current at α_4 subtypes at 1 μM but at 10 and 30 μM concentrations the current observed was greater at α_6 than at α_4 ion channels.

Examination of additional studies in oocytes expressing the α_4 subunit along with the delta subunit ($\alpha_4\beta_3\delta$) indicated no XHe-III-74–mediated augmentation of GABA ([EC_3])–induced currents, even at the highest concentration of XHe-III-74 tested (10 μM; data not shown; n = 4). Similarly, at 10 μM CMD-45 showed only a modest augmentation of GABA-induced currents ($116\pm3\%$ of current induced by a GABA EC_3 concentration alone, $P < 0.05$, $n = 4$) at δ subtypes. The CMD-45 did not significantly augment GABA-induced currents at δ subtypes either at lower concentrations (data not shown). These studies demonstrate the selectivity of CMD-45 and XHe-III-74 for $\alpha_4\beta_3\gamma_2$ subunit–containing receptors, and also demonstrate that they have very little to no activity at receptors containing the α_4/δ subunit combination. This is an important result.
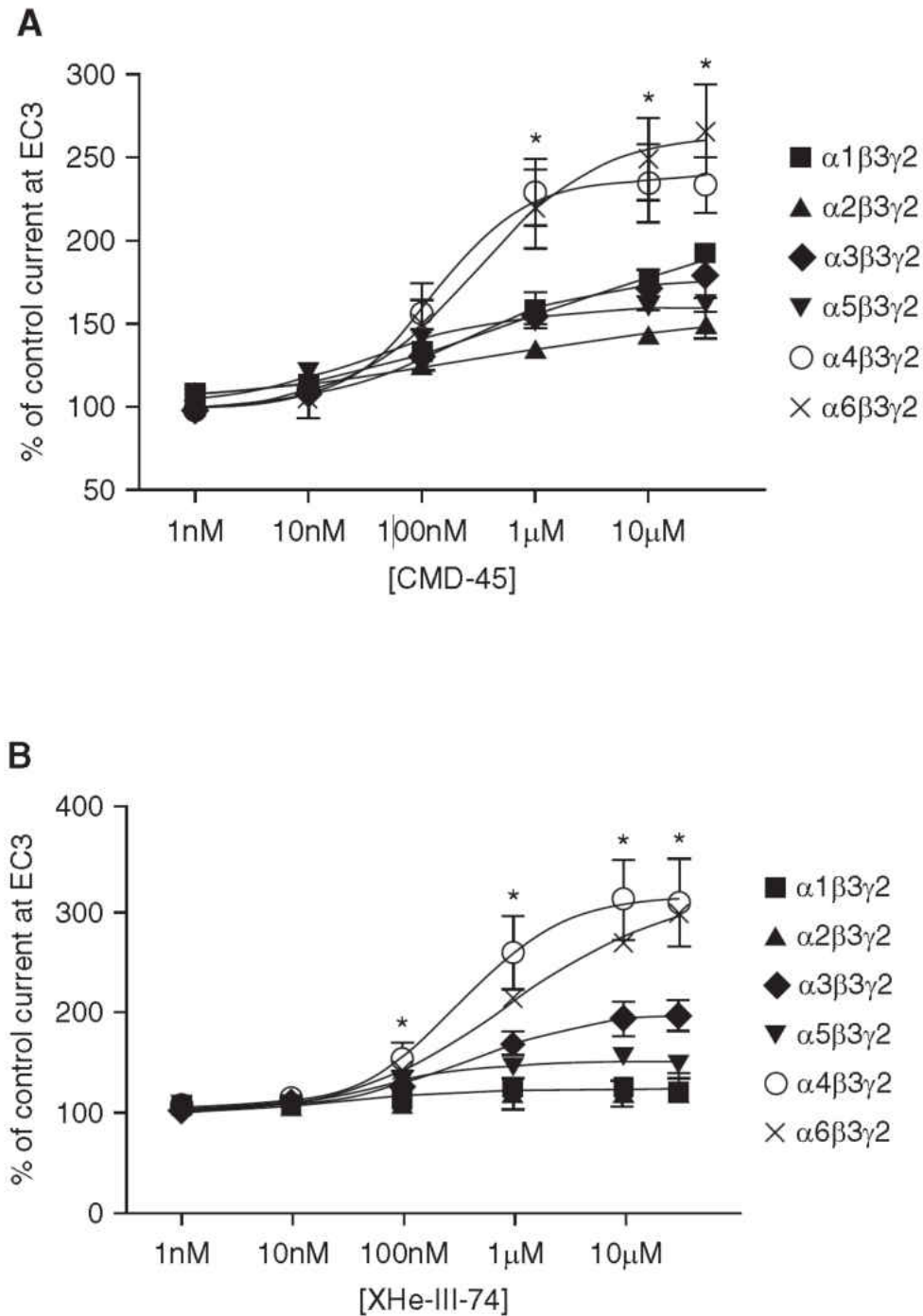
Figure 12. Augmentation of GABA-induced currents in oocytes expressing GABA$_A$Rs of specified subunit composition. At multiple concentrations, both CMD-45 and XHe-III-74 led to significantly greater augmentation of GABA$_A$R-mediated currents in oocytes expressing α$_4$ or α$_6$ subunits in combination with β$_3$/γ$_2$ subunits (when each is compared with α$_1$ as a reference in two-way repeated measures ANOVA with Bonferroni post test comparisons). Data are presented as a percent of current induced by a 3% maximal effective concentration (EC$_3$) of GABA. This demonstrates the subunit selectivity of these novel, positive allosteric modulators of the GABA$_A$R (*P < 0.05 for both α$_4$ and α$_6$ as compared with the α$_1$ subtype by Bonferroni _post hoc_ analysis; n = 3–4; mean ± SE). Modified from the figure in Yocum, et al.[2]

34

3.3.2 Mouse Tracheal Ring Organ Bath Studies on XHE-III-74 and CMD-45[2]

In *ex vivo* organ bath experiments carried out by Yocum and Emala, CMD-45 and XHE-III-74 were evaluated for their ability to relax pre-contracted mouse tracheal rings. The treatment of ACh-contracted WT (wild type) mouse tracheal rings with CMD-45 and XHe-III-74 led to a significant relaxation (Figure 13). The tracheal rings from $GABA_A$ receptor α_4 knock out (KO) mice also exhibited a response to CMD-45 and XHe-III-74, which indicated relaxation, but was significantly less than in wild type (WT) mice for both ligands at multiple concentrations. This finding further confirmed that the α_4 subtype $GABA_A R$ selectivity of these imidazoles and the mechanistic role of the α_4 $GABA_A R$ activation in the relaxation of ASM. In these experiments too, XHE-III-74 was found to be more potent than CMD-45 in relaxation of pre-contracted mouse tracheal rings. This is consistent with the electrophysiological data presented previously here, which demonstrated a larger $GABA_A R$-mediated current with exposure to XHe-III-74 as compared to that with CMD-45 at equal concentrations (Figure 11). The prorelaxant effects of both compounds were reversible in WT tracheal rings at the highest doses tested (100 µM for CMD-45 and 50 µM for XHe-III-74) after repeated buffer changes. This was demonstrated by showing that both XHe-III-74– or CMD-45–treated rings contracted with equal force to 80 mM KCl treated rings as compared with vehicle-treated rings after these repeated buffer changes (data not shown). **The data from these "wash out" experiments was significant.**
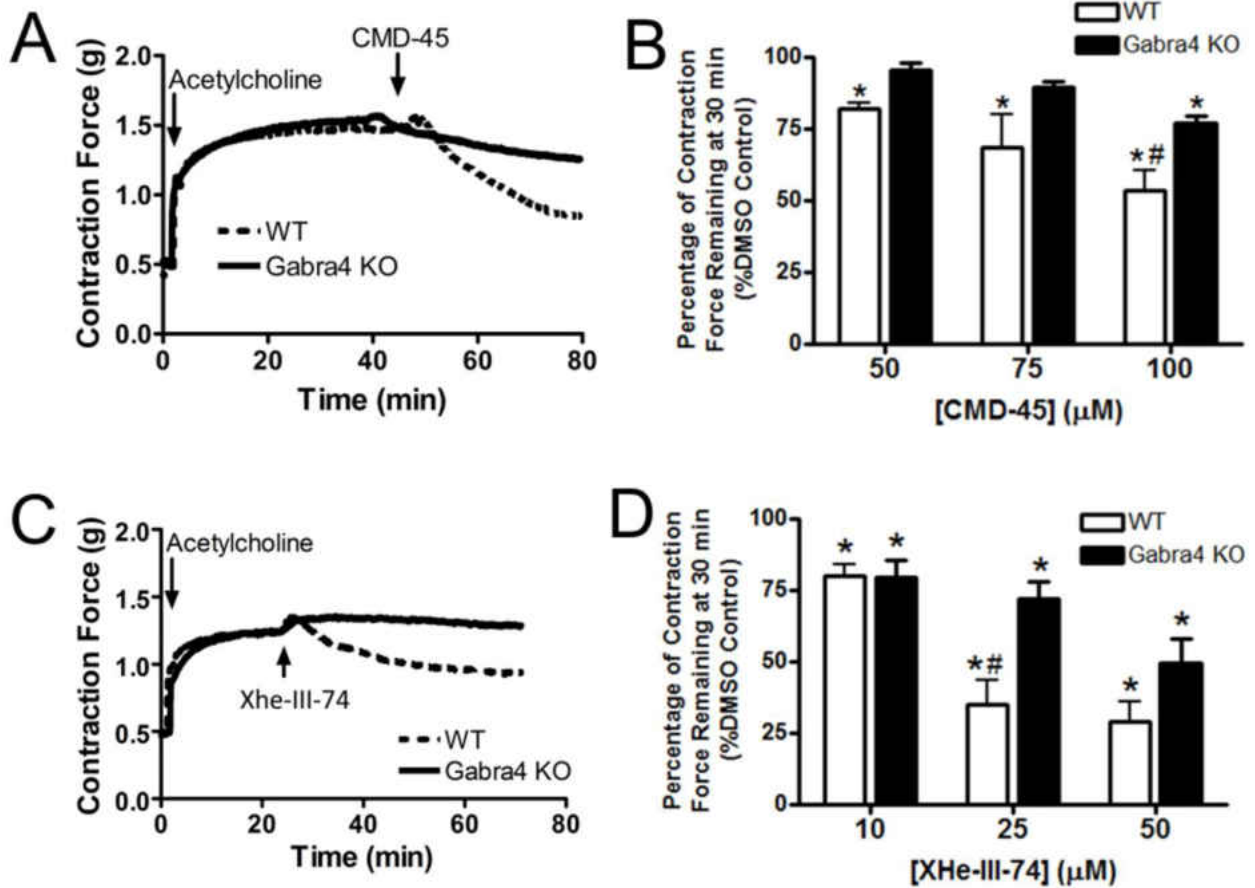
Figure 13. Mouse tracheal ring contraction force in *ex vivo* organ bath preparations. (A and C) Representative muscle force tracings of acetylcholine (ACh)–contracted murine tracheal rings. (B) CMD-45 significantly relaxed precontracted wild-type (WT) murine tracheal rings but not rings from Gabra4 knockout (KO) mice, at 50 μM (*n* = 3) and 75 μM (*n* = 3), consistent with heightened selectivity for the Gabra4 subunit, as demonstrated in Figure 12. (D) XHe-III-74 led to significant relaxation of precontracted murine tracheal rings as compared with vehicle (0.1% DMSO) in both WT and Gabra4 KO mice at 10 μM (*n* = 5), 25 μM (*n* = 5), and 50 μM (*n* = 3). At 25 μM XHe-III-74, tracheal rings from WT mice relaxed to a greater extent than rings from Gabra4 KO mice, consistent with the heightened Garbra4 selectivity. Contraction force is presented as percent of DMSO vehicle control for WT and Gabra4 KO tracheal rings (*$P<0.05$ in comparison to DMSO control, #$P<0.05$ in comparison to drug-exposed Gabra4 KO; ANOVA with Bonferroni *post hoc* comparison; mean ± SE). Modified from the figure in Yocum, et al.[2]

3.3.3 Effect of XHE-III-74 and CMD-45 on Human Airway Smooth Muscle[2]

To further evaluate the pro relaxant properties of these two ligands, human tracheal airway smooth muscle (ASM) strips were used in *ex vivo* organ bath experiments. This work by Yocum and Emala employed healthy human tracheal rings that were part of a surgery resection. Both CMD-45 and XHe-III-74 led to a significant reduction in contractile force in ACh-contracted human ASM strips at 50 µM ($n = 5$) and 100 µM ($n = 6$, Figures 14A and 14B $P < 0.05$ for both compounds, as compared to vehicle control at 50 and 100 µM). In separate experiments low concentrations of both CMD-45 and XHe-III-74 (25 µM) potentiated the albuterol induced relaxation of human ASM contracted with ACh *ex vivo*, which led to a full log decrease in the albuterol EC_{50} (Figure 14C; albuterol EC_{50} was 807.0 nM for DMSO, 69.3 nM for the CMD-45 treatment group, and 87.9 nM for the XHe-III-74 treatment group; n = 4, $P < 0.01$ for change in albuterol EC_{50} compared with CMD-45 or XHe-III-74 to vehicle [DMSO]).
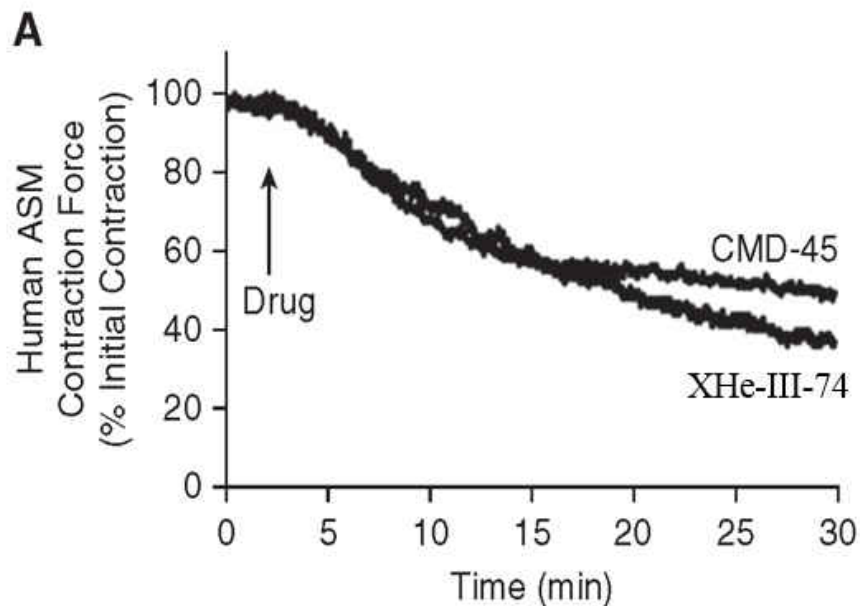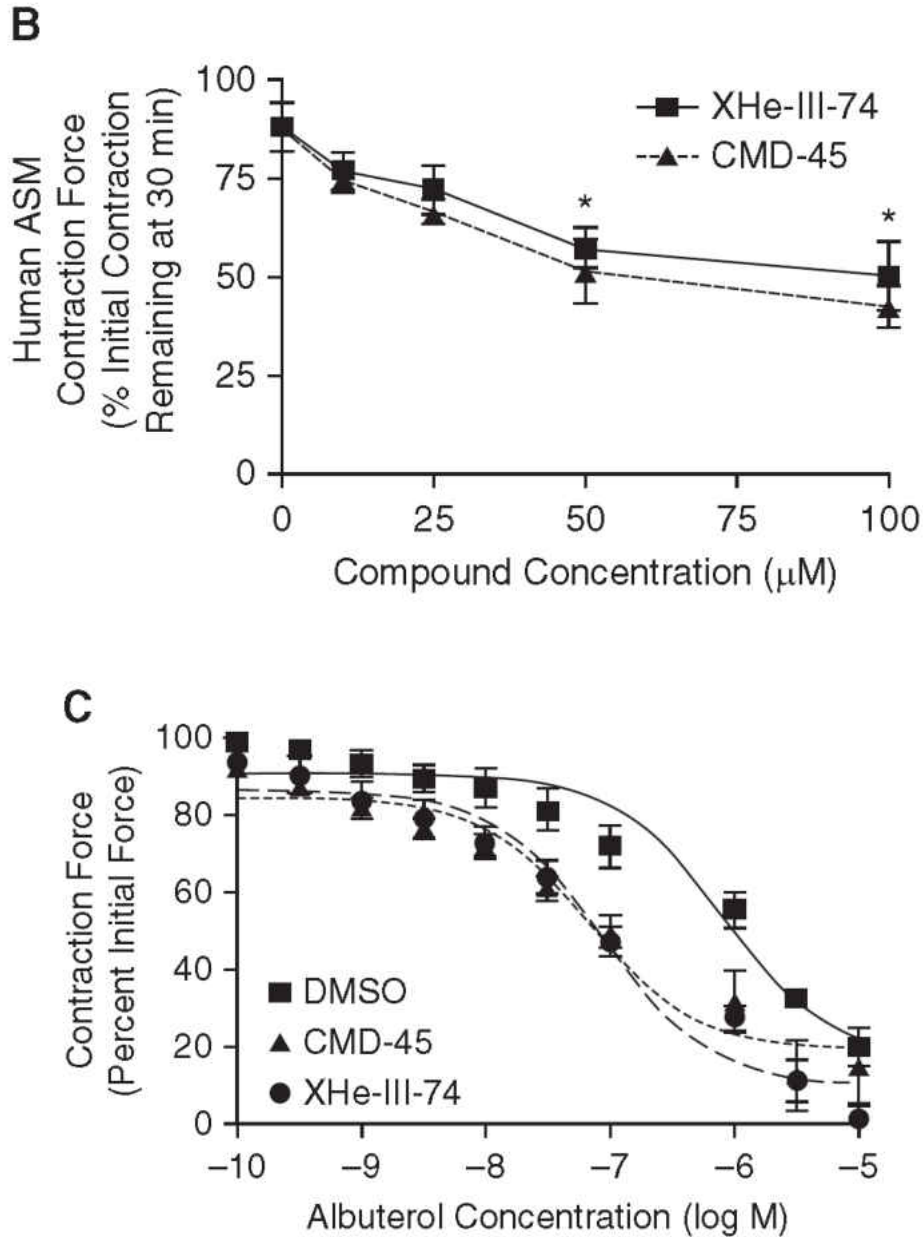
Figure 14. Human tracheal airway smooth muscle (ASM) strips in *ex vivo* organ bath preparations. (A) Representative muscle force tracings of the 100 μM CMD-45– and XHe-III-74–induced direct relaxation of ACh [EC$_{50}$]–precontracted human tracheal ASM strips. (B) CMD-45 or XHe-III-74 (50 and 100 μM) induced significant relaxation of ACh-precontracted tracheal ASM strips compared with vehicle (0.2% DMSO) controls at 30 minutes (*n* for 0, 10, 25, 50, and 100 μM, respectively: CMD-45, 6, 6, 4, 5, and 6; XHe-III-74, 6, 4, 3, 5, and 6. *P<0.05 for both CMD-45 and XHe-III-74 as compared with vehicle control, ANOVA with Bonferroni *post hoc* comparison). (C) CMD-45 (short dashed line) and XHe-III-74 (long dashed line) at low dose (25 μM) both induced significant leftward shifts in the dose–response curve for albuterol (β$_2$-adrenoceptor–selective agonist)-mediated human ASM relaxation as compared with the DMSO control (solid line). The EC$_{50}$ concentration of albuterol with coadministration of CMD-45 was 69.3 nM, and with coadministration of XHe-III-74 was 87.9 nM as compared with 807.0 nM for DMSO (*n* = 4 per group; *P<0.01 for leftward shift in EC$_{50}$ for both ligands compared with vehicle; mean ± SE). Modified from the figure in Yocum, et al.[2]

3.3.4 Effect of XHE-III-74 and CMD-45 on Resistance (*in vivo*) on the Mouse Respiratory System[2]

To evaluate the relaxant or respiratory system resistant potential of these ligands, when administered as an aerosol, the dose was applied by inhalation to an asthmatic subject (HDM sensitized WT-mouse model) before introducing the challenge. The better compound of the two ligands in the earlier experiments, XHe-III-74 (25 µl, 10 mM), when administered by inhalation 10 minutes before a bronchoconstrictive challenge, led to a significant reduction in R_{RS}, as measured by the forced oscillation technique (flexiVent) in asthmatic (HDM-sensitized) mice (Figure 15; area under the curve analysis, $P<0.05$, $n = 3$ for vehicle, 4 for XHe-III-74). This demonstrated the potential of this compound to be administered therapeutically by inhalation to treat bronchospasms.
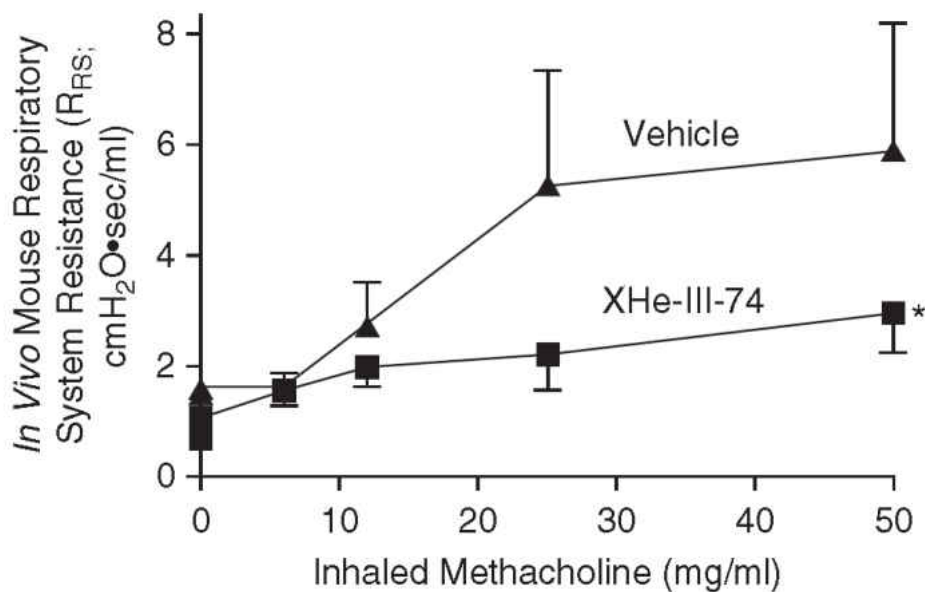
Figure 15. *In vivo* mouse respiratory system resistance (R_{RS}) tests. Inhalation of XHe-III-74 10 minutes before a bronchoconstrictive challenge (methacholine) significantly reduced R_{RS} in house dust mite antigen–sensitized WT mice (asthma model) as compared with inhaled vehicle control (*$P<0.05$ for area under the curve analysis; $n = 3$ for vehicle control, 4 for XHe-III-74; mean ± SE). Modified from the figure in Yocum, et al.[2]

3.3.5 Effect of XHE-III-74 and CMD-45 on ASM Calcium Dynamics[2]

The pretreatment of human ASM cells with CMD-45 and XHe-III-74 inhibited histamine-induced increases in intracellular calcium concentrations *in vitro*, an effect that was lost when calcium was omitted from the extracellular buffer. This phenomenon suggests that inhibition of calcium influx due to alterations in plasma membrane potential may play a role in the mechanism of ASM relaxation.

In *in vitro* studies using a fluorescent intracellular calcium indicator, the removal of calcium from the external buffer led to a 29.8% diminution in histamine-mediated increases in intracellular calcium in primary cultures of human ASM cells ($P < 0.001$ comparing 0 [$n = 28$] to 2 mM [$n = 14$] external calcium in DMSO-pretreated and histamine-stimulated cells). In the absence of extracellular calcium, the addition of 100 µM CMD-45 ($n = 17$) or XHe-III-74 ($n = 20$) did not further augment this inhibition of the histamine-induced intracellular calcium response (Figure 16A; $P =$ not significant). However, in the presence of 2 mM external calcium, CMD-45 and XHe-III-74 (25 and 50 µM) inhibited the histamine-mediated increase in intracellular calcium in cultured primary human ASM cells to an extent similar to removal of external calcium (25.0% and 30.0% for 50 µM CMD-45 and XHe-III-74, respectively, $P<0.05$ and $P<0.001$, respectively; Figures 16B and 16C). This suggests that these two ligands lead to ASM relaxation by limiting the calcium influx from the extracellular space, likely as a result of altered plasma membrane potential.

A

B
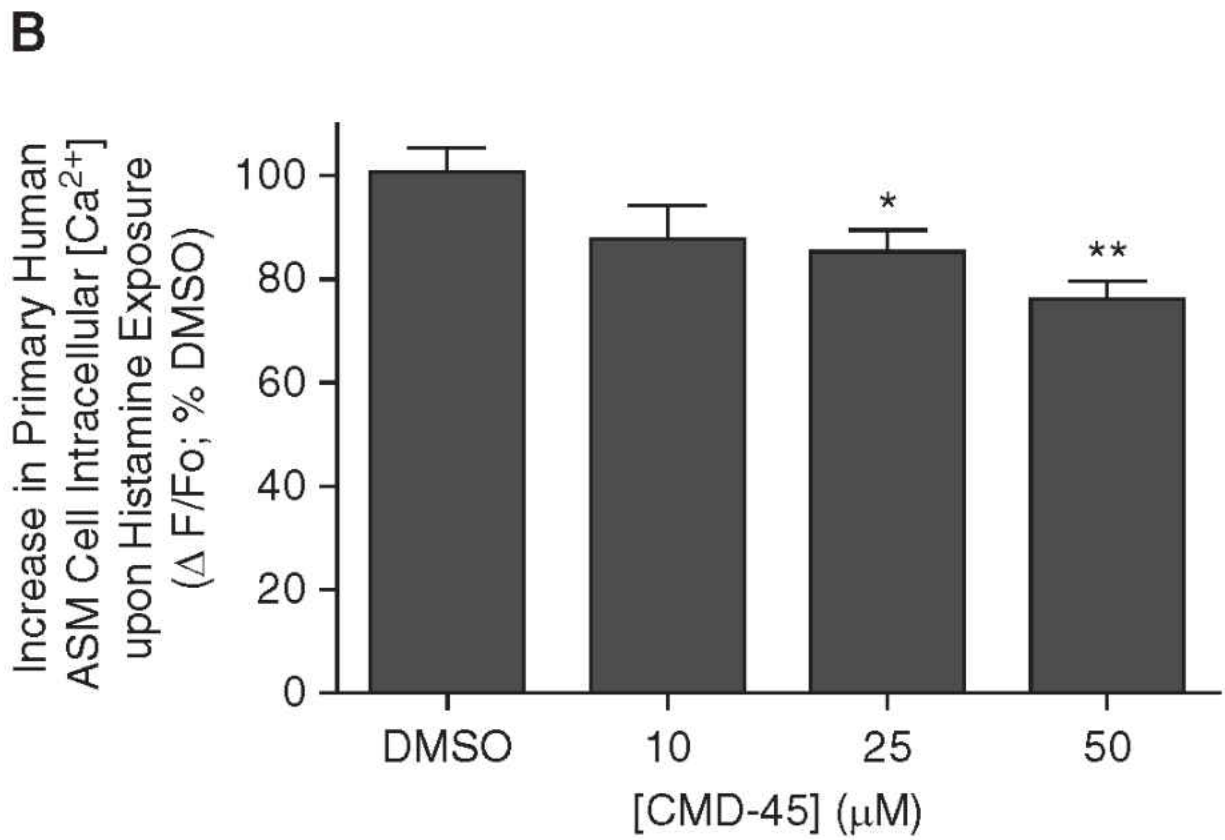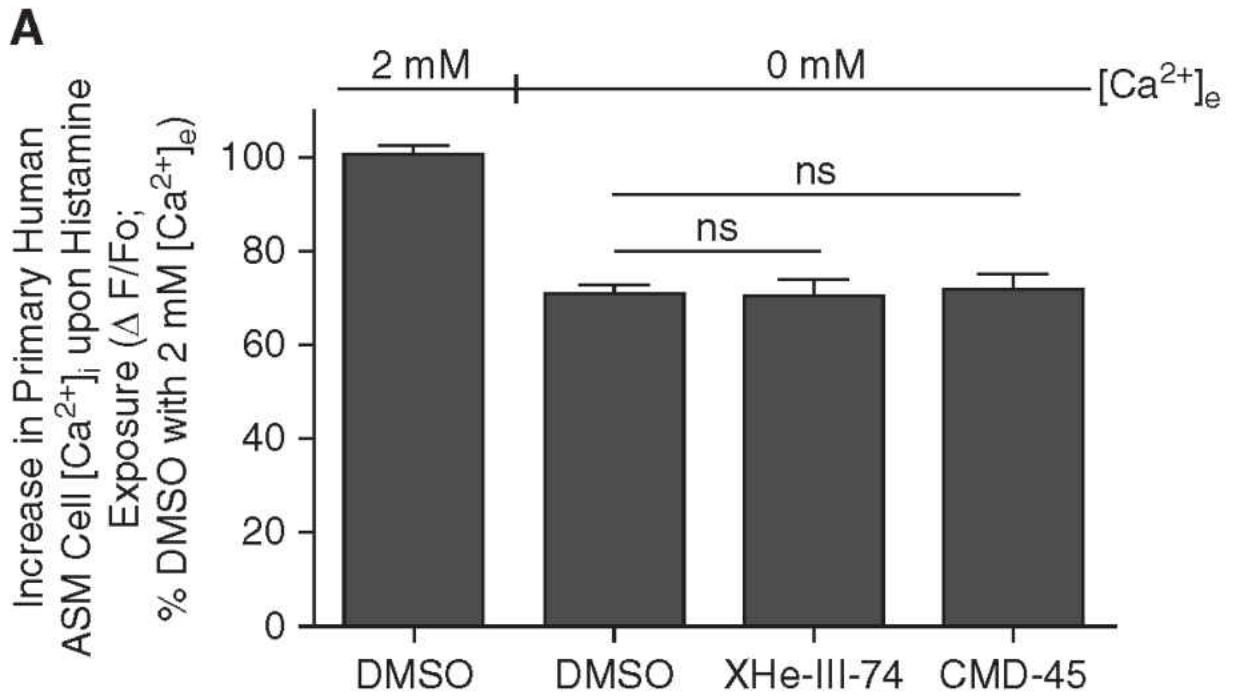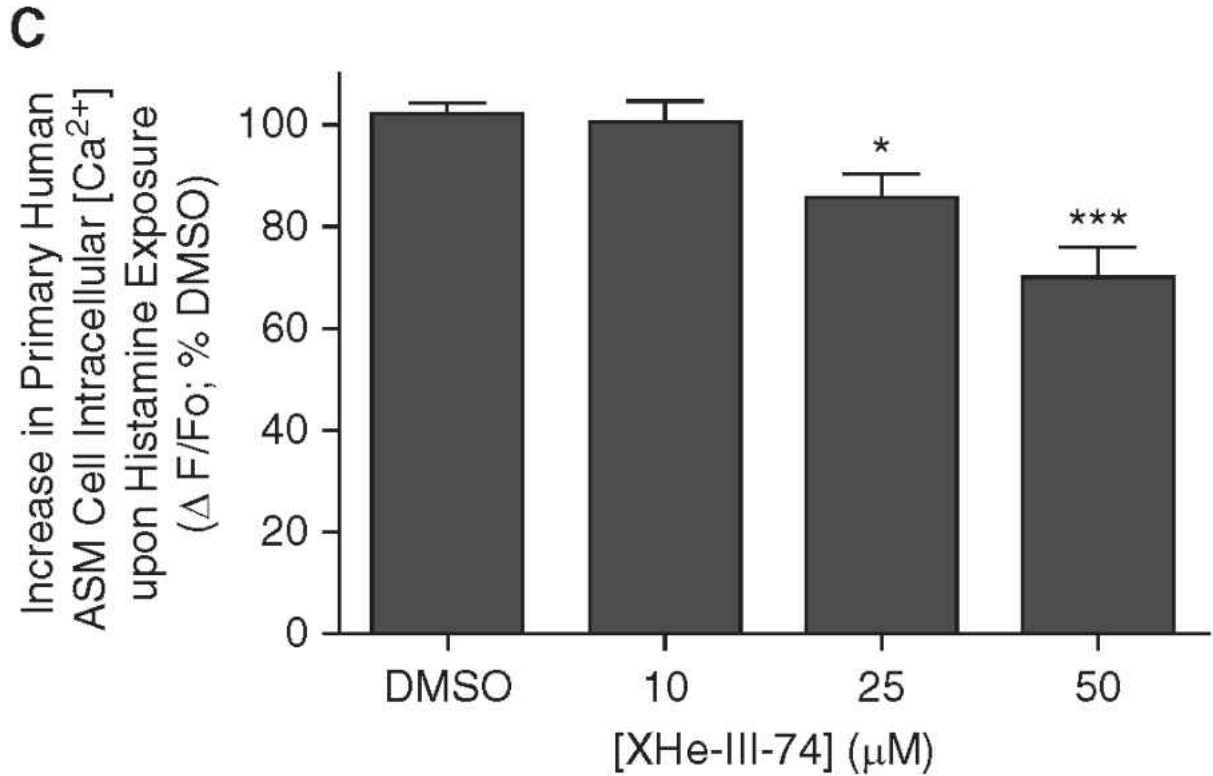
Figure 16. *In vitro* primary human ASM cell calcium dynamics. (A) The increase in intracellular calcium concentrations ([Ca^{2+}]$_i$) in primary human ASM upon exposure to 10 μM histamine is inhibited 29% ($P<0.05$; $n = 28$) by the removal of extracellular calcium ([Ca^{2+}]$_e$; 0 mM). The addition of 100 μM XHe-III-74 ($n = 20$) or CMD-45 ($n = 17$) does not further inhibit histamine-induced increases in [Ca^{2+}]$_i$ (P>0.05). (B and C) In contrast, in the presence of 2 mM external calcium, pretreatment with 25 or 50 μM CDM-45 or XHe-III-74 significantly inhibited subsequent histamine-induced increases in peak [Ca^{2+}]$_i$ (n [DMSO, 10, 25, and 50 μM]: [B] (CMD-45): 12, 9, 11, 9; [C] (XHe-III-74): 16, 10, 14, 14; human ASM cell lines established from three donor patients; data are presented as percent of average of simultaneously tested vehicle control wells; n = total plate wells; *$P< 0.05$, **$P< 0.01$, ***$P< 0.001$, ANOVA with Bonferroni *post hoc* comparison; mean ± SE). ΔF/Fo, peak change in fluorescence/baseline fluorescence; ns, not significant. Modified from the figure in Yocum, et al.[2]

In *in vitro* experiments, CMD-45 and XHE-III-74 blocked the Ca^{2+} influx and inhibited the increase by 25-30% in intracellular [Ca^{2+}]$_i$ concentration induced by histamine. However, in the absence of extracellular Ca^{2+} these ligands did not potentiate any inhibition which gave important mechanistic insight into the role of [Ca^{2+}]$_i$ in regulating ASM tone. The effects of $GABA_AR$ modulators on ASM are likely via membrane potential since $GABA_AR$ is a chloride ion channel. In a resting ASM, the internal chloride concentration is higher and the activation of the $GABA_AR$

is likely to result in depolarization of the membrane potential. The membrane potential of the ASM increases from a resting value (-50 to -60 mV) to a potential of -20 mV, which is predicted to be crossing the chloride equilibrium potential. This would result in opening of the chloride channel which favors chloride influx and relative hyperpolarization. These conditions may pose an inhibition of voltage-sensitive Ca^{2+} entry mechanisms. This is in agreement with the *in vitro* data of CMD-45 and XHE-III-74, which led to a significant retardant in raising the intracellular $[Ca^{2+}]_i$ in histamine-exposed ASM. In addition, in the absence of extracellular Ca^{2+} these compounds do not further inhibit calcium intake even at higher concentrations (100 μM) which further reinforces the hypothesis of the mechanism of action of these compounds is *via* inhibition of calcium influx.

3.3.6 The Outcome of the Comparative Studies on CMD-45 and XHE-III-74

It was demonstrated that the two novel compounds, CMD-45 and XHe-III-74, are positive allosteric modulators of the $GABA_AR$ and have superior selectivity for receptors containing the α_4/α_6 subunit. Both compounds acutely relaxed ASM from mice and humans. These selective compounds offer the potential to treat bronchoconstriction *via* a novel therapeutic mechanism, while reducing or avoiding unwanted CNS side effects.

Consideration of the inference from the experimental evidence, XHE-III-74 was deemed to be a better ligand (better selectivity, higher efficacy and more desirable properties) than CMD-45 and it was selected for further development and SAR studies. The logic behind this choice includes:

1. It is known that human ASM also express α_5 subunits of $GABA_ARs$.[151] It was also purportedly demonstrated that α_5-subtype selective PAM's were responsible for memory impairment[164] and post anesthesia cognitive impairment associated with upregulation of α_5 $GABA_AR$ in the brain.[2,165]

In addition, activation of α_2 and α_5 in human airway epithelium was reported to increase mucus production.[158] Since CMD-45 exhibited a much higher α_5 subtype selectivity in addition to the useful α_4 selectivity as compared to XHE-III-74, targeting only the α_4 (i.e., XHE-III-74) GABA$_A$R ion channel would avoid any potential undesired effects associated with α_5 receptors.

2. XHE-III-74 exhibited better properties than CMD-45 in the oocyte electrophysiology studies, in *ex vivo* organ bath studies (both murine and human), as well as *in vitro* human ASM calcium dynamics.

3. Finally the materials required for the synthesis of CMD-45 were much more expensive, as compared to the materials for synthesis of XHE-III-74. This means XHE-III-74 was better suited for additional studies.

The GABA$_A$R plays a prominent role in inhibitory neurotransmission and off target binding of ligands to undesired GABA$_A$ receptors containing the α_1, α_2, or α_5 subtypes may cause unwanted CNS effects, especially if the drug is administered intravenously (iv). To evaluate the potential of these compounds in the exhibition of such unwanted side-effects, the Savic group at the University of Vienna performed several experiments (see Appendix for details). The basket test was used to assess the effect of XHE-III-74 and CMD-45 on motor performance. Both ligands caused sensorimotor deficits in C57BL/6 mice at higher doses in Dr. Savic's laboratory (30 mg/kg, Appendix, Table A1). To evaluate the anti-anxiety effects of XHE-III-74 and CMD-45, a step-down test was performed on trained C57BL/6 mice (Appendix, Table A2). Neither of the ligands exhibited any hint of anti-anxiety properties in keeping with their activity at α_4 diazepam insensitive subtypes. To further evaluate the effects of these two α_4-preferring ligands on motor performance, the rotarod experiment was undertaken (Appendix, Table A3). Both XHE-III-74 and CMD-45 showed ataxia at higher doses [10 mg/kg (XHE-III-74) and 15 mg/kg (CMD-45) i.p.

administration]. In addition, locomotor activity was performed separately on adult male and female Wistar rats to access the sedative effects of the two ligands in consideration. Both showed pronounced sedative effects (Appendix, Table A4) at 10 mg/kg i.p. dose. Furthermore, the plasma and brain distribution of XHE-III-74 after iv administration (solution and nanoemulsion) was evaluated by pharmacokinetic studies. Significant concentrations of XHE-III-74 were detected in both brain and plasma up to 12 hours after iv administration (Appendix, Figure A1).

3.4 Strategies for Further Optimization of the Lead Compound, XHE-III-74 (7)

From the oocyte efficacy and organ bath experiments, it was clear that XHE-III-74, as mentioned, was better suited than CMD-45 for further development for the treatment of asthma by targeting the airway smooth muscle in the lung. This was a promising novel strategy for asthma management. However, the negative CNS side effects which were found in the evaluation of sedative effects by Savic *et al*. (unpublished result) was likely due to the brain penetration of these drugs. Since α_1, α_2, and α_5 subunits are expressed in higher concentrations in the brain, the binding to the GABA$_A$ receptor containing these subunits would certainly evoke the negative undesired effects such as, sedation and ataxia that were observed by Savic *et al*. (unpublished results). By considering the outcome of all the experiments discussed above, the following strategy was taken:

- Since the expression of the α_4 subunit was more pronounced in lungs, which were also devoid of other subtypes (except α_5) which caused the negative GABA$_A$R-induced effects, XHE-III-74 should be further developed to deliver readily to the lung e.g. via an aerosol formulation.

- To inhibit brain penetration of XHE-III-74, this lead compound should be modified to increase polarity (reduced lipophilicity) while retaining α_4 selectivity, which would retard BBB penetration. This would avoid adverse CNS side-effects exhibited by XHE-III-74 itself.

- Potential ligands should be synthesized only after consulting molecular modeling and the pharmacophore model to reduce the number of ligands to be synthesized.

- A library of XHE-III-74 ligands with different substitution at C-3, C-4, and C-8 would be of high interest.

Therefore, XHE-III-74 (7) was selected as the lead compound for further development based on the above hypothesis. Consequently, further improvements in this ligand were deemed beneficial in the search for better asthma drugs with the novel mechanism of action described above and with less CNS activity.

3.5 Novel XHE-III-74 Analogs Based on the Pharmacophore Model

3.5.1 Molecular Modeling and the Pharmacophore Model[13,14]
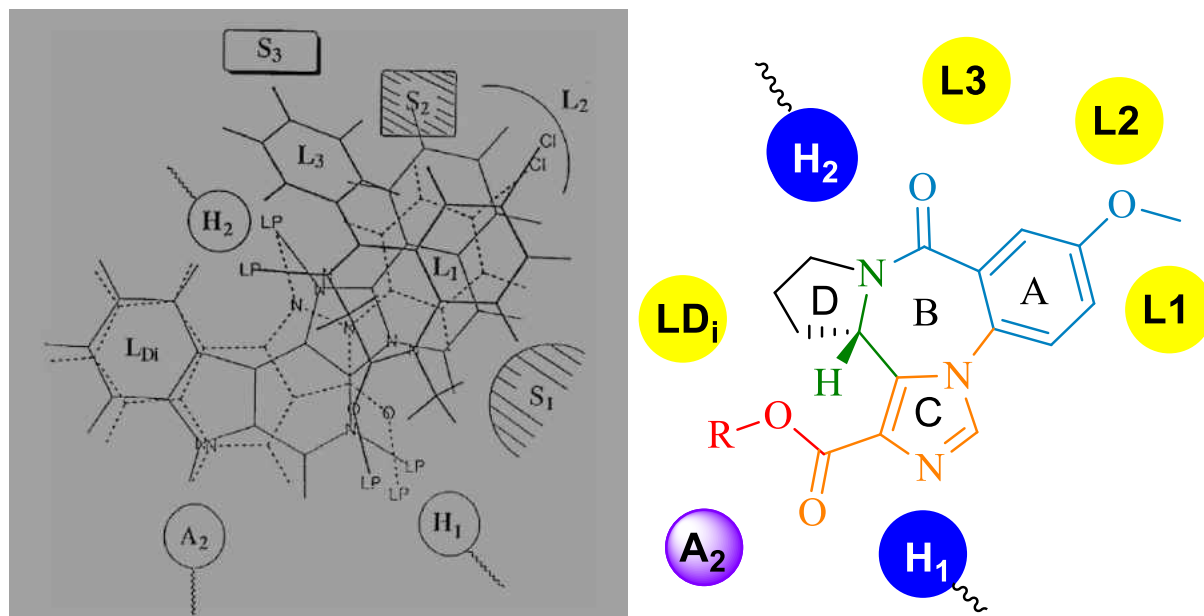
Figure 17. a) The pyrazolo[3,4-c]quinolin-3-one CGS-9896 (dotted line), diazepam (thick line), and planar diazadiindole (thin line) fitted to a schematic representation of the inclusive pharmacophore model for the BzR. The descriptors H$_1$ and H$_2$ designate hydrogen bond donor sites on the receptor protein while A$_2$ represents a hydrogen bond acceptor site necessary for potent inverse agonist activity *in vivo*. L$_1$, L$_2$, L$_3$, and L$_{Di}$ are four lipophilic regions in the binding pharmacophore. Agonist activity requires interaction with H$_1$, H$_2$, L$_1$, L$_2$, and/or L$_3$. Receptor descriptors S$_1$, S$_2$, and S$_3$ are regions of negative steric repulsion. Lp=lone pair electrons. [Modified from the review published in 2007 (Clayton et al)][13,14] b) A simplified representation of the interaction of XHE-III-74 inside the pharmacophore pocket according to the homology model.

Molecular modeling is necessary to decrease the number of potential ligands to be synthesized. This strategy provides a list of potential ligands that fit the target receptor and should show higher binding affinity. The group in Milwaukee developed a unified and comprehensive pharmacophore model for benzodiazepine receptor site employing about 30 rigid planar ligands to map out the protein repulsive regions (S$_1$, S$_2$, S$_3$). In Figure 16, this two-dimensional representation of the

pharmacophore model contains lipophilic pockets (designated L), steric regions of protein-ligand repulsion (designated S), and hydrogen bond donor sites (designated H) and acceptor sites (designated A). This model was employed to design new ligands.

The substituents of varying lipophilicity or size at position C-8 could have a profound effect on receptor subtype selectivity since groups at this position can interact with the lipophilic pocket L_2.

The alkyl group of the esters at position C-3 were proposed to interact with the lipophilic pocket L_{Di} in the pharmacophore model. Thus, variation of the alkyl substituents on this position could be profound in terms of efficacy and subtype selectivity, as well as effects on metabolism.

The chiral center at C-4 was significant in the determination of affinity. The different stereochemistry at this position both 4(S) and 4(R) along with various ring sizes (4-6 membered rings) interact differently with the lipophilic pocket L_{Di} thus resulting in very different effects on affinity.

Consequently, analysis of the pharmacophore model revealed that these three positions are preferred for further variations to achieve a better α_4 GABA$_A$R agonist to treat asthma. The structure activity relationship (SAR) studies of the analogs at these positions would facilitate this process.

3.5.2 Proposed New Ligands[17]
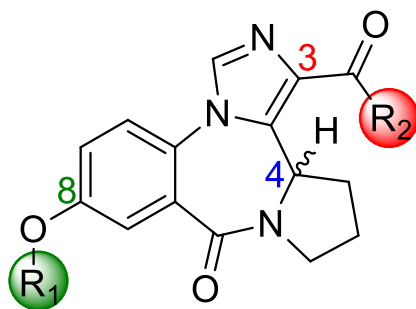
Position C-8: R_1 =
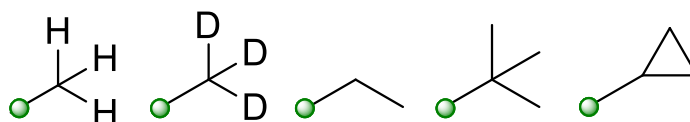
Position C-4: Both (*R*)- and (*S*)-enantiomers

Position C-3: R_2 =
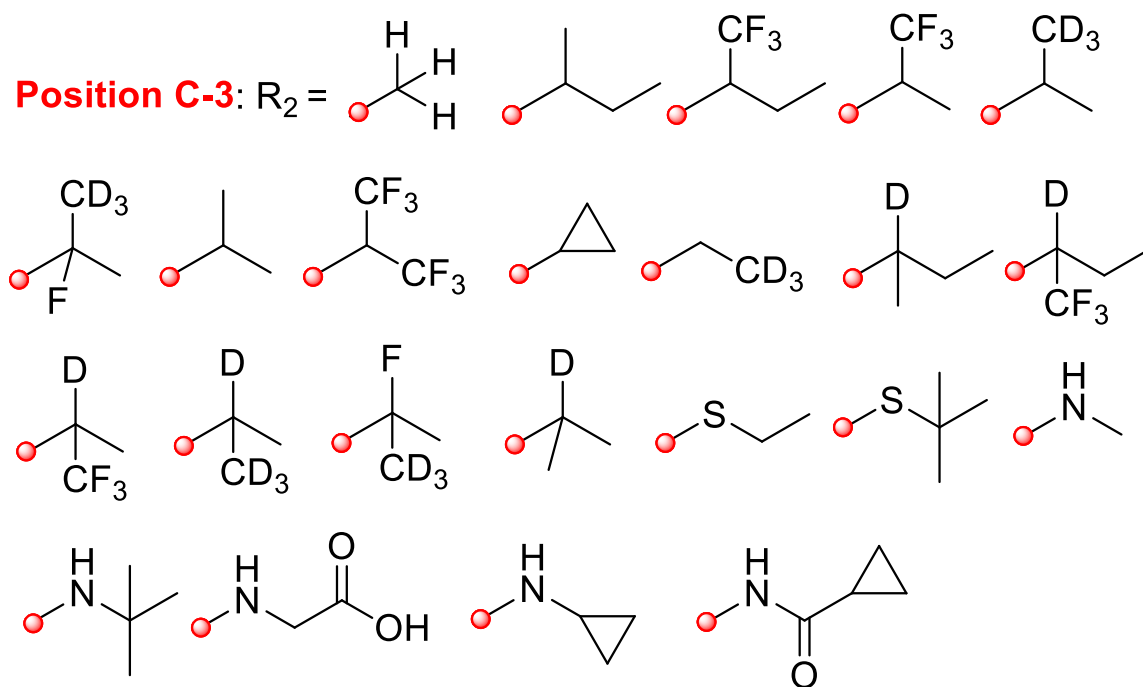
3.6 Synthesis of Novel XHE-III-74 (7) Analogs

3.6.1 Synthesis of Analogs at the C(3) Position of XHE-III-74 (7)

The ethyl ester **5** was saponified to give the acid **9** and this was treated with thionyl chloride to make the corresponding acid chloride. The acid chloride was converted into the amides, esters and thioesters (**11**-**19**) by treating the acylchloride with suitable nucleophiles in the presence of triethylamine to scavenge the HCl which formed. The methyl ester **10** was formed by trans esterification in the presence of NaOMe in methanol.

The chiral esters (**20** and **21**) were prepared via trans-esterification of the ethyl ester with (*R*) and (*S*)-2-butanol. The cyclopropyl ester **22** was prepared from the carboxylic acid **9** with cyclopropyl bromide and Cs_2CO_3 in DMF. The deuterated ethyl ester **23** was prepared from deuterated ethyl bromide and Cs_2CO_3 in DMF.

Scheme 3. Synthesis of C-3 analogs; see experimental for exact details
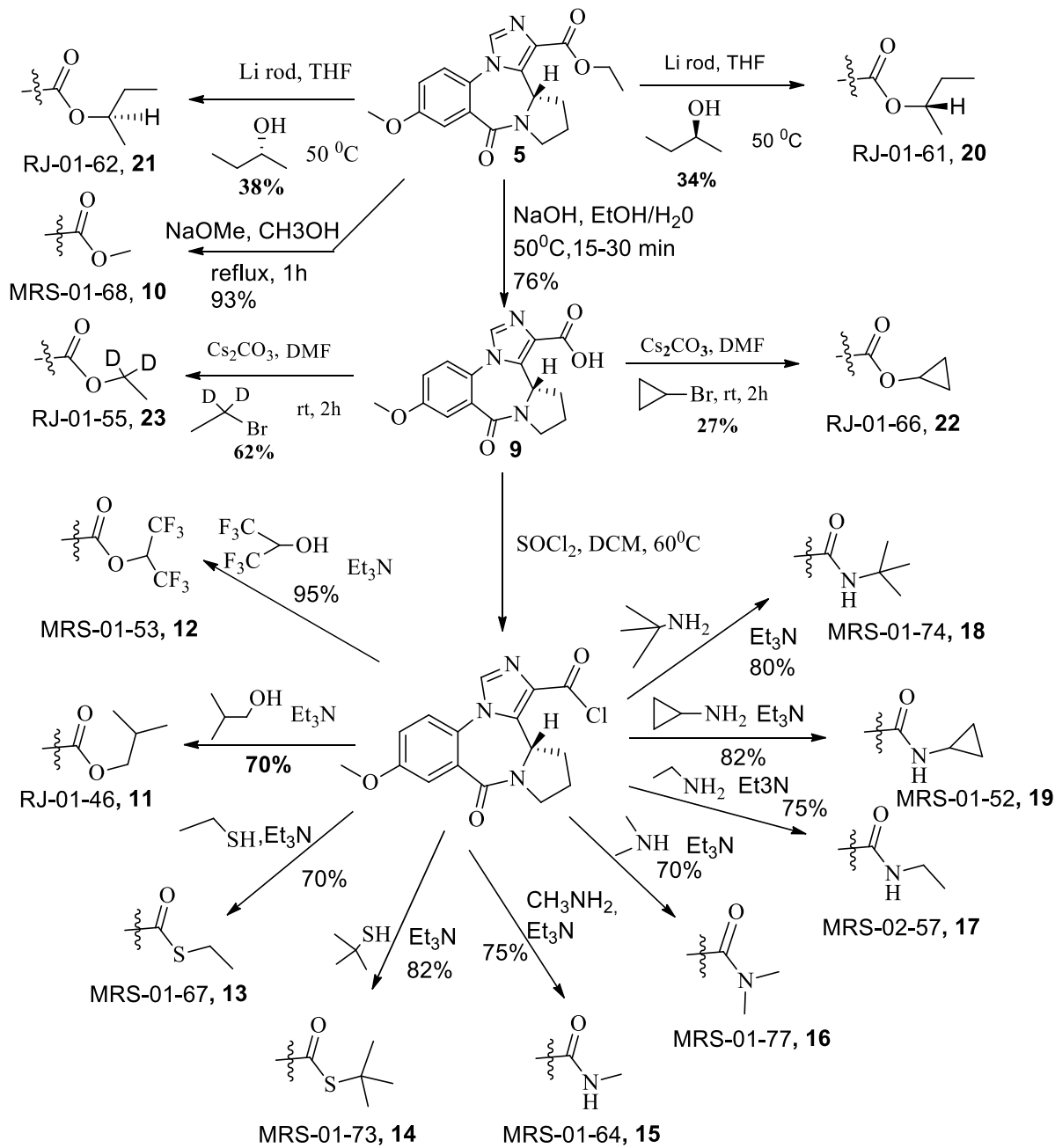
3.6.2 Synthesis of the Analogs of XHE-III-74 (7) at C(4) Position

When the known[16] isatoic anhydride **3** was heated with D-proline in DMSO, the corresponding benzodiazepine **4′** was obtained. This was converted into the imidazodiazepine following the reported procedure to provide the (*R*) enantiomer of XHE-III-74 ethyl ester **5′.** This material was converted into the (*R*) enantiomer of the tert-butyl analog of XHE-III-74 **7′** with a Li rod in ᵗBuOH on multi-gram scale.

Scheme 4. Synthesis of C-4 analog

3

10 g

DMSO
160 °C
4h
90%

D-proline

ᵗBuOK, THF at -20 °C to rt;
(EtO)₂POCl, -20 °C to rt;

CNCH₂CO₂Et, ᵗBuOK, -20 °C to rt
61%

5′
2.5 g

4'

5 g

50 °C
30min
65%

Li rod
THF
t-BuOH

7'

XHE-III-74 (*R*- enantiomer)
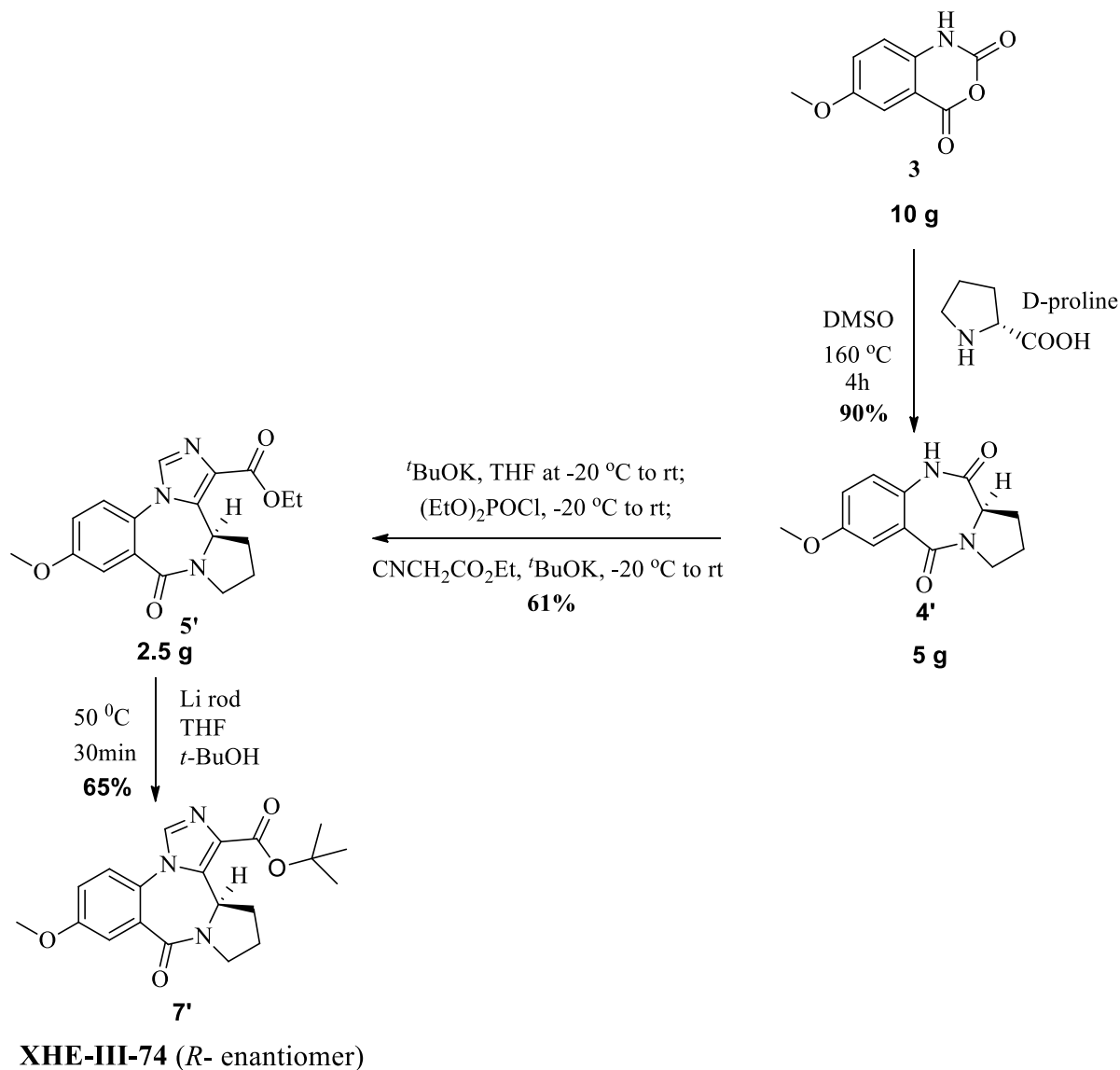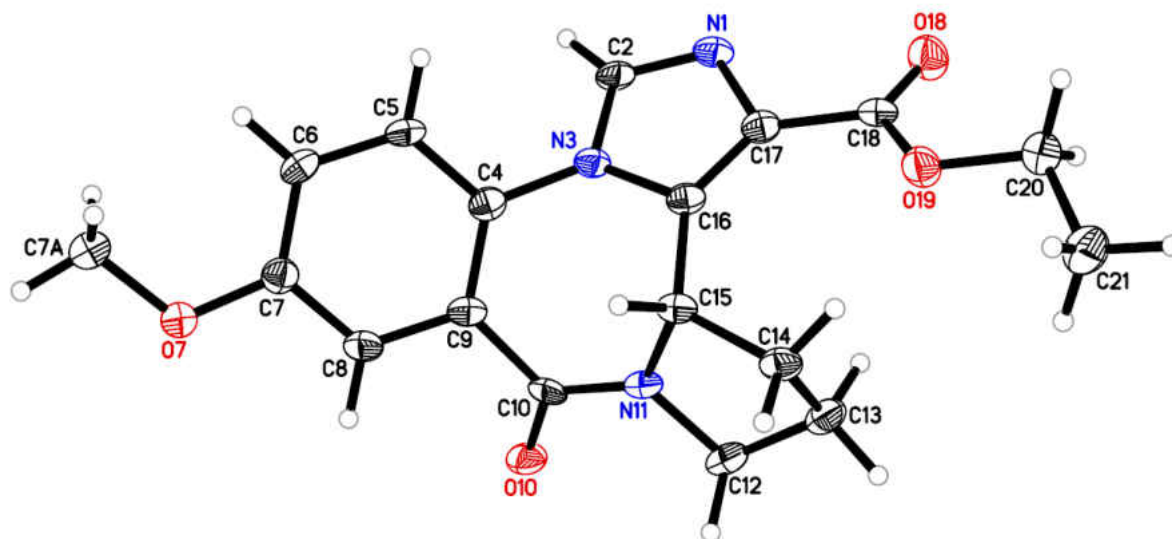
Figure 18. ORTEP representation of XHE-III-74EE(*S* isomer), 5
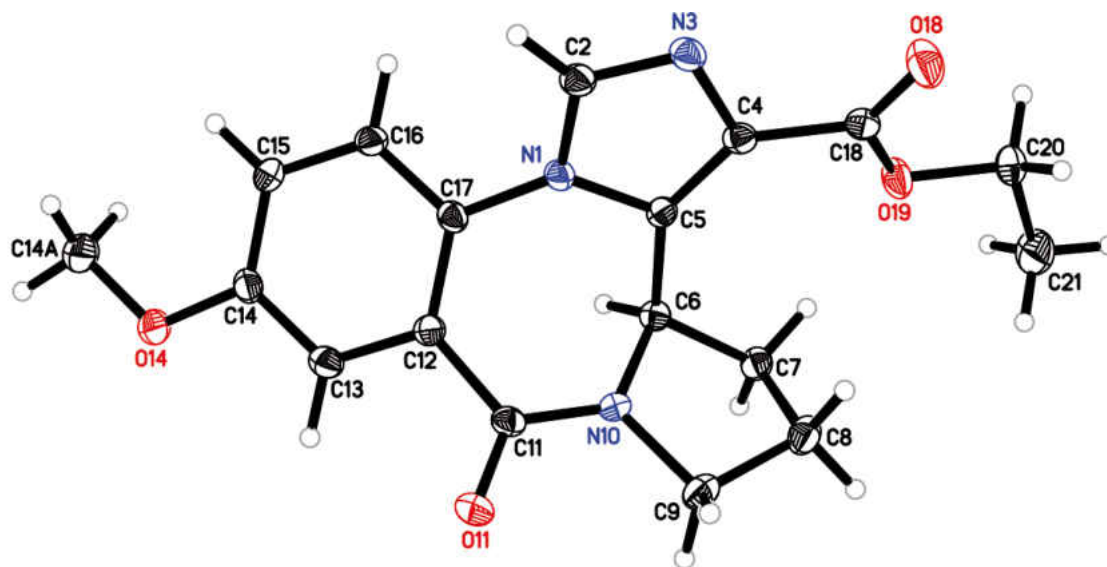
Figure 19. ORTEP representation of XHE-III-74EE (*R* isomer), 5′

53

3.6.3 Synthesis of Analog at the C(8) Position of XHE-III-74 (7)

To optimize compounds for therapeutic use in patients, it is planned to increase metabolic stability *in vivo* and druggability. In addition, it is critical to understand the rate and mechanism of the overall clearance of the molecule. It is certainly more complex when the drug is metabolized by more than one metabolic pathway. As a result, it necessitates the knowledge of the extent of each metabolic pathway involved in the overall metabolism of the molecule. In addition, one would like to know the mechanism of the metabolic enzymes, and whether there should be a kinetic isotopic effect (KIE) in the rate of metabolism and clearance.[166] Incorporation of deuterium into a molecule which exhibits low-to moderate clearance would increase both systemic exposure and bioavailability (half-life). In contrast, introduction of deuterium into a metabolically fragile molecule would only increase their systemic exposure but not the half-life.[166] The carbon-deuterium (C-D) bond is approximately 9 times stronger than carbon-hydrogen (C-H) bond.[167] As a result, the metabolic stability of compounds which contain the C-D bond at a key metabolic position would be expected to be greater than that of compounds which contain a C-H bonds.[166] This does not hold true in every case, for sometimes blocking the metabolism with the C-D substituents leads to a different metabolic pathway and a toxic metabolite. The OCH_3 group at C-8 is susceptible to metabolic action; cleavage of the C-H bond would give the more polar phenolic (OH) ligand, which in turn could be excreted from the body via conjugation to the glucuronide on second pass metabolism and excretion. Thus, replacing the OCH_3 group with an OCD_3 group would be expected to improve the pharmacokinetics of the potential drug for the treatment of asthmatics.
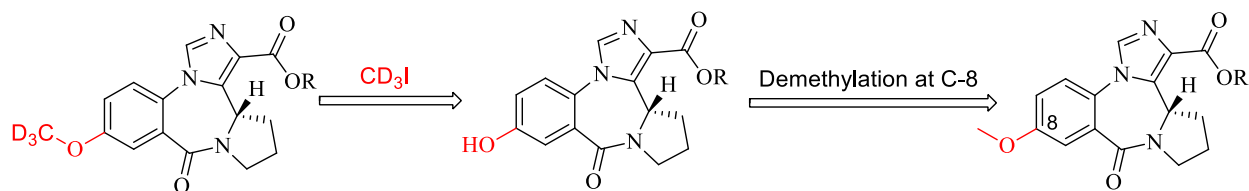
Figure 20. Retrosynthesis of C-8 deuterated analogs *via* demethylation followed by deutero methyl-alkylation

In the case of the C-8 OCD_3 analogs of XHE-III-74, it was felt it was more practical to incorporate the deuterated methoxy function into ring-A at the end of the synthetic route instead of carrying the OCD_3 substituent through the entire route because of the expense of CD_3I. Instead, the OCH_3 version was felt to be more appropriate if a facile method of conversion of the 8-methoxy group into a phenolic function was available. The methoxy function would be easily substituted for by the deuterated methoxy function simply by de-methylation of XHE-III-74 to give the phenol, followed by re-methylation of the phenol with CD_3I (Figure 10). Although an aryl-methoxy function is a robust protecting group for phenols, numerous deprotection methods have been reported.[168-170]

A number of methods were available and screened to find a suitable reagent for this essential transformation (Scheme 5). Surprisingly, most of the known reagents that have been reported as facile for this transformation either did not furnish the phenol or furnished it in trace amounts and/or accompanied by decomposition of the starting material.

The lithium chloride-dimethylformamide combination (Krapcho conditions) has been used as a mild method for the demethylation of aryl-alkyl ethers.[169,171-174] When the desired demethylation was attempted using LiCl in DMF under thermal and microwave irradiation, no product was detected. Introduction of additives such as NMP and *p*-TSA were not successful as well.

Boron tribromide (BBr₃)-mediated demethylation of an aromatic methoxy function is the most common and popular method.[175-177] Besides, BBr₃ mediated demethylation is a milder condition and can be carried out in the presence of sensitive functional groups.[169] This method has been employed in the total synthesis of a number of natural products.[178-184] Consequently, BBr₃ was employed to perform the desired transformation. It was realized, after numerous trials with BBr₃ under many different conditions that the OCH₃ function in XHE-III-74 was surprisingly resistant to BBr₃-mediated cleavage and this lead ligand failed to undergo the desired transformation.

Scheme 5. Attempted demethylation of the C-8 OCH₃ functional group under different conditions
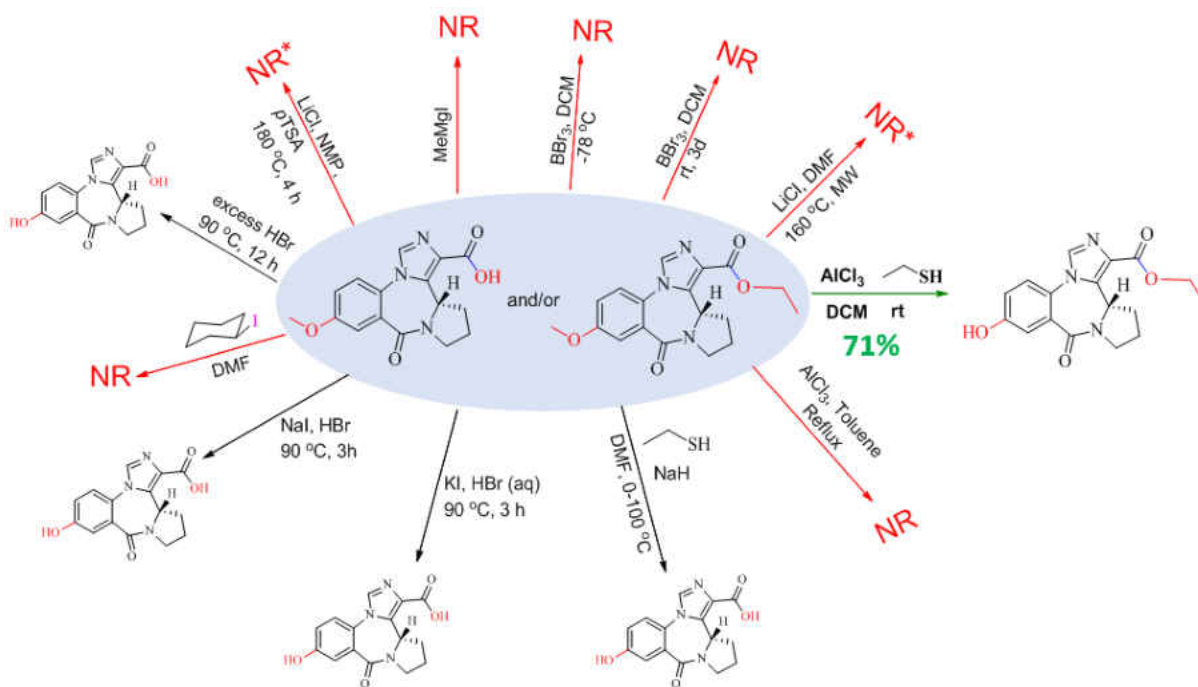
NR: No reaction, SM recovered; NR*: No reaction with decomposition

Demethylation of aryl methyl ethers using Lewis acids such as $AlCl_3$ to furnish phenols have been well studied and reported.[185-189] A number of phenolic natural products have been accessed employing this method of demethylation.[189-191] Consequently, the desired transformation was attempted using aluminum chloride at low temperature and this was followed by heating to elevated temperature. Upon repeated attempts in refluxing toluene for longer times, the demethylation process failed to furnish any demethylated product. Only the starting methyl ether was recovered.

Methyl magnesium iodide[192-194] has been successfully employed in the total synthesis of several phenolic natural products for cleavage of aryl methyl ethers in high yields. Upon heating the aryl methyl ether starting material in the presence of MeMgI at 160 °C, this process failed to perform the desired transformation.

Strong acids such as HI and HBr have been reported for the dealkylation of aryl alkyl ethers.[169,170,195,196] Although such harsh conditions are not generally desired for most substrates these have been successfully employed in many cases.[197] Using strong hydrogen halide acid such as HI may result in decomposition of most heterocyclic organic compounds. To avoid exposure of the substrate to a high concentration of HI, reagents that slowly release HI upon heating could be a useful way around problems with decomposition.[195] Iodoalkanes are able to release HI slowly via an elimination process upon heating, which has been used to perform the desired demethylation in high yields in several cases.[198-201] Iodocyclohexane in DMF under reflux conditions was reported to generate HI in situ and performed demethylation or aryl methyl ethers in high yield.[195] Consequently, the aryl methyl ether was heated in the presence of iodocyclohexane in DMF but this method failed to facilitate the desired transformation, as well. On the contrary, treatment with an excess of aqueous HBr[195,202] both in the presence or absence of KI or NaI as an additive did

cleave the desired methyl ether but also cleaved the ester function, as well. This process was further complicated by the decomposition of the material since only trace amounts of demethylated phenolic carboxylic acid were isolated.

Sodium ethanethiolate in aprotic solvents such as DMF has been reported to be an efficient dealkylating reagent for aryl alkyl ethers.[169,203,204] Upon treatment of the methyl ether starting material with ethanethiol and sodium hydride in DMF at 0-100 °C. This process resulted in cleavage of the ether function, accompanied by the cleavage of the ester function. In addition, only a small amount of product could be isolated which turned out impractical for the synthesis of the desired phenol, as well.

The combination of a hard acid with a soft nucleophile has been reported to be successful in an efficient deprotection of aryl methyl ethers.[190,196,205-208] Aluminum chloride in the presence of ethanethiol is such a combination. If desired, the stench associated with low molecular weight thiols could be avoided by using long chain thiols such as 1-dodecanethiol.[206]

Gratifyingly, at last, the mixture of aluminum chloride and ethanethiol was found to be the only effective method among the methods and reagents screened for this transformation on this particular substrate, to date. The mixture of $AlCl_3$, EtSH in DCM at rt furnished the desired phenolic compound in >70% isolated yield (>85% based on recovered SM).

After the successful demethylation of the aryl-methyl ether, re-alkylation with CD_3I under standard conditions failed to furnish the 8-CD_3 substituted analog **5a**. For example, methylation of phenols with CH_3I in the presence of K_2CO_3 or Cs_2CO_3 in DMF is well known. But in this case the reaction process with Cs_2CO_3 and CD_3I in DMF provided only a trace amount of the analog, while K_2CO_3 in DMF furnished the 8-OCD_3 ligand only in a mediocre yield of 43% (Scheme 6). Other bases;

e.g., NaH, ^{t}BuOK and solvents e.g., DCM, THF, acetone were also attempted (Table 3). Gratifyingly, Cs_2CO_3 in DCM was found to be the best combination, which furnished the desired deuterated analog in a clean 84% yield ending a long-standing deadlock for the synthesis of this important 8-OCD$_3$ ethyl ester target **5a**. It was felt this deuterated analog **5a** would have more desirable metabolic properties required for a better drug candidate for asthma. This was based on the long-standing research on the metabolism of aryl methoxy groups to phenols for later conjugation and excretion.

Scheme 6. Successful access to the C-8 OCD$_3$ variant of XHE-III-74EE 5a
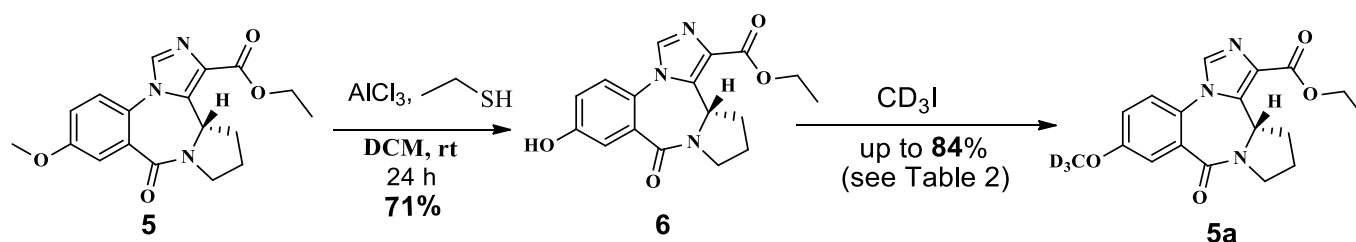
Table 3. Alkylation of the C-8 phenolic function of 8-hydroxy ethyl ester 6 under different conditions

Base	Solvent	Isolated Yield[a]
K_2CO_3	DMF	43%
K_2CO_3	DCM	50%
K_2CO_3	Acetone	45%
NaH	THF	40%
^{t}BuOK	THF	Trace
Cs_2CO_3	DMF	Trace
Cs_2CO_3	DCM	84%

a: SM recovered; all reactions were carried out at rt

The ester **5a** was converted into its *tert*-butyl analog **7a** *via* trans esterification (Li rod in ^{t}BuOH) in good yield. Additionally, the corresponding methyl ester **10a** was readily available in excellent yield by reacting **5a** with NaOMe in methanol. The carboxylic acid **9a** was also prepared from **5a** by saponification and this was followed by acidification in excellent yield. The deuterated acid **9a** was employed as the starting point for the synthesis of the corresponding deuterated versions (**11a-19a**) of **11-19** employing the same procedure as described in Scheme 3 (Scheme 7).

In addition, phenol **6** was also converted into its tert-butyl analog **8** via *trans*-esterification with lithium pieces in the presence of *tert*-butanol in THF at 50 ^{o}C (Scheme 8).

Scheme 7. Synthesis of C-8 deuterated analogs 10a-19a
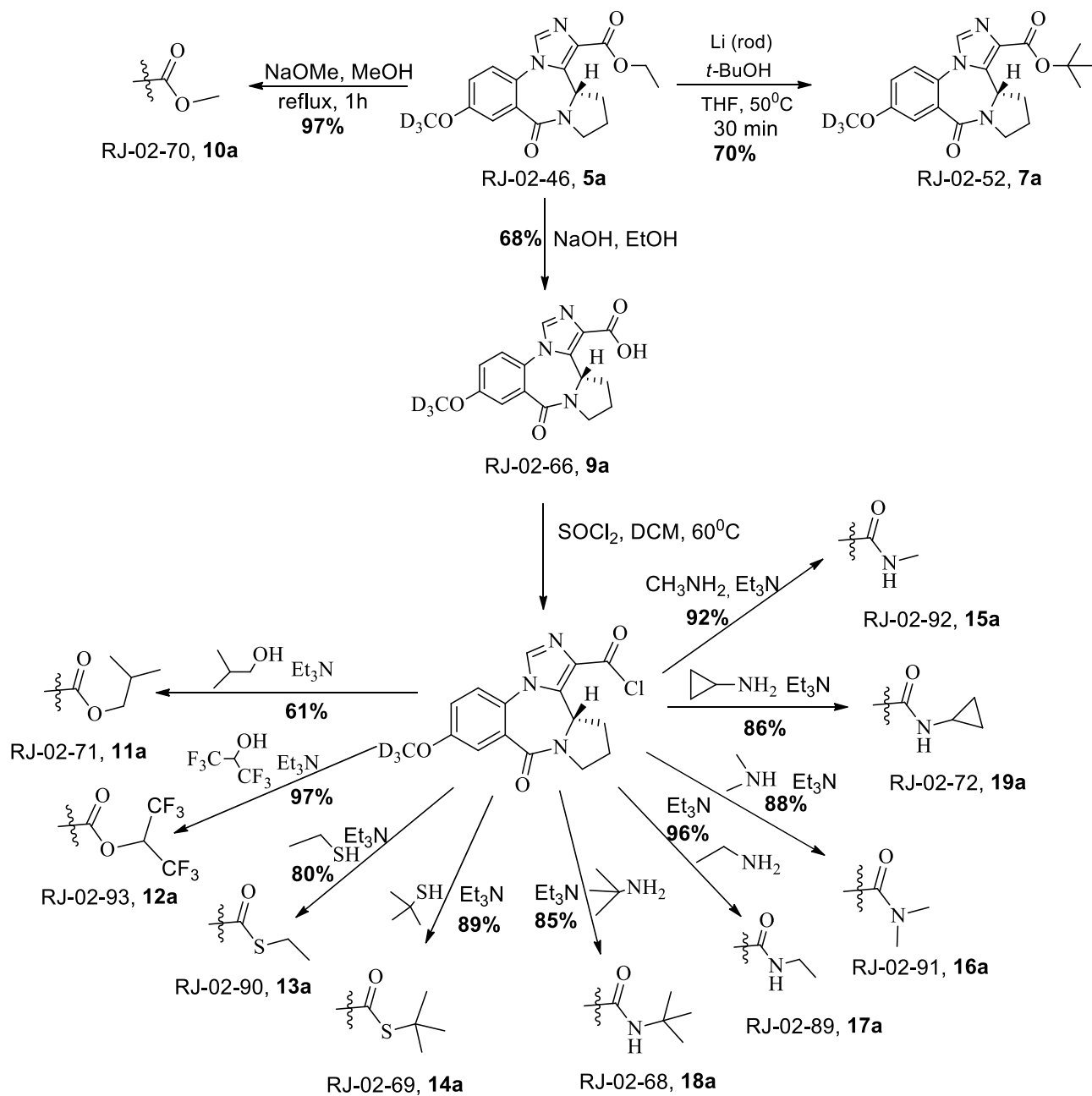
Scheme 8. Preparation of C-8 phenolic XHE-III-74 (RJ-02-67, 8)
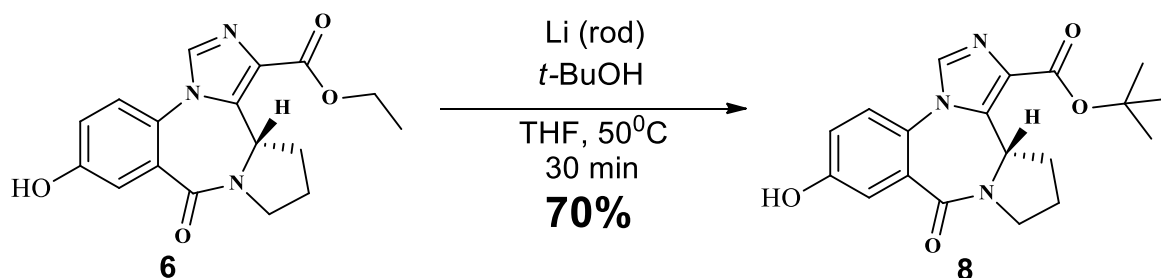
3.7 Biological Evaluation of Analogs of XHE-III-74 Derivatives

Earlier, Forkuo et al illustrated in *ex vivo* organ bath experiment that XHE-III-74 **7** was capable of inducing relaxation in precontracted ASM in mice. In addition, *in vivo* aerosol administration of XHE-III-74 **7** could reduce lung resistance in a house dust mite (HDM) mice model of asthma.[2,15] These encouraging results lead to further evaluation of XHE-III-74 **7** including evaluation of in vitro and in vivo metabolic stability and ability in vivo to relax ASM in the lung.

3.7.1 In vitro Microsomal Stability of XHE-III-74 (7) and XHE-III-74EE (5), and XHE-III-74A (9)[15]

The metabolic stability of XHE-III-74 **7** was investigated in vitro prior to the evaluation of its effectiveness in the reduction of methacholine-induced resistance in mouse lungs. The XHE-III-74 **7** and two related compounds XHE-EE **5**, and XHE-acid **9** were incubated for 1 h with human liver microsomes (HLM) and mouse liver microsomes (MLM), the metabolism of which was monitored by mass spectroscopy on a LCMS. The metabolism of XHE-III-74 **7** was much faster

in MLM, as you would expect, than HLM, which had 24.1% and 92.1% remaining after 1 hour, respectively. This corresponds to the half-life of XHE-III-74 **7** in MLM to be less than 24 min. The ethyl ester version of XHE-III-74 (XHE-EE) **5** was much more stable than XHE-III-74 **7** itself both in HLM (99.2% remaining after 1 h) and MLM (86.3%), as well as in the respective S9 liver fractions (95.6% and 98.4% in MLM and HLM S9, respectively). This corresponded to a predicted half-life of several hours (Table 4). The metabolite of XHE-III-74 was identified by mass spectroscopy as the corresponding carboxylic acid **9**. Consequently, the carboxylic acid derivative XHE-III-74A **9** was also evaluated for microsomal stability against both HLM and MLM and their corresponding S9 liver fractions. Just like the parent ligand, in the case of XHE-III-74A **9** too species-specific metabolism was not observed and acid **9** was found to be metabolized faster than ester **5** both in HLM and MLM with the % remaining, after 1h of 56.1 ± 0.6 % and 51.3 ± 0.4 %, respectively (Table 4). The half-lives of acid **9** and ester **5** were 80.1 ± 10.1 min and 73.4 ± 6.5 min in HLM and MLM, respectively. Similar metabolic stability was also observed in the corresponding S9 fractions. Interestingly, the acid **9** was metabolized faster than XHE-III-74 **7** in HLM but in MLM the acid was twice as stable than XHE-III-74 **7** (Table 4). Both ester **5** and acid **9** were stable in blood plasma for at least one hour. To further confirm the metabolic stability of XHE-III-74EE *in vivo*, a single dose (5 mg/kg i.p. administration) pharmacokinetics study was performed in mice (Figure 21A).

Table 4. In Vitro Metabolic Stability of XHE-III-74 (7), XHE-III-74EE (5), and XHE-III-74A (9)[15]

	XHE-III-74	XHE-III-74EE	XHE-III-74A
human liver microsomes % remaining after 1 h	92.1 ± 1.0	99.2 ± 0.15	56.5 ± 0.6
mouse liver microsomes % remaining after 1 h	24.1 ± 0.7	86.3 ± 0.3	51.3 ± 0.4
human S9 fraction % remaining after 1 h		95.6 ± 0.3	82.5 ± 0.2
mouse S9 fraction % remaining after 1 h		98.4 ± 0.4	64.2 ± 0.2
mouse plasma		92.6 ± 0.2	91.9 ± 0.4

3.7.2 Pharmacokinetic Profiles of XHE-III-74EE (5), and XHE-III-74A (9)[15]

The ester **5** was rapidly absorbed and distributed in blood and lung with a T_{max} of 10 and 3 min, respectively with a higher concentration in the blood [$C_{max\ (blood)}/C_{max\ (lung)} > 2$]; $AUC_{(lung)}/AUC_{(blood)} = 0.6$ (Figure 21A). These results confirm good absorption and distribution of ester **5** into the target organ for potential treatment of asthma (lungs). In addition, ester **5** was rapidly metabolized in lung as indicated by the half-life of only 17.6 min. Besides, there was a significant concentration of XHE-III-74EE **5** observed in brain [$AUC_{(brain)}/AUC_{(blood)} = 0.79$] with a longer half-life (36.7 min). This indicated that ester **5** was able to penetrate the BBB and exhibits higher relative stability in the brain. In order to distinguish between clearance (via conjugation) and metabolism of XHE-III-74EE in blood, lung, and brain, the metabolic product XHE-III-74A was quantified (Figure 21B). Interestingly, a quantifiable amount of XHE-III-74A **9** was present only in the blood $AUC_{(74A)}/AUC_{(74EE)} = 0.75$, which indicated that the rate of metabolism of

XHE-III-74EE **5** in blood is much faster than the rate of excretion of XHE-III-74A **9**. Since, XHE-III-74EE **5** is stable in blood plasma, the metabolism is likely to occur in the liver much like the anxiolytic ethyl ester XHE-III-053, as observed by BMS in human patients. On the other hand, since XHE-III-74A **9** was not found in a quantifiable amount in brain and lung, there may not be any metabolism of XHE-III-74EE **5** taking place in these organs. When a similar pharmacokinetic study (5 mg/kg) was performed on XHE-III-74A **9**, it underwent a rapid absorption and distribution similar to XHE-III-74EE (T_{max} 10 min, Figure 21C). Comparable AUC values of XHE-III-74A **9** in blood and lung were observed, which indicated excellent distribution of XHE-III-74A **9** in lung tissue. In this case as well, the half-lives in lung and blood were 11.0 and 13.1 min, respectively, which indicates rapid clearance of XHE-III-74A **9** from both lung and blood. Unlike, XHE-III-74EE **5**, XHE-III-74A **9** was present at a very low concentration in the brain which indicated that XHE-III-74A **9** had poor BBB penetration. This negates potential CNS side effects. The high levels of XHE-III-74A **9** were detected in urine, as compared to the brain, upon quantification after 30 min of administration (Figure 21D) as expected. A high concentration of XHE-III-74A **9** in the kidneys supports the hypothesis that most of acid **9** is excreted from the body chemically unaltered. On the other hand, the concentration of acid **9** in the liver was much lower (4% of blood conc.) than other organs which indicated the liver was the probable site of metabolism in this mice model.

A

XHE-III-74EE

	Blood	Lung	Brain
C_{max} (ng/ml)	216.9	120.7	84.8
T_{max} (min)	10	3	40
AUC (ng*min/ml)	5737	3358	4516
$T_{1/2,E}$ (min)	16.3	17.6	22.9
$T_{1/2,D}$ (min)	6.6	2.2	36.7

Legend: Brain, Lung, Blood

y-axis: ng XHE-III-74EE per g tissue or blood

x-axis: Time (min)
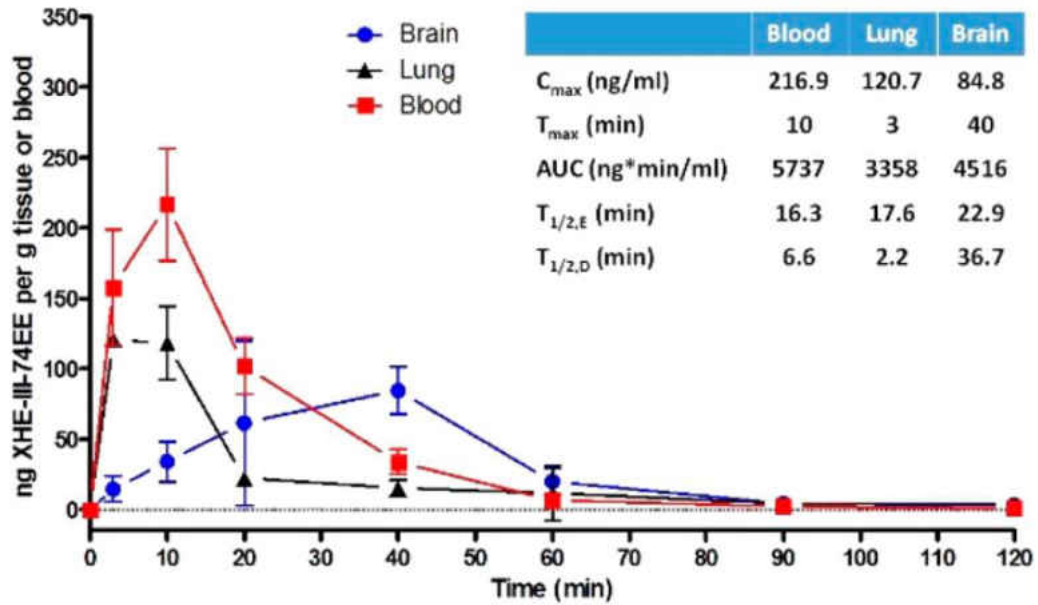
B

XHE-III-74A metabolized from XHE-III-74EE

	Blood
C_{max} (ng/ml)	102.3
T_{max} (min)	10
AUC (ng*min/ml)	4282.3
$T_{1/2,E}$ (min)	11.6
$T_{1/2,D}$ (min)	2.8

Legend: Brain, Lung, Blood

y-axis: ng formed XHE-III-74A per g tissue or blood

x-axis: Time (min)

C

XHE-III-74A

	Blood	Lung	Brain
C_{max} (ng/ml)	269.3	136.4	2.3
T_{max} (min)	10	10	3
AUC (ng*min/ml)	5332	5257	52.8
$T_{1/2,E}$ (min)	13.1	11.0	13.1
$T_{1/2,D}$ (min)	9.3	3.9	0.9

D

XHE-III-74A (30min)
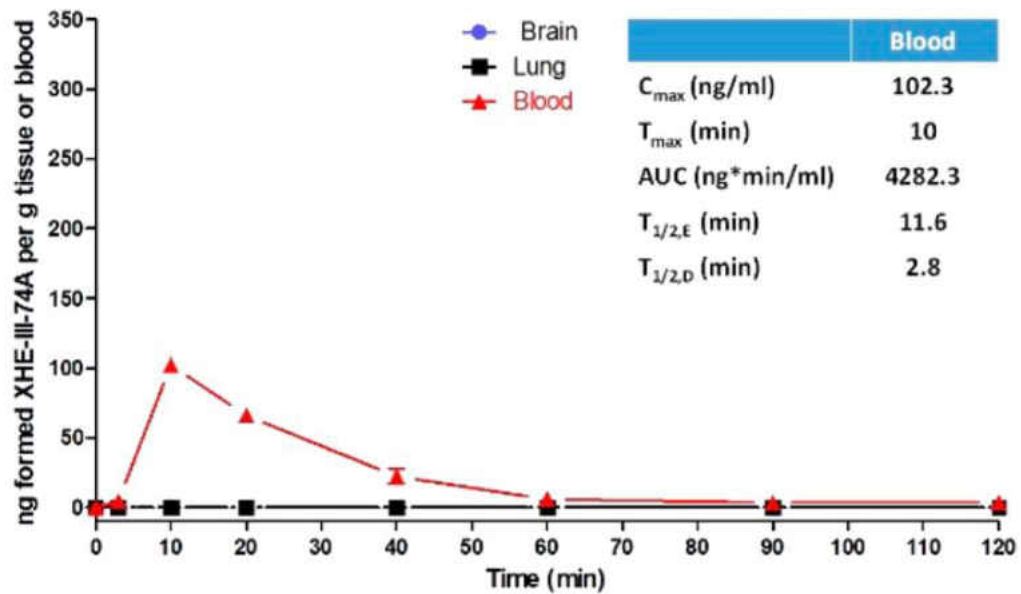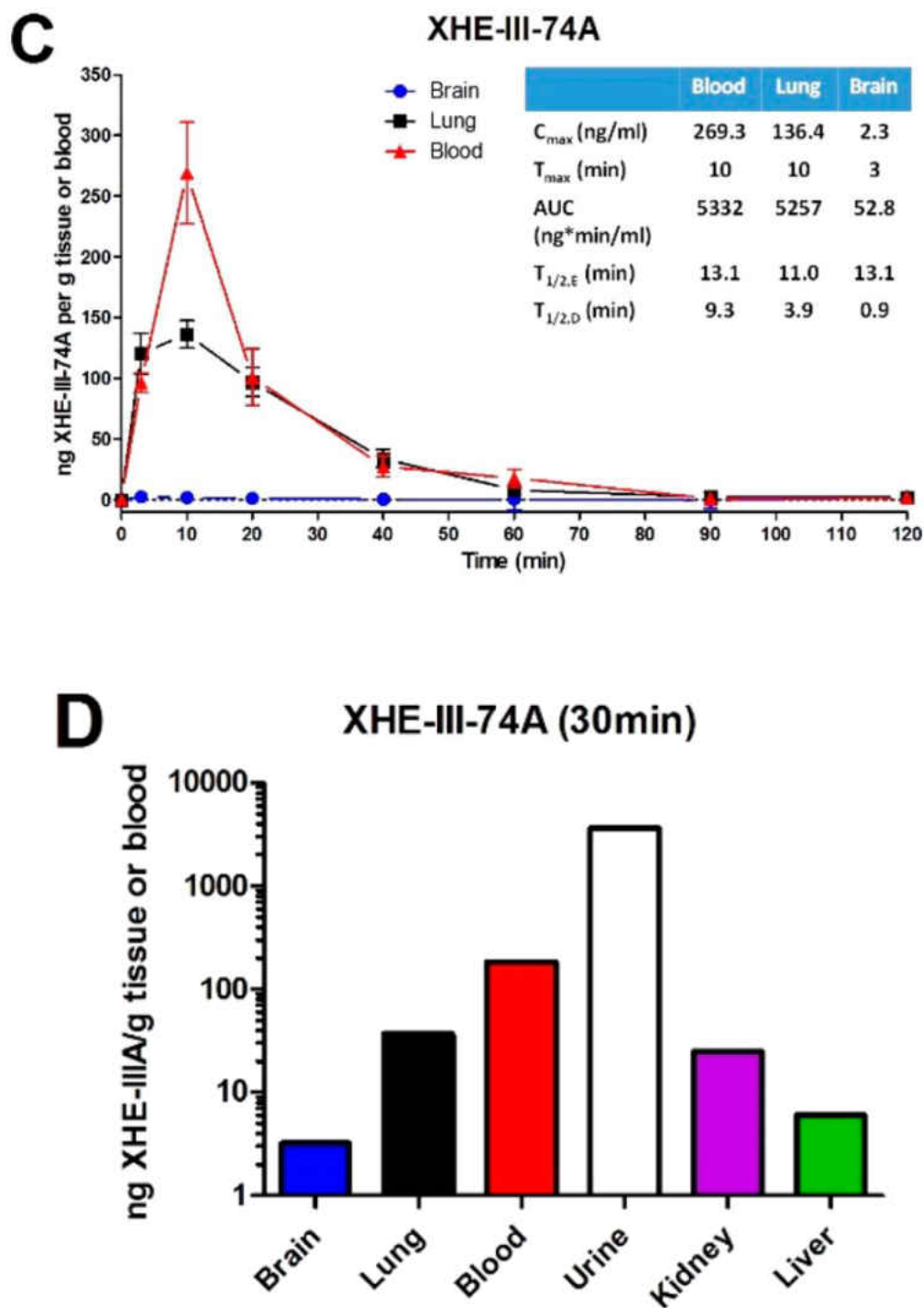
Figure 21. Pharmacokinetic profile of XHE-III-74 EE and XHE-III-74A in mice brain, lung, and blood (N = 3). (A) Time-dependent distribution of XHE-III-74EE (5 mg/kg, i.p.). (B) Time-dependent distribution of metabolite XHE-III-74A given as XHE-III-74EE (5 mg/kg, i.p.). (C) Time dependent distribution of XHE-III-74A (5 mg/kg, i.p.). (D) Distribution of XHE-III-74A (5 mg/kg, i.p.) at 30 min in different tissue and fluids (N =1). Modified from the figure in Gloria, et al.[15]

67

3.7.3 Oocyte Efficacies of XHE-III-74EE 5 and XHE-III-74A 9[15]

Ligand ester **5** is known as an $\alpha_4\beta_3\gamma_2$ subtype selective GABA$_A$R allosteric modulator with weak activity at the $\alpha_6\beta_3\gamma_2$ GABA$_A$R at >1 μM concentration.[209] The efficacy of acid **9** was evaluated in oocytes individually expressing single α (α_{1-5}) subunits in combination with β_3 and γ_2 subunits in comparison with XHE-III-74EE (Figure 22). Gratifyingly XHE-III-74A **9** showed significant positive modulatory effects only at the α_4 and α_5 GABA$_A$Rs and was mostly inactive at the α_1, α_2, and α_3 sites. XHE-III-74A showed selectivity biased to $\alpha_4\beta_3\gamma_2$ at a concentration of 3 μM, while it reached a plateau at $\alpha_5\beta_3\gamma_2$.
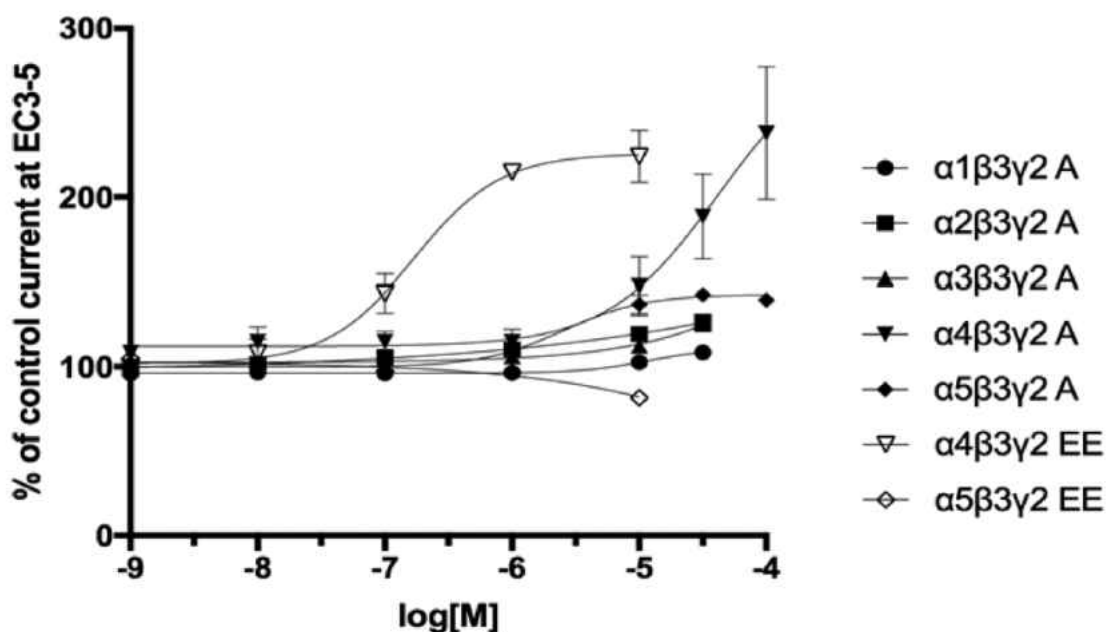
Figure 22. GABA$_A$ receptor subtype selectivity. Dose-dependent modulation of GABA (EC3−5 concentration) elicited currents by XHE-III-74A (A) and XHE-III-74EE (EE) on Xenopus oocytes expressing GABA$_A$ receptor subtypes $\alpha_1\beta_3\gamma_2$, $\alpha_2\beta_3\gamma_2$, $\alpha_3\beta_3\gamma_2$, $\alpha_4\beta_3\gamma_2$, and $\alpha_5\beta_3\gamma_2$. Data points represent means ± SEM from 2−8 oocytes from two batches, normalized to control currents (100%) in the absence of compound. XHE-III-74EE modulation of a set of GABA$_A$R subtypes has been published previously,[27] and only $\alpha_4\beta_3\gamma_2$ and $\alpha_5\beta_3\gamma_2$ are shown here for comparison. XHE-III-74EE modulation of $\alpha_5\beta_3\gamma_2$ GABA$_A$R was measured at GABA EC$_{20}$. Modified from the figure in Gloria, et al.[15]

3.7.4 Sensorimotor Effects of XHE-III-74EE (5) and XHE-III-74A (9)[15]

A rotarod experiment was performed to evaluate the possible CNS side-effects of XHE-III-74EE

5 which results from its ability to cross the BBB (Figure 23). The XHE-III-74EE **5** did not show

any motor sensory impairment at 20 mg/kg while the positive control diazepam induced significant

impairment at 5 mg/kg. However, XHE-III-74EE **5** did exhibit motor impairing effects at 40

mg/kg. On the other hand, XHE-III-74A **9** did not exhibit any sensory motor impairment at 20

mg/kg, as expected, which confirms its inability to travel across the blood brain barrier. There was

no loss of righting response as well.
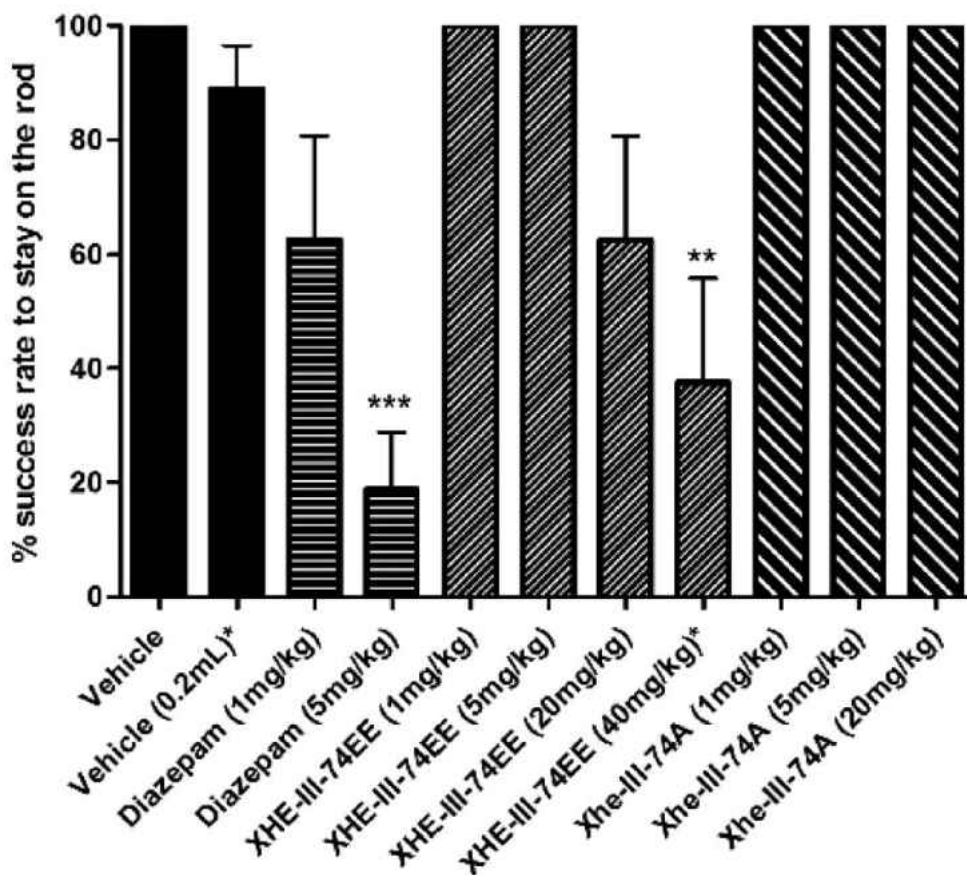
Figure 23. Effect of XHE-III-74EE and XHE-III-74A on sensorimotor coordination. The Balb/c mice were tested on a rotarod at 15 rpm for 3 min. Mice received a single i.p. injection of test compound or control compound. A fail was assigned to a mouse that fell from the rotarod prior to 3 min. The % success rate is expressed as mean ± SEM ($N = 8$). ∗∗, ∗∗∗ indicates $p < 0.01$, $p < 0.001$ significance compared to vehicle-treated mice. Modified from the figure in Gloria, et al.[15]

3.7.5 Effect of XHE-III-74EE (5) and XHE-III-74A (9) on Airway Hyperresponsiveness[15]

Based on the results from the previous experiments, the ligands **5** and **9** were evaluated for their effectiveness in the ovalbumin sensitized mouse asthma model. In this model of asthma, the mice are first sensitized by Ova to establish airway inflammation by i.p. administration, and this was followed by an intranasal challenge, which generated airway hyper-responsiveness (AHR), mucus hypersecretion, and airway inflammation. Both XHE-III-74EE **5** or XHE-III-74A **9** were administered i.p. to primed mice during the Ova challenge phase (chronic repeated dosing) or 40 min (acute) before measuring AHR (Figure 24).

The asthmatic mice exhibited a reduction in methacholine-induced airway hyper-responsiveness after 5 days treatment with XHE-III-74EE (twice daily) of 20 mg/kg doses (Figure 24A). A single dose (10 or 20 mg/kg), however did not reduce AHR (Figure 24B, 24C). Since it was known from previous experiments that XHE-III-74EE **5** is metabolized fast and XHE-III-74A **9** is cleared rapidly, a minipump was implanted surgically to administer the dose over 7 days which results in a steady blood concentration of 27.2 ± 2.7 ng/g on the day of AHR measurement. The pump delivery of XHE-III-74EE **5** was effective in reducing AHR for methacholine concentration up to 6.25 mg/mL. However, at higher doses, no significant AHR reduction was observed (Figure 24D). A similar trend was also observed for the positive control and known anti-inflammatory drug dexamethasone (24E). In addition, acute (20 mg/kg, i.p. 40 min prior to measurement) administration of XHE-III-74A **9** did not result in reduction of methacholine-induced AHR (Figure 24F).
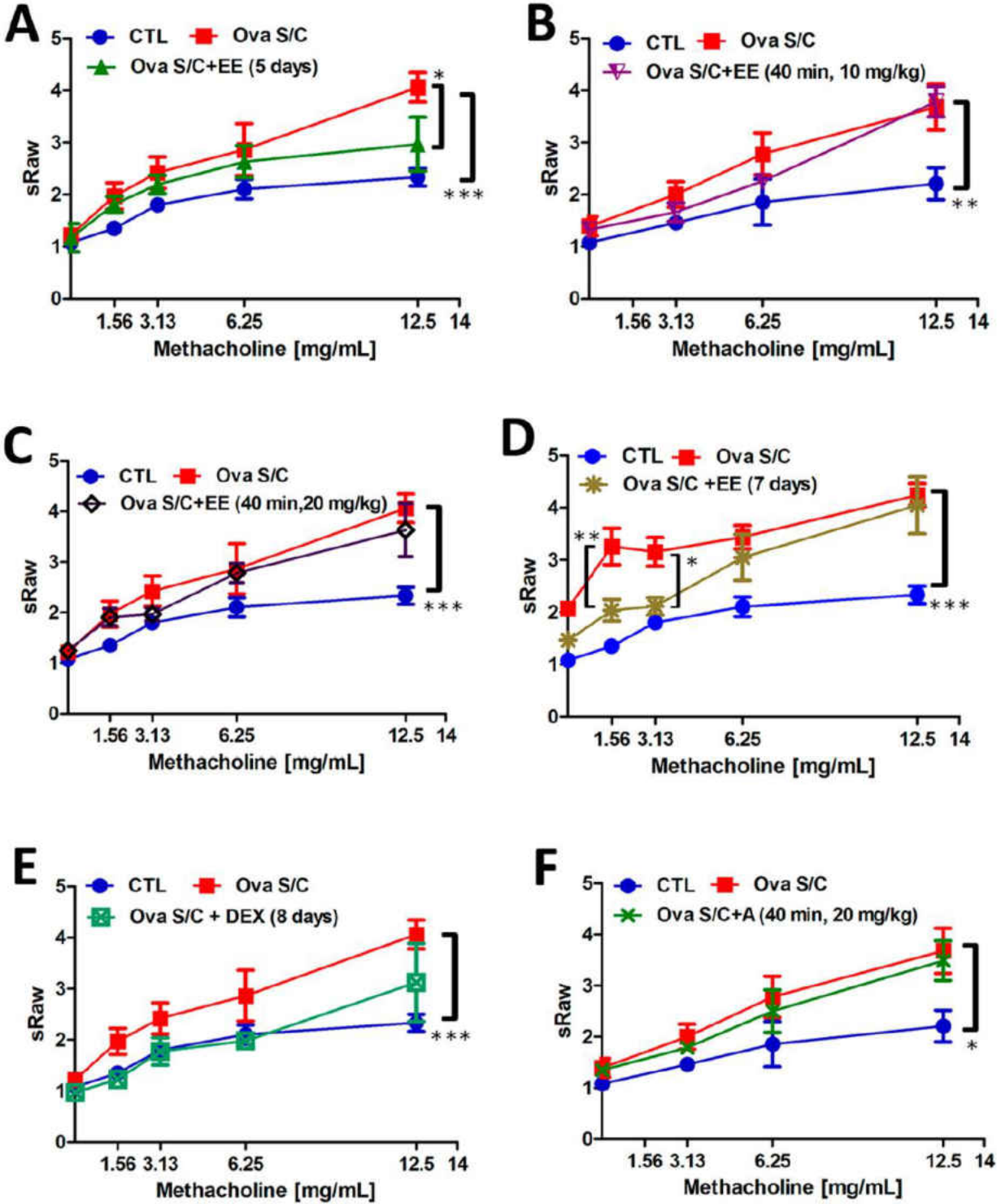
Figure 24. Effect of XHE-III-74EE (EE) and XHE-III-74A (A) on airway hyperresponsiveness. Specific airway resistance (sRaw) to increasing doses of methacholine measured by DSI's Buxco FinePointe noninvasive airway mechanics instrument. Balb/c mice were administered (A) XHE-III-74EE, two 20 mg/kg i.p. injections daily for

5 days; (B) XHE-III-74EE, single i.p. injection 10 mg/kg 40 min prior to analysis; (C) XHE-III-74EE, single i.p. injection 20 mg/kg 40 min prior to analysis; (D) XHE-III-74EE via osmotic pump, 20 mg/kg daily for 7 days; (E) DEX, single 4 mg/kg i.p. injection daily for 8 days; and (F) XHE-III-74A, single i.p. injection 20 mg/kg 40 min prior to analysis. Data represent mean ± SEM from 4−7 mice in each group. ∗, ∗∗, and ∗∗∗ indicate p < 0.05, p < 0.01, or p < 0.001 significance, respectively, compared to vehicle treated Ova S/C Balb/c mice. Modified from the figure in Gloria, et al.[15]

3.7.6 Effects of ligands 5 and 9 on Mucus Hypersecretion[15]

To evaluate and compare mucus hypersecretion in treated and untreated Ova sensitized mice, lung sections were stained with PAFS stain (Figure 25). A significant increase in mucus production was observed in Ova S/C mice. An 8-day treatment with dexamethasone (4 mg/kg, i.p. daily) significantly decreased mucous metaplasia in Ova S/C mice compared to vehicle treated mice whereas, XHE-III-74EE **5** and XHE-III-74A **9** did not induce a noticeable reduction in mucin production both in chronic repeated and acute doses.
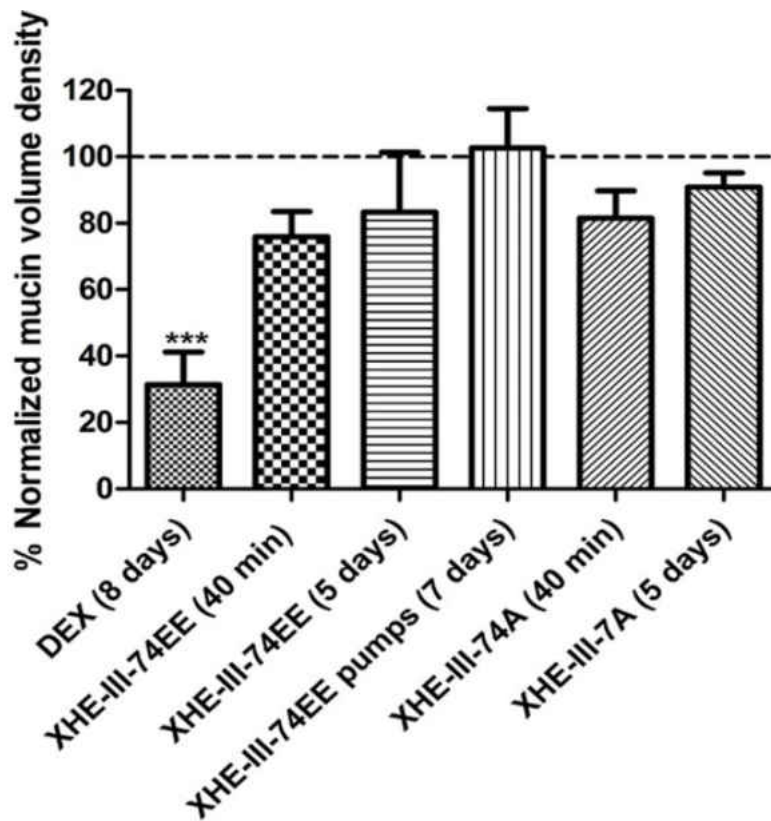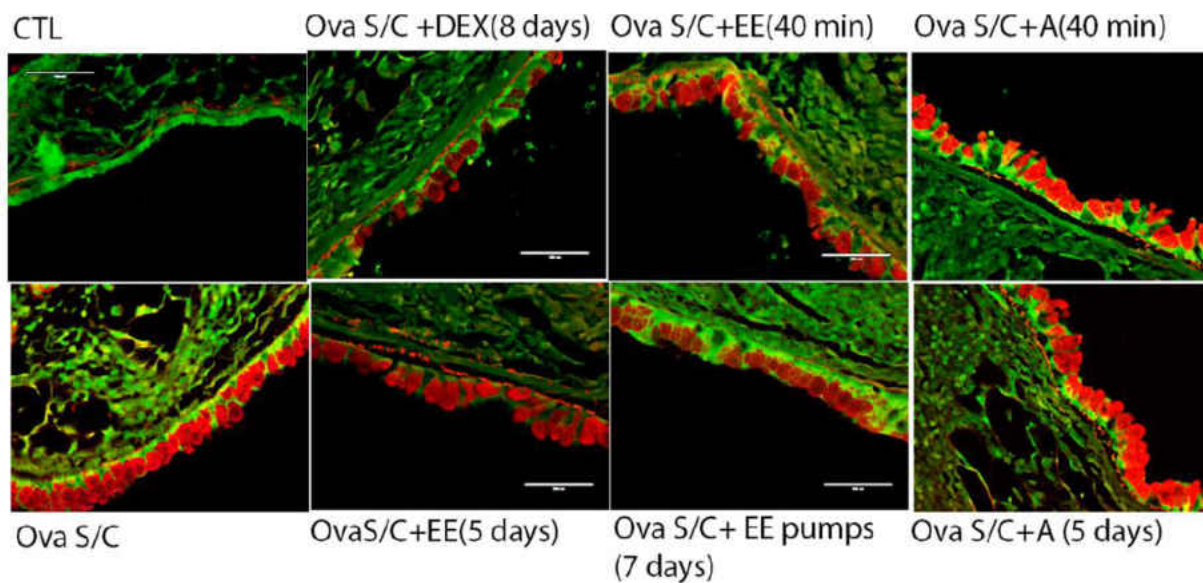
Figure 25. Effect of XHE-III-74EE (EE) and XHE-III-74A on mucin production. (A) Morphometric quantification of mucin volume density and (B) representative images of mucin (red) in the airway epithelium (green) with periodic acid fluorescent Schiff's stain. Balb/c mice were administered once daily 4 mg/kg i.p. DEX (dexamethasone) injections for 8 days, a single 20 mg/kg i.p. injection of XHE-III-74EE 40 min prior to analysis, two XHE-III-74 EE 20 mg/kg i.p. injections daily for 5 days, 20 mg/kg XHE-III-74EE for 7 days via osmotic pump, XHE-III-74 EE single 20 mg/kg i.p. injection 40 min prior to analysis, or two XHE-III-74A 20 mg/kg i.p. injection daily for 5 days. Data represent % normalized mucin volume density relative to CTL and Ova S/C Balb/c mice from 5−7 mice in each group. ∗∗ indicates p < 0.01 significance compared to vehicle treated Ova S/C Balb/c mice. Scale bar represents 100 μm. Modified from the figure in Gloria, et al.[15]

3.7.7 Effect of XHE-III-74EE (5) and XHE-III-74A (9) on Airway Eosino-philia[15]

Additionally, the immune response in the lungs of Ova S/C mice was quantified by collecting the bronchoalveolar lavage fluid (BALF), and this was followed by the quantification of eosinophils (Figure 26).
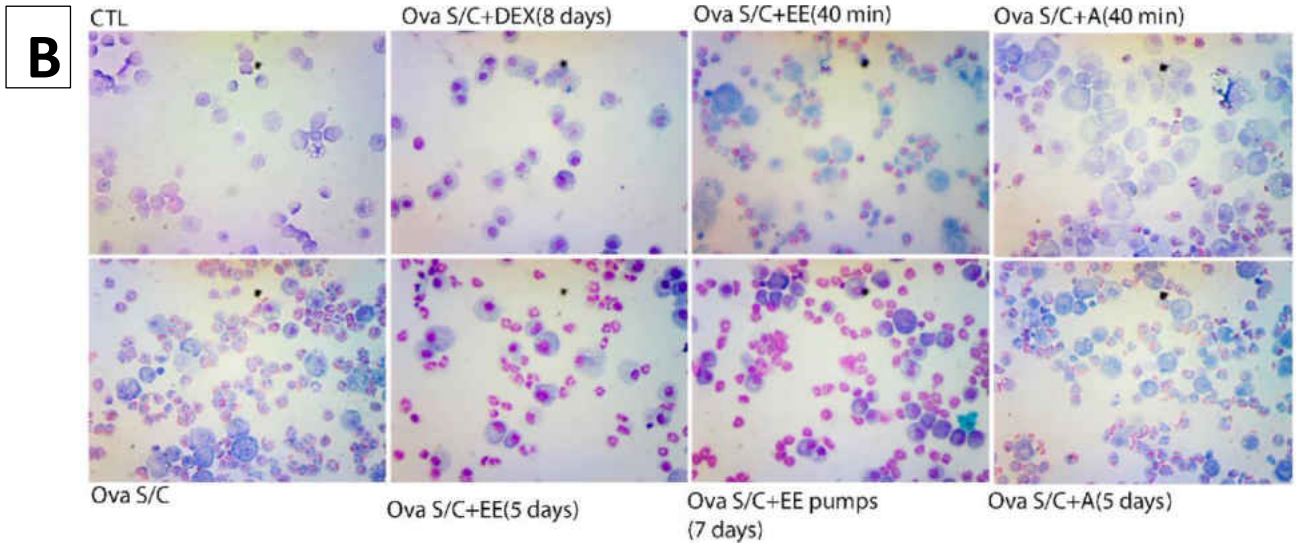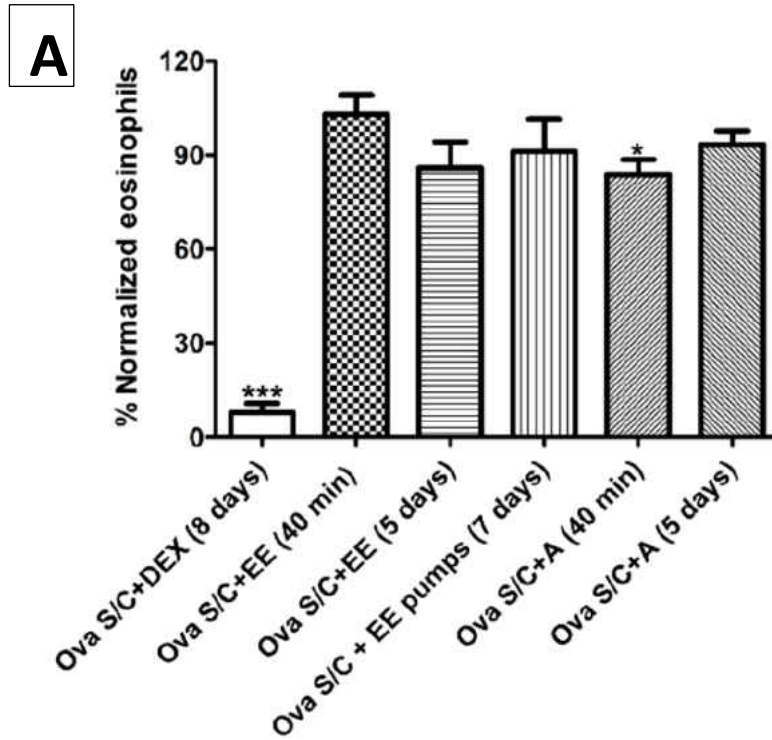
Figure 26. Effect of XHE-III-74EE (EE) and XHE-III-74A (A) on airway eosinophilia. (A) Quantification of airway eosinophilia and (B) representative images of Wright Giemsa stained slides. Balb/c mice were administered single 4 mg/kg i.p. DEX injection daily for 8 days, XHE-III-74 EE single 20 mg/kg i.p. injection 40 min prior to analysis, two XHE-III-74 EE 20 mg/kg i.p. injections daily for 5 days, 20 mg/kg XHE-III-74 EE via osmotic pump for 7 days, XHE-III-74 EE single 20 mg/kg i.p. injection 40 min prior to analysis, and two XHE-III-74A 20 mg/kg i.p. injections daily for 5 days. Data represent % normalized eosinophils relative to CTL (negative control) and Ova S/C Balb/c mice (positive control) from 5−7 mice in each group. ∗ and ∗∗∗ indicate p < 0.05 and p < 0.001 significance compared to vehicle treated Ova S/C Balb/c mice. Modified from the figure in Gloria, et al.[15]

It is known that the Ova asthma model demonstrates mainly eosinophil driven inflammation in the lung.[210] Treatment with the anti-inflammatory agent dexamethasone significantly decreased airway eosinophilia.[211] However, treatment with XHE-III-74EE **5** did not effect any change in airway eosinophilia. In contrast, significant reduction in airway eosinophilia was observed in acute (40 min, i.p., 20 mg/kg) treatment with XHE-III-74A **9**. Although, acid **9** is a metabolite of XHE-III-74EE **5**, the absence of any such effect in the case of acute treatment with XHE-III-74EE **5** was not observed probably because XHE-III-74EE **5** is metabolized in the blood but not in the lung.

3.7.8 Modulation of Immune Response by XHE-III-74EE (5) and XHE-III-74A (9)[15]

To further investigate the direct effect of XHE-III-74EE **5** and its metabolite XHE-III-74A **9** on immune cells, the effects on human Jurkat T-cells was investigated in vitro. The stimulation by phytohemagglutinin (PHA) and phorbol myristate acetate (PMA) resulted in a sudden increase in intracellular $[Ca^{2+}]_i$ and a significant amount of IL-2 production, which can be used for measuring cell activation.[212,213] The natural ligand of the $GABA_AR$ is known to depolarize Jurkat cell plasma membranes where different α-subunits which contain $GABA_ARs$ (including $α_4$) are expressed. The direct effect of GABA is the release of IL-2 in PMA and PHA stimulated Jurkat cells (Figure 27A). The GABA did decrease IL-2 production at 100 nM but was not effective at 1 nM concentration. The XHE-III-74A did reduce IL-2 secretion at 100 pM concentration while XHE-III-74EE did not show IL-2 reduction under the same conditions (Figure 27A).
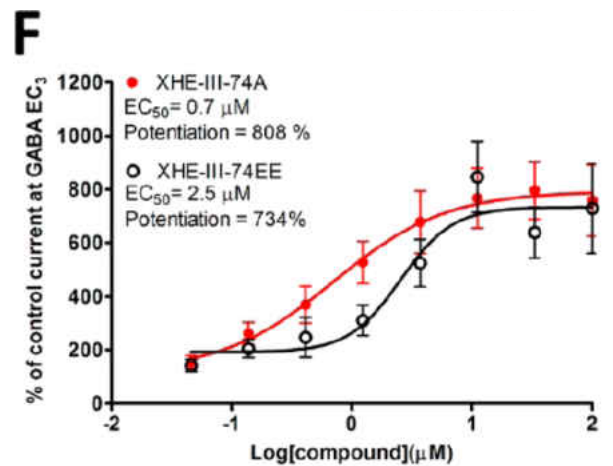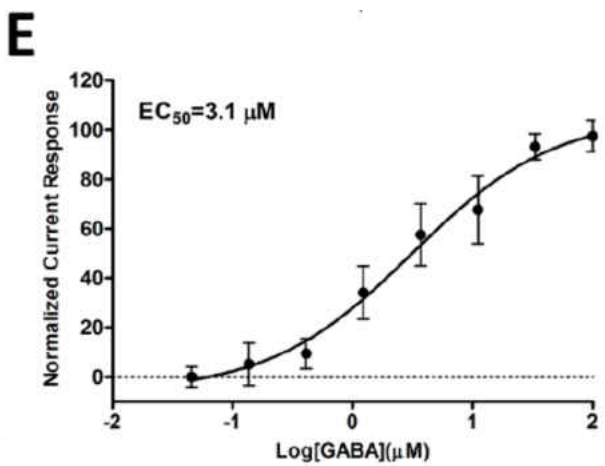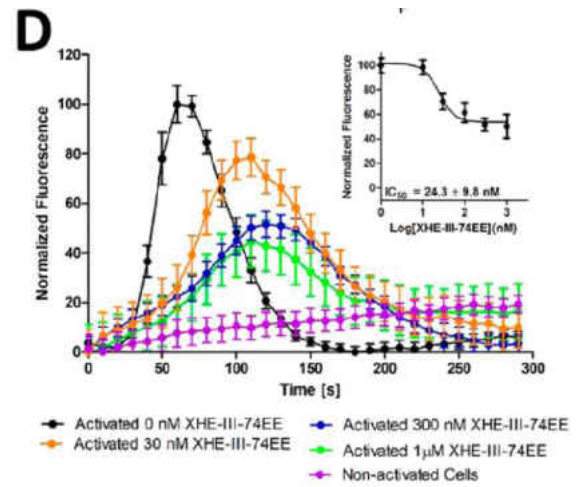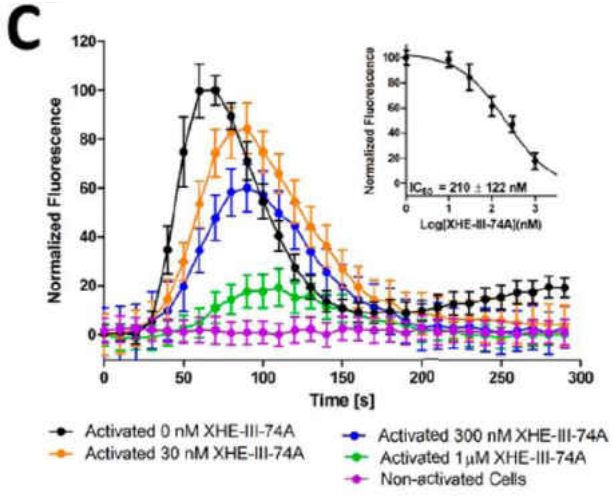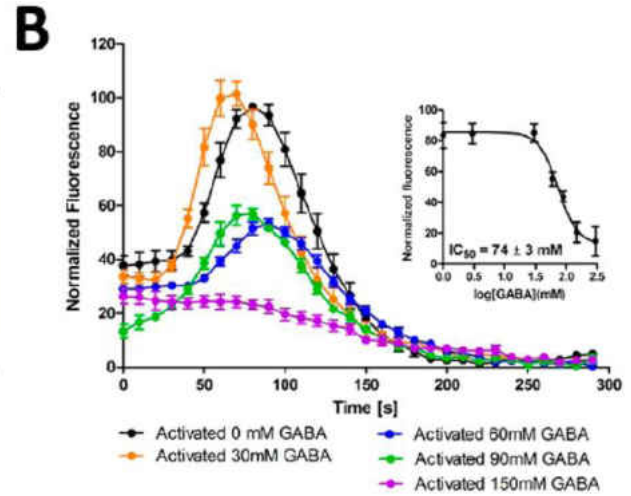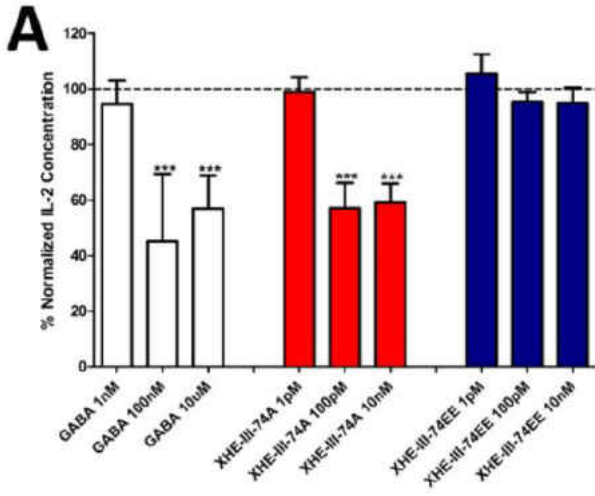
Figure 27. Modulation of immune response. GABA$_A$R ligands inhibit intracellular calcium spike and increased IL-2 production in PMA/PHA stimulated Jurkat cells. (A) IL-2 in the presence of different concentrations of GABA, XHE-74EE, and XHE-74A. (B, C, D) Decrease of [Ca^{2+}]$_I$ concentration in Jurkat cells measured with a cell-permeable fluorescence probe Fluo-4 in the presence of different concentrations GABA, XHE-III-74A, and XHE-III-74EE. (E) Patch-clamped change of Jurkat current response in the presence of GABA. (F) Patch-clamped change of Jurkat current response in the presence of 300 nM GABA and XHE-III-74A and XHE-III-74EE. ∗∗∗ indicates p < 0.001 significance compared to vehicle treated activated Jurkat cells. Modified from the figure in Gloria, et al.[15]

The increment in intracellular Ca^{2+} concentration by GABA and GABAergic ligands in response to PMA and PHA; the Ca^{2+} concentration peaked at 50 s after this PMA/PHA treatment. The GABA did decrease the [Ca^{2+}]$_i$ in a dose-dependent manner and fully suppressed it at 150 mM GABA IC$_{50}$ = 74 ± 3 mM (Figure 27B). In contrast, XHE-III-74A **9** significantly reduced PMA/PHA-induced [Ca^{2+}]$_i$ increase at much lower concentrations, IC$_{50}$ = 210 ± 122 nM (Figure 27C). XHE-III-74EE, on the other hand, caused only partial inhibition of the PMA/PHA induced increase in [Ca^{2+}]$_i$, IC$_{50}$ = 24.3 ± 9.8 nM (Figure 27D).

GABA has been reported to depolarize human jurkat T-cells at 100 μM concentration. The GABA level showed a dose-dependent effect on jurkat cell membrane current with EC$_{50}$ = 3.1 μM (Figure 27E). In the presence of GABA (EC$_3$ conc.) and the positive modulator XHE-III-74EE **5**, a significant dose-dependent change of current was observed. A GABA-induced current potentiation of 734% and 808% was observed with XHE-III-74EE **5** (EC$_{50}$ = 2.5 μM) and XHE-III-74A **9** (EC$_{50}$ = 0.7 μM, Figure 27F), respectively.

3.7.9 Relaxation of Pre-Contracted Guinea Pig ASM by XHE-III-74 (7), XHE-III-74EE (5), and XHE-III-74A (9)[15]

In ex vivo organ bath experiments on pre-contracted (by substance P) guinea pig tracheal rings XHE-III-74 **7**, XHE-III-74EE **5**, and XHE-III-74A **9** eicited relaxation of ASM (Figure 28).
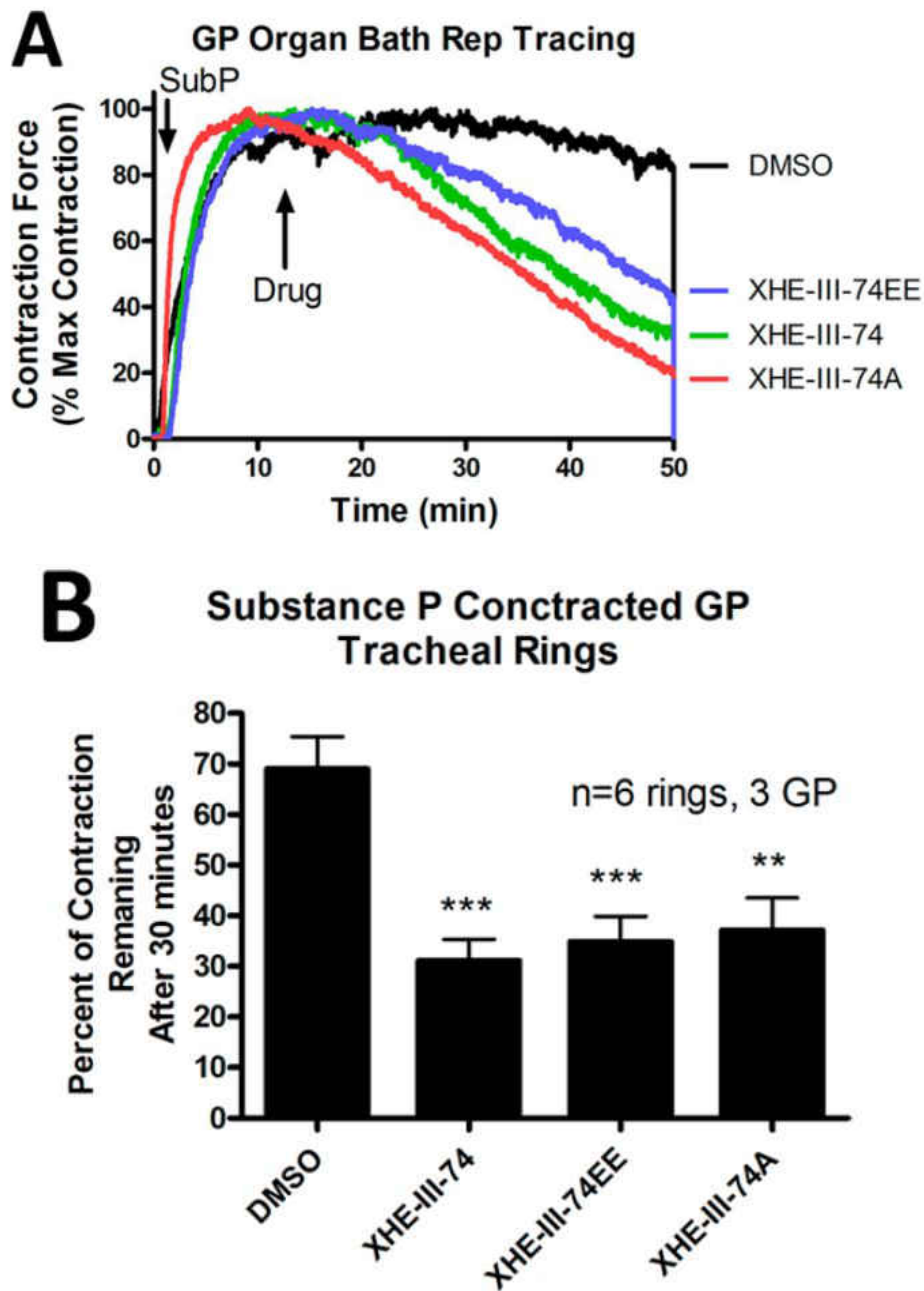
Figure 28. Muscle force measurements in guinea pig tracheal rings. (A) Time-dependent change of muscle contraction in the presence of substance P and GABAergic compounds. (B) Force remaining 30 min after drug addition is shown. Tracheal rings were contracted with 1 μM substance P and at the peak of muscle contraction 100 μM (in 0.1% DMSO) was added and the percent of remaining force was measured at 30 min. ∗∗∗ p < 0.001, ∗∗ p < 0.01 compared to vehicle, n = 6 rings from three guinea pigs (GP). Modified from the figure in Gloria, et al.[15]

3.7.10 In vitro Liver Microsomal Stability of Deuterated and Non-Deuterated XHE-III-74 Analogs[3]

In addition, a liver microsomal stability of HLM and MLM was investigated to identify metabolically labile compounds and deuterated compounds which should be more stable than their nondeuterated counterparts. The results of this study are summarized in Table 5. The parent compound XHE-III-74 (**7**) was metabolized rapidly by mouse liver microsomes with 16.2% remaining after 1 h (Table 5, Entry 4). The corresponding half-life was less than 24 minutes. However, ligand **7** was stable in the presence of human liver microsomes, similar to the majority of compounds investigated. Less than 80% of the parent compound was observed after 1 h for acid **9**; esters **11**, **11a**, **12a**; and cyclopropyl amide **19** (Table 5, Entries **7**, **11**, **12**, **14** and **27**). For acid **9** and amide **19**, stability of the deuterated analogs (**9a** and **19a**) was significantly increased (Table 5, Entries **7**, **8**, **27**, and **28**). A smaller number of compounds were stable in the presence of mouse liver microsomes for 1 h. The most stable compounds (as judged by less than 20% loss at 1 h on microsomes) were esters **5**, **5a**; phenol **6**, deuterated acid **9a**, deuterated methyl ester **10a**; amides **16**, **16a**, **17a**, **19**, and **19a** (Table 5, Entries **1**, **2**, **3**, **8**, **10**, **21**, **22**, **24**, **27**, and **28**). All compounds that exhibited good stability in mouse liver microsomes were also stable in the presence of human liver microsomes. Importantly, different metabolic rates for deuterated and non-deuterated compounds in the presence of mouse liver microsomes were observed for acid **9**, esters **10**, **11**, and amide **17** and their corresponding deuterated analogs (Table 5, Entries **7-12**, **23**, **24**).

Table 5. *In vitro* liver microsomal stability of XHE-III-74 analogs[3]

Entry	Compound	Microsomal stability (human) % remaining after 1 hour	Microsomal stability (mouse) % remaining after 1 hour
1	**5**	99.1 ± 0.1	85.4 ± 0.3
2	**5a**	92.8 ± 0.3	85.5 ± 0.3
3	**6**	91.7 ± 0.2	91.1 ± 0.1
4	**7**	92.1 ± 1.0	16.2 ± 0.2
5	**7a**	91.9 ± 0.4	17.6 ± 0.2
6	**8**	90.6 ± 0.2	46.6 ± 0.3
7	**9**	56.1 ± 0.5	52.9 ± 0.5
8	**9a**	84.6 ± 0.3	84.6 ± 0.2
9	**10**	89.7 ± 0.2	70.3 ± 0.2
10	**10a**	92.9 ± 0.2	85.9 ± 0.2
11	**11**	77.8 ± 0.2	13.4 ± 0.9
12	**11a**	78.7 ± 0.2	22.4 ± 0.3
13	**12**	-[a]	-[a]
14	**12a**	77.1 ± 0.2	62.5 ± 0.3
15	**13**	-[a]	-[a]
16	**13a**	-[a]	-[a]
17	**14**	-[a]	-[a]
18	**14a**	-[a]	-[a]
19	**15**	93.8 ± 0.3	54.3 ± 0.2
20	**15a**	94.9 ± 0.2	56.8 ± 0.3
21	**16**	92.4 ± 0.2	82.5 ± 0.3
22	**16a**	96.3 ± 0.3	83.1 ± 0.2
23	**17**	90.7 ± 0.3	50.1 ± 0.2
24	**17a**	93.5 ± 0.2	94.8 ± 0.2
25	**18**	92.8 ± 0.5	4.2 ± 0.2
26	**18a**	95.6 ± 0.2	9.4 ± 0.4
27	**19**	79.9 ± 0.2	91.3 ± 0.2
28	**19a**	88.1 ± 0.2	94.1 ± 0.2

[a] Compound was not soluble at 10 mM in PBS with 1% DMSO. Data were acquired by two independent experiments carried out in triplet.

3.7.11 Cytotoxicity Evaluation of XHE-III-74 Analogs[3]

Further characterization of these compounds included the determination of their cytotoxicity using three different cell lines; HEK293 kidney cells, HepG2 liver cells, and BEAS2B lung epithelial cells (Table 6).

Table 6. *In vitro* cytotoxicity of XHE-III-74 analogs[3]

Entry	Compound	Toxicity in HEK293 (Kidney) LD_{50} (µM) [a]	Toxicity in HEPG2 (Liver) LD_{50} (µM) [a]	Toxicity in BEAS 2B (Lung) LD_{50} (µM) [a]
1	**5**	>400	>400	>400
2	**5a**	>400	>400	>400
3	**6**	>400	>400	>400
4	**7**	>100	>400	>200
5	**7a**	>100	>400	>200
6	**8**	>400	>400	>400
7	**9**	>400	>400	>400
8	**9a**	>400	>400	>400
9	**10**	>400	>400	>400
10	**10a**	>400	>400	>400
11	**11**	>100	>200	>200
12	**11a**	>100	>200	>200
13	**12**	>200	>400	>400
14	**12a**	>200	>400	>400
15	**13**	>100	>100	>100
16	**13a**	>100	>100	>100
17	**14**	18.8 ± 2.4	>100	>100
18	**14a**	16.8 ± 2.0	>100	>100
19	**15**	>100	>400	>400
20	**15a**	>100	>400	>400
21	**16**	>400	>400	>400
22	**16a**	>400	>400	>400
23	**17**	>400	>400	>400
24	**17a**	>400	>400	>400
25	**18**	>200	>400	>400
26	**18a**	>200	>400	>400
27	**19**	>200	>400	>400
28	**19a**	>200	>400	>400

Compounds were incubated at different concentrations with specified cells for 48 h, followed by detection of viability using Cell-Titer Glo (Promega). The results were normalized using DMSO (negative) and 3-dibutylamino-1-(4-hexyl-phenyl)-propan-1-one (150 mM in DMSO final concentration, positive). Data were acquired by three independent experiments carried out in quadruplet.

Most of the compounds exhibited no major cytotoxicity at the concentrations tested. The compounds with the most pronounced cytotoxicity were thioesters **13**, **13a**, **14**, and **14a** (Table 6, Entries **15**-**18**). Among the compounds identified as stable in human and mouse liver microsomes, only cyclopropyl amide **19** and **19a** showed any toxicity in HEK293 cells (Table 6, Entries **27** and **28**) and it was at a concentration much higher than a therapeutic dose.

3.7.12 Sensorimotor Effects of Analogs of XHE-III-74 (7)[3]

In addition, possible adverse CNS sensorimotor effects were evaluated using a rotarod apparatus (Figure 29).

The Swiss Webster mice were injected i.p. with 40 mg/kg of the indicated compound. The sensorimotor test was carried out after 10, 30 and 60 min. All compounds, including the diazepam positive control, showed the greatest impairment of sensorimotor steadiness at 10 min, followed by 30 and 60 min. The compounds that caused the most severe motor impairment were esters **10a**, **11a**; amides **15** and **18a**. In addition, some of the esters and thioesters **11**, **12**, **12a**, **13**, **13a**, **14** and **14a** were not soluble in the vehicle (50% PBS, 40% propylene glycol, 10% DMSO) and could not be tested. Similar rotarod data were published previously for ester **5** and acid **9**, which indicated that ester **5** weakly induced sensorimotor impairment whereas acid **9** did not, this is likely due to the inability of the acid to penetrate the blood brain barrier.[15] The lead **7** (XHE-III-74) induced sensorimotor impairment in rats at 15 mg/kg (unpublished results). Taken together, compounds in

this series that are stable in the presence of human and mouse liver microsomes and exhibited

neither cytotoxicity nor sensorimotor impairment are phenol **6**, acid **9a**, amides **16**, **16a**, and **17a**.
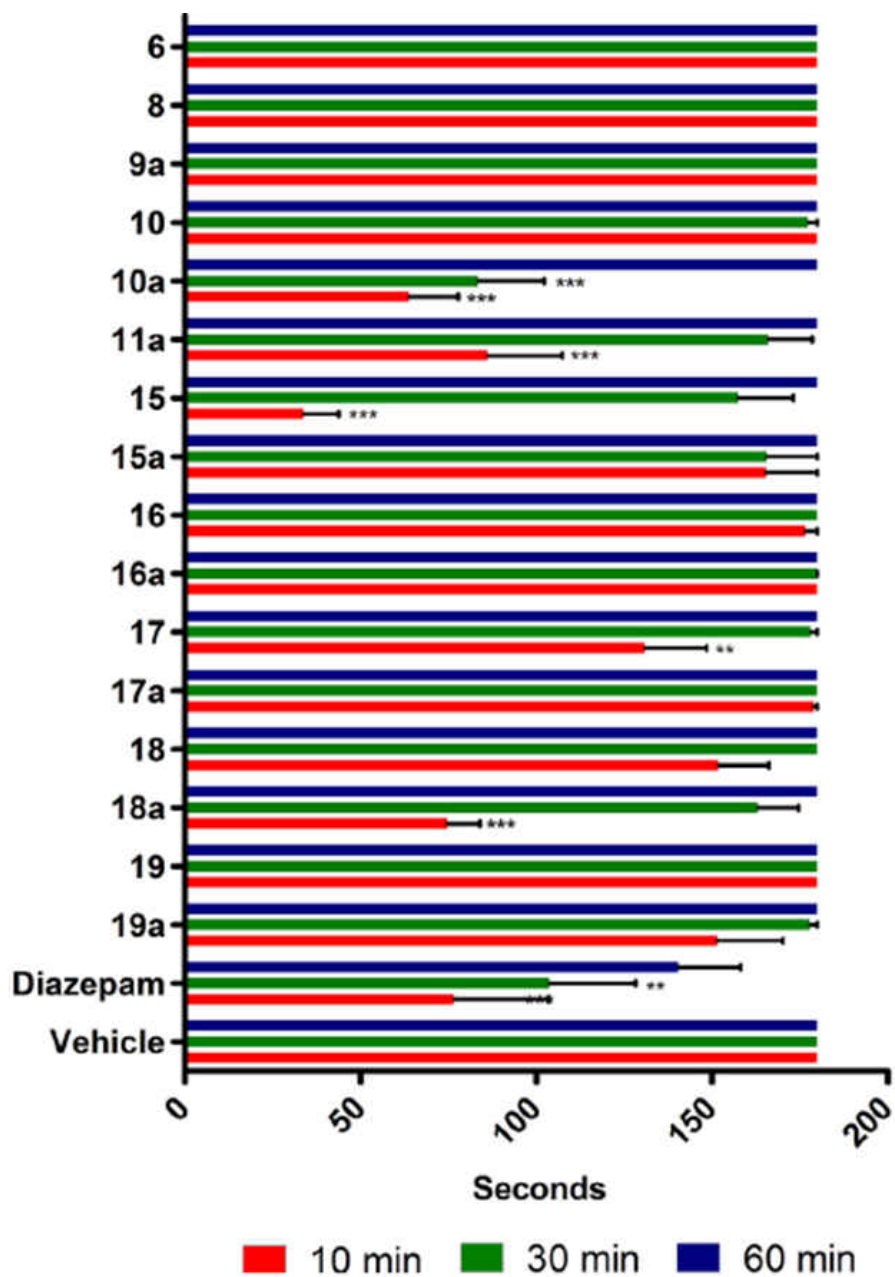
Figure 29. Effect of compounds on sensorimotor coordination. Swiss Webster mice were tested on a rotarod at 15 rpm for 3 min at 10, 30, and 60 min following compound exposure. Mice (N ¼ 10) received a single i.p. injection of test compound (40 mg/kg), diazepam (5 mg/kg), or vehicle (50% PBS, 40% propylene glycol, 10% DMSO). The time of fall was recorded if it occurred prior to 3 min. Data are expressed as mean ± SEM (N ¼ 10). ** (p < 0.01) or *** (p < 0.001) significance compared to vehicle-treated mice. Compounds 11, 12, 12a, 13, 13a, 14, 14a did not dissolve in the vehicle. Modified from the figure in Jahan, et al.[3]

From the above data dimethyl amide **16/16a** showed the most promising performance of the nondeuterated/deuterated pairs of compounds.

3.8 Further Evaluation of the Most Promising Analog, Dimethyl Amide 16[3]

The $\alpha_4\beta_3\gamma_2$ GABA$_A$R subtype selectivity of **16** was confirmed by comparison of its GABA induced current potentiation with the $\alpha_1\beta_3\gamma_2$ GABA$_A$R (Figure A2).

At a concentration of 1 mM of amide **16**, 161% potentiation was observed for the $\alpha_1\beta_3\gamma_2$ GABA$_A$R in contrast to 319% potentiation for the $\alpha_4\beta_3\gamma_2$ GABA$_A$R in the presence of a GABA EC$_{20}$ concentration. To investigate if amide **16**, like other analogs of XHE-III-74, exhibited the ability to relax airway smooth muscle, an ex vivo assay, which employed tracheal rings precontracted with substance P (Figure 30), was carried out.

Examination of the results indicated that amide **16** reduced the contractile force of substance P in guinea pig tracheal rings over a period of 1 hour. The greatest significance was observed after 30 min with a $p < 0.001$. Consequently, amide **16** was able to relax airway smooth muscle consistent with other analogs of XHE-III-74.[3,15]

In addition, it was investigated if amide **16** could reduce airway hyperresponsiveness in a mouse asthma model. To establish an asthma-like disease, model male BALB/c mice were sensitized with three i.p. injections of ovalbumin (2 mg/kg/d emulsified in 2 mg of alum on days 0, 7 and 14, in a total volume of 100 µL). This was followed by intra-nasal challenge (1.6 mg/kg/d ovalbumin for 5 days on days 23-27). The control mice were sensitized with ovalbumin but challenged with saline.[15] The separate groups of ovalbumin induced (S/C) BALB/c mice received a single 40 mg/kg i.p. dose of **16** at 40 minutes before the measurement or twice daily 40 mg/kg of **16** i.p. for a

duration of five days during the ovalbumin challenge period for chronic studies (Figure 31A and

31B).
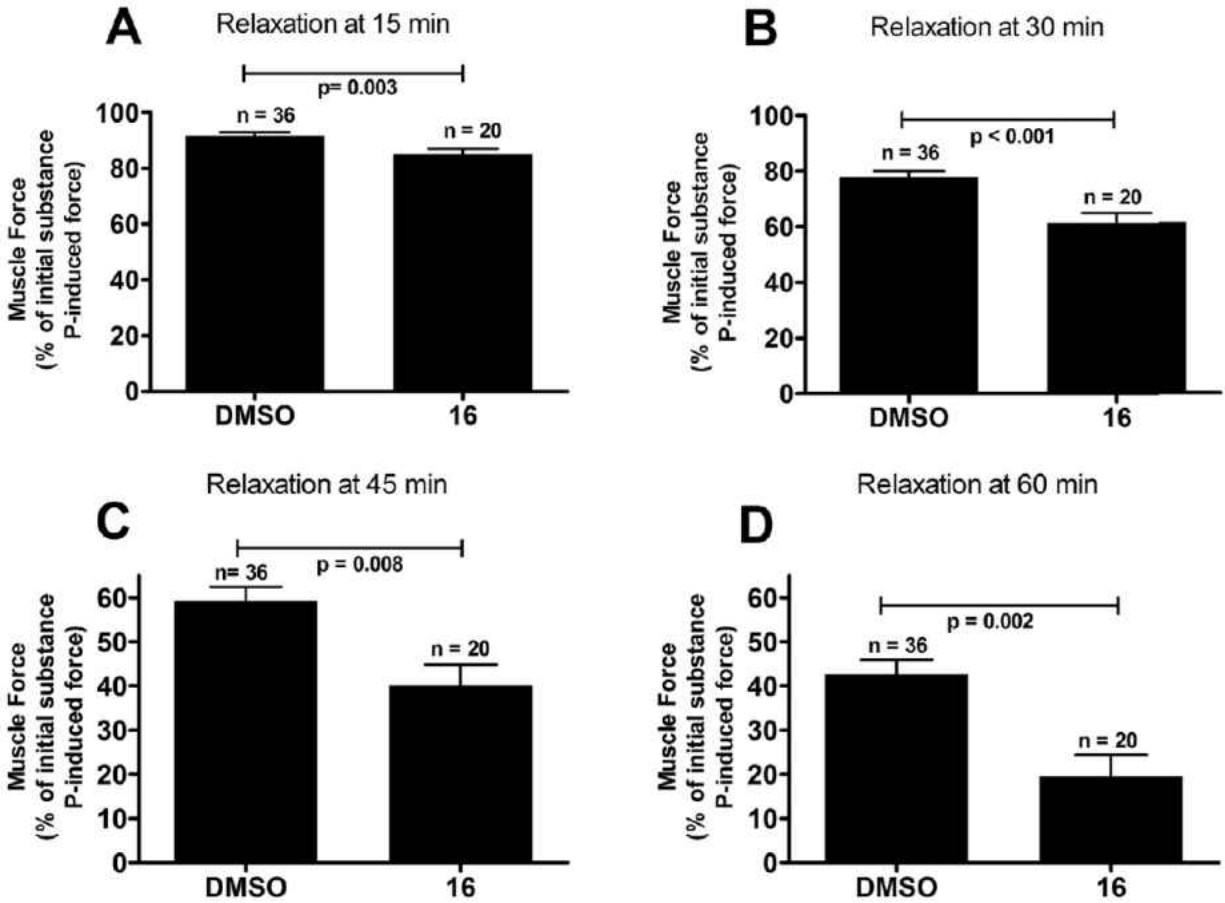
Figure 30. Airway smooth muscle contractile force in guinea pig tracheal rings. Tracheal rings were contracted with 1 μM substance P and then treated with 50 μM of 16 (or the vehicle control 0.1% DMSO). The percent of remaining contractile force was measured at various time points and expressed as a percent of the initial substance P induced contractile force. N and p-values are given for each condition. Modified from the figure in Jahan, et al.[3]
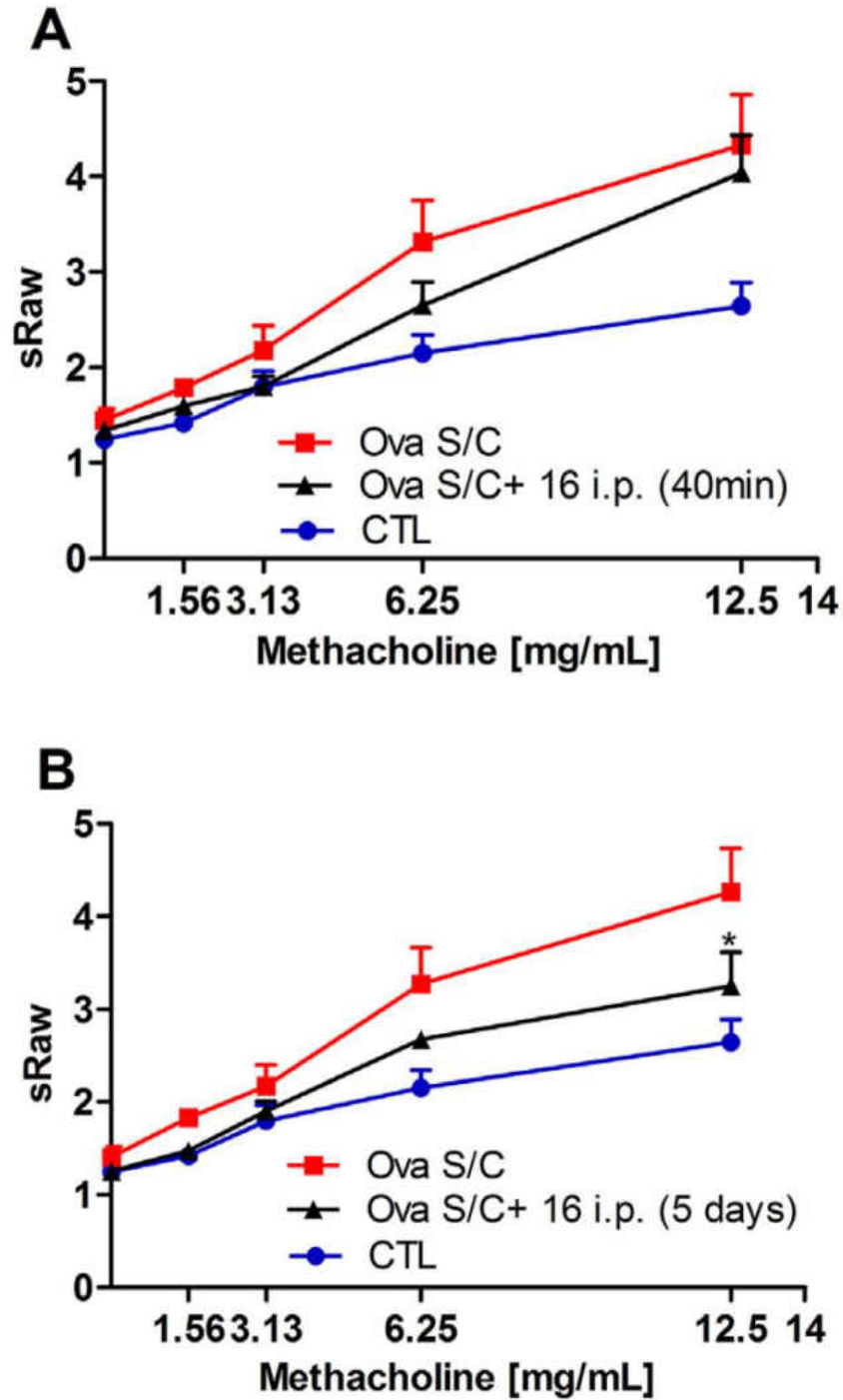
Figure 31. Effect of amide 16 on airway hyperresponsiveness: Specific airway resistance (sRAW) to increasing doses of methacholine measured by DSI's Buxco® FinePointe non-invasive airway mechanics instrument. (A) Balb/c mice were administered 40 mg/kg of 16 single i.p. injection 40 min prior to analysis; (B) administration of 16 at 40 mg/kg i.p. injections daily for 5 days. Data represent mean ± SEM from 4 to 7 mice in each group. * indicates p < 0.05 significance compared to vehicle-treated mice. Modified from the figure in Jahan, et al.[3]

For animals treated with a single dose of ligand **16**, no statistical significant specific airway resistance (sRAW) differences in comparison to the vehicle-treated group were observed at any of the methacholine concentrations tested. Importantly, significant reduction in sRAW ($p < 0.05$) was observed at the 12.5 mg/mL methacholine challenge for animals given amide **16** over a 5 day treatment course.

In light of the observed partial in vivo efficacy of **16** in reducing airway hyperresponsiveness, a pharmacokinetic study to investigate the stability in vivo of amide **16** (Figure 32) was carried out.

A

	Blood	Brain	Lung
t_{max} (min)	3	10	3
C_{max} (ng/g)	691	123	30
E_{rate} (min^{-1})	0.078	0.067	0.059
$t_{1/2}$ (min)	8.8	10.3	11.7
AUC_{0-t} (ng*min/g)	6205	2701	764
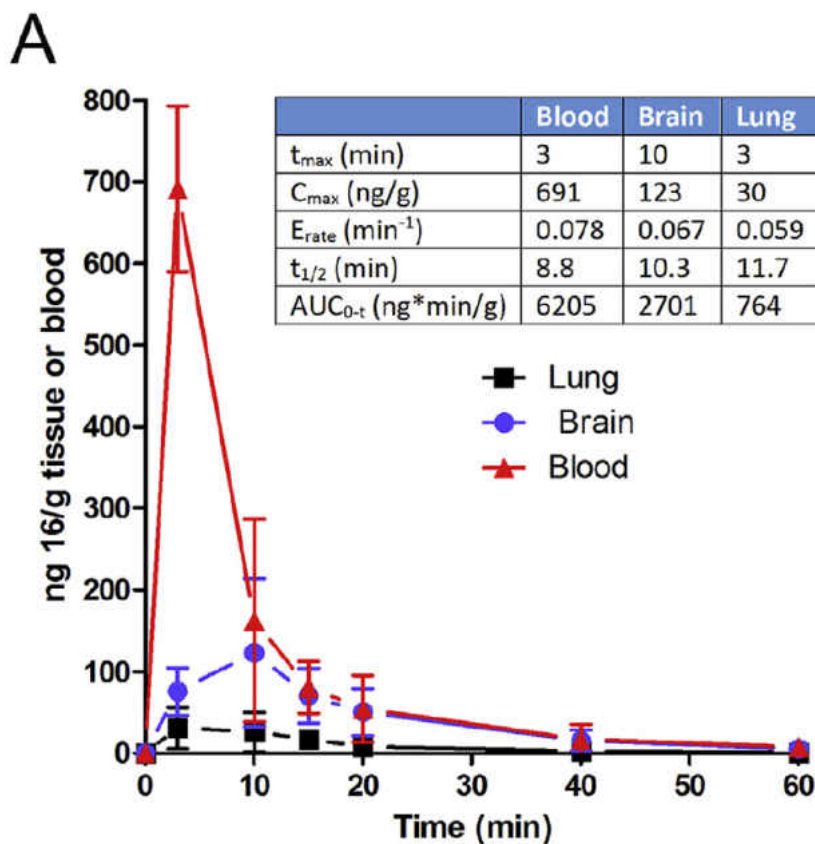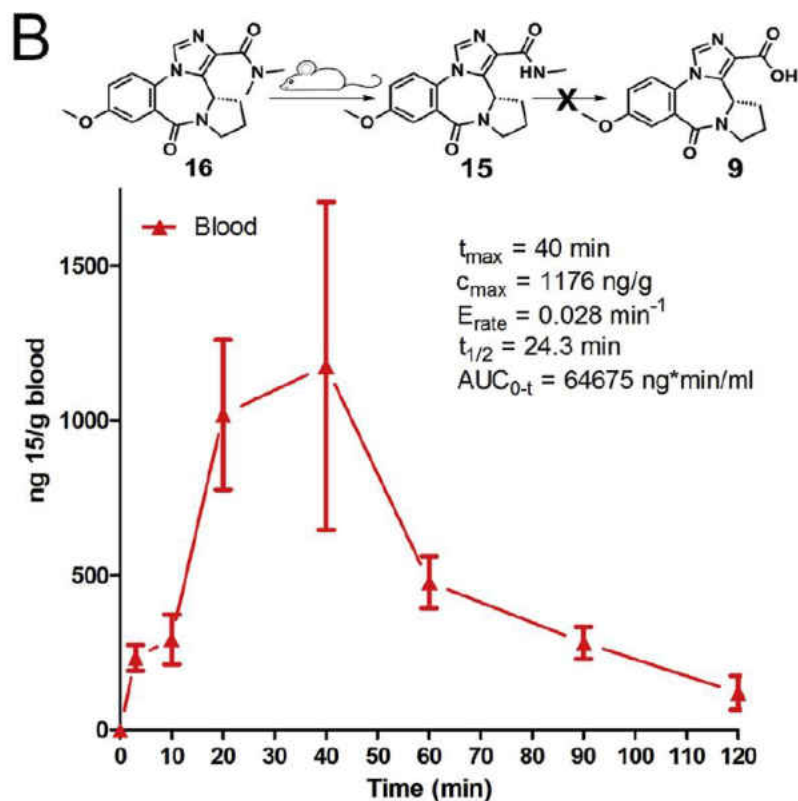
Figure 32. Pharmacokinetic analysis. A) Concentration changes of compound 16 in mouse brain, lung, and blood over time when given as a 5 mg/kg, i.p. injection. B) Quantification of metabolite 15 in mouse blood at indicated time points. Modified from the figure in Jahan, et al.[3]

The concentrations following an i.p. dose of 5 mg/kg, amide **16** were quantified in blood, brain, and lung at different time points (Figure 32A). the ligand **16** reached a maximum absorption within minutes (t_{max} = 3 min) but also was cleared very rapidly, with a half-life of 8.8 min. The overall exposure of amide **16** (AUC = 6205 ng*min/ml) was not very high. A markedly decreased distribution of dimethyl amide **16** was observed in brain and lung. The amide **16** did penetrate the blood brain barrier but reached only a very low C_{max} of 123 ng/g. The distribution in the lung was even less pronounced with an AUC of 764 ng*min/ml in comparison to an AUC = 6205 ng*min/ml in blood. The presence of two likely metabolites of dimethyl amide **16**, principally methyl amide **15** (formed by N-demethylation) and acid **9** (formed by peptidase-mediated hydrolysis or by

hydrolases) were then investigated. The metabolite **15** was observed in substantial amounts in blood after only 3 min after injection (Figure 32B). The peak blood concentration was higher than the parent compound and occurred later, as expected for a metabolite. Overall, the distribution of methyl amid **15** was superior to dimethyl amide **16** with an AUC of 64675 ng*min/ml. Acid **9** however, which was shown previously to reduce airway hyperresponsiveness, was not detected in any blood samples.[15]

3.9 Biological Evaluation of the XHE-III-74 Ethyl Ester with the Phenolic Hydroxyl Function at the C-8 Position (Ligand 6)[4]

It has been shown previously that XHE-III-74[3] **7** and XHE-III-74EE **5**,[15] can cross the blood−brain barrier (BBB) and induce CNS effects at higher concentrations. To reduce the compounds ability to travel across the BBB it was decided to reduce the lipophilicity of XHE-III-74EE and related derivatives. The C-8 methoxy substituted compounds XHE-III-74 **7**, XHE-III-74-EE **5**, and XHE-III-74A **9** could relax airway smooth muscle but all of them exhibited a poor pharmacokinetic profile. The analog XHE-III-74A **9** was devoid any CNS side-effects, while XHE-III-74 **7** and its EE derivative **5** exhibited undesired CNS effects. More importantly, XHe-III-74 and XHe-III-74EE reduced airway hyper-responsiveness but acid **9** did not show any AHR reduction. On the other hand, XHe-III-74A could reduce inflammation while XHe-III-74 and XHe-III-74EE did not exhibit any reduction of inflammation.[15] This led to a further search for a GABA$_A$R ligand which would show all of the desired properties: **better microsomal stability, a good PK profile, no CNS effects, relaxation of ASM, reduction of AHR, and reduction of inflammation**. The C-8 phenol variant of XHE-III-74EE **6**, which is in fact an intermediate for the synthesis of other

investigated derivatives above, might potentially have the desired properties. Consequently, phenol **6** was evaluated for the above-mentioned properties.

3.9.1 Relaxation of Airway Smooth Muscle by Phenol 6 Analog[4]

The airway smooth muscle relaxation capability of phenol **6** was investigated using two different *ex vivo* models (Figure 33). One of the models utilized substance P-induced guinea pig tracheal muscle constriction, which was mediated by Gq-coupled neurokinin receptors. The other one utilized the application of acetylcholine to human tracheal airway smooth muscle strips that affect the muscarine acetylcholine receptors (Gi and Gq-proteins).

In the guinea pig ASM, phenol **6** effected significant attenuation of the substance P-induced contraction at 15, 30, 45, and 60 minutes (Figure 33A). Although, substance P-induced contractile force spontaneously decreased over a period of 1 h, ligand **6** exhibited significant reduction of the contraction at 50 µM at each time point and, in a dose dependent manner (Figure 33B).
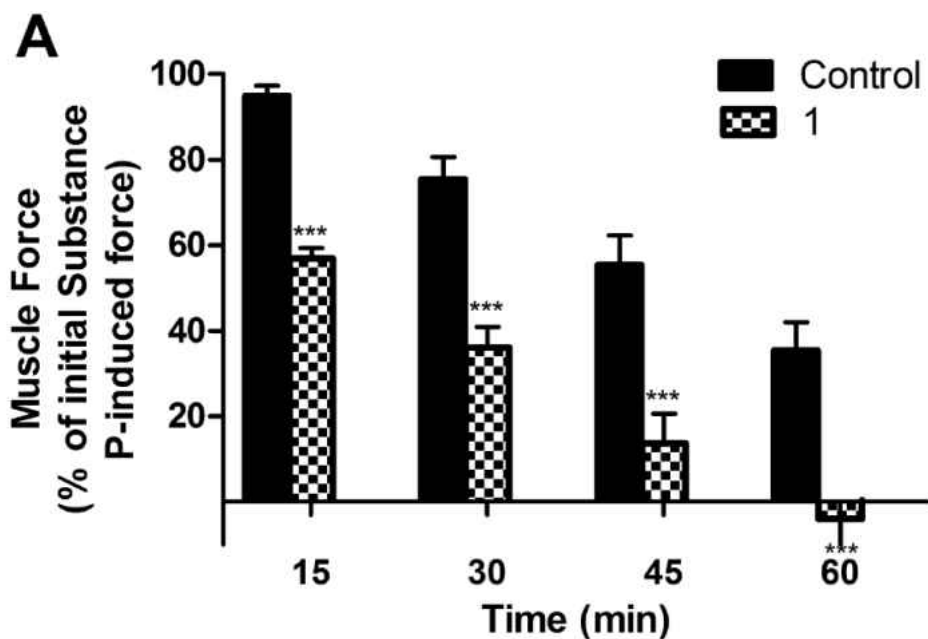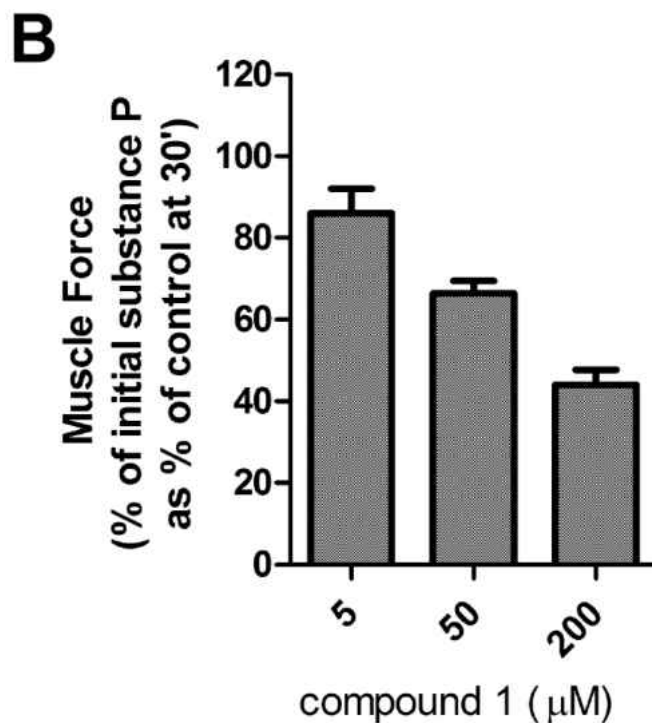
Figure 33. Smooth muscle contractile force measurement in the presence of phenol 6 (compound 1). (A, B) Airway smooth muscle contractile force in guinea pig tracheal rings. Tracheal rings were contracted with 1 μM substance P and then treated with (A) 50 μM of 6 (or the vehicle control 0.1% DMSO). The percent of remaining contractile force was measured at various time points and expressed as a percent of the initial substance P induced contractile force (N = 4). (B) Tracheal rings were contracted with 1 μM substance P and then treated with 6 at different concentrations. The percent of remaining contractile force was measured at 30 min and expressed as a percent of the initial substance P induced contractile force as a percent of control (N = 3). Modified from the figure in Gloria, et al.[4]

3.9.2 Distribution of Phenol 6 in Different Organs After Oral Administration in Mice[4]

To ensure the delivery of the drug molecule **6** to the target organ or tissue at a pharmacologically active concentration, a pharmacokinetic profile was investigated. This would permit manipulation and further dose optimization to achieve the desired pharmacological effects. The pharmacokinetic profile of ligand **6** is illustrated in Figure 34.
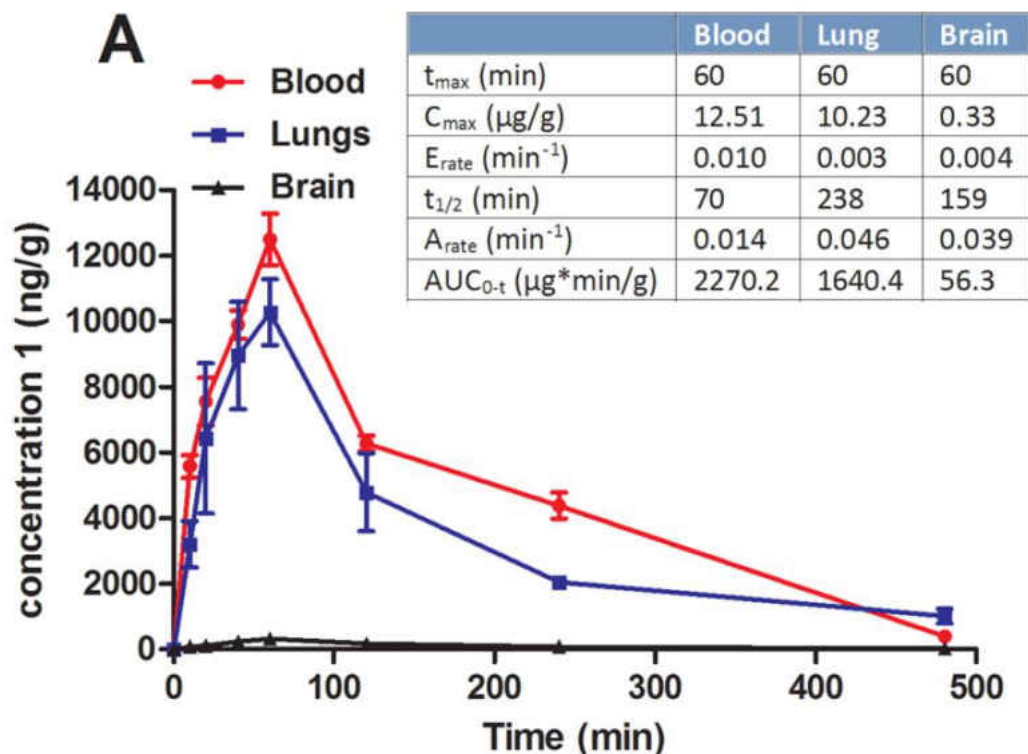
Figure 34. Time dependent pharmacokinetic distribution of phenol 6 in mice blood, lungs, and brain (25 mg/kg via oral gavage). Modified from the figure in Gloria, et al.[4]

The ligand **6** was absorbed within one hour after a 25 mg/kg oral dose. Excellent distribution in blood and lung (T_{max} = 60 min, AUC = 2270.2 µg.min/g) was observed, as well. The ligand **6** was present in the blood at a higher concentration (C_{max} 10.23 µg/g) than in the lung. The half-life of phenol **6** was higher in the lung (238 min) than in the blood and was detected in the lung even after 8 hours (Figure 35). More importantly, the level of phenol **6** was rather insignificant in the brain. In addition, to evaluate any undesired CNS effects induced by a higher dose, **6** was administered orally at a 100 mg/kg dose. Ligand **6** did not induce any motor sensory impairment which was clear from the rotarod assay (Figure A3). In addition, phenol **6** exhibited low efficacy toward the $\alpha_1\beta_3\gamma_2$ GABA$_A$R, which would mediate sedation and tolerance (Figure A4).

3.9.3 Anti-Inflammatory Properties of Phenol 6[4]

To evaluate the effect of ligand **6** on inflammatory cells, ova s/c BALB/c mice were treated with twice a day dose of 100 mg/kg for 5 days and the subsequent changes of inflammatory cells in bronchoalveolar lavage fluid was quantified using flow cytometry (Figure 35A-F). Ova s/c mice that usually exhibit asthma-like inflammation contained a significantly high amount of white blood cells in BALF. The 5-day oral treatment with phenol **6** showed an anti-inflammatory effect which was demonstrated by the reduced number of leukocytes in BALF (Figure 35A). To further confirm the anti-inflammatory properties of phenol **6**, eosinophilia in BALF was quantified in ova s/c mice using Wright Geimsa stain (Figure 35B). A five-days b.i.d. treatment with ligand **6** showed significant reduction in eosinophil counts in mouse BALF. Similar studies were also performed on $CCR3^+$, $GR1^+$, $CD4^+$, and $CD11b^+$ immune cells. In all these cases ligand **6**-treated mice exhibited a lower cell count compared to the untreated ova s/c mice (Figure 35C-F). In addition, the change in transmembrane current in the presence of phenol **6** in isolated $CD4^+$ T cells (from the spleen of ova s/c mice) was determined using patch clamp. There was a dose-dependent increment in current caused by phenol **6** (Figure 35G). Overall, ligand **6** exhibited more pronounced electro-physiological effects on $CD4^+$ T cells than another clinical asthma drug candidate (MIDD-0301, Figure 35I).[4]
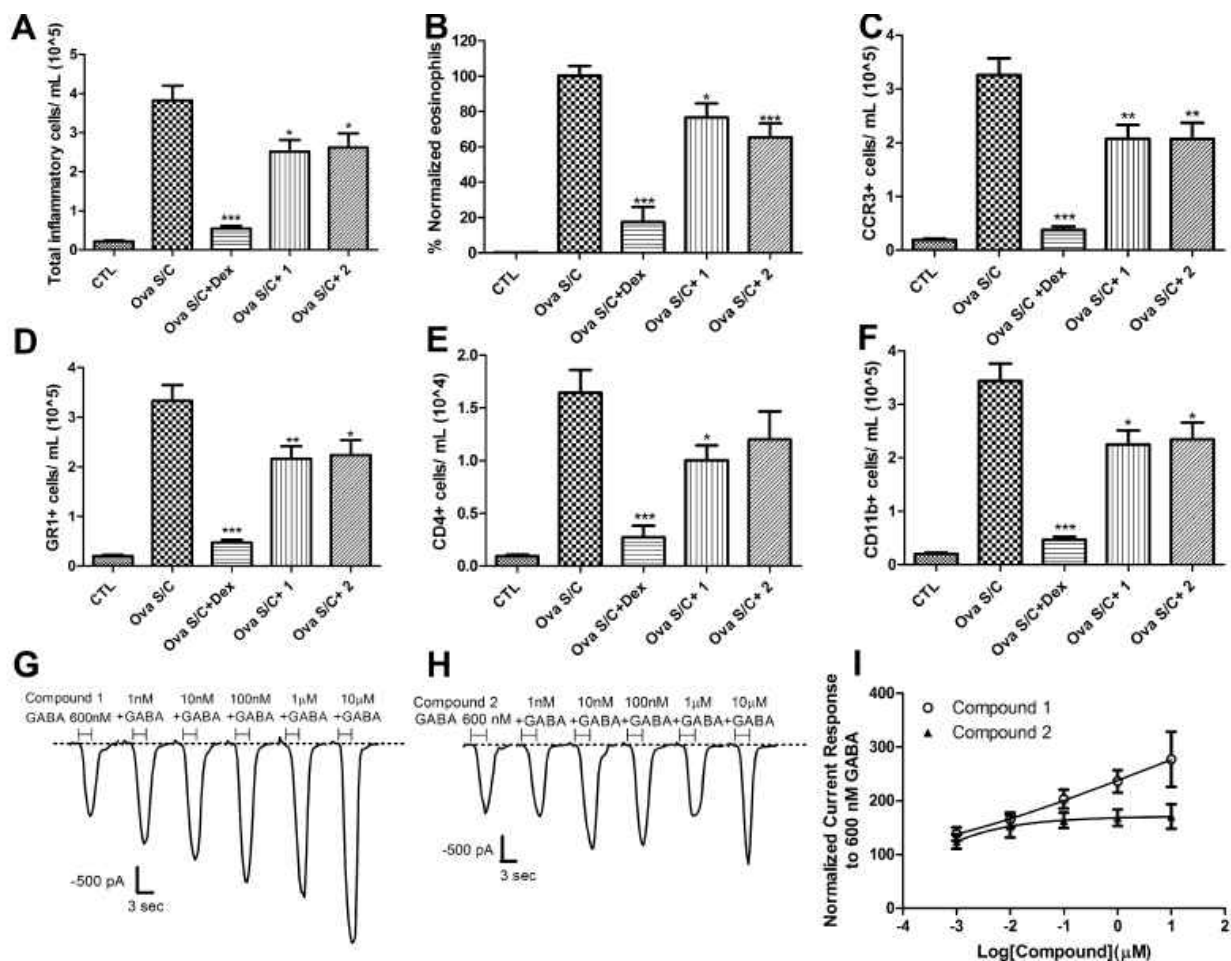
Figure 35. Effect of compounds 1 (phenol 6) and 2 (MIDD-0301, structure not shown) on inflammatory cells. Groups of 10 ova s/c BALB/c mice were administered dexamethasone i.p., 4 mg/kg daily for 8 days; compound 1 via oral gavage, 100 mg/kg twice daily for 5 days, and compound 2 via oral gavage, 100 mg/kg twice daily for 5 days. BALF was harvested from each animal and used for (A) quantification of total inflammatory cells. Cells were stained with mouse CD45 APC antibody, and samples were analyzed with BD FACS Calibur on high flow rate (60 μL/min) for 180 s. The gated positive events in the fourth channel (FL4) were used to calculate the total inflammatory cell count as cells/mL. (B) Quantification of Wright Giemsa stained airway eosinophils. Data represent % normalized eosinophil count relative to CTL (negative control) and ova s/c mice (positive control). (C−F) Quantification of specific leukocyte population. (C) CCR3+, (D) GR1+, (E) CD4+, and (F) CD11b+ cell populations were stained with specific antibodies and detected by flow cytometry. Data represent mean ± SEM from 10 mice in each group. *, **, and *** indicate $p < 0.05$, $p < 0.01$, and $p < 0.001$ significance, respectively, compared to vehicle treated ova s/c BALB/c mice. (G) Current recordings in the presence of 600 nM GABA and increasing concentration of compound 1 applied together for 3 s using CD4+ T-cells isolated from ova s/c BALB/c mice spleen. (H) Current recordings in the presence of 600 nM GABA and increasing concentrations of compound 2 applied together for 3 s using CD4+ T-cells isolated from ova s/c BALB/c mice spleen. (I) Concentration-dependent current responses of CD4+ T-cells from ova s/c BALB/c mice spleen in the presence of 600 nM GABA and increasing concentration of compound 1 or 2. Current readings were normalized to 600 nM GABA response set as 100% (n = 16). Modified from the figure in Gloria, et al.[4]

3.9.4 Alleviation of Airway Hyperresponsiveness by Phenol 6[4]
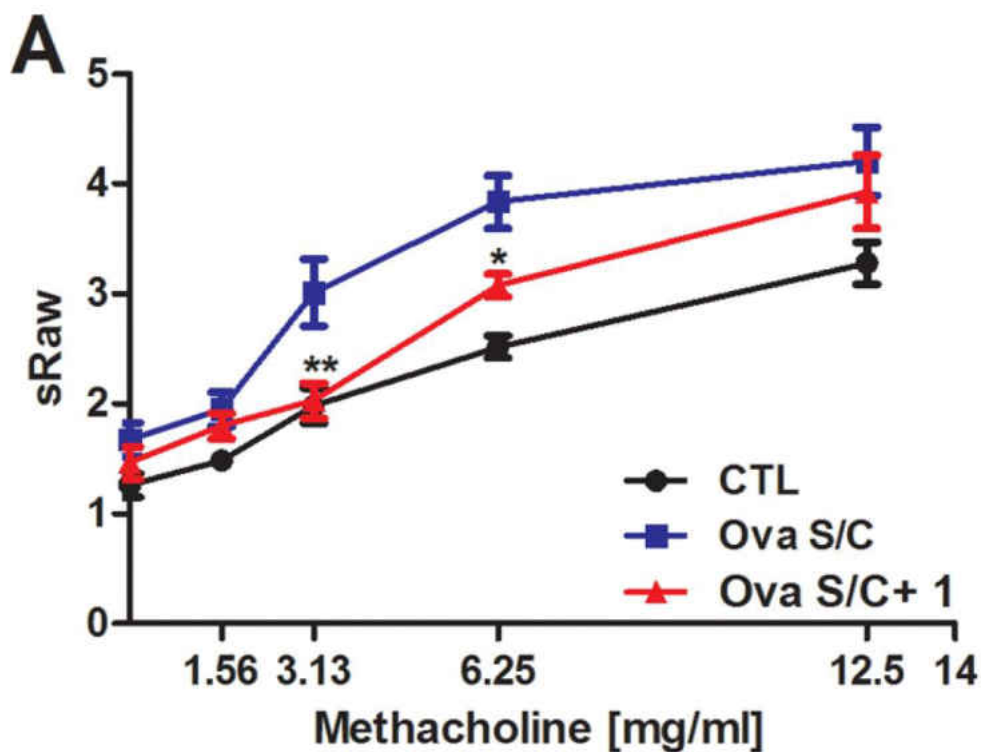
Figure 36. Effect of 6 on airway hyperresponsiveness. Specific airway resistance (sRaw) was measured at increasing dosages of methacholine by a DSI's Buxco FinePointe noninvasive airway mechanics instrument. Ova s/c BALB/c mice were administered 6 via oral gavage, 100 mg/kg twice daily for 5 days. Data represent mean ± SEM from 10 mice in each group. *, **, and * indicate p < 0.05, p < 0.01, and p < 0.001 significance, respectively, compared to vehicle treated ova s/c BALB/c mice. Modified from the figure in Gloria, et al.[4]**

Airway hyperresponsiveness is characterized by the physiologic agitation of cholinergic agonists and is a primary aspect of the symptoms of asthma.[214] The specific airway resistance (sRaw) in ova s/c mice was measured in the presence of an increasing amount of aerosolized methacholine to investigate the pharmacodynamic properties of phenol **6** after oral administration (Figure 36). Significant AHR was observed for methacholine at 6.25 and 12.5 mg/mL. After a 5-day treatment with ligand **6** (100 mg/kg, b.i.d. and 30 min before the measurement), this resulted in a significant

reduction in sRaw values for $C_{methacoline}$ = 3.13 and 6.25 mg/mL (Figure 26) which was in agreement with a previous report.[15] In addition, ligand **6** did not cause significant mucous metaplasia after oral administration (Figure A5).

In summary, phenol **6** demonstrated for the first time, the potential of this novel oral drug strategy for asthma by relaxing ASM, and alleviating AHR without mucous metaplasia. This novel asthma drug candidate will be further optimized for even better properties to combat AHR and airway inflammation which are responsible for the symptoms of asthma and perhaps COPD. In part, the method of administration might be the most important aspect of future research on phenol **6**.

3.10 The Synthesis of Heterocyclic Bioisosteres of XHe-III-74 at the C-3 Ester Position

Isostere, as a concept, was first contemplated by Moir in 1909, which was later refined by Grimm and experimentally established by Langmuir.[215-218] It was initially based on the octet theory of valence electrons. According to Langmuir, if two compounds or chemical species existed with the same number of atoms and electrons, they would arrange themselves in a similar manner and would exert similar properties.[218] As predicted based on this concept, diazomethane would have physical properties similar to ketene. Bioisosteres, on the other hand, are structurally distinct compounds that have similar biological properties or are recognized similarly by biological systems. This concept was developed by Erlenmeyer and Landsteiner in the 1930s.[217,219] Although the term "bioisostere" did not appear until 1950, when Friedman defined and distinguished between isosteres and bioisoteres.[220] Isostereic compounds are not necessarily bioisosteric, and vice versa.[217] Bioisosteres are generally not structural mimetics but biochemical mimetics. In the

design of bioisosteres factors that play key roles in molecular recognition and mimicry include size, shape, electronic distribution, lipophilicity, dipole moment, pKa, etc.[217] In current medicinal chemistry and modern drug discovery strategies, bioisosteres have become a fundamental tactic in the design and development of drugs.[215-217,221-223] The application of this strategy encompasses improving potency, increasing selectivity, reducing or altering metabolism, and acquiring intellectual property of the drug candidate.[217] Although established initially for a medicinal chemistry context, this concept has found useful and productive applications in optimization and development of organocatalysts.[224]

Classical bioisosteres can be as simple as the replacement of a hydrogen with a deuterium or fluorine atoms, an amine function with a hydroxyl function, etc. On the other hand, non-classical bioisosteres can range from a subtle to a sophisticated alteration of the molecule which may be completely different in terms of functionality, structure, and topology.[217] For example, a benzothiazole[225] moiety can be a bioisostere for a phenol function, a tetrazole function can be a carboxylic acid bioisostere,[217,226] an oxadiazole for an ester, a trifluoromethylamine function for an amide function, etc.[217]

3.10.1 Synthesis of Bioisosteres of Ligands 24-26, 28, 29 and 31

The ester function at C-3 was converted into a series of heterocyclic bioisosteres; 1,2,4-oxadiazoles with an alkyl substituent (Me, Et, iPr) at the C-3 position of the heterocycle.

For the 1,2,4-oxadiazoles, oximes with appropriate alkyl substituents were first stirred with NaH in THF before the introduction of the ethyl ester **5** and the reaction mixture, which resulted, was stirred at room temperature until completion (usually 2 hours), as indicated on analysis by TLC (silica gel) to furnish the 3-alkyl-1,2,4-oxidiazoles (Scheme 9) in excellent yields.[9]

Scheme 9. Synthesis of 3-alkyl-1,2,4-oxadiazoles (24-26)

THF, 3A MS, NaH

rt, 2h-5h

R= iPr,84%,RJ-03-12(**24**)
= Et,42%, RJ-03-13(**25**)
=Me,69%,RJ-03-14(**26**)
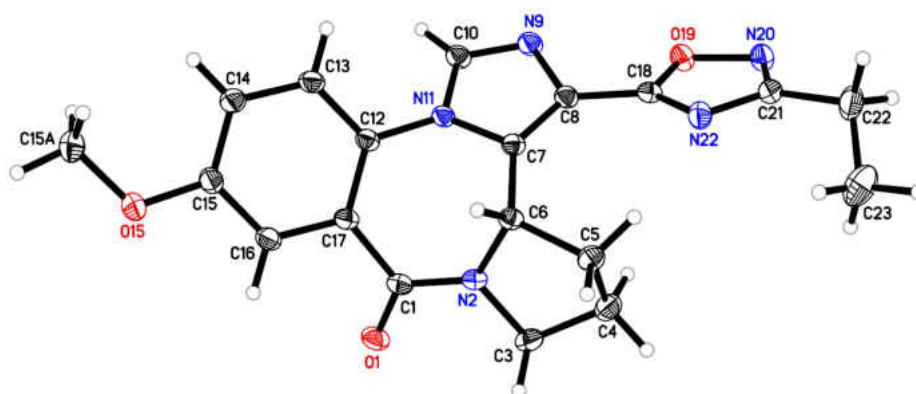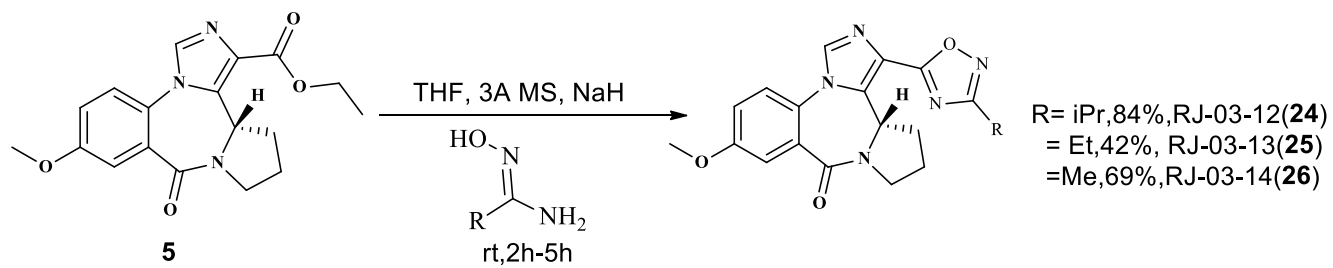
Figure 37. ORTEP representation of oxadiazole 25
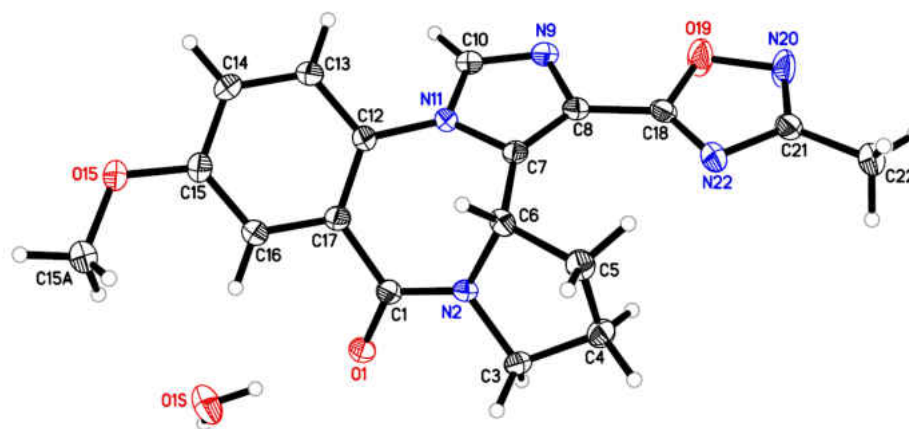
Figure 38. ORTEP representation of oxadiazole 26

The oximes required for these transformations were prepared earlier by the reaction of hydroxylamine with the corresponding alkyl nitriles in aqueous methanol at elevated temperature (Scheme 10).[9]

Scheme 10. Synthesis of the oximes[9]

$$R-CN + H_2N-OH \cdot HCl \xrightarrow[\text{reflux, 16h.}]{K_2CO_3, \text{ MeOH, } H_2O}$$

R = Me, Et, iPr
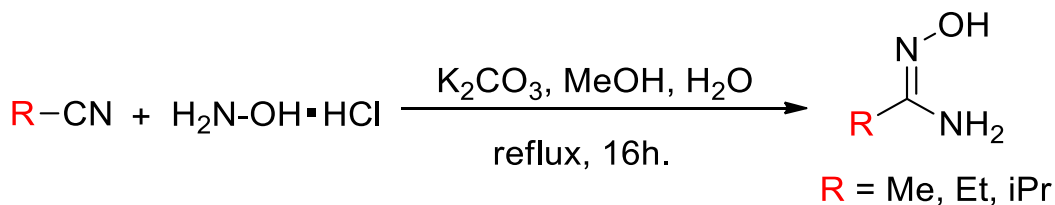
These three bioisosteres were analyzed for their potential cytotoxicity on HEK293, HEP2 and BEAS 2B lung cells (Appendix, Table A5, unpublished results). These bioisosteres were not cytotoxic at any concentration related to a therapeutic concentration of **24**, **25**, and **26** required for treatment of asthma. Moreover, importantly there was no cytotoxicity in lung cells.

In addition to the 1,2,4-oxadiazoles, a 1,3-oxazole, which is not a usual bioisosteric replacement for an ester but has been used before,[144] was also prepared as a bioisostere of the ester. The five-membered heterocyclic ring in a 1,3-oxazole is comparable to a methyl ester in size but electronically more related to the oxadiazoles. It does have two sites of electron density (O, N) which can interact with the protein in similar fashion to the oxygen atoms of an ester function.

The reaction of aldehyde **27** with TosMIC in the presence of potassium carbonate in methanol[227] furnished the oxazole KRM-II-68 **28** in good yield, while the required aldehyde **27** was prepared from the ethyl ester **5** by reduction with DIBAL-H at -78 °C (Scheme 11). The synthesis of aldehyde **27** was further improved by using SDBBA (Figure 38).[228,229] The SDBBA was prepared (Scheme 12) and used *in situ* from sodium *tert*-butoxide and DIBAL-H in excellent yield.[228] The SDBBA mediated reduction of the ester was more facile because the reaction was carried out at

99

room temperature (not in –78 °C). In this process the aldehyde was formed quickly from the hindered hydride reagent and the reaction was stopped before the aldehyde could be reduced to the alcohol byproduct.

Scheme 11. Synthesis of the aldehyde 27 and this was followed by conversion into the 1,3 oxazole 28 at the C-3 position
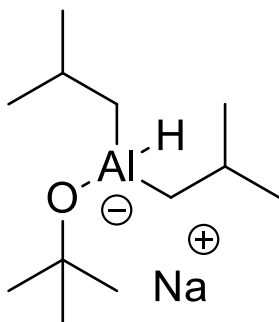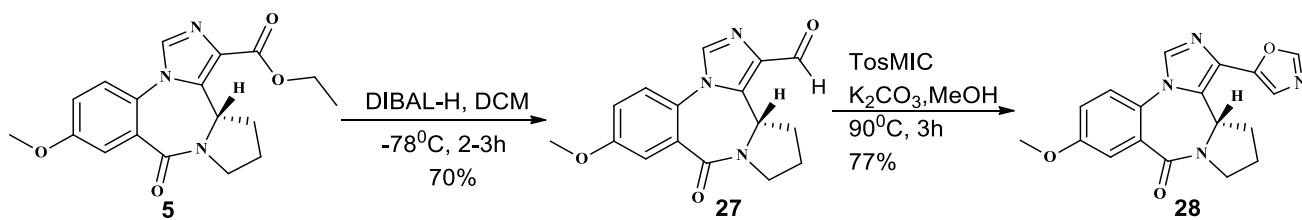
Figure 39. Structure of SDBBA
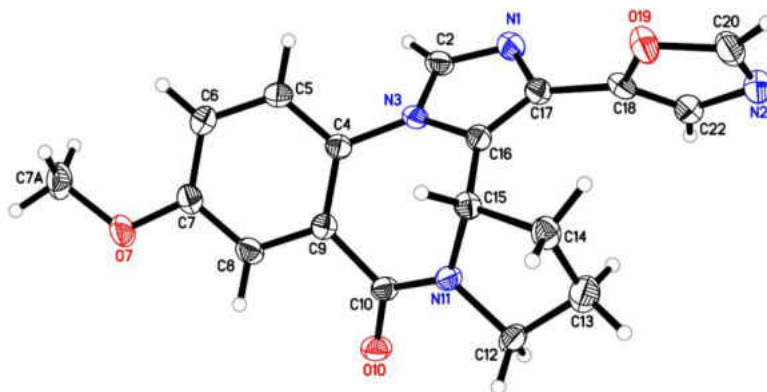
Figure 40. ORTEP representation of oxazole 28

Scheme 12. Improved synthesis of the aldehyde 27 at the C-3 position from ester 5 with *in situ* formed SDBBA[228,229]
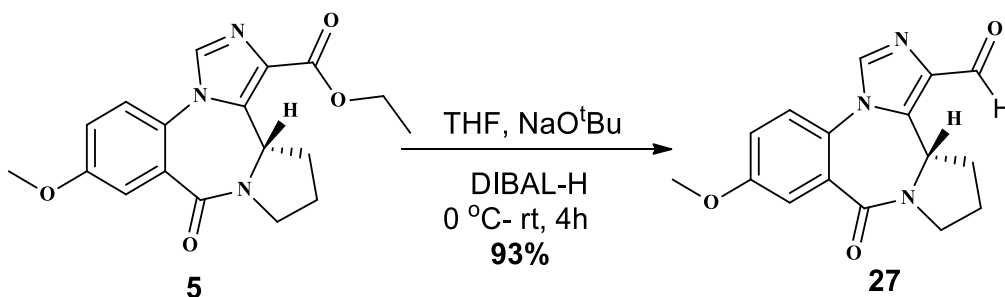
The 1,3-oxazole **28** did not show any cytotoxicity at a concentration up to 400 µM in the three different cell lines; HEK293 kidney cells, HEP2 liver cells and BEAS2B lung epithelial cells (see Appendix, Table A6, unpublished results).

In pre-contracted (with 1 mM substance P) guinea pig tracheal rings, oxazole **28** reduced the constriction of airway smooth muscle after 15 minutes for a period of at least 60 minutes (comparable with XHE-III-74; Appendix, Figure A6, unpublished results). The effect of oxazole

28 on sensorimotor gating at 40mg/kg was performed and it showed profound motor impairment beginning at 10 minutes all the way through 60 minutes on the rotorod (Appendix, Figure A7, unpublished results).

Although 1,3-oxazole **28** was not cytotoxic and it exhibited the desired relaxation of ASM, it passed through the BBB which led to CNS side effects. Consequently, the more polar variant, the C-8 phenolic C-3 oxazole **29** (RJ-03-30) was prepared *via* the previously mentioned ethanethiol and ALCl₃ mediated demethylation of oxazole **28** in excellent yield (Scheme 13).

Scheme 13. Synthesis of C-8 phenolic C-3 oxazole 29[229]
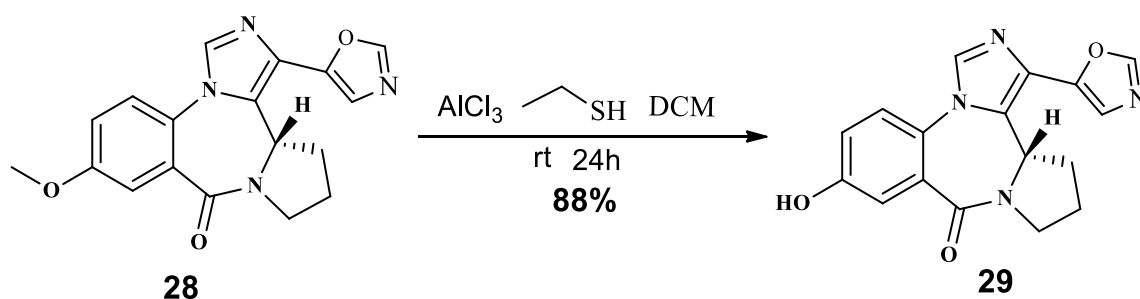
The phenolic, C-3 substituted oxazole **29** was very stable on both human and mouse liver microsomes (see Appendix, Table A7). The oxazole **29** did not show cytotoxicity at a concentration of $400\,\mu M$ in HEK293 kidney cells and HEPG2 liver cells, as well (Appendix, Table A8). In addition, it was found to exhibit relaxation of guinea pig airway smooth muscle which began at 15 minutes, which was very promising (Appendix, Figure A8). As expected, ligand **29** did not show any sensory motor impairment at 100 mg/kg in the rotarod assay, which indicated the lack of distribution in the brain because of the more polar nature, which, presumably, prevented it from traveling across the BBB (Appendix, Figure A9). Although oxazole **29** did not

show alleviation of airway hyper-responsiveness (Appendix, Figure A10), and did not modulate inflammatory cells in the preliminary experiments (Appendix, Figure A11), it evoked a very pronounced GABA induced current in electrophysiological measurement of $CD4^+$ T lymphocytes (Appendix, Figure A12).[229] Consequently, it is still a promising candidate for further development because of its desirable properties in other criteria. It is important that further biology be carried out on this molecule.

It is known that 1,2,3,4-tetrazoles are excellent bioisosteres for carboxylic acids. The synthesis of tetrazole **31** (RJ-03-57) began from the XHE-III-74 ethyl ester **5** already in hand. The ethyl ester **5** was first converted into the aldehyde **27** using SDBBA, and this was followed by conversion into the corresponding nitrile **30** by reaction of **27** with I_2 in aqueous ammonia in excellent yield with no chromatography required for purification.[228] Subsequently, the nitrile **30** was treated with sodium azide in the presence of zinc bromide at elevated temperature (refluxing THF) to furnish the desired tetrazole **31** (Scheme 14).[230]

Scheme 14. Synthesis of 1,2,3,4-tetrazole 31 from ester 5[228-230]
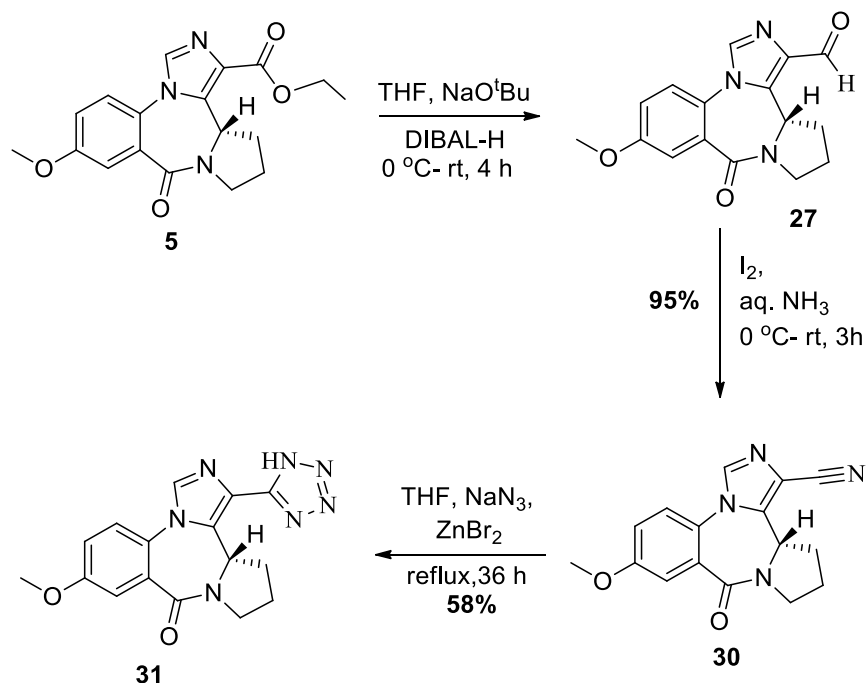
Tetrazole **31** was much more stable than the acid **9** in the microsomal enzyme stability assay (Appendix, Table A7)**.** In human liver microsomes 98.5 ± 0.2% of tetrazole **31** remained (acid **9** was 56.1 ± 0.5%) after 1 hour, while in mouse liver microsomes 94.3 ± 0.1% remained (acid **9** was 52.9 ± 0.5%) of **31** after 1 hour. It did not show cytotoxicity at a concentration of 400 µM in HEK293 kidney cells and HEPG2 liver cells at a therapeutic dose, as well (Appendix, Table A8).[229]

As expected, tetrazole **31** did not show any sensorimotor impairments on the rotarod assay when dosed at 40 mg/kg (Appendix, Figure A9). But this compound could not reduce the constriction of guinea pig airway smooth muscle after 15 minutes for a period of at least 60 minutes (Appendix, Figure A8). Unfortunately, it also was not able to alleviate airway hyperresponsiveness (AHR) (Appendix, Figure A10). The pharmacokinetic profile of tetrazole **31** in mice blood, lungs, and brain, when administered at 25 mg/kg *via* oral gavage, indicated a moderate absorption and fast

clearance had occurred (Appendix, Figure A13).[229] This was not suitable for treatment of asthma, it was felt.

Subsequently, the phenolic ethyl ester **6** was saponified and this was followed by acidification to furnish the phenolic acid (RJ-03-90) **32**, as shown in Scheme 15 below.

Scheme 15. Synthesis of phenolic acid 32 from ester 6

NaOH, EtOH,H$_2$O
50$^{\rm O}$C, 15 min; 1 N HCL

65%

6

32
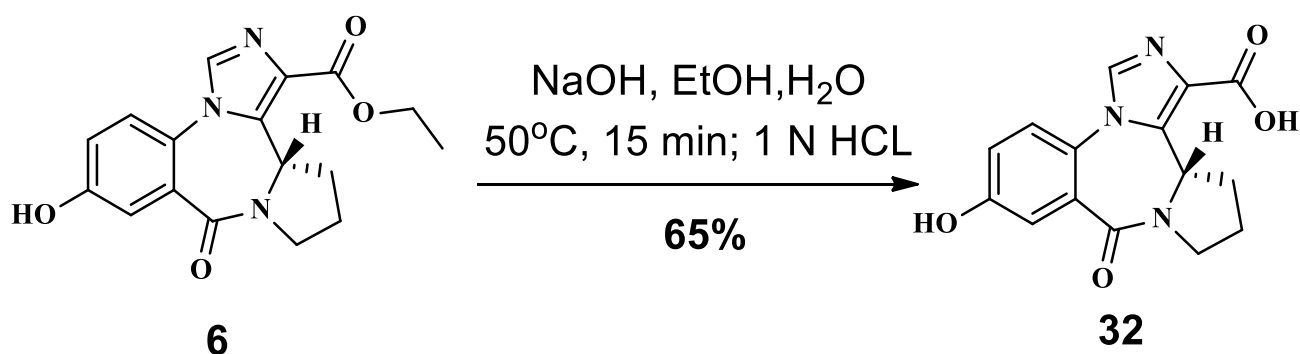
The phenolic acid **32** did not show any sedative effects on the rotarod at 100 mg/kg on oral dosing (Appendix, Figure A9). When the effect on inflammatory cells was performed, acid **32** did not modulate the numbers of inflammatory cells when ova s/c BALB/c mice were administered **32** at 100 mg/kg twice daily for 5 days (Appendix, Figure A11).[229] **However, this is only preliminary data. It is hoped that this compound will be rescreened for AHR and anti-inflammatory properties in the near future.**

Scheme 16. Synthesis of amides 33 and 34 from acid 9[229]

9

(i) SOCl$_2$, DCM, 1 h;
(ii) NH$_2$OMe, Et$_3$N 5h
70%

33 (MRS-III-87)

(i) SOCl$_2$, DCM, 1 h;
(ii) NH$_2$CN, Et$_3$N 5h
70%

34 (MRS-III-90)
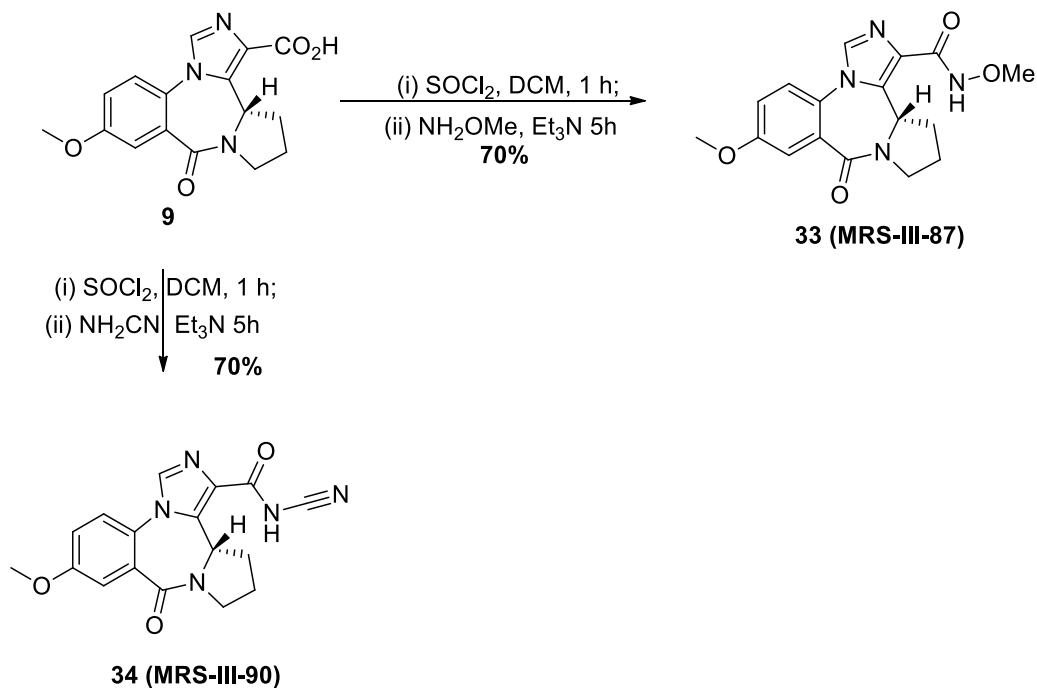
Scheme 17. Synthesis of alkyl ethers 35-39 from phenol 6

6

(i) Cs$_2$CO$_3$, DCM, Alkyl
halide, 24 h

(ii) NaOH, H$_2$O, EtOH
50 °C, 15 min
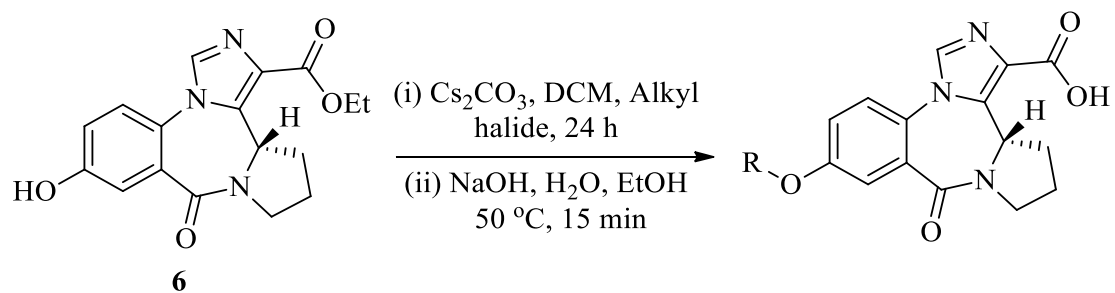
R = CH$_2$CH$_3$, 70% ,**35** (MRS-IV-05)
= CD$_2$CD$_3$, 65%,**36** (MRS-IV-14)
= Cyclopropyl , 30%,**37** (MRS-IV-12)
= CH(CH$_3$)$_2$,70%,**38** (MRS-IV-06)
= C(CH$_3$)$_3$,65%,**39** (MRS-IV-08)

Additionally, the carboxylic acid at C-3 was converted into methoxyamide **33** and cyanamide **34** in cooperation with Dr. Michael Stephen. The carboxylic acid **9** was converted to corresponding acyl chloride by reaction with thionyl chloride and this was followed by the treatment of methoxylamine and cyanimide in the presence of triethylamine to furnish amides **33** and **34**, respectively (Scheme 16). Furthermore, the phenolic function at C-8 of ester **6** was converted to alkyl ethers **35**-**39** for additional C-8 ether derivatives. The phenol function was alkylated by reaction with alkyl halides in the presence of cesium carbonate in DCM to convert them into their corresponding ethers (individually). The ester function was saponified subsequently to furnish the C-8 alkyl ether containing carboxylic acids **35**-**39** in good to excellent yield (Scheme 17).

The biological evaluation of these promising α$_4$-subtype selective GABA$_A$R agonists is yet to be performed. It is hoped that these compounds will be screened in the near future.

4. Discussion

There are only a limited number of options available for the long-term management of chronic asthma. The beta 2 adrenergic receptor (β_2AR) agonists and inhaled anti-inflammatory corticosteroids have been the mainstays in ameliorating asthmatic symptoms in moderate to severe incessant asthma.[4,231,232] In this case administration of the drugs through inhalation offers a more direct approach since it promises targeted delivery of the drug to the lung in high dosages, while avoiding undesirable adverse effects from systemic exposure. Despite this apparent advantage, prolonged use of corticosteroids may result in drug adherence and compliance issues.[233,234] In addition, asthma therapeutics that offer the inhaler route may not be economically viable in many circumstances and have to be carried-with always.[4,233] It is a considerable encumbrance for children and elderly asthma patients since improper technique of the inhaler use often causes incorrect dosage and poor efficacy of the drug. This ultimately contributes to the poor management of asthma and increased asthma related morbidity and mortality.[4,233,234] On the contrary, administration through the oral route is widely accepted and can be supervised by relatives and caregivers. In addition, if the oral drug can be formulated into a slow-release form, it would ensure a long-lasting exposure of the drug and consequently, it will ensure pharmacological benefits around-the-clock.

Esters and amides are common functional groups in many FDA approved drugs, although a number of such compounds are prodrugs that rely on endogenous enzymes such as peptidases to be activated. The lead XHE-III-74 **7**, has a tert-butyl ester function which was shown to be labile in the presence of mouse liver microsomes, while relatively stable in vitro in human liver microsomes. Nevertheless, XHE-III-74 **7** reduces airway hyperresponsiveness when given by aerosol delivery in mice.[2] Consequently, the stability of XHE-III-74 **7** was sufficient in mice when

administered directly to the target organ. Other compounds with limited half-lives in the presence of mouse liver microsomes are **18** and **18a** bearing a tert-butyl amide, **8** bearing a tert-butyl ester, and **11**, **11a** bearing a isobutyl ester.[3] Therefore, it was found that esters and amides with longer and more branched carbon chains are metabolically less stable than their shorter carbon chain analogs. Another aspect of the SAR determined herein was the comparison of deuterated and non-deuterated compounds. Overall, a trend, that deuterated compounds are equally or more stable than their corresponding non-deuterated analogs was found. This effect was very pronounced for acids **9** and **9a**, probably because a hydrolysable carboxylic ester or amide group inherent to other analogs in this series was missing.[3] Thus, for **9** and **9a**, oxidation of the methoxy group (deuterated or non-deuterated) to the corresponding hemiacetal followed by hydrolysis might be the rate-determining step of metabolism. This specific route of metabolism can be species dependent. For instance, ethyl amides **17** and **17a** had similar stability on human liver microsomes; however, in the presence of mouse liver microsomes the non-deuterated amide **17** was notably less stable.[3] Therefore, it was confirmed that small molecule metabolism was highly species dependent and involved many different metabolic reactions that are structure dependent. The cytotoxicity of XHE-III-74 analogs was not very pronounced. The analysis showed that 50% of all compounds have LD_{50} values greater than 400 µM for the sensitive HEK293 kidney cells. For the BEAS2B lung cells, 71% of the compounds were not toxic. The compounds with the highest toxicity were thioesters **14** and **14a**.[3] Interestingly, the deuterium protecting effect was less pronounced for cytotoxicity, although small differences were observed (Appendix, Figure A11). This is as expected, for if a molecule is cytotoxic as is, increasing the duration may well not decrease toxicity. The only way to affect cytotoxicity is to block metabolism to a toxic metabolite. Sensorimotor impairment is another important screen for unwanted side effects in a possible asthma drug.

Among the different GABA$_A$R in the CNS, the $\alpha_1\beta_3\gamma_2$ GABA$_A$R's subtype is known to mediate sedation, which in turn compromises sensorimotor skills.[3,235] Therefore, compounds with high efficacy toward this receptor subtype are expected to induce sedation in vivo, as seen for diazepam.[209] However, due to the unique scaffold of XHE-III-74 and its analogs, low efficacy towards $\alpha_1\beta_3\gamma_2$ GABA$_A$R and high efficacy towards $\alpha_4\beta_3\gamma_2$ GABA$_A$R was shown, e.g. XHE-III-74 **7**,[2] XHE-III-74EE **5**,[209] and XHE-III-74A **9**.[15] Only a few of the compounds described herein induced sensorimotor effects comparable to diazepam; however, at concentrations that were eight times greater. At 40 mg/kg the deuterated analogs, in comparison to non-deuterated parents are more likely to impair sensorimotor abilities. This effect correlated with their better metabolic stability. For instance, 30% of methyl ester **10** was metabolically converted into the acid after 1 h, whereas only 15% of deuterated ester **10a** was converted into the acid during the same time. Accordingly, ester **10** did not induce any sensorimotor impairment in contrast to deuterated ester **10a**. Thus, increasing the half-life of a drug candidate using deuterium substitution in the present case amplified not only the therapeutic effect but also potentiated possible side effects.[3] The only compounds investigated herein that were stable in mouse and human liver microsomes and did not induce sensorimotor impairment were phenol **6**, acid **9a**, as well as amides **16**, **16a**, and **17a**. Amide **16**, like other compounds in this series e.g. esters **5**, **7**, and acid **9**,[15] significantly reduced airway muscle constriction caused by substance P. Airway smooth muscle relaxation is an important hallmark of an efficacious asthma treatment and amide **16** mediated this effect within 15 min. In vivo, using ovalbumin S/C mice, ligand **16** reduced airway hyperresponsiveness at high methacholine challenge when given chronically.[3] Similar effects were reported for ethyl ester **5** when given repeatedly over five days.[15] Both ligands (**5** and **16**) are metabolically stable in vitro and non-toxic, however, their effect was less pronounced in vivo probably due to sub-

pharmacological concentrations. Ethyl ester **5** was shown to be absorbed and cleared slower with a $t_{1/2}$ of 16.3 minutes instead of 8.8 minutes in comparison to dimethyl amide **16**. Using the same dose, the AUC for lung exposure decreased from 4516 ng*min/ml for ester **5**-to 764 ng*min/ml for amide **16**.[3] Finally, it was shown that ester **5** metabolized to acid **9** probably by mouse esterases and acid **9** decreased airway eosinophilia.[15] In contrast, dimethyl amide **16** metabolized to methyl amide **15** (demethylation) but no hydrolysis took place to yield acid **9** was detected. Thus, the incremental weaker pharmacodynamic effects of amide **16**, presumably is due in part by its short half-life and the inability to form the anti-inflammatory acid **9**.[3]

The common GABA$_A$R positive allosteric modulators (PAMs) suffer from significant distribution in the brain which elicits undesirable side effects. In contrast, phenol **6**, a novel PAM for GABA$_A$R, demonstrated pharmacological effects to treat asthma, while maintaining an extremely low brain concentration. No detectable murine sensorimotor impairment at high doses in the rotarod assay confirmed the low brain exposure and no corresponding CNS adverse effects (Appendix, Figure A12).[4] The active key chemical composition was realized by incorporating a hydrophilic function such as phenolic hydroxyl group attached to a well-established imidazobenzodiazepine scaffold (phenol **6**) into the molecule. The improvement in hydrophilicity (pKa) resulted in reduction in brain distribution almost entirely. In addition, phenol **6** exhibited excellent pharmacokinetic properties with very high concentrations in blood and lung, as well as a longer in vivo half-life which would facilitate the management of asthma.[4] It was demonstrated that a five day long oral b.i.d administration of ligand **6** during an ovalbumin challenge (following ovalbumin sensitization) could significantly diminish airway hyperresponsiveness (AHR) at low concentrations of methacholine. This observation was in accord with the results from a prior investigation with α$_4$

subtype selective GABA$_A$R PAM XHE-III-74EE **5**.[15] The in vivo effects of phenol **6** on ASM were similar to its positive effect on ex vivo ASM relaxation. In organ bath experiments on guinea pig tracheal smooth muscle (ex vivo), phenol **6** significantly relaxed substance P induced contraction.[4] Other useful pharmacological properties of ligand **6** include the anti-mucogenic property for treatment of asthmatics.[4]

To formulate a single compound that can mitigate both AHR and airway inflammation, GABA$_A$R proteins expressed on immune/inflammatory cells were targeted, which would respond similarly to the effects of GABA on GABA$_A$Rs expressed in the brain. It has been demonstrated that CD4$^+$ T lymphocytes responded proportionately to phenol **6** in the presence of GABA. The lung eosinophilic inflammation due to ovalbumin allergen was attenuated, as well. Ligand **6** demonstrated a significant decrease in CD4$^+$ T cells in BALF and changed transmembrane current in a dose dependent manner, although the exact mechanism of transmembrane current mediated reduction in T-cell population is yet to be elucidated.[4]

The 3-alkyl-1,2,4-oxadiazoles **24**-**26** were designed as bioisosteric replacements of the C-3 ester function since such alteration often results in superior drug properties which include longer in vivo duration of drug-action. These compounds showed promising results in a cytotoxicity assay on several cell-lines where none of them were cytotoxic anywhere near therapeutic dose for asthma. Gratifyingly, cytotoxicity was not observed in lung cells. The 1,3-oxazole **28**, which is a non-conventional ester bioisostere, did not exhibit any cytotoxicity up to 400 µM in three different cell lines. Although oxazole **28** showed significant sensorimotor impairment in a rotorod assay at high concentrations, it showed pronounced relaxation in pre-contracted guinea pig tracheal rings, which was comparable with XHE-III-74 **7**. As indicated by the CNS side effects, oxazole **28** could travel across the BBB. As inferred from this observation, a more polar derivative (i.e., higher

hydrophilicity) was designed. The C-8 phenolic C-3 1,3-oxazole **29** showed superior microsomal stability both on human and murine liver microsomes. The phenolic oxazole **29** was also not cytotoxic up to 400 µM in kidney and liver cells. As desired, oxazole **29** did not show any sensorimotor impairment in rotorod assay at a dose as high as 100 mg/kg, obviously due to low brain distribution, while showing promising relaxation in guinea pig ASM. **Although in initial experiments, oxazole 29 did not show desired promise in alleviating AHR and modulating inflammatory cells, it evoked very strong GABA induced current in CD4$^+$ T lymphocytes in electrophysiological measurements.[229] It is hoped that oxazole 29 could be an excellent lead for further developments because of its promising properties in other useful criteria.**

Tetrazole **31** was designed as a carboxylic acid bioisostere. The tetrazole exhibited much better stability as compared to the parent carboxylic acid **9** both in human and mouse liver microsomes. It did not show any cytotoxicity in several cell lines and did not exhibit CNS side effects in the rotorod assay. Unfortunately, tetrazole **31** failed to show promising pharmacokinetic properties due to its rapid excretion after oral administration.[229]

5. Conclusion

Classical benzodiazepines have demonstrated many useful clinical applications as evidenced by their presence in the market for the last five decades lacking a better replacement. Over the years, numerous promising candidates to treat asthma have appeared, but failed due to poor pharmacokinetic properties and adverse CNS effects. The primary goal of this research was to further develop the promising α_4-subtype selective $GABA_AR$ ligand, lead compound XHE-III-74, for better subtype selectivity, efficacy, *in vivo* stability, as well as superior modulation of airway hyper-responsiveness, and effective and rapid relaxation of ASM constriction. All the while avoiding brain exposure to prevent CNS related adverse effects consequently, work toward development of novel asthma drug with an innovative mechanism of action. Specifically to find a new drug candidate for the treatment of asthma by targeting the $GABA_ARs$ expressed in the lung airway smooth muscle (ASM) and inflammatory cells of the peripheral nervous system. This is a novel mechanism of action and has now shown promising developments toward a novel treatment to manage asthma. This approach should not only be economically more viable but would be a direct and sustainable approach.

The relaxation of ASM and reduction of AHR by XHE-III-74 **7** has been confirmed but it did not show any reduction in airway inflammation. In addition, poor microsomal stability and an inferior pharmacokinetic profile, as well as CNS side effects indicated the requirement for further modification and optimization of this drug candidate. Subsequently, the ethyl ester analog **5** (XHE-III-74EE) elicited better microsomal stability, ASM relaxation, AHR reduction, and reduction of inflammation. However, it suffered from poor pharmacokinetic properties and CNS adverse effects. Fortunately, further modification at the same position (C-3) gave another good candidate,

the dimethyl amide **16** which did not show any CNS activity but also suffered from a poor PK profile and inability in mitigating airway inflammation. In continuation of the development process, the carboxylic acid derivative XHE-III-74A **9,** while showing promise in microsomal stability, ASM relaxation, avoiding CNS exposure and reduction in inflammation, suffered from lack of AHR reduction and inferior PK properties. This led to the development of phenolic ethyl ester derivative of XHE-III-74 **6**, which has shown desirable properties in all the criteria for treatment of asthma since it has exhibited good metabolic stability, better pharmacokinetic properties, and no CNS activity. Furthermore, phenol **6** exhibited ASM relaxation, AHR mitigation properties, as well as reduction of airway inflammation. However, despite the fundamental successes with **6** and 3 other analogs to treat asthma modifications built on the results obtained thus far, may provide even better ligands to treat asthmatic patients.

In addition, a number of other derivatives were prepared which include different C-8 alkyl substituents and ester as well as carboxylic acid bioisosteric moieties at C-3 still await their complete biological evaluation. It is hoped that those experiments would result in GABA$_A$R ligands with superior drug properties in all aspects, or at the least, will provide important leads for further development of next generation asthma drug candidates using the current strategy.

In conclusion, the goal of this research was not only to understand the chemical aspects of the GABA$_A$Rs and the effects of subtype selective ligands on the GABA$_A$R, but also to apply current knowledge in this area to design novel GABA$_A$R ligands to address unmet clinical demands to treat asthmatic patients young and old. In terms of outcome, the purpose was to provide aid and a better treatment option to the individuals who live with asthmatic symptoms. It is felt some of the ligands developed here can do just that. It is expected that the framework of this research will lead toward those objectives.

6. Methods

Reagents[2]

Indomethacin, acetylcholine, N-vanillylnonanamide, histamine, and pyrilamine (Sigma; St. Louis, MO, USA); MK501 (Tocris Bioscience; Ellisville, MO, USA); tetrodotoxin (Calbiochem; San Diego, CA, USA); test compounds CMD-45 and XHe-III-74 (designed and synthesized by Dr. James Cook's laboratory in the Department of Chemistry and Biochemistry, University of Wisconsin-Milwaukee); purified house dust mite (HDM) antigen (Greer Laboratories; Lenoir, NC, USA).

Experimental Animals[2]

All studies were approved by the Columbia University Institutional Animal Care and Use Committee. The 8 to 10 week old male mice with a global genetic deletion of the $GABA_AR$ α_4 subunit (gabra4 KO; originally a gift of Dr. Gregg Homanics, University of Pittsburgh)[236] and/or their corresponding background wild type C57/Bl6 mice (WT) were utilized for all mouse studies. Prior to tissue harvests, all animals were euthanized with an overdose of intraperitoneal (i.p.) phenobarbital (100 mg/kg). For in vivo airway resistance testing, wild type C57/Bl6 mice underwent house dust mite (HDM) antigen sensitization to induce an asthmatic phenotype. Briefly, all mice were exposed to 30 Eg of intranasal purified HDM or vehicle (PBS) during isoflurane anesthesia daily for 3 weeks prior to airway resistance testing.

Human Tissue[2]

Human trachea and bronchi samples were collected from healthy donor lungs at the time of lung transplant surgery (surgical discards). All experiments using these tissues were deemed non-human subjects research after review by Columbia University's Institutional Review Board.

6.1 Oocyte Electrophysiological Studies (Dr. Margot Earnst at the Medical University of Vienna)[2]

To generate the respective mRNAs, cDNAs of rat $GABA_A$ receptor subunits (each α subunit with $β_3$ and $γ_2$, or $α_4$ with $β_3$ and δ) were used, which were then injected into Xenopus laevis oocytes (Nasco, Fort Atkinson, WI, USA) as described previously.[209] For electrophysiological recordings, oocytes were placed on a nylon-grid in a bath of Xenopus Ringer solution (XR, containing (in mM): 90 NaCl, 5 HEPES-NaOH (pH 7.4), 1 $MgCl_2$, 1 KCl and 1 $CaCl_2$). The oocytes were impaled with two microelectrodes (2-3 mυ, filled with 2 mM KCl) for current measurements. The oocytes were constantly washed by a flow of 6 ml/min XR, which could be switched to XR containing GABA and/or ligands (CMD-45 or XHe-III-74). Both ligands were diluted into XR from DMSO-solutions which resulted in a final concentration of 0.1% DMSO. The ligands, CMD-45 and XHe-III-74 were pre-applied for 30 sec prior to the addition of GABA, which was co-applied with the drugs until a peak response was observed. As identical peak responses were observed after pre-applied ligand compared to co-applied ligand, the datasets were completed by co-application of GABA at EC_3 with the ligand. To ensure full recovery from desensitization, between two applications, oocytes were washed in XR for up to 15 minutes. All recordings were performed at room temperature at a holding potential of -60 mV using a Dagan TEV-200A two electrode voltage clamp or a Dagan CA-1B Oocyte Clamp (Dagan Corporation, Minneapolis, MN). Data were digitized and recorded using a Digidata 1322A data acquisition system (Axon Instruments, Union City, CA, USA).

117

6.2 Mouse Tracheal Ring Organ Bath Experiments (Dr. Charles Emala at Columbia University)[1,2]

Mouse tracheas were removed from WT and gabra4 KO mice and placed in modified Krebs-Henseleit (KH) buffer of the following composition in mM: 115 NaCl, 2.5 KCl, 1.91 $CaCl_2$, 2.46 $MgSO_4$, 1.38 NaH_2PO4, 25 $NaHCO_3$, and 5.56 D-glucose at pH 7.4. The tracheas were then mounted on wire pins in a myograph system (DMT, Ann Arbor, MI) and held at a resting tension of 5 mN for one hour in buffer that was continuously bubbled with 95% O_2/5% CO_2 (buffer was exchanged every 15 minutes) at 37°C. By following this equilibration period, three acetylcholine (ACh) dose-response curves were constructed (100 nM-1 mM) with extensive buffer exchanges and a resetting of resting tension to 5 mN between dose-response challenges. After determining the ACh EC_{50} for each tracheal ring, the rings were contracted with their respective EC_{50} concentration of ACh, their contraction force was allowed to plateau, and the rings were exposed to concentration ranges of CMD-45 (25 to 100 µM), XHe-III-74 (10 to 50 µM) or DMSO (0.2%; vehicle). The amount of residual contractile force was measured after 30 minutes and compared to the initial contractile force to determine the percent of relaxation. Each ring was only exposed to a single concentration of CMD-45, XHe-III-74, or DMSO once (multiple concentrations and/or compounds were not tested on the same ring).

6.3 Human Airway Smooth Muscle Strip Organ Bath Experiments (Dr. Charles Emala at Columbia University)[2]

Human ASM strips were dissected from trachea and mainstem bronchi samples and the epithelium was removed. Strips were suspended at 1.5 g resting tension in KH buffer with 10 EM indomethacin (to block endogenous release of prostanoids), as previously described (5-7). Briefly, strips were suspended in a water-jacketed, 2 ml glass organ baths at 37° C (Radnoti Glass

Technology, Inc., Monrovia, CA, USA) and attached to Grass FT03 force transducers (Grass Telefactor, West Warwick, RI) coupled to a computer using BioPac hardware and Acqknowledge 7.3.3 software (Biopac Systems, Inc., Goleta, CA, USA). The KH buffer was continuously bubbled with 95% O_2/5% CO_2 and tissues were allowed to equilibrate at 1.5 g isotonic force for 1 hour with fresh KH buffer changes every 15 min.

The ACh EC_{50} was calculated for each strip (based on three cycles of exposure to 100 nM-100 EM ACh). Tetrodotoxin (1 EM; antagonist of endogenous neuronal-mediated effects), pyrilamine (10 EM; H1 histamine receptor antagonist), and MK571 (10 EM; leukotriene D4 antagonist) were then added to the buffer to eliminate potentially confounding effects of endogenous contractile mediators. Each strip was then contracted with its EC50 concentration of ACh. After the contractile force reached steady state, the strips were exposed to concentration ranges (10-100 μM) of CMD-45, XHe-III-74, or 0.2% DMSO. The amount of residual contractile force was measured after 30 minutes and compared to the initial contractile force to determine the percent of relaxation. Each strip was only exposed to CMD-45, XHe-III- 74, or DMSO once (multiple concentrations and/or compounds were not tested on the same strip).

Separate human ASM organ bath experiments were conducted to determine if CMD-45 or XHe-III-74 potentiated the relaxation induced by the β2-agonist albuterol (first-line asthma rescue therapy). In these studies, human ASM was contracted to a stable plateau of force with an EC_{50} concentration of acetylcholine and then increasing concentrations of albuterol were added to each organ bath at 7 minute intervals (half-log increments 100 pM – 10 μM). Concurrent with the 500 pM albuterol addition, a single exposure of CMD-45, XHe-III-74 (25 μM each) or vehicle (0.2% DMSO) was added to each bath.

6.4 In Vivo Mouse Respiratory System Resistances Testing (Dr. Charles Emala at Columbia University)[2]

In vivo airway resistances were assessed using a flexiVent FX1 module with an in-line nebulizer (SciReq, Montreal, QC, Canada), as described previously,[1,237] using HDM-sensitized WT mice. Briefly, the mice were anesthetized with pentobarbital (i.p., 50 mg/kg), paralyzed with succinylcholine (i.p., 10 mg/kg), and mechanically ventilated via a tracheostomy (tidal volume 10mg/kg, 150 breaths/min). Mice were nebulized by XHe-III-74 (25 μl, 10 mM) or vehicle (25% ethanol in PBS) 10 minutes prior to measuring respiratory system resistances (RRS) by the forced oscillatory technique during a graded, nebulized methacholine challenge (0-50 mg/ml). Throughout the experiment EKG and temperature monitoring were performed. Lung resistance values for each mouse at each methacholine dose represent an average of three measurements.

6.5 In Vitro Human Airway Smooth Muscle Cell Calcium Dynamics (Dr. Charles Emala at Columbia University)[2]

Primary human airway smooth muscle cells (collected from healthy lung transplantation donor tissue)[238] were grown to 80% confluence as monolayers in phenol red-free 50%/50% DMEM/F12 media containing 10% FBS and 1X antibiotics/antimycotics on clear-bottomed, black-walled 96 well plates. The cells were incubated in serum-free basal media for 48 hours, prior to each experiment. The cells were then washed with Hank's balanced salt solution (HBSS) containing the following in mM: NaCl 138, KCl 5.3, $CaCl_2$ 2.5, $MgSO_4$ 0.4, $MgCl_2$ 0.49, Na_2HPO_4 0.34, $NaHCO_3$ 4.2, KH_2PO_4 0.44, dextrose 5.5, hepes 20, pH 7.4. Cells were then incubated in HBSS containing the calcium indicator Fura-2 AM (5 μM; Life Technologies, Grand Island, NY, USA) for 45 minutes at 37°C. Following the dye loading, cells were washed with HBSS three times, pretreated

with concentration ranges (10-50 µM) of CMD-45, XHe-III-74, or DMSO (0.1%), and allowed to rest 15 minutes at 37°C. The cells were then continuously excited (alternatively at 340 and 380 nm) every 4 seconds and the resultant emission at 510 nM was recorded using a FlexStation3 microplate reader (Molecular Devices, Sunnyvale, CA) at 37°C during the addition of 10 µM histamine using the injection feature of the FlexStation3. In separate experiments, after dye loading, the cells were washed with Hank's balanced salt solution containing no calcium. The cells remained in this buffer during pretreated with 100 µM CMD-45, XHe-III-74, or DMSO (0.1%) and during fluorescent recording with histamine exposure.

Experimental animals[3]

The 5-10 week old male BALB/c and Swiss Webster mice (Charles River Laboratory, WIL, MA) and adult (425-450 g) male Hartley guinea pigs (Charles River Laboratory, WIL, MA) were used for the experiments. The animals were housed under specific pathogen free conditions, under standard conditions of humidity, temperature and a controlled 12 h light and dark cycle and had free access to food and water. All animal experiments were in compliance with the University of Wisconsin, Milwaukee or Columbia University Institutional Animal Care and Use Committees (IACUC).

6.6 Microsomal Stability Assay Procedure (Revathi Kodali at UWM)[3]

The 4 µL of 1 mM test compound at a final concentration of 10 µM in DMSO were preincubated at 37°C for 5 minutes on a digital heating shaking dry bath (Fischer Scientific, Pittsburgh, PA) in a mixture containing 282 µL of water, 80 µL of phosphate buffer (0.5 M, pH 7.4) 20 µL of NADPH Regenerating System Solution A (BD Bioscience, San Jose, CA) and 4 µL of NADPH Regenerating System Solution B (BD Bioscience, San Jose, CA) in a total volume of 391.2 µL.

Following preincubation, the reaction was initiated by addition of 8.8 μL of either human liver microsomes (BD Gentest, San Jose, CA) or mouse liver microsomes (Life technologies, Rockford, IL) at a protein concentration of 0.5 mg/mL. Aliquots of 50 μL were taken at time intervals of 0 (without microsomes), 10, 20, 30, 40, 50 and 60 minutes. Each aliquot was added to 100 μL of cold acetonitrile solution containing 1 μM of verapamil HCl as an internal standard. This was followed by sonication for 10 seconds and centrifugation at 10,000 rpm for 5 minutes. Then 100 μL of the supernatant was transferred into Spin-X HPLC filter tubes (Corning Incorporated, NY) and centrifuged at 13,000 rpm for 5 minutes. The filtrate was diluted 100 fold and subsequently analyzed by LC-MS/MS with a Shimadzu LCMS 8040, (Shimadzu Scientific Instruments, Columbia, MD). The ratio of the peak areas of the internal standard and the test compound was calculated for every time point and the natural log of the ratio was plotted against time to determine the linear slope (k). The metabolic rate (k*C0/C), half-life (0.693/k), and internal clearance (V*k) were calculated, where k is the slope, C0 is the initial concentration of test compound, C is the concentration of microsomes, and V is the volume of incubation in μL per microsomal protein in mg. All experiments were repeated three times in duplicates.

6.7 Cytotoxicity Assay (Dr. Michael Stephen and Dr. Gloria Forkuo at UWM)[3]

Human liver hepatocellular carcinoma (HEPG2), human embryonic kidney 293T (HEK293T) and human bronchial epithelial (BEAS 2B) cell lines were purchased (ATCC) and cultured in 75 cm2 flasks (CellStar). Cells were grown in DMEM/High Glucose (Hyclone, #SH3024301) media to which non-essential amino acids (Hyclone, #SH30238.01), 10 mM HEPES (Hyclone, #SH302237.01), 5 x 106 units of penicillin and streptomycin (Hyclone, #SV30010), and 10% of heat inactivated fetal bovine serum (Gibco, #10082147) were added. Cells were harvested using 0.05% Trypsin (Hyclone, #SH3023601), washed with PBS, and dispensed into sterile white,

optical bottom 384-well plates (NUNC, #142762). After three hours, small molecule solutions were transferred with a Tecan Freedom EVO liquid handling system equipped with a 100 nL pin tool (V&P Scientific). The controls were 3-dibutylamino-1-(4-hexyl-phenyl)-propan-1-one (25 mM in DMSO, positive control) and DMSO (negative control). The cells were incubated for 48 hours followed by the addition of CellTiter-Glo™, a luminescence-based cell viability assay (Promega, Madison, WI). All luminescence readings were performed on a Tecan Infinite M1000 plate reader. The assay was carried out in quadruplet with three independent runs. The data was normalized to the controls and analyzed by nonlinear regression (GraphPad Prism).

6.8 Rotarod Assay (Nicholas Zahn at UWM)[3]

The swiss Webster mice were trained to maintain balance at a constant speed of 15 rpm on the rotarod apparatus (Omnitech Electronics Inc. Nova Scotia, Canada) until mice could perform for 3 min at three consecutive time points. Separate groups of mice received intraperitoneal (i.p.) injections of vehicle (10% DMSO, 40% propylene glycol and 50% PBS) or test compounds. Diazepam was used as a positive control compound (5 mg/kg) in an approximate volume of 100 ml. Ten minutes after each injection, mice were placed on the rotarod for 3 min. A fail was assigned for each mouse

that fell from the rotarod prior to 3 min. Mice were rested two to three days before administration of another dose or a different compound.

6.9 Guinea Pig Airway Smooth Muscle Organ Bath (Dr. Charles Emala at Columbia University)[3]

Guinea pigs were anesthetized with intraperitoneal pentobarbital (100 mg/kg). Their tracheas were then surgically removed and transected into cross-sectional sections containing two cartilaginous rings as described previously.[15] The epithelium was removed with cotton swabs and the rings were suspended by two silk threads in 4 mL jacketed organ baths (Radnoti Glass Technology). One thread was attached to a Grass FT03 force transducer (Grass- Telefactor) coupled via Biopac hardware to a computer with Acknowledge 7.3.3 software (Biopac Systems) for continuous digital recording of muscle tension. The rings were bathed in 4 mL of KH buffer solution (composition in mM: 118 NaCl, 5.6 KCl, 0.5 $CaCl_2$, 0.2 $MgSO_4$, 25 $NaHCO_3$, 1.3 NaH_2PO_4, 5.6 D-glucose) with 10 mM indomethacin (DMSO vehicle final concentration of 0.01%), which was continuously bubbled with 95% O_2 and 5% CO_2 at pH 7.4, at 37 ^{O}C. The rings were equilibrated at 1 g of isotonic tension for 1 h with new KH buffer added every 15 min. All rings were precontracted with 10 mM N-vanillylnonanamide (capsaicin analog) and then two cycles of cumulatively increasing concentrations of acetylcholine (0.1-100 µM) with extensive buffer washes between and after those two cycles with resetting of the resting tension to 1.0 g. To eliminate the confounding effects of airway nerves and histamine receptors, tetrodotoxin (1 µM) and pyrilamine (10 µM) were added to the buffer. After a stable baseline tension of 1.0 g was established, tracheal rings were contracted with 1 µM substance P. After the peak contraction was reached, 50 µM of compound **16** (or the vehicle control 0.1% DMSO) was added to each bath. The percentage of initial contraction remaining at 15, 30, 45, and 60 min after compound exposure was compared between groups.

6.10 Human Airway Smooth Muscle Organ Bath (Dr. Charles Emala at Columbia University)[4]

The human trachea were obtained from healthy donor lungs incidental to lung transplantations and airway smooth muscle strips were dissected from them. All the studies were reviewed by the Columbia University IRB and deemed not to be human subject research. The strips were suspended as above in organ baths in oxygenated KH buffer at 37 °C at 1.5g of resting tension. This was followed by equilibration for 1h with buffer exchanges every 15 min, after which the strips were contracted with 3 cycles of increasing concentrations of acetylcholine (100 nM - 1 mM) with extensive buffer exchanges between and after these pre-contractile challenges. Before each strip was contracted to its individually calculated EC_{50} concentration of acetylcholine MK571 (10 μM), pyrilamine (10 μM) and tetrodotoxin (1 μM) were added to the buffer. When a plateau in the increase in contractile force was achieved (typically 15 min), 100 μM of test compound or its vehicle (0.2% ethanol) was added to the buffer and the maintenance of contractile force was continuously measured over 1h. The remaining contractile force at 15, 30, 45 and 60 min was expressed as a percentage of the initial acetylcholine-induced contractile force.

6.11 Assessment of Airway Hyper-Responsiveness (Dr. Gloria Forkuo at UWM)[3]

Airway hyper-responsiveness to methacholine in conscious, spontaneously breathing animals was measured by DSI's Buxco® FinePointe Non-Invasive Airway Mechanics (NAM) instrument.[15] Before measurements were taken, mice were acclimated to the chamber for 15 min daily for 5 days. The chambers were also calibrated each time before data collection. Briefly, the nasal chamber in combination with the thoracic chamber permits computation of Specific Airway Resistance (sRaw). The FinePointe software computes sRaw with all other ventilatory parameters derived by the NAM analyzer. Mice were exposed to aerosolized PBS (for the baseline

measurement) or methacholine (1.56-12.5 mg/mL) for 1 min and readings were taken and averaged for 3 min after each nebulization. Data obtained were presented as sRaw versus aerosolized methacholine concentration (mg/ml). Data analysis was carried out using 2way ANOVA repeated measures with Bonferroni post-test. Overall p-value was 0.0937 and F = 1.763. The Bonferroni post-test gave significance for 12.5 mg methacholine as indicated in Figure 30.

6.12 Pharmacokinetic Study (Revathi Kodali at UWM)[3]

The female Swiss Webster mice received i.p. injections of vehicle or each ligand formulated in DMSO/ propylene glycol/ PBS, 10:40:50, v/v/v) and injected at a dose of 5 mg/kg. At different time points, the blood (collected into heparinized tubes, 50 µL of 1 mg/mL heparin), lungs, and brain were harvested and the samples were stored in liquid nitrogen until analysis.

Blood samples were thawed on ice, vortexed for 10 seconds, and a 100 µL aliquot was taken and added to 400 µL cold acetonitrile containing [20 nM] internal standard 1 (Hz166). Samples were vortexed for 30 seconds and centrifuged at 13,000 RPM for 3 minutes. The supernatant layer was then transferred to clean tubes and evaporated overnight. The residue was reconstituted with 300 µL of mobile phase and spin-filtered through 0.22 µm nylon centrifugal filter units (Costar). After reconstitution, verapamil (internal standard 2) was added and 5 µL of the sample was injected into the LC–MS/MS.

The brain and lung tissue samples were stored in liquid nitrogen prior to homogenization and extraction. The whole organs were thawed over ice, weighed, and homogenized directly into 500 µL of ACN containing internal standard 1 (HZ166) using a Benchmark Scientific BeadBug Homogenizer with three 3.2mm stainless steel beads. Samples were homogenized for 30 seconds,

and centrifuged for 3 minutes at 13,000 RPM. This process was repeated for a total of three extractions.

The supernatants were combined and prepared in the same manner as the blood samples for LC-MS/MS analysis.

High performance liquid chromatography (HPLC) was performed with Shimadzu Nexera X2 LC30AD series pumps (Shimadzu, Kyoto, Japan) that include a 20A5R degassing unit, SIL 30AC autosampler and a 20A column oven. Analytes were separated by a Restek Ultra Biphenyl II column (2.1 mm × 50 mm, 5 um particle size, Restek, California, US) under gradient elution at a flow rate of 0.6 mL/min. The mobile phase was acetonitrile and water (both containing 0.1% formic acid). Time program: 10% B → 99% B (3 min), hold at 99% B (3.75 min), return to 10% B (4 min), hold (4.5 min). Column Temperature: 50°C.

Analytes were monitored under positive mode on a Shimadzu 8040 triple quadrupole mass analyzer (Shimadzu, Kyoto, Japan) electrospray (ESI) and atmospheric pressure ionization (APCI) run in dual (DUIS) mode. The following transitions were monitored in multiple reaction monitoring (MRM) mode. Ion transition pairs for 17 are 340.85 > 296.00, 340.85 > 277.95, 340.85 > 268.10 and 340.85 > 227.15. Transition pairs for HZ-166 are m/z 356.90 > m/z 311.15, m/z 356.90 > m/z 283.15, and m/z 356.90 > m/z 282.15. Transition pairs for verapamil (internal standard) are 454.70 > 165.15, 454.70 > 150.20, and 454.70 > 303.30. Collision energy was optimized for each transition to obtain optimal sensitivity. The mass spectrometer was operated with the heat block temperature of 400°C, drying gas flow of 15 L/min, desolvation line temperature of 250 °C, nebulizing gas flow of 1.5 L/min, and both needle and interface voltages of 4.5 kV. The response acquisition was performed using LabSolutions software.

The sample preparation of calibration standards and quality control for LC–MS/MS: HZ-166 was chosen as an internal standard (I.S.) because it has a similar chemical structure as that of **17** and was therefore used to account for sample dilution, evaporation, and matrix effects. Verapamil was also used as a second standard to monitor instrumental variations. The stock solutions of all were prepared at a concentration of 2 mg/mL separately in ACN and stored in a −20 °C freezer, with the exception of the acid which was prepared in 80:20 ACN:water. The intermediate working solutions of each were prepared by serial dilution with mobile phase (80:20, ACN:water with 0.1% formic acid). Calibration curve cocktails were prepared at concentrations of 1, 5, 10, 15, 25, 50, 75, 100, and 150 nM.

The intra-run/within-run validation was performed at concentrations of 10, 25 and 75 nM with three replicates for each concentration. For separate validations, separate standard curves were freshly prepared. The standard curves were fitted by a linear regression and the validation samples were calculated back by the calibration curve of that day. The mean and the coefficient of variance (CV) were calculated accordingly. Accuracy was calculated by comparing calculated concentrations to corresponding nominal.

Pharmacokinetic parameters were calculated with PK solutions software 2.0 and fitted to the following equation: $c = A \cdot e^{-at} + B \cdot e^{-bt}$. Due to the rapid absorption two phases could be identified as the distribution/absorption phase and the elimination phase.

6.13 Patch clamp assay (Amanda Neiman at UWM)[3]

HEK293T stably expressing $\alpha_1\beta_3\gamma_2$ GABA$_A$R or $\alpha_4\beta_3\gamma_2$ were maintained RPMI 1640 medium with L-glutamine supplemented with 10% (v/v) fetal bovine serum and 1% penicillin/streptomycin. Automated patch-clamp studies were conducted as described previously.[15] Briefly, the IonFlux plate layout consists of units of 12 wells: two wells contain intracellular solution (ICS containing 140 mM CsCl, 1 mM CaCl$_2$, 1 mM MgCl$_2$, 11 mM EGTA, 10 mM HEPES, pH 7.2 with CsOH), one contains cells diluted in extracellular solution (ECS containing 140 mM NaCl, 5.4 mM KCl, 1 mM CaCl$_2$, 10 mM D-glucose monohydrate, and 10 mM HEPES, pH 7.4 with NaOH), eight contain different concentration of amide **16** in the presence of GABA at 0.1% DMSO. Well 1 is for waste collection. The cells are captured from suspension by applying suction to microscopic channels in ensemble recording arrays. Once the array is fully occupied, the applied suction breaks the membranes of captured cells, which establishes the whole cell voltage clamp. For compound applications, pressure is applied to the appropriate compound wells, which introduces the compound into the extracellular solution rapidly flowing over the cells. For recording GABA$_A$R induced currents, cell arrays were voltage clamped at a hyperpolarizing holding potential of -80 mV. Prior to use on the automated patch clamp, cells were centrifuged at 380g for 5 minutes and resuspended gently in ECS. This was repeated two more times before the cells were dispensed into the plate. All compound applications were carried out for 3 seconds and this was followed by a 5 second washout.

7. Experimental

7.1 5-Methoxyanthranilic acid (2)

A solution of 2-nitro-5-methoxybenzoic acid **1** (60.3 g, 306 mmol) in EtOAc (1.5 L) was degassed under reduced pressure and refilled with argon (repeated 3 times). Palladium (10% w/w on carbon, 3.9g, 1.2 mol%) was added to the above solution. The reaction flask was evacuated under reduced pressure and refilled with H_2 from a balloon (repeated 3-4 times to make sure that the solution was saturated with H_2). The reaction mixture was stirred at rt for 6 h. After the completion of the reaction (TLC, silica gel), the solution was filtered over a bed of celite to remove the Pd. The solids were washed with ethyl acetate. The solvent was removed under reduced pressure to yield acid **2** as a yellow solid in 97% (49.7 g) yield: M.p = 147-149 ˚C; ^{1}H NMR (300 MHz, CDCl$_3$) δ 3.66 (s, 3H), 6.71 (d, 1H, J = 9.0 Hz), 6.94 (dd, 1H, J = 9.0 Hz, 3.0 Hz), 7.19 (d, 1H, J = 3.0 Hz), 8.40 (bs, 2H). The spectral data matched the reported values[16]. This material was employed directly in the next step.

7.2 5-Methoxyisatoic anhydride (3)

The 5-methoxyanthranilic acid **2** (30 g, 179 mmol) was dissolved in a mixture of H_2O (1.2 L) and conc HCl (15 mL), and this was followed by the addition of triphosgene (63.8 g, 215 mmol). The contents were stirred at rt for 3-4 h until the completion of the reaction (TLC, silica gel). A white solid precipitated from the solution after completion. The solids were collected by filtration and washed with H_2O (4 L). The solids were dried under vacuum to give pure anhydride **3** in 89% (30.7 g) yield: M.p = 237-239 ˚C; ^{1}H NMR (300 MHz, CDCl$_3$) δ 3.65 (s, 3H), 7.11 (d, 1H, J = 8.9 Hz), 7.35 (dd, 1H, J = 8.9 Hz, 2.7 Hz), 7.19 (d, 1H, J = 2.7 Hz), 11.61 (bs, 1H). The spectral data were identical with the reported values[16]. This material was employed directly in the next step.

Triphosgene reacts to give toxic phosgene; care must be exercised. The phosgene itself smells like new mown hay. Do not breath it.

7.3 (S)-2,3-Dihydro-7-methoxy-1H-pyrrolo[2,1-c][1,4]benzodiazepine-5,11(10H,11aH)-dione (4)

A mixture of 5-methoxyisotoic anhydride **3** (30.7 g, 158.9 mmol) and L-proline (20.2 g, 174.8 mmol) in dry DMSO (300 mL) was heated with stirring at 160 ˚C for 2 h. The white turbid reaction mixture, which resulted, became a clear brown solution as the temperature was increased to above 80 ˚C. After the completion of the reaction, on examination by TLC (silica gel), the solution was cooled to rt. The mixture was poured into 250 mL of ice water to yield benzodiazepine **4** as a white solid. The solids were collected by vacuum filtration and washed with ice cold water (2 X 50 mL). The filtrate was extracted with ethyl acetate and the solvent was removed under reduced pressure to yield solid diazepine **4**. The combined solids were dried in a vacuum oven at 80 ˚C for 4 h. The yield of **4** was 96% (37.9 g): M.p = 214-216 ˚C; $[\alpha]_D^{25}$= +444.40 (c 1%, in CH_2Cl_2); ^{1}H NMR (300 MHz, $CDCl_3$) δ 1.82-2.01 (m, 3H), 2.50-2.51 (m, 1H), 3.40-3.49 (m, 1H), 3.56-3.63 (m, 1H), 3.78 (s, 3H), 4.07-4.10 (m, 1H), 7.07 (d, 1H, J = 8.7 Hz), 7.13 (dd, 1H, J = 8.7 Hz, 3.0 Hz), 7.26 (d, 1H, J = 3.0 Hz), 10.30 (bs, 1H). The spectral data were identical to the reported values[16]. This material was employed directly in the next step.

7.4 (S)-Ethyl-7-methoxy-9-oxo-11,12,13,13a-tetrahydro-9H-benzo[e]imidazo[5,1-c]pyrrolo-[1,2-a][1,4]diazepine-1-carboxylate (5)

A well dried reaction flask was evacuated completely and flushed with argon. The flask was then charged with diazepine **4** (37 g, 150.2 mmol) in dry THF (800 mL). The turbid solution was cooled to -20 ˚C. Potassium *tert*-butoxide (good material, 33.7 g, 300.4 mmol) was added to the flask and

the solution was stirred at rt for 1 h. Good diethyl chlorophosphate (43.4 mL, 300.4 mmol) was then slowly added to the reaction mixture at -20 ˚C and it was allowed to stir at rt over a period of 2-3 h. The cloudy reaction mixture became a clear golden-brown solution. After complete consumption of the starting material **4** (TLC, silica gel), the reaction was cooled to -20 ˚C, after which ethyl isocyanoacetate (32.8 mL, 300.4 mmol) and potassium *tert*-butoxide (33.7 g, 300.4 mmol) were added. The reaction mixture was stirred at rt for 8 h. The reaction was quenched with a saturated aq solution of $NaHCO_3$ (80 mL). The THF was removed under reduced pressure and the aq layer was extracted with CH_2Cl_2 (300 mL X 3). The combined organic layer was separated and washed with brine (400 mL) and dried (Na_2SO_4). The CH_2Cl_2 was removed under reduced pressure and the dark brown pasty liquid residue, which resulted, was washed with ether to yield the crude ethyl ester **5**. This crude solid was recrystallized from CH_2Cl_2 to yield ethyl ester **5** as a pure white solid in 60% (30.85 g) yield: M.p = 195-197 ˚C; (Lit. report: 175-176 ˚C)[16]; $[\alpha]_D^{25}=$ +18.00 (c 0.5%, in CH_2Cl_2); ^{1}H NMR (300 MHz, $CDCl_3$) δ 1.44 (t, 3H, *J* = 7.2 Hz), 2.15-2.31 (m, 3H), 3.49-3.61 (m, 2H), 3.75-3.85 (m, 1H), 3.91 (s, 3H), 4.41 (q, 2H, *J* = 7.2 Hz), 4.75 (d, 1H, *J* = 6.9 Hz), 7.15 (dd, 1H, *J* = 8.9 Hz, 3.0 Hz), 7.32 (d, 1H, *J* = 8.9 Hz), 7.59 (d, 1H, *J* = 3.0 Hz), 7.82 (s, 1H); ^{13}C NMR (75 MHz, $CDCl_3$) δ 14.3, 24.3, 28.4, 46.6, 53.4, 55.8, 61.2, 114.5, 119.7, 124.6, 126.0, 127.3, 130.6, 135.8, 137.6, 159.4, 162.6, 163.7; HRMS (ESI) $(M+Na)^+$, calcd. for $C_{18}H_{19}N_3O_4Na$ 364.1273; Found 364.1279. The spectral data were identical to the reported values[16]. This material was employed directly in the next step.

7.5   (S)-Ethyl-7-hydroxy-9-oxo-11,12,13,13a-tetrahydro-9H-benzo[e]imidazo[5,1-c]pyrrolo-[1,2-a][1,4]diazepine-1-carboxylate (6)

In an oven dried round bottom flask, dry CH_2Cl_2 (50 ml) was added and it was cooled to 0 ˚C. Then $AlCl_3$ (3 g, 22.8 mmol) and good ethanethiol (4.5 ml, 60.8 mmol) were added to the above

flask slowly at 0 ˚C. The ice bath was removed and the reaction was allowed to warm to rt. After the AlCl₃ dissolved completely, ester **5** (2.6 g, 7.62 mmol) was added to the mixture at rt and the mixture was stirred for 24 h under Ar. The reaction time will vary with the scale of the reaction. After completion of the reaction (TLC, silica gel), the solution was poured onto ice and was acidified using an aq 2N HCl solution. The solution was extracted 7 times with CH_2Cl_2 and 4 times with EtOAc, separately. Since the product was soluble in water, the extraction procedure was carried out until there was no more product observed in the aq layer (TLC, silica gel). The combined organic layer was washed with brine and dried (Na_2SO_4). The solvent was removed under reduced pressure and the residue was purified by flash column chromatography on [silica gel, 4% MeOH in CH_2Cl_2] to furnish the phenolic ethyl ester **6** as a solid (2.1 g) in 84% yield: M.p = >260 ˚C (decomp.); ¹H NMR (300 MHz, CDCl₃) δ 1.44 (t, 3H, J = 7.1 Hz), 2.19-2.42 (m, 3H), 3.55-3.64 (m, 2H), 3.81-3.89 (m, 1H), 4.42 (q, 2H, J = 7.1 Hz), 4.82 (d, 1H, J = 7.3 Hz), 7.13 (dd, 1H, J = 8.7 Hz, 2.6 Hz), 7.27-7.31 (m, 1H), 7.85 (s, 1H), 7.91 (d, 1H, J = 2.6 Hz), 9.22 (s, 1H); ¹³C NMR (75 MHz, CDCl₃) δ 14.3, 24.4, 28.4, 46.9, 53.8, 61.2, 117.5, 120.8, 124.9, 125.2, 127.7, 129.5, 136.0, 137.2, 157.6, 162.8, 164.6; HRMS (ESI) (M+H)⁺, calcd. for $C_{17}H_{18}N_3O_4$ 328.1292; Found 328.1293.

7.6 (S)-Ethyl-7-(²H₃)-methoxy-9-oxo-11,12,13,13a-tetrahydro-9H-benzo[e]imidazo[5,1-c]py-rolo[1,2-a][1,4]diazepine-1-carboxylate (5a)

To a solution of phenol **6** (1.5 g, 4.6 mmol) in CH_2Cl_2 (30 mL), Cs_2CO_3 (3 g, 9.2 mmol) was added and the mixture stirred at rt for 30 min. Then CD₃I (2.3 ml, 36.8 mmol) was added slowly and the reaction mixture was stirred at rt for 24 h. After completion of the reaction (TLC, silica gel), the mixture was quenched with cold water and extracted with CH_2Cl_2. The combined organic layer was washed with brine and dried (Na_2SO_4). The solvent was removed under reduced pressure and

the residue was purified by flash column chromatography [silica gel, 2% CH_3OH in CH_2Cl_2] to furnish ester **5a** as a solid (1.36 g) in 86% yield: M.p = 195-196 ˚C; $[\alpha]_D^{25}$= +20.00 (c 0.5%, in CH_2Cl_2); ^1H NMR (300 MHz, $CDCl_3$) δ 1.46 (t, 3H, J = 7.1 Hz), 2.17-2.36 (m, 3H), 3.54-3.63 (m, 2H), 3.77-3.84 (m, 1H), 4.43 (q, 2H, J = 7.1 Hz), 4.77 (d, 1H, J = 7.3 Hz), 7.16 (dd, 1H, J = 8.8 Hz, 2.8 Hz), 7.33 (d, 1H, J = 8.8 Hz), 7.60 (d, 1H, J = 2.8 Hz), 7.82 (s, 1H); ^{13}C NMR (75 MHz, $CDCl_3$) δ 14.3, 24.3, 28.3, 46.5, 53.4, 61.1, 114.4, 119.7, 124.5, 126.0, 127.6, 130.5, 135.8, 137.6, 159.3, 162.8, 163.7; HRMS (ESI) (M+H)$^+$, calcd. for $C_{18}H_{17}{}^2H_3N_3O_4$ 345.1637; Found 345.1635. The $\underline{^{13}C}$-D signal was not observed due to the long relaxation time, line broadening, reduced NOE effect, and spin-spin coupling.

7.7 (S)-tert-Butyl-7-methoxy-9-oxo-11,12,13,13a-tetrahydro-9H-benzo[e]imidazo[5,1-c]py-rolo[1,2-a][1,4]diazepine-1-carboxylate (7)

A flame dried round bottom flask was charged with dry THF (30 mL) and lithium rod (excess, cut into small pieces) was added. Dry *tert*-butanol (2.6 mL, 27.1 mmol) was added to the above flask at rt and the mixture which resulted was heated to 45-50 ˚C under Ar until the *tert*-butanol reacted completely. This freshly prepared lithium *tert*-butoxide solution was transferred carefully with a cannula to another flame dried round bottom flask charged with ester **5** (1.0 g, 2.71 mmol) and stirred at 50 ˚C under Ar for 30 min. After the completion of the reaction (TLC, silica gel), the flask was cooled to rt and the THF removed under reduced pressure. Ice water (10 mL) was added to the residue and it was then extracted with EtOAc. The organic layer was washed with water (2 X 10 mL) and brine (15 mL). The solvent was removed under reduced pressure and the residue was purified by flash column chromatography [silica gel, EtOAc/hexane (7:3)] to yield *tert*-butyl ester (XHE-III-74) **7** as a solid (0.72 g) in 67% yield: M.p = 115-117 ˚C (119-121 ˚C)[16]; $[\alpha]_D^{25}$= +36.00 (c 0.5%, in CH_2Cl_2); ^1H NMR (300 MHz, $CDCl_3$) δ 1.63 (s, 9H), 2.14-2.28 (m, 3H), 3.47-

3.61(m, 2H), 3.74-3.81 (m, 1H), 3.90 (s, 3H), 4.73 (d, 1H, J = 6.9 Hz), 7.14 (dd, 1H, J = 8.8 Hz, 3.0 Hz), 7.30 (d, 1H, J = 8.8 Hz), 7.57 (d, 1H, J = 3.0 Hz), 7.83 (s, 1H); ^{13}C NMR (75 MHz, CDCl$_3$) δ 24.3, 28.2, 28.3, 46.7, 53.4, 55.9, 81.9, 114.5, 119.7, 124.6, 126.1, 128.9, 130.5, 135.6, 136.5, 159.4, 162.2, 163.8; HRMS (ESI) (M+Na)$^+$, calcd. for C$_{20}$H$_{23}$N$_3$O$_4$Na 392.1586; Found 392.1574. The spectral data were identical to the reported values.[17]

Alternative Synthesis: The acid **9a** (0.1 g, 0.32 mmol) was suspended in dry toluene (15 ml) in an oven dried round bottom flask and the mixture which resulted, was heated to reflux. *N,N*-dimethylformamaide di-*tert*-butyl acetal (0.3 ml, 1.28 mmol) was added dropwise to the above refluxing mixture. The mixture was refluxed until the reaction was complete (30 mins, confirmed by TLC, silica gel). After that, the reaction mixture was cooled to rt, and then quenched with an ice cold aq NaHCO$_3$ solution followed by extraction with EtOAc (2x 10 mL). The combined organic layer was washed with brine and dried (Na$_2$SO$_4$). The solvent was then removed under reduced pressure and the residue was purified by flash column chromatography [silica gel, EtOAc/hexane (7:3)] to yield *tert*-butyl ester (XHE-III-74) **7** as a solid (0.07 g) in 60% yield.

7.8   (S)-tert-Butyl-7-(^{2}H$_3$)-methoxy-9-oxo-11,12,13,13a-tetrahydro-9H-benzo[e]imidazo[5,1-c]pyrolo[1,2-a][1,4]diazepine-1-carboxylate (7a)

The *tert*-butyl ester **7a** was prepared from ethyl ester **5a** by following the same procedure employed for preparation of *tert*-butyl ester **7** in 67% yield: M.p = 114-115 ˚C; ^{1}H NMR (300 MHz, CDCl$_3$) δ 1.65 (s, 9H), 2.15-2.34 (m, 3H), 3.50-3.63 (m, 2H), 3.77-3.84 (m, 1H), 4.75 (d, 1H, J = 7.2 Hz), 7.15 (dd, 1H, J = 8.8 Hz, 2.8 Hz), 7.27-7.32 (m, 1H), 7.59 (d, 1H, J = 2.8 Hz), 7.79 (s, 1H); ^{13}C NMR (75 MHz, CDCl$_3$) δ 24.4, 28.2, 28.4, 46.7, 53.5, 81.8, 114.4, 119.8, 124.6, 126.3, 129.3, 130.6, 135.7, 136.5, 159.3, 162.6, 163.8; HRMS (ESI) (M+H)$^+$, calcd. for C$_{20}$H$_{21}$^{2}H$_3$N$_3$O$_4$ 373.1950; Found 373.1951.

7.9 (S)-tert-Butyl-7-hydroxy-9-oxo-11,12,13,13a-tetrahydro-9H-benzo[e]imidazo[5,1-c]pyrrolo[1,2-a][1,4]diazepine-1-carboxylate (8)

The *tert*-butyl ester **8** was prepared from phenolic ethyl ester **6** following the same procedure employed for the preparation of *tert*-butyl ester **7** in 65% yield: M.p = 174-175 °C; ^{1}H NMR (300 MHz, CDCl$_3$) δ 1.63 (s, 9H), 2.09-2.34 (m, 3H), 3.50-3.62 (m, 2H), 3.77-3.85 (m, 1H), 4.79 (d, 1H, *J* = 7.1 Hz), 7.10 (dd, 1H, *J* = 8.6 Hz, 2.2 Hz), 7.23-7.28 (m, 1H), 7.77 (bs, 1H), 7.85 (s, 1H), 9.75 (bs, 1H); ^{13}C NMR (75 MHz, CDCl$_3$) δ 24.4, 28.2, 28.3, 46.9, 53.7, 82.0, 117.4, 120.7, 124.9, 125.1, 129.1, 129.6, 135.8, 136.2, 157.7, 162.3, 164.6; HRMS (ESI) (M+H)$^+$, calcd. for C$_{19}$H$_{22}$N$_3$O$_4$ 356.1605; Found 356.1615.

7.10 (S)-7-Methoxy-9-oxo-11,12,13,13a-tetrahydro-9H-benzo[e]imidazo[5,1-c]pyrrolo[1,2-a][1,4]diazepine-1-carboxylic acid (9)

The ester **5** (2.12 g, 6.21 mmol) was dissolved in a mixture of EtOH (4 mL) and H$_2$O (3 mL), after which solid NaOH (1.2 g, 31.0 mmol) was added to the solution. This reaction mixture was heated to 50 °C for 15 min and the EtOH was removed under reduced pressure. The remaining aq solution was stirred at 0 °C for 10 min and then conc HCl was added dropwise to the solution until the pH was 3-4 (pH paper). A pale yellow precipitate which formed was left in the solution and the mixture was allowed to stir at rt for 2 h. The precipitate was collected by filtration, washed with cold water (2 X 5 mL), and the aq layer also was allowed to stand at rt for 10 h to obtain additional solid **9**. The combined solids were dried in a vacuum oven at 80 °C for 7 h to get pure acid **9** in 80 % yield: M.p = 210-211 °C; [α]$_D^{25}$= +8.00 (c 0.25%, in CH$_3$OH); ^{1}H NMR (300 MHz, DMSO) δ 2.03-2.16 (m, 3H), 3.50-3.63 (m, 3H), 3.87 (s, 3H), 4.84 (d, 1H, *J* = 7.5 Hz), 7.31 (dd, 1H, *J* = 8.9 Hz, 3.0 Hz), 7.41 (d, 1H, *J* = 3.0 Hz), 7.63 (d, 1H, *J* = 8.9 Hz), 8.21 (s, 1H); ^{13}C NMR (75 MHz, DMSO) δ 24.9, 28.7, 47.3, 53.6, 56.8, 115.3, 119.9, 126.7, 127.0, 128.6, 131.0, 137.4, 137.5, 159.5, 164.0,

165.3; HRMS (ESI) (M+H)$^+$, calcd. for $C_{16}H_{16}N_3O_4$ 314.1141; Found 314.1141. The spectral data were identical to the reported values[16]. This material was employed directly in the next step.

7.11 (S)-11,12,13,13a-Tetrahydro-7-($^2H_3$)-methoxy-9-oxo-9H-imidazo[1,5-a]pyrrolo[2,1-c]-[1,4]benzodiazepine-1-carboxylic acid (9a)

The acid **9a** was prepared from ester **5a** following the procedure employed for the preparation of acid **9** in 82% yield: M.p = 210-212 ˚C; $[\alpha]_D^{25}$= +8.00 (c 0.25%, in CH_3OH); ^{1}H NMR (300 MHz, CDCl$_3$) δ 2.17-2.34 (m, 3H), 3.48-3.83 (m, 3H), 4.72 (d, 1H, J = 7.1 Hz), 7.17 (dd, 1H, J = 8.7 Hz, 2.3 Hz), 7.31-7.35 (m, 1H), 7.60 (d, 1H, J = 2.3 Hz), 7.82 (s, 1H); ^{13}C NMR (75 MHz, CDCl$_3$) δ 24.4, 28.5, 46.7, 53.2, 114.7, 119.8, 124.5, 125.7, 126.7, 130.8, 134.8, 137.5, 159.7, 161.5, 163.6; HRMS (ESI) (M+H)$^+$, calcd. for $C_{16}H_{13}{}^2H_3N_3O_4$ 317.1324; Found 317.1328. This material was employed directly in a later step.

7.12 (S)-Methyl-7-methoxy-9-oxo-11,12,13,13a-tetrahydro-9H-benzo[e]imidazo[5,1-c]pyro-lo[1,2-a][1,4]diazepine-1-carboxylate (10)

To an oven dried two neck round bottom flask, ethyl ester **5** (0.30 g, 0.87 mmol) was added in dry methanol (10 mL) and then NaOMe (0.2g, 3.48 mmol) was added to the solution. The mixture was heated to reflux until the reaction was complete (~1h, confirmed by TLC, silica gel). Then the reaction mixture was quenched with an ice cold aq NaHCO$_3$ solution. The solvent was removed under reduced pressure and the residue was dissolved in water and extracted with EtOAc (2x 20 mL). The combined organic layer was then washed with brine and dried (Na$_2$SO$_4$). The solvent was removed under reduced pressure and the residue was purified by flash column chromatography [silica gel, EtOAc/hexane (1:1)] to yield pure methyl ester **10** as a solid (0.286 g) in 93% yield: M.p = 180-182 ˚C; $[\alpha]_D^{25}$= +8.00 (c 0.25%, in CH_2Cl_2); ^{1}H NMR (300 MHz, CDCl$_3$)

δ 2.16-2.35 (m, 3H), 3.52-3.61 (m, 2H), 3.75-3.81 (m, 1H), 3.91 (s, 3H), 3.94 (s, 3H), 4.75 (d, 1H, J = 6.9 Hz), 7.16 (dd, 1H, J = 8.7 Hz, 2.7 Hz), 7.34 (d, 1H, J = 8.7 Hz), 7.59 (d, 1H, J = 2.7 Hz), 7.88 (s, 1H); ^{13}C NMR (75 MHz, CDCl$_3$) δ 24.4, 28.4, 46.6, 52.2, 53.4, 55.9, 114.5, 119.8, 124.7, 125.9, 126.9, 130.6, 135.9, 137.9, 159.5, 162.9, 163.7. HRMS (ESI) (M+Na)$^+$, calcd. for C$_{17}$H$_{17}$N$_3$O$_4$Na 350.1117; Found 350.1125.

7.13 (S)-Methyl-7-(^{2}H$_3$)-methoxy-9-oxo-11,12,13,13a-tetrahydro-9H-benzo[e]imidazo[5,1-c]-pyrolo-[1,2-a][1,4]diazepine-1-carboxylate (10a)

The methyl ester **10a** was prepared from acid **5a** following the procedure employed for preparation of methyl ester **10** in 97% yield: M.p = 182-183 ˚C; ^{1}H NMR (300 MHz, CDCl$_3$) δ 2.17-2.37 (m, 3H), 3.50-3.63 (m, 2H), 3.75-3.83 (m, 1H), 3.95 (s, 3H), 4.76 (d, 1H, J = 7.0 Hz), 7.17 (dd, 1H, J = 8.8 Hz, 2.9 Hz), 7.34 (d, 1H, J= 8.8 Hz), 7.60 (d, 1H, J = 2.9 Hz), 7.82 (s, 1H); ^{13}C NMR (75 MHz, CDCl$_3$) δ 24.4, 28.4, 46.6, 52.2, 53.5, 114.5, 119.8, 124.6, 126.0, 127.3, 130.6, 135.9, 137.9, 159.4, 163.2, 163.7. HRMS (ESI) (M+H)$^+$, calcd. for C$_{17}$H$_{15}$^{2}H$_3$N$_3$O$_4$ 331.1480; Found 331.1486.

7.14 General method for the synthesis of esters and amides (11, 11a- 19, and 19a)

A mixture of acid (**9 or 9a**, 0.32 mmol) individually, thionyl chloride (5.12 mmol) and dry CH$_2$Cl$_2$ (8 mL) was added to an oven dried round bottomed flask under argon. This suspension was allowed to reflux at 52 ˚C (the outside oil bath temperature was at 60 ˚C) for 1 h under an atmosphere of argon. The solution became a clear yellow color. The absence of the starting material was confirmed by the examination by TLC (silica gel). The organic solvent and excess thionyl chloride were removed under reduced pressure. This evaporation was repeated a couple of times with dry CH$_2$Cl$_2$ (5 mL) to remove excess thionyl chloride and any HCl. The yellow residue, which was obtained, was dissolved in dry CH$_2$Cl$_2$ (10 mL) and cooled to 0 ˚C for 10 min under argon. The

appropriate nucleophile (alcohol/thiol/amine, 3.2 mmol), followed by Et$_3$N (1.6 mmol) was added to the reaction mixture at 0°C and the mixture was then allowed to warm to rt and stirred for 2-7 h. After the completion of the reaction (TLC, silica gel), the solvent was removed under reduced pressure. The residue was quenched with ice cold water (5 mL) and extracted with CH$_2$Cl$_2$ (8 mL X 2). The combined organic layer was washed with brine (5 mL). The solvent was removed under reduced pressure and the residue was purified by flash column chromatography (silica gel) to yield the corresponding pure esters, thioesters and amides whose properties are depicted below. **Note: We observed in a control experiment that the mixture of dichloromethane plus thionyl chloride boils at 52 °C.**

7.15 (S)-Isobutyl-7-methoxy-9-oxo-11,12,13,13a-tetrahydro-9H-benzo[e]imidazo[5,1-c]pyro-lo[1,2-a][1,4]diazepine-1-carboxylate (11)

The isobutyl ester **11** was prepared from acid **9** following the general procedure with dry isobutanol as the nucleophile. The crude residue was purified by flash column chromatography [silica gel, EtoAc/hexane (7:3)] to yield pure isobutyl ester **11** as a solid in 70% yield: M.p = 126-127 °C (104-106 °C)[16]; ^{1}H NMR (300 MHz, CDCl$_3$) δ 1.04 (d, 6H, J = 6.7 Hz), 2.13-2.37 (m, 4H), 3.49-3.63 (m, 2H), 3.76-3.84 (m, 1H), 3.92 (s, 3H), 4.14 (d, 2H, J = 6.9 Hz), 4.76 (d, 1H, J = 6.9 Hz), 7.17 (dd, 1H, J= 8.8 Hz, 2.9 Hz), 7.33 (d, 1H, J = 8.8 Hz), 7.60 (d, 1H, J = 2.9 Hz), 7.82 (s, 1H); ^{13}C NMR (75 MHz, CDCl$_3$) δ 19.3, 24.4, 27.8, 28.4, 46.6, 53.5, 55.9, 71.2, 114.5, 119.8, 124.6, 126.2, 127.8, 130.6, 135.9, 137.6, 159.4, 163.1, 163.8. HRMS (ESI) (M+Na)$^+$, calcd. for C$_{20}$H$_{23}$N$_3$O$_4$Na 392.1586; Found 392.1594. The spectral data were identical to the reported values[16].

7.16 (S)-Isobutyl-7-(^{2}H$_3$)-methoxy-9-oxo-11,12,13,13a-tetrahydro-9H-benzo[e]imidazo[5,1-c]py-rrol-o[1,2-a][1,4]diazepine-1-carboxylate (11a)

The isobutyl ester **11a** was prepared from acid **9a** following the general procedure with dry isobutanol as the nucleophile. The crude residue was purified by flash column chromatography [silica gel, EtOAc/hexane (7:3)] to yield pure isobutyl ester **11a** as a solid in 61% yield: M.p = 125-127 ˚C; ^{1}H NMR (300 MHz, CDCl$_3$) δ 1.03 (d, 6H, J = 6.7 Hz), 2.12-2.31 (m, 4H), 3.51-3.62 (m, 2H), 3.76-3.82 (m, 1H), 4.14 (d, 2H, J = 6.9 Hz), 4.76 (d, 1H, J = 6.9 Hz), 7.16 (dd, 1H, J = 8.8 Hz, 2.9 Hz), 7.32 (d, 1H, J = 8.8 Hz), 7.59 (d, 1H, J = 2.9 Hz), 7.81 (s, 1H); ^{13}C NMR (75 MHz, CDCl$_3$) δ 19.1, 24.2, 27.6, 28.2, 46.4, 53.3, 71.0, 114.3, 119.5, 124.5, 125.9, 127.5, 130.4, 135.7, 137.4, 159.2, 162.8, 163.5. HRMS (ESI) (M+H)$^+$, calcd. for C$_{20}$H$_{21}$^{2}H$_3$N$_3$O$_4$ 373.1950; Found 373.1955.

7.17 (S)-1,1,1,3,3,3-Hexafluoropropan-2-yl-7-methoxy-9-oxo-11,12,13,13a-tetrahydro-9H-benzo[e]-imidazo[5,1-c]pyrrolo[1,2-a][1,4]diazepine-1-carboxylate (12)

The hexafluoro isopropyl ester **12** was prepared from acid **9** following the general procedure with dry 1,1,1,3,3,3-hexafluoropropan-2-ol as the nucleophile. The crude residue was purified by flash column chromatography [silica gel, EtOAc/hexane (1:1)] to yield pure ester **12** as a solid in 95% yield: M.p = 204-205 ˚C; [α]$_D^{25}$= +16.67 (c 0.3%, in CH$_2$Cl$_2$); ^{1}H NMR (300 MHz, CDCl$_3$) δ 2.16-2.29 (m, 3H), 3.38-3.40 (m, 1H), 3.52-3.62 (m, 1H), 3.79-3.85 (m, 1H), 3.92 (s, 3H), 4.77 (d, 1H, J = 7.3 Hz), 5.98-6.08 (m, 1H), 7.18 (dd, 1H, J = 8.8 Hz, 2.8 Hz), 7.33 (d, 1H, J = 8.8 Hz), 7.61 (d, 1H, J = 2.8 Hz), 7.87 (s, 1H); ^{13}C NMR (75 MHz, CDCl$_3$) δ 24.3, 28.3, 46.6, 53.4, 55.9, 66.7 (sep, J = 34.5 Hz), 114.7, 119.9, 120.6 (q, J = 279 Hz), 124.3, 124.6, 125.6, 130.6, 136.8, 140.6, 159.4, 159.7, 163.6; HRMS (ESI) (M+Na)$^+$, calcd. for C$_{19}$H$_{15}$F$_6$N$_3$O$_4$Na 486.0864; Found 486.0875.

7.18 (S)-1,1,1,3,3,3-Hexafluoropropan-2-yl-7-(^{2}H$_3$)-methoxy-9-oxo-11,12,13,13a-tetrahydro-9H-benzo[e]imidazo[5,1-c]pyrrolo[1,2-a][1,4]diazepine-1-carboxylate (12a)

The hexafluoro isopropyl ester **12a** was prepared from acid **9a** following the general procedure with dry 1,1,1,3,3,3-hexafluoropropan-2-ol as the nucleophile. The crude residue was purified by column chromatography [silica gel, EtOAc/hexane (7:3)] to yield pure ester **12a** as a solid in 97% yield: M.p = 204-206 ˚C; ^{1}H NMR (300 MHz, CDCl$_3$) δ 2.15-2.34 (m, 3H), 3.38-3.42 (m, 1H), 3.53-3.63 (m, 1H), 3.80-3.86 (m, 1H), 4.79 (d, 1H, J = 7.3 Hz), 5.98-6.10 (sep, 1H, J = 6.1 Hz), 7.19 (dd, 1H, J = 8.8 Hz, 2.9 Hz), 7.34 (d, 1H, J = 8.8 Hz), 7.62 (d, 1H, J = 2.9 Hz), 7.89 (s, 1H); ^{13}C NMR (75 MHz, CDCl$_3$) δ 24.3, 28.3, 46.6, 53.4, 66.7 (sep, J = 34.5 Hz), 114.6, 119.9, 120.6 (q, J = = 279 Hz), 124.3, 124.6, 125.6, 130.6, 136.8, 140.6, 159.5, 159.7, 163.6; HRMS (ESI) (M+Na)$^+$, calcd. for C$_{19}$H$_{13}$^{2}H$_3$F$_6$N$_3$O$_4$ 467.1228; Found 467.1230.

7.19 (S)-S-Ethyl-7-methoxy-9-oxo-11,12,13,13a-tetrahydro-9H-benzo[e]imidazo[5,1-c]pyrrolo[1,2-a][1,4]diazepine-1-carbothioate (13)

The thio ethyl ester **13** was prepared from acid **9** following the general procedure with dry ethanethiol as the nucleophile. The crude residue was purified by flash column chromatography [silica gel, EtOAc/hexane (8:2)] to yield pure thio ester **13** as a solid in 70% yield: M.p = 228-230 ˚C; [α]$_D^{25}$= -14.29 (c 0.28%, in CH$_2$Cl$_2$); ^{1}H NMR (300 MHz, CDCl$_3$) δ 1.35 (t, 3H, J = 7.4 Hz), 2.14-2.25 (m, 3H), 3.00 (q, 2H, J = 7.4 Hz), 3.42-3.60 (m, 2H), 3.74-3.82 (m, 1H), 3.91 (s, 3H), 4.71 (d, 1H, J = 7.2 Hz), 7.15 (dd, 1H, J = 8.8 Hz, 2.8 Hz), 7.31 (d, 1H, J = 8.8 Hz), 7.59 (d, 1H, J = 2.8 Hz), 7.79 (s, 1H); ^{13}C NMR (75 MHz, CDCl$_3$) δ 14.6, 23.1, 24.4, 28.6, 46.5, 53.3, 55.9, 114.5, 119.8, 124.5, 125.9, 130.6, 132.5, 134.6, 135.5, 159.5, 163.6, 188.1. HRMS (ESI) (M+Na)$^+$, calcd. for C$_{18}$H$_{19}$N$_3$O$_3$SNa 380.1045; Found 380.1047.

7.20 (S)-S-Ethyl-7-(^{2}H$_3$)-methoxy-9-oxo-11,12,13,13a-tetrahydro-9H-benzo[e]imidazo[5,1-c]pyrrolo[1,2-a][1,4]diazepine-1-carbothioate (13a)

The thio ethyl ester **13a** was prepared from **9a** following the general procedure with dry ethanethiol as the nucleophile. The crude residue was purified by flash column chromatography [silica gel, EtOAc/hexane (8:2)] to yield pure thio ester **13a** as a solid in 80% yield: M.p = 229-231 °C; ^{1}H NMR (300 MHz, CDCl$_3$) δ 1.36 (t, 3H, J = 7.4 Hz), 2.18-2.26 (m, 3H), 3.02 (q, 2H, J = 7.4 Hz), 3.44-3.61 (m, 2H), 3.76-3.83 (m, 1H), 4.73 (d, 1H, J = 6.9 Hz), 7.17 (dd, 1H, J = 8.8 Hz, 2.9 Hz), 7.33 (d, 1H, J = 8.8 Hz), 7.60 (d, 1H, J = 2.9 Hz), 7.81 (s, 1H); ^{13}C NMR (75 MHz, CDCl$_3$) δ 14.6, 23.1, 24.4, 28.6, 46.5, 53.4, 114.6, 119.8, 124.5, 125.9, 130.7, 133.6, 134.6, 135.5, 159.5, 163.6, 188.1. HRMS (ESI) (M+H)$^+$, calcd. for C$_{18}$H$_{17}$^{2}H$_3$N$_3$O$_3$S 361.1408; Found 361.1405.

7.21 (S)-S-tert-Butyl-7-methoxy-9-oxo-11,12,13,13a-tetrahydro-9H-benzo[e]imidazo[5,1-c]-pyrolo[1,2-a][1,4]diazepine-1-carbothioate (14)

The thio *tert*-butyl ester **14** was prepared from acid **9** following the general procedure with dry *tert*-butyl mercaptan as the nucleophile. The crude residue was purified by flash column chromatography [silica gel, EtOAc/hexane (8:2)] to yield pure thio ester **14** as a solid in 82% yield: M.p = 130-132 °C; $[α]_D^{27}$= -23.54 (c 0.17% in CH$_2$Cl$_2$); ^{1}H NMR (300 MHz, CDCl$_3$) δ 1.57 (s, 9H), 2.18-2.20 (m, 3H), 3.41-3.59 (m, 2H), 3.74-3.80 (m, 1H), 3.90 (s, 3H), 4.69 (d, 1H, J = 7.2 Hz), 7.14 (dd, 1H, J = 8.9 Hz, 3.0 Hz), 7.29 (d, 1H, J = 8.9 Hz), 7.58 (d, 1H, J = 3.0 Hz), 7.74 (s, 1H); ^{13}C NMR (75 MHz, CDCl$_3$) δ 24.3, 28.5, 29.7, 46.4, 47.1, 53.3, 55.8, 114.4, 119.6, 124.5, 125.9, 130.5, 134.2, 135.1, 159.3, 163.5, 188.7 ; HRMS (ESI) (M+H)$^+$, calcd. for C$_{20}$H$_{24}$N$_3$O$_3$S 386.1533; Found 386.1532.

7.22 (S)-S-tert-Butyl-7-(^{2}H$_3$)-methoxy-9-oxo-11,12,13,13a-tetrahydro-9H-benzo[e]imidazo-[5,1-c]pyrrolo[1,2-a][1,4]diazepine-1-carbothioate (14a)

The thio *tert*-butyl ester **14a** was prepared from **9a** following the general procedure with dry *tert*-butyl mercaptan as the nucleophile. The crude residue was purified by flash column chromatography [silica gel, EtOAc/hexane (1:1)] to yield pure thio ester **14a** as a solid in 89% yield: M.p = 129-131 ˚C; ^{1}H NMR (300 MHz, CDCl$_3$) δ 1.52 (s, 9H), 2.11-2.20 (m, 3H), 3.31-3.53 (m, 2H), 3.69-3.75 (m, 1H), 4.67 (d, 1H, *J* = 5.9 Hz), 7.08-7.13 (m, 1H), 7.26-7.30 (m, 1H), 7.52 (d, 1H, *J* = 2.0 Hz), 7.72 (s, 1H); ^{13}C NMR (75 MHz, CDCl$_3$) δ 24.4, 28.6, 29.8, 46.5, 47.1, 53.4, 114.5, 119.7, 124.6, 126.0, 130.6, 134.3, 134.4, 135.2, 159.4, 163.6, 188.8 ; HRMS (ESI) (M+H)$^+$, calcd. for C$_{20}$H$_{21}$^{2}H$_3$N$_3$O$_3$S 389.1721; Found 389.1725.

7.23 (S)-7-Methoxy-N-methyl-9-oxo-11,12,13,13a-tetrahydro-9H-benzo[e]imidazo[5,1-c]-pyrolo[1,2-a][1,4]diazepine-1-carboxamide (15)

The *N*-methyl amide **15** was prepared from acid **9** following the general procedure with a solution of methylamine (33 wt % in absolute ethanol, 3 mL) as the nucleophile. The crude residue was purified by flash column chromatography [neutral alumina, 1% MeOH in CH$_2$Cl$_2$] to yield pure amide **15** as a solid in 75% yield: M.p = 180-182 ˚C; [α]$_D^{25}$= +3.70 (c 0.5%, in CH$_2$Cl$_2$); ^{1}H NMR (300 MHz, CDCl$_3$) δ 2.12-2.25 (m, 2H), 2.30-2.41 (m, 1H), 2.98 (d, 1H, *J* = 4.6 Hz), 3.50-3.62 (m, 1H), 3.73-3.89 (m, 2H), 3.91 (s, 3H), 4.73 (d, 1H, *J* = 7.8 Hz), 7.16 (dd, 1H, *J* = 8.6 Hz, 2.3 Hz), 7.32 (d, 1H, *J* = 8.6 Hz), 7.59 (d, 1H, *J* = 2.3 Hz), 7.72 (brs, 1H), 7.91 (s, 1H); ^{13}C NMR (75 MHz, CDCl$_3$) δ 24.5, 26.2, 28.7, 46.8, 53.5, 55.9, 114.7, 119.8, 124.7, 125.6, 128.5, 130.9, 134.2, 135.6, 159.8, 161.3, 163.5. HRMS (ESI) (M+Na)$^+$, calcd. for C$_{17}$H$_{18}$N$_4$O$_3$Na 349.1277; Found 349.1300.

7.24 (S)-7-(^{2}H$_3$)-Methoxy-N-methyl-9-oxo-11,12,13,13a-tetrahydro-9H-benzo[e]imidazo[5,1-c]-pyrrolo[1,2-a][1,4]diazepine-1-carboxamide (15a)

The *N*-methyl amide **15a** was prepared from acid **9a** following the general procedure with a solution of methylamine (33 wt % in absolute ethanol, 3 mL) as the nucleophile. The crude residue was purified by flash column chromatography [neutral alumina, 1% MeOH in CH$_2$Cl$_2$] to yield pure amide **15a** as a solid in 92 % yield: M.p = 180-182 ˚C; ^{1}H NMR (300 MHz, CDCl$_3$) δ 2.12-2.25 (m, 2H), 2.30-2.42 (m, 1H), 2.97 (d, 1H, *J* = 5.0 Hz), 3.50-3.60 (m, 1H), 3.74-3.91 (m, 2H), 4.73 (d, 1H, *J* = 7.6 Hz), 7.14 (dd, 1H, *J* = 8.8 Hz, 2.9 Hz), 7.29 (d, 1H, *J* = 8.8 Hz), 7.48-7.54 (bm, 1H), 7.58 (d, 1H, *J* = 2.9 Hz), 7.70 (s, 1H); ^{13}C NMR (75 MHz, CDCl$_3$) δ 24.5, 25.8, 28.6, 46.5, 53.4, 114.3, 119.4, 124.4, 126.2, 130.2, 130.6, 134.5, 134.9, 159.1, 162.8, 163.7. HRMS (ESI) (M+H)$^+$, calcd. for C$_{17}$H$_{16}$^{2}H$_3$N$_4$O$_3$ 330.1640; Found 330.1637.

7.25 (S)-7-Methoxy-N,N-dimethyl-9-oxo-11,12,13,13a-tetrahydro-9H-benzo[e]imidazo[5,1-c]pyrrolo[1,2-a][1,4]diazepine-1-carboxamide (16)

The *N, N*-dimethyl amide **16** was prepared from acid **9** following the general procedure with a solution of *N*,*N*-dimethylamine (11% in ethanol, 5 mL) as the nucleophile. The crude residue was purified by flash column chromatography [neutral alumina, 5% MeOH in CH$_2$Cl$_2$] to yield pure dimethyl amide **16** as a solid in 70% yield: M.p = 186-188 ˚C; [α]$_D$^{25}= +52.00 (c 0.25%, in CH$_2$Cl$_2$); ^{1}H NMR (300 MHz, CDCl$_3$) δ 2.01-2.08 (m, 2H), 2.25-2.38 (m, 1H), 2.89-2.94 (m, 1H), 3.08 (s, 3H), 3.14 (s, 3H), 3.63-3.82 (m, 2H), 3.91 (s, 3H), 4.73 (dd, 1H, *J* = 8.4, 3.0 Hz), 7.15 (dd, 1H, *J* = 8.9 Hz, 2.9 Hz), 7.34 (d, 1H, *J* = 8.9 Hz), 7.57 (d, 1H, *J* = 2.9 Hz), 7.97 (s, 1H); ^{13}C NMR (75 MHz, CDCl$_3$) δ 23.9, 27.8, 35.3, 39.1, 47.2, 52.3, 55.8, 114.9, 119.7, 124.2, 126.1, 130.1, 131.0, 132.0, 134.8, 159.1, 164.2, 165.7. HRMS (ESI) (M+Na)$^+$, calcd. for C$_{18}$H$_{20}$N$_4$O$_3$Na 363.1433; Found 363.1410.

7.26 (S)-7-(²H₃)-Methoxy-N,N-dimethyl-9-oxo-11,12,13,13a-tetrahydro-9H-benzo[e]imida-zo[5,1-c]pyrrolo[1,2-a][1,4]diazepine-1-carboxamide (16a)

The *N, N*-dimethyl amide **16a** was prepared from acid **9a** following the general procedure with a solution of *N,N*-dimethylamine (11% in ethanol, 5 mL) as the nucleophile. The crude residue was purified by flash column chromatography [neutral alumina, 5% MeOH in CH_2Cl_2] to yield pure amide **16a** as a solid in 88% yield: M.p = 185-186 ˚C; ^{1}H NMR (300 MHz, CDCl₃) δ 2.01-2.10 (m, 2H), 2.24-2.37 (m, 1H), 2.89-2.98 (m, 1H), 3.07 (s, 3H), 3.14 (s, 3H), 3.63-3.82 (m, 2H), 4.72 (dd, 1H, *J* = 8.3 Hz, 2.9 Hz), 7.13 (dd, 1H, *J* = 8.7 Hz, 2.9 Hz), 7.29 (d, 1H, *J* = 8.7 Hz), 7.56 (d, 1H, *J* = 2.9 Hz), 7.77 (s, 1H); ^{13}C NMR (75 MHz, CDCl₃) δ 23.9, 27.9, 35.3, 39.1, 47.2, 52.3, 114.9, 119.7, 124.2, 126.3, 130.1, 131.4, 132.0, 134.9, 159.0, 164.3, 166.1. HRMS (ESI) (M+H)⁺, calcd. for $C_{18}H_{18}{}^2H_3N_4O_3$ 344.1796; Found 344.1798.

7.27 (S)-N-Ethyl-7-methoxy-9-oxo-11,12,13,13a-tetrahydro-9H-benzo[e]imidazo[5,1-c]pyro-lo[1,2-a][1,4]diazepine-1-carboxamide (17)

The *N*-ethyl amide **17** was prepared from acid **9** following the general procedure with a solution of ethylamine (2.0 M in THF, 1 mL) as the nucleophile. The crude residue was purified by flash column chromatography [neutral alumina, EtOAc/hexane (8:2)] to yield pure ethyl amide **17** as a solid in 75% yield: M.p = 175-177 ˚C; $[\alpha]_D^{27}$=+8.33 (c 0.12%, in CH_2Cl_2); ^{1}H NMR (300 MHz, CDCl₃) δ 1.25 (t, 3H, *J* = 7.3 Hz), 2.13-2.41 (m, 3H), 3.40-3.59 (m, 3H), 3.74-3.87 (m, 2H), 3.90 (s, 3H), 4.72 (d, 1H, *J* = 7.8 Hz), 7.14 (dd, 1H, *J* = 8.7 Hz, 3.0 Hz), 7.28 (d, 1H, *J* = 8.7 Hz), 7.48-7.50 (bm, 1H), 7.58 (d, 1H, *J* = 2.7 Hz), 7.69 (s, 1H); ^{13}C NMR (75 MHz, CDCl₃) δ 14.9, 24.6, 28.8, 34.0, 46.7, 53.6, 55.8, 114.4, 119.6, 124.5, 126.3, 130.3, 130.7, 134.5, 135.2, 159.3, 162.0, 163.8; HRMS (ESI) (M+H)⁺, calcd. for $C_{18}H_{21}N_4O_3$ 341.1608; Found 341.1601.

7.28 (S)-N-Ethyl-7-(^{2}H$_3$)-methoxy-9-oxo-11,12,13,13a-tetrahydro-9H-benzo[e]imidazo[5,1-c]pyrrolo[1,2-a][1,4]diazepine-1-carboxamide (17a)

The *N*-ethyl amide **17a** was prepared from **9a** following the general procedure with a solution of ethylamine (2.0 M in THF, 1 mL) as the nucleophile. The crude residue was purified by flash column chromatography [neutral alumina, EtOAc/hexane (8:2)] to yield pure amide **17a** as a solid in 96 % yield: M.p = 176-177 ˚C; ^{1}H NMR (300 MHz, CDCl$_3$) δ 1.25 (t, 3H, *J* = 7.3 Hz), 2.12-2.24 (m, 2H), 2.30-2.42 (m, 1H), 3.40-3.60 (m, 3H), 3.74-3.91 (m, 2H), 4.72 (d, 1H, *J* = 7.7 Hz), 7.14 (dd, 1H, *J* = 8.8 Hz, 2.9 Hz), 7.29 (d, 1H, *J* = 8.8 Hz), 7.47-7.53 (bm, 1H), 7.58 (d, 1H, *J* = 2.9 Hz), 7.70 (s, 1H); ^{13}C NMR (75 MHz, CDCl$_3$) δ 14.9, 24.6, 28.8, 34.0, 46.7, 53.6, 114.4, 119.6, 124.5, 126.4, 130.4, 130.7, 134.6, 135.2, 159.3, 162.1, 163.8; HRMS (ESI) (M+H)$^+$, calcd. for C$_{18}$H$_{18}$^{2}H$_3$N$_4$O$_3$ 344.1796; Found 344.1797.

7.29 (S)-N-(tert-Butyl)-7-methoxy-9-oxo-11,12,13,13a-tetrahydro-9H-benzo[e]imidazo[5,1-c]pyrrolo[1,2-a][1,4]diazepine-1-carboxamide (18)

The *N-tert*-butyl amide **18** was prepared from acid **9** following the general procedure with *tert*-butyl amine as the nucleophile. The crude residue was purified by flash column chromatography [neutral alumina, EtOAc/hexane (8:2)] to yield pure amide **18** as a solid in 80 % yield: M.p = 152-154 ˚C; $[\alpha]_D^{27}$= +170.00 (c 0.10%, in CH$_2$Cl$_2$); ^{1}H NMR (300 MHz, CDCl$_3$) δ 1.47 (s, 9H), 2.11-2.37 (m, 3H), 3.50-3.60 (m, 1H), 3.74-3.86 (m, 2H), 3.91 (s, 3H), 4.71 (d, 1H, *J* = 7.8 Hz), 7.14 (dd, 1H, *J* = 8.7 Hz, 3.0 Hz), 7.26-7.29 (m, 1H), 7.45 (bs, 1H), 7.58 (d, 1H, *J* = 3.0 Hz), 7.77 (s, 1H); ^{13}C NMR (75 MHz, CDCl$_3$) δ 24.5, 28.8, 46.7, 50.9, 53.6, 55.8, 114.4, 119.6, 124.6, 126.3, 130.7, 131.2, 134.3, 134.9, 159.2, 161.5, 163.8; HRMS (ESI) (M+H)$^+$, calcd. for C$_{20}$H$_{25}$N$_4$O$_3$ 369.1921; Found 369.1920.

7.30 (S)-N-(tert-Butyl)-7-(^{2}H$_3$)-methoxy-9-oxo-11,12,13,13a-tetrahydro-9H-benzo[e]imida-zo[5,1-c]pyrrolo[1,2-a][1,4]diazepine-1-carboxamide (18a)

The *N-tert*-butyl amide **18a** was prepared from acid **9a** following the general procedure with *tert*-butyl amine as the nucleophile. The crude residue was purified by flash column chromatography [neutral alumina, EtOAc/hexane (8:2)] to yield pure amide **18a** as a solid in 85% yield: M.p = 153-155 ˚C; ^{1}H NMR (300 MHz, CDCl$_3$) δ 1.49 (s, 9H), 2.12-2.39 (m, 3H), 3.51-3.61 (m, 1H), 3.75-3.94 (m, 2H), 4.73 (d, 1H, *J* = 7.9 Hz), 7.14 (dd, 1H, *J* = 8.8 Hz, 2.9 Hz), 7.27-7.30 (m, 1H), 7.39 (bs, 1H), 7.59 (d, 1H, *J* = 2.9 Hz), 7.68 (s, 1H); ^{13}C NMR (75 MHz, CDCl$_3$) δ 24.6, 28.9, 46.7, 50.9, 53.7, 114.4, 119.7, 124.5, 126.5, 130.7, 131.4, 134.3, 134.8, 159.3, 161.7, 163.8; HRMS (ESI) (M+H)$^+$, calcd. for C$_{20}$H$_{21}$^{2}H$_3$N$_4$O$_3$ 372.2108; Found 372.2109.

7.31 (S)-N-Cyclopropyl-7-methoxy-9-oxo-11,12,13,13a-tetrahydro-9H-benzo[e]imidazo[5,1-c]py-rrolo[1,2-a][1,4]diazepine-1-carboxamide (19)

The *N*-cyclopropyl amide **19** was prepared from acid **9** following the general procedure with dry cyclopropylamine as the nucleophile. The crude residue was purified by flash column chromatography [neutral alumina, EtOAc/hexane (1:1)] to yield pure amide **19** as a solid in 82% yield: M.p = 189-190 ˚C; [α]$_D^{25}$= -6.67 (c 0.3%, in CH$_2$Cl$_2$); ^{1}H NMR (300 MHz, CDCl$_3$) δ 0.54-0.59 (m, 2H), 0.76-0.82 (m, 2H), 2.06-2.18 (m, 2H), 2.25-2.36 (m, 1H), 2.75-2.81 (m, 1H), 3.43-3.53 (m, 1H), 3.68-3.81 (m, 2H), 3.84 (s, 3H), 4.65 (d, 1H, *J* = 8.1 Hz), 7.07 (dd, 1H, *J* = 8.7 Hz, 2.8 Hz), 7.19-7.22 (m, 1H), 7.50 (bs, 1H), 7.52 (d, 1H, *J* = 2.8 Hz), 7.61 (s, 1H); ^{13}C NMR (75 MHz, CDCl$_3$) δ 6.5, 6.6, 22.3, 24.6, 28.8, 46.6, 53.6, 55.8, 114.4, 119.6, 124.4, 126.3, 130.0, 130.7, 134.5, 135.3, 159.3, 163.7, 163.8; HRMS (ESI) (M+Na)$^+$, calcd. for C$_{19}$H$_{20}$N$_4$O$_3$Na 375.1433; Found 375.1440.

7.32 (S)-N-Cyclopropyl-7-(^{2}H$_3$)-methoxy-9-oxo-11,12,13,13a-tetrahydro-9H-benzo[e]imida-zo[5,1-c]pyrrolo[1,2-a][1,4]diazepine-1-carboxamide (19a)

The *N*-cyclopropyl amide **19a** was prepared from acid **9a** following the general procedure with dry cyclopropylamine as the nucleophile. The crude residue was purified by column chromatography [neutral alumina, EtOAc/hexane (1:1)] to yield pure amide **19a** as a solid in 86% yield: M.p = 189-190 ˚C; ^{1}H NMR (300 MHz, CDCl$_3$) δ 0.62-0.67 (m, 2H), 0.84-0.90 (m, 2H), 2.12-2.26 (m, 2H), 2.33-2.46 (m, 1H), 2.83-2.89 (m, 1H), 3.51-3.60 (m, 1H), 3.75-3.93 (m, 2H), 4.73 (d, 1H, *J* = 8.2 Hz), 7.15 (dd, 1H, *J* = 8.8 Hz, 2.9 Hz), 7.27-7.31 (m, 1H), 7.57-7.60 (m, 2H), 7.69 (s, 1H); ^{13}C NMR (75 MHz, CDCl$_3$) δ 6.5, 6.6, 22.3, 24.7, 28.8, 46.7, 53.6, 114.4, 119.7, 124.5, 126.3, 130.1, 130.8, 134.6, 135.3, 159.3, 163.7, 163.8; HRMS (ESI) (M+H)$^+$, calcd. for C$_{19}$H$_{18}$^{2}H$_3$N$_4$O$_3$ 356.1796; Found 356.1796.

7.33 (S)-(^{2}H$_3$)--ethyl-7-methoxy-9-oxo-11,12,13,13a-tetrahydro-9H-benzo[e]imidazo[5,1-c]-pyrolo[1,2-a][1,4]diazepine-1-carboxylate (23)

To an oven dried round bottom flask, acid **9** (0.6 g, 1.92 mmol) and Cs$_2$CO$_3$ (1.3 g, 3.8 mmol) were dissolved in dry DMF (5 mL) at rt. The 1,1-dideuterated bromoethane (0.2 ml, 2.9 mol) was added via a syringe in one portion and the reaction was stirred for 2 hr at rt. The reaction mixture was then filtered to remove precipitate (CsBr), and the solid was rinsed with EtOAc (2ml). The organic layers were combined, and the solvent was removed under reduced pressure. The residue, that resulted, was purified by flash chromatography (silica gel, 10% methanol in DCM) which provided pure C(3) substituted *d*^{2}-ethyl ester **23** as a white solid (0.398 g) in 61% yield: ^{1}H NMR (300 MHz, CDCl$_3$) δ 7.81 (s, 1H), 7.59 (d, *J* = 2.9 Hz, 1H), 7.31 (t, *J* = 8.4 Hz, 1H), 7.16 (dd, *J* = 8.8, 3.0 Hz, 1H), 4.75 (d, *J* = 7.0 Hz, 1H), 3.91 (s, 3H), 3.87 – 3.70 (m, 1H), 3.70 – 3.35 (m, 2H), 2.50 – 2.03 (m, 3H), 1.43 (s, 3H); ^{13}C NMR (75 MHz, CDCl$_3$) δ 163.8, 162.9, 159.4, 137.7, 135.9,

130.6, 127.7, 126.2, 124.6, 119.8, 114.5, 60.6 (quint), 55.9, 53.5, 46.6, 28.4, 24.4, 14.2. LCMS (ESI, *m/z*, relative intensity (ESI), calcd. for $C_{18}H_{17}D_2N_3O_4$ (M+H)$^+$ 343.37; Found 343.07.

7.34 (S)-1-(3-isopropyl-1,2,4-oxadiazol-5-yl)-7-methoxy-11,12,13,13a-tetrahydro-9H-benzo-[e]imidazo[5,1-c]pyrrolo[1,2-a][1,4]diazepin-9-one (24)

The ethyl ester **5** (0.20 g, 0.58 mmol) was dissolved in dry THF (20 mL) under argon at rt. In a separate oven dried round bottom flask which contained 3Å molecular sieves, *N'*-hydroxyisobutyrimidamide (0.24 g, 2.34 mmol) was dissolved in dry THF (20 mL) under argon and treated with sodium hydride (60% dispersion in mineral oil, 0.058 g, 1.46 mmol). The mixture, which resulted, was then stirred for 15 min at which point the solution of ethyl ester **5** was added. The reaction mixture, which resulted, was stirred at rt for 2h. After completion of the reaction (TLC, silica gel), the mixture was quenched with a saturated aq NaHCO$_3$ solution (5 mL). Then water (30 mL) was added and the product was extracted with EtOAc (3 x 50 mL). The combined organic layer was then washed with brine and dried (Na$_2$SO$_4$). The solvent was removed under reduced pressure and the residue was purified by flash column chromatography [silica gel, EtOAc/hexane (1:1)] to yield pure isopropyl oxadiazole **24** as a solid (0.19 g) in 84% yield: ^{1}H NMR (300 MHz, CDCl$_3$) δ 7.93 (s, 1H), 7.58 (d, *J* = 2.8 Hz, 1H), 7.36 (d, *J* = 8.8 Hz, 1H), 7.16 (dd, *J* = 8.8, 2.8 Hz, 1H), 4.82 (d, *J* = 7.7 Hz, 1H), 3.90 (s, 3H), 3.78 (dd, *J* = 14.6, 5.2 Hz, 1H), 3.58 (dd, *J* = 19.4, 9.6 Hz, 2H), 3.17 (dt, *J* = 13.8, 6.9 Hz, 1H), 2.43 – 1.92 (m, 3H), 1.37 (d, *J* = 6.3 Hz, 6H); ^{13}C NMR (75 MHz, CDCl$_3$) δ 175.2, 170.7, 163.7, 159.5, 137.3, 135.6, 130.5, 125.9, 124.6, 122.1, 119.7, 114.7, 55.9, 53.1, 46.6, 28.1, 26.7, 24.2, 20.5; HRMS (ESI) (M+H)$^+$, calcd. for $C_{20}H_{22}N_5O_3$ 380.1717; Found 380.1710.

7.35   (S)-1-(3-Ethyl-1,2,4-oxadiazol-5-yl)-7-methoxy-11,12,13,13a-tetrahydro-9H-benzo[e]-imidazo[5,1-c]pyrrolo[1,2-a][1,4]diazepin-9-one (25)

The ethyl ester **5** (0.20 g, 0.58 mmol) was dissolved in dry THF (20 mL) under argon at rt. In a separate oven dried round bottom flask, which contained 3Å molecular sieves, *N′*-hydroxypropionimidamide (0.21 g, 2.34 mmol) was dissolved in dry THF (20 mL) under argon and treated with sodium hydride (60% dispersion in mineral oil, 0.058 g, 1.46 mmol). The mixture, which resulted, was then stirred for 15 min at which point the solution of ethyl ester **5** was added. The reaction mixture which resulted was stirred at rt for 2h. After completion of the reaction (TLC, silica gel), the mixture was quenched with a saturated aq NaHCO₃ solution (5 mL). Then water (30 mL) was added and the product was extracted with EtOAc (3 x 50 mL). The combined organic layer was then washed with brine and dried (Na₂SO₄). The solvent was removed under reduced pressure and the residue was purified by flash column chromatography [silica gel, EtOAc/hexane (1:1)] to yield pure ethyl oxadiazole **25** as a solid (0.09 g) in 42% yield: ^{1}H NMR (300 MHz, CDCl₃) δ 7.95 (s, 1H), 7.61 (d, *J* = 2.9 Hz, 1H), 7.38 (d, *J* = 8.8 Hz, 1H), 7.18 (dd, *J* = 8.8, 3.0 Hz, 1H), 4.91 – 4.72 (m, 1H), 3.93 (s, 3H), 3.87 – 3.71 (m, 1H), 3.71 – 3.49 (m, 2H), 2.85 (q, *J* = 7.6 Hz, 2H), 2.43 – 2.07 (m, 3H), 1.39 (t, *J* = 7.6 Hz, 3H). ^{13}C NMR (75 MHz, CDCl₃): δ 171.9, 170.9, 163.8, 159.5, 137.3, 135.6, 130.5, 125.9, 124.6, 122.1, 119.8, 114.7, 55.9, 53.1, 46.7, 28.1, 24.2, 19.7, 11.4. HRMS (ESI) (M+H)$^+$, calcd. for C₁₉H₂₀N₅O₃ 366.1561; Found 366.1566.

7.36 (S)-7-Methoxy-1-(3-methyl-1,2,4-oxadiazol-5-yl)-11,12,13,13a-tetrahydro-9H-benzo[e]-imidazo[5,1-c]pyrrolo[1,2-a][1,4]diazepin-9-one (26)

The ethyl ester **5** (0.20 g, 0.58 mmol) was dissolved in dry THF (20 mL) under argon at rt. In a separate oven dried round bottom flask, which contained 3Å molecular sieves, *N'*-hydroxyacetimidamide (0.17 g, 2.34 mmol) was dissolved in dry THF (20 mL) under argon and treated with sodium hydride (60% dispersion in mineral oil, 0.058 g, 1.46 mmol). The mixture, which resulted, was then stirred for 15 min at which point the solution of ethyl ester **5** was added. The reaction mixture which resulted was stirred at rt for 2h. After completion of the reaction (TLC, silica gel), the mixture was quenched with a saturated aq $NaHCO_3$ solution (5 mL). Then water (30 mL) was added and the product was extracted with EtOAc (3 x 50 mL). The combined organic layer was then washed with brine and dried (Na_2SO_4). The solvent was removed under reduced pressure and the residue was purified by flash column chromatography [neutral alumina, 5% CH_3OH in CH_2Cl_2] to yield pure methyl oxadiazole **26** as a solid (0.15 g) in 69% yield: ^{1}H NMR (300 MHz, $CDCl_3$) δ 7.94 (s, 1H), 7.59 (d, *J* = 2.9 Hz, 1H), 7.37 (d, *J* = 8.8 Hz, 1H), 7.17 (dd, *J* = 8.8, 3.0 Hz, 1H), 4.91 – 4.75 (m, 1H), 3.91 (s, 3H), 3.77 (ddd, *J* = 10.5, 7.2, 3.0 Hz, 1H), 3.67 – 3.44 (m, 2H), 2.47 (s, 3H), 2.37 – 1.93 (m, 3H). ^{13}C NMR (75 MHz, $CDCl_3$) δ 171.0, 167.5, 163.8, 159.5, 137.3, 135.7, 130.5, 125.9, 124.6, 122.0, 119.8, 114.7, 55.9, 53.1, 46.7, 28.1, 24.2, 11.8. HRMS (ESI) $(M+H)^+$, calcd. for $C_{18}H_{18}N_5O_3$ 352.1404; Found 352.1400.

Representative example: ethyl oxime "*N'*-hydroxypropionimidamide"

Hydroxylamine hydrochloride (9.73 g, 0.14 mol) and potassium carbonate (41.5 g, 0.3 mol) were added into methanol (400 mL) and water (80 mL). The suspension, which resulted, was stirred at rt for 15 min after which it was heated to reflux. The propionitrile (7.1 mL, 0.1 mol) was added dropwise and the reaction, which resulted, was stirred at reflux for 16 h. After that, the reaction

mixture was cooled to 0 °C and the precipitate which formed was filtered off. The solvent from the filtrate was removed under reduced pressure. The solid residue was dissolved in EtOAc and washed with water, brine, and dried (Na_2SO_4), after which the solvent was removed under reduced pressure to afford the ethyl oxime as a white solid (6.05 g, 69%): **HPLC-MS** (ESI) *m/z* (M+H) 89.06. This material was used for the next step without further characterization.

By following the same procedure with isobutyronitrile (6.49 mL, 72.3 mmol), this process furnished isopropyl oxime "*N'*-hydroxyisobutyrimidamide" (5.54 g, 75%). The same process with acetonitrile (12.7 mL, 0.24 mol) furnished the methyl oxime "*N'*-hydroxyacetimidamide (9.92 g, 55%).

7.37 (S)-7-hydroxy-1-(oxazol-5-yl)-11,12,13,13a-tetrahydro-9H-benzo[e]imidazo[5,1-c]pyrrolo[1,2-a][1,4]diazepin-9-one (29)

The DIBAL-H (1.2 M, 6.2 mL, 7.4 mmol) was added at 0 ˚C to a solution of NaO^{t}Bu (0.76 g, 7.9 mmol) in 20 mL of dry THF. The mixture which resulted, was stirred for 1 h at rt under an argon atmosphere. The compound **5** (1.5 g, 4.4 mmol) was then added to the above solution at 0 ˚C and the mixture was stirred for 3 h (or until the complete consumption of **5**) at room temperature under Ar. After completion of the reaction, excess DIBAL-H was quenched by careful addition of methanol (~ 15 mL), and this was followed by 5% aq HCl (20-30 mL) at 0 ˚C. After this the mixture, which resulted, was allowed to warm to rt. The aq layer was extracted with CH_2Cl_2 (2x 50 mL). The combined organic layers were washed with brine and dried (Na_2SO_4). The solvent was removed under reduced pressure to afford the crude aldehyde **27**. This residue was purified by flash chromatography (2:1 ethyl acetate/hexane) to afford the pure diazepine aldehyde **27** as a white solid, (3.325 g, 93%). ^{1}H NMR (300 MHz, CDCl$_3$) δ 10.05 (s, 1H), 7.91 (s, 1H), 7.61 (d, *J* = 3.0 Hz, 1H), 7.38 (d, *J* = 9.0 Hz, 1H), 7.19 (dd, *J* = 3.0, 9.0 Hz, 1H), 4.72 (d, *J* = 8.4 Hz, 1H),

3.93 (s, 3H), 3.78-3.86 (m, 1H), 3.51-3.61 (m, 1H), 3.41-3.45 (m, 1H), 2.14-2.34 (m, 3H). ^{13}C

NMR (75 MHz, CDCl$_3$) δ 186.9, 163.5, 159.6, 137.3, 136.8, 134.7, 130.7, 125.6, 124.5, 119.8,

114.8, 55.9, 53.0, 46.6, 28.8, 24.3; LCMS (ESI *m/z*) 298.35 (M+H)$^+$.

The toluenesulfonylmethyl isocyanide, TosMIC (3.28 g, 16.8 mmol), was placed in a dry two neck

round bottom flask and dissolved in dry MeOH (40 mL) under an argon atmosphere. At rt, K$_2$CO$_3$

(4.64 g, 33.57 mmol) was added, as well as the aldehyde **27** (3.325 g, 11.18 mmol) to the reaction

and the mixture was heated to reflux for 3 h. After completion of the reaction, as indicated by TLC

(silica gel), the reaction mixture was quenched with cold water. After this, 1/3 of the solvent was

removed under reduced pressure and the remainder extracted with EtOAc (3x 20 mL). The

combined organic layers were washed with water and brine successively and dried (Na$_2$SO$_4$). The

solvent was then removed under reduced pressure and the residue was purified by silica gel flash

chromatography to give the pure oxazole **28** as white solid (2.83 g, 75 %). M.p: 228-230 ºC. ^{1}H

NMR (300 MHz, CDCl$_3$) δ 8.03 (s, 1H), 8.00 (s, 1H), 7.60 (d, *J* = 2.7 Hz, 1H), 7.42 (s, 1H), 7.38

(d, *J* = 8.7 Hz, 1H), 7.18 (dd, *J* = 3.0, 8.7 Hz, 1H), 4.82 (dd, *J* = 2.7, 8.1 Hz, 1H), 3.93 (s, 3H),

3.62-3.81 (m, 2H), 2.64-2.72 (m, 1H), 2.22-2.35 (m, 1H), 1.94-2.04 (m, 2H). ^{13}C NMR (75 MHz,

CDCl$_3$) δ 164.1, 159.1, 150.7, 145.5, 136.3, 131.9, 130.1, 126.3, 126.1, 124.4, 123.6, 119.7, 114.8,

55.87, 52.5, 46.9, 27.8, 23.8; HRMS (ESI) (M+H)$^+$, calcd. for C$_{18}$H$_{17}$N$_4$O$_3$ 337.1301; found

337.1299.

In an oven dried round bottom flask, dry CH$_2$Cl$_2$ (50 mL) was added and then cooled to 0 ˚C. Then

AlCl$_3$ (3.33 g, 24.97 mmol) and ethanethiol (5.0 ml, 67.52 mmol) were added to the above flask

slowly at 0 ˚C. The ice bath was removed and the reaction was allowed to warm to rt. After the

AlCl$_3$ dissolved completely, the oxazole **28** (2.8 g, 8.32 mmol; dissolved in DCM) was added to

the mixture at rt and the mixture was stirred for 24h under Ar. After completion of the reaction

(TLC, silica gel) the solution was poured onto ice and the mixture was acidified using 2N aq HCl solution. The solution was extracted 5-7 times with CH_2Cl_2 and 3-4 times with EtOAc, separately. The combined organic layer was washed with brine and dried (Na_2SO_4). The solvent was removed under reduced pressure and the residue was purified by flash column chromatography [silica gel, 4% MeOH in CH_2Cl_2] to furnish phenol **29** as a solid (2.36 g) in 88% yield: ^{1}H NMR (500 MHz, $CDCl_3$): δ 1.97-2.08 (m, 2H), 2.25-2.35 (m, 1H), 2.65-2.73 (m, 1H), 3.63-3.71 (m, 1H), 3.76-3.84 (m, 1H), 4.84-4.88 (m, 1H), 7.10 (dd, 1H, J = 8.6, 2.2 Hz), 7.30 (d, 1H, J = 5.3 Hz), 7.40 (s, 1H), 7.75 (d, 1H, J = 1.9 Hz), 7.95 (s, 1H), 8.02 (s, 1H), 9.85 (s, 1H); ^{13}C NMR (125 MHz, $CDCl_3$): δ 23.9, 27.8, 47.2, 52.8, 117.6, 120.8, 123.5, 124.7, 125.3, 126.2, 129.3, 131.9, 136.5, 145.4, 150.9, 157.5, 164.8; HRMS (ESI) $(M+H)^+$, calcd. for $C_{17}H_{15}N_4O_3$ 323.1139; found 323.1130.

7.38 (S)-7-Methoxy-1-(1H-tetrazol-5-yl)-11,12,13,13a-tetrahydro-9H-benzo[e]imidazo[5,1-c]pyrrolo[1,2-a][1,4]diazepin-9-one (31)

The DIBAL-H (1.2 M, 6.2 mL, 7.4 mmol) was added at 0 ˚C to a solution of NaO^{t}Bu (0.76 g, 7.9 mmol) in 20 mL of dry THF. The mixture which resulted, was stirred for 1 h at rt under an argon atmosphere. The ethyl ester **5** (1.5 g, 4.4 mmol) was then added to the above solution at 0 ˚C and the mixture was stirred for 3 h (or until the complete consumption of **5**) at rt under Ar. Then, concentrated aq NH_3 (28%, 20 mL) and I_2 (4.57 g, 18.0 mmol) were added at 0 ˚C and the mixture which resulted, was stirred at rt for 3h. After complete disappearance of the aldehyde intermediate, the reaction mixture was treated with a saturated solution of sodium thiosulfate (~10 mL) and extracted with EtOAc (3x 30 mL). The combined organic layer was washed with brine, dried (Na_2SO_4) and the solvent was removed under reduced pressure. The residue was purified by silica gel flash column chromatography (70% EtOAc in hexanes) to furnish the nitrile **30** as a white solid, 1.22 g, 95%. At this point, to a solution of the nitrile **30** (0.295 g, 1.0 mmol) in 30 mL of

THF, ZnBr$_2$ (0.34 g, 1.50 mmol) and NaN$_3$ (78 mg, 1.20 mmol) were added and the mixture was heated to reflux for 36 h (or until complete consumption of **30,** by TLC, silica gel). The solution was then treated with aq 1M HCl to dissolve the solid material and bring the pH of the solution to 1 by pH paper. The solution, which resulted, was extracted with EtOAc (4x 40 mL). The solvent was evaporated under reduced pressure and the residue was passed through a short pad of silica gel with 7% MeOH in DCM to furnish 196 mg of **31**, (yield,58 %). ^{1}H NMR (300 MHz, DMSO-d$_6$): δ 1.96-2.14 (m, 2H), 2.23-2.40 (m, 1H), 3.40-3.50 (m, 1H), 3.5-3.66 (m, 1H), 3.89 (s, 3H), 3.96-4.10 (m, 1H), 4.95 (d, 1H, *J* = 8.34 Hz), 7.31-7.38 (m, 1H), 7.43 (d, 1H, *J* = 2.8 Hz), 7.69 (d, 1H, *J* = 8.8 Hz), 8.60 (s, 1H); ^{13}C NMR (75 MHz, DMSO-d$_6$): δ 24.7, 27.9, 46.6, 52.3, 56.3, 115.1, 119.2, 123.5, 126.0, 126.5, 130.9, 137.7, 155.4, 159.3, 163.3; HRMS (ESI) (M+H)$^+$, calcd. for C$_{16}$H$_{16}$N$_7$O$_2$ 336.1360; found 336.1357.

7.39 (S)-7-Hydroxy-9-oxo-11,12,13,13a-tetrahydro-9H-benzo[e]imidazo[5,1-c]pyrolo[1,2-a]-[1,4]di-azepine-1-carboxylic acid (32)

The ester **6** (1.52 g, 4.6 mmol) was dissolved in a mixture of EtOH (4 mL) and H$_2$O (3 mL), after which solid NaOH (1.0 g, 25.0 mmol) was added to the solution. This reaction mixture was heated to 50 ˚C for 15 min and the EtOH was removed under reduced pressure. The remaining aq solution was stirred at 0 ˚C for 10 min and then conc HCl was added dropwise to the solution until the pH was 3-4 (pH paper). A pale-yellow precipitate, which formed, was left in the solution and the mixture was allowed to stir at rt for 2 h. Then the precipitate was collected by filtration, washed with cold water (2-5 mL) and the aq layer was allowed to stand at rt for 10 h to obtain additional solid acid **32**. The combined solids were dried in a vacuum oven at 80 ˚C for 7 h to get pure dry **32** in 65% yield: ^{1}H NMR (300 MHz, CD$_3$OD): δ 2.14-2.29 (m, 3H), 3.50-3.63 (m, 2H), 3.70-3.78 (m, 1H), 4.95 (d, 1H, merged with solvent peak), 7.15 (d, 1H, *J* = 8.7 Hz, 3.0 Hz), 7.38-7.43 (m,

1H), 7.53 (d, 1H, J = 8.76 Hz), 8.48 (m, 1H); ^{13}C NMR (75 MHz, CD$_3$OD) δ 24.0, 27.7, 46.2, 53.4, 116.2, 119.8, 124.5, 125.4, 128.4, 130.2, 136.2, 137.5, 158.2, 162.5, 164.4; HRMS (ESI) (M+H)$^+$, calcd. for C$_{15}$H$_{14}$N$_3$O$_4$ 300.0979; found 300.0990.

7.40   (S)-N,7-Dimethoxy-9-oxo-11,12,13,13a-tetrahydro-9H-benzo[e]imidazo[5,1-c]pyrolo-[1,2-a][1,4]diazepine-1-carboxamide (33)

A mixture of acid **9** (0.15 g), thionyl chloride (1 mL) and dry CH$_2$Cl$_2$ (8 mL) was added to an oven dried round bottomed flask under argon. This suspension was allowed to reflux at 52 ºC (the outside oil bath temperature was at 60 ºC) for 1 h under an atmosphere of argon. The solution became a clear yellow color. The absence of the starting material was confirmed by the examination of the solution by TLC (silica gel). The organic solvent and excess thionyl chloride were removed under reduced pressure. This flash evaporation with dry DCM was repeated two times with dry CH$_2$Cl$_2$ (5 mL) to remove excess thionyl chloride and any HCl. The yellow residue, which was obtained, was dissolved in dry CH$_2$Cl$_2$ (10 mL) and cooled to 0 ºC for 10 min under argon. Then methyl hydroxylamine hydrochloride (2.5 eq), followed by Et$_3$N (5 eq) was added to the reaction mixture at 0 ºC and the mixture was then allowed to warm to rt and stirred for 4 h. After the completion of the reaction (TLC, silica gel), the solvent was removed under reduced pressure and acetone (4 mL) was added to the residue. The salt was removed by filtration and the solvent was removed under reduced pressure to provide MRS-III-87 in 70 % yield: 1H NMR (300 MHz, CDCl3) δ 2.14-2.22 (m, 2H), 2.30-2.39 (m, 1H), 3.08-3.10 (m, 1H), 3.51-3.57 (m, 1H), 3.75-3.80 (m, 1H), 3.88 (s, 3H), 3.91 (s, 3H), 4.72 (d, 1H, J = 8.0 Hz), 7.14 (dd, 1H, J = 8.8 Hz, 2.7 Hz), 7.28 (d, 1H, J = 8.8 Hz), 7.58 (d, 1H, J = 2.7 Hz), 7.69 (s, 1H), 9.84 (bs, 1H); LCMS (ESI, m/z, relative intensity (ESI), calcd. For C$_{17}$H$_{17}$N$_4$O$_4$ (M-H)$^+$ 341.35; Found 341.00.

7.41 (S)-N-Cyano-7-methoxy-9-oxo-11,12,13,13a-tetrahydro-9H-benzo[e]imidazo[5,1-c]py-rrolo[1,2-a][1,4]diazepine-1-carboxamide (34)

A mixture of acid **9** (0.15 g), thionyl chloride (1 mL) and dry CH_2Cl_2 (8 mL) was added to an oven dried round bottomed flask under argon. This suspension was allowed to reflux at 52 ℃ (the outside oil bath temperature was at 60 ℃) for 1 h under an atmosphere of argon. The solution became a clear yellow color. The absence of the starting material was confirmed by the examination of the solution by TLC (silica gel). The organic solvent and excess thionyl chloride were removed under reduced pressure. This evaporation was repeated a couple of times with dry CH_2Cl_2 (5 mL) to remove excess thionyl chloride and any HCl. The yellow residue, which was obtained, was dissolved in dry CH_2Cl_2 (10 mL) and cooled to 0 ℃ for 10 min under argon. The methyl cyanamide (2.5 eq), followed by Et_3N (5 eq.) was added to the reaction mixture at 0 ℃ and the mixture was then allowed to warm to rt and stirred for 5 h. After the completion of the reaction (TLC, silica gel), the solvent was removed under reduced pressure and acetone (4 mL) was added to the residue. The salt was filtered off and the solvent was removed under reduced pressure to obtain MRS-III-90 in 70% yield. ^{1}H NMR (300 MHz, DMSO-d6) δ 2.10-2.13 (m, 2H), 3.34-3.58 (m, 3H), 3.88 (s, 3H), 3.91 (s, 3H), 4.73 (d, 1H, J = 7.5 Hz, major rotamer 83%), 4.84 (d, J = 7.5 Hz, minor rotamer, 17%), 7.27-7.29 (m, 1H, major rotamer), 7.31-7.33 (m, minor rotamer), 7.38 (d, 1H, J = 2.0 Hz, major rotamer), 7.41 (d, J = 2.5 Hz, minor rotamer), 7.57 (d, 1H, J = 8.5 Hz, major rotamer), 7.64 (d, J = 9.0 Hz, minor rotamer), 8.00 (s, 1H, major rotamer), 8.21 (s, minor rotamer), 9.49-10.11 (bs, 1H); LCMS (ESI, m/z, relative intensity (ESI), calcd. for $C_{17}H_{14}N_5O_3$ (M-H)$^+$ 336.33; Found 336.00.

7.42 General method for the synthesis of alkyl ethers at the C-8 position (35-39)

To a solution of phenol **6** (0.15 g) in CH_2Cl_2 (5 mL), Cs_2CO_3 (0.3 g) was added and the mixture was stirred at rt for 30 min. Then the alkyl halide [ethyl iodide; ethyl iodide-d_5; cyclopropyl bromide; isopropyl iodide or *t*-butyl bromide (0.5 mL)] was added (individually) slowly and the reaction mixture was stirred at rt for 24 h. After completion of the reaction (TLC, silica gel) the mixture was quenched with cold water and extracted with CH_2Cl_2. The combined organic layer was washed with brine and dried (Na_2SO_4). The solvent was removed under reduced pressure and the solid residue (ester) was used directly for the next step. The ester [from first step], was dissolved in a mixture of EtOH (4 mL) and H_2O (3 mL), after which solid NaOH (5 eq) was added to the solution. This reaction mixture was heated to 50 ºC for 15 min and then the EtOH was removed under reduced pressure. The remaining aq solution was stirred at 0 ºC for 10 min and then conc. HCl was added dropwise to the solution until the pH was 3-4 (pH paper). A pale yellow precipitate, which formed, was left in the solution and the mixture was allowed to stir at rt for 2 h. The precipitate was collected by filtration, washed with cold water (2 X 5 mL) and the aq layer also was extracted with CH_2Cl_2 (2 to 3 X). The combined organic layer was washed with brine and dried (Na_2SO_4). The solvent was removed under reduced pressure to provide additional amounts (individually) of acids **35-39**.

7.43 (*S*)-7-Ethoxy-9-oxo-11,12,13,13*a*-tetrahydro-9*H*-benzo[*e*]imidazo[5,1-*c*]pyrrolo[1,2-*a*]-[1,4]diazepine-1-carboxylic acid (35)

70 % yield: ^{1}H NMR (500 MHz, DMSO-d_6) δ 1.38 (t, 3H, *J* = 7.0 Hz), 2.06-2.16 (m, 3H), 3.30-3.32 (m, 1H), 3.42-3.46 (m, 1H), 3.59-3.62 (m, 1H), 4.15 (q, 2H, *J* = 7.0 Hz), 4.86 (d, 1H, *J* = 7.5

Hz), 7.30 (dd, 1H, J = 9.0 Hz, 3.0 Hz), 7.39 (s, 1H), 7.64-7.66 (m, 1H), 8.77-8.89 (bs, 1H); LCMS (ESI, m/z, relative intensity (ESI), calcd. for $C_{17}H_{16}N_3O_4$ (M-H)$^+$ 326.33; Found 326.00

7.44   (*S*)-7-(²H₅)Ethoxy-9-oxo-11,12,13,13*a*-tetrahydro-9*H*-benzo[*e*]imidazo[5,1-*c*]pyrrolo-[1,2-*a*][1,4]diazepine-1-carboxylic acid (36)

65 % yield: ^1H NMR (500 MHz, DMSO-d₆) δ 2.04-2.17 (m, 2H), 3.42-3.46 (m, 4H merged with DMSO+H₂O peak), 4.83(d, 1H, J = 7.5 Hz), 7.29 (dd, 1H, J = 9.0 Hz, 3.0 Hz), 7.37-7.38 (m, 1H), 7.61 (d, 1H, J = 9.0 Hz), 8.20 (s, 1H); ^2H NMR (500 MHz, DMSO, number of scans =128) δ 1.25 (3D) and 4.04 (2D). LCMS (ESI, m/z, relative intensity (ESI), calcd. for $C_{17}H_{13}D_5N_3O_4$ (M+H)$^+$ 333.37; Found 333.25.

7.45 (*S*)-7-Cyclopropoxy-9-oxo-11,12,13,13*a*-tetrahydro-9*H*-benzo[*e*]imidazo[5,1-*c*]pyrrolo-[1,2-*a*][1,4]diazepine-1-carboxylic acid (37)

30 % yield: ^1H NMR (500 MHz, CDCl₃) δ 2.19-2.29 (m, 3H), 3.35-3.57 (m, 1H), 3.68-3.71 (m, 1H), 3.77-3.81 (m, 1H), 4.61- 4.69 (m, 2H), 4.72 (d, 1H, J = 7.0 Hz), 5.35 (d, 1H, J = 13.5 Hz), 5.46 (d, 1H, J = 13.5 Hz), 6.02-6.10 (m, 1H), 7.19 (dd, 1H, J = 8.5 Hz, 2.3 Hz), 7.31-7.33 (m, 1H), 7.61 (d, 1H, J = 2.3 Hz), 7.78 (s, 1H); LCMS (ESI, m/z, relative intensity (ESI), calcd. for $C_{18}H_{18}N_3O_4$ (M+H)$^+$ 340.35; Found 340.20.

7.46   (*S*)-7-Isopropoxy-9-oxo-11,12,13,13*a*-tetrahydro-9*H*-benzo[*e*]imidazo[5,1-*c*]pyrrolo-[1,2-*a*][1,4]diazepine-1-carboxylic acid (38)

70 % yield: ^1H NMR (500 MHz, CDCl₃) δ 1.38 (d, 3H, J = 6.3 Hz), 1.40 (d, 3H, J = 6.3 Hz), 2.19-2.26 (m, 3H), 3.51-3.57 (m, 1H), 3.65-3.68 (m, 1H), 3.77-3.80 (m, 1H), 4.66-4.74 (m, 2H), 7.13-7.16 (m, 1H), 7.39 (bs, 1H), 7.57 (d, 1H, J = 2.5 Hz), 7.89 (bs, 1H); LCMS (ESI, m/z, relative intensity (ESI) calcd. for $C_{18}H_{20}N_3O_4$ (M+H)$^+$ 342.36; Found 342.30.

7.47 (*S*)-7-(*tert*-Butoxy)-9-oxo-11,12,13,13*a*-tetrahydro-9*H*-benzo[*e*]imidazo[5,1-*c*]pyrrolo-[1,2-*a*][1,4]diazepine-1-carboxylic acid (39)

65 % yield: ^{1}H NMR (500 MHz, CDCl$_3$) δ 1.43 (s, 9H), 2.20-2.29 (m, 3H), 3.51-3.57 (m, 1H),3.67-3.69 (m, 1H), 3.76-3.80 (m, 1H), 4.74 (d, 1H, *J* = 7.0 Hz), 7.23 (dd, 1H, *J* = 8.7 Hz, 2.2 Hz), 7.30 (d, 1H, *J* = 8.7 Hz), 7.72 (d, 1H, *J* = 2.2 Hz), 7.39 (s, 1H), 7.83 (bs, 1H); LCMS (ESI, m/z, relative intensity (ESI), calcd. for C$_{19}$H$_{22}$N$_3$O$_4$ (M+H)$^+$ 356.39; Found 356.25.

PART II

1. Introduction

Type A γ-aminobutyric acid receptors (GABA$_A$) is the primary target receptor for GABA, which is the major inhibitory neurotransmitter of the central nervous system.[94,227] These systems are ligand-gated chloride ion pores that are transmembrane hetero-pentameric in structure. Since it is the principal target receptor for its indigenous ligand (GABA), GABA$_A$ receptors regulate a wide range of functions within the brain and the across the central nervous system.[239] A variety of GABA-ergic ligands can positively or negatively modulate different subtypes of GABA$_A$ receptors and thus can exert various CNS effects (see Part I, Table 1). As described earlier in part I, benzodiazepines (BZDs) are a class of drugs that binds to GABA$_A$Rs and exerts allosteric effects on GABAR efficacy.[227,239] It is known that classical BZDs such as diazepam bind to the extracellular region at the interface between the $\alpha^+\gamma^-$ protein subunits and acts as a positive modulator (PAM) at $\alpha_{1-3,5}\beta\gamma_2$ subtypes of the GABA$_A$Rs.[13,227,239,240] BZDs have been used in clinic for more than five decades, although these drugs exhibit various undesired adverse CNS effects.[227,239] Diazepam, for instance, though among the very limited options available for CNS disorders including anxiety, convulsions and insomnia, can evoke side effects such as sedation, ataxia, amnesia, and addiction.[132,239,241-243] Moreover, it is not effective in all patients and has a limited long-term application as a prescription drug due to some of these adverse effects. On the other hand, due to the absence of suitable replacements in terms of better subtype selectivity and efficacy that are devoid of the undesired effects, they are still among the mainstays for treatment of CNS disorders.[227,239,243]

A large number of studies suggest that the development of novel $\alpha_2\beta_{2/3}\gamma_2$ and $\alpha_3\beta_{2/3}\gamma_2$ subtype selective GABA$_A$R ligands is a promising avenue for the development of better agnostic efficacy. These subtype selective agents would exert anxiolytic, antinociceptive, and anticonvulsant

activity, while avoiding the undesired effects, which stem from efficacy at $\alpha_2\beta_{2/3}\gamma_2$.[132,227,239,244-251,252,253] According to the recent literature this class of $\alpha_{2/3}$ subtype selective GABA$_A$R allosteric modulators are believed to be better treatments for seizures,[235,254] antihyperalgesia,[255,256] and anxiety[132-134] without causing sedation, amnesia, ataxia, addiction and dependence, as well as tolerance.[257-259] As a consequence of rigorous studies and development in this vein, a number of promising drug candidates[227,235,244,248,260,261] have appeared, but most of them failed to remain in the development process due to poor pharmacokinetic properties[227,262] and/or adverse CNS effects.[227,244,263,264] As a consequence, due to the unmet demands for drugs with superior $\alpha_{2/3}$ subtype efficacy, which lack the undesired CNS side effects from efficacy at α_1 subtypes, there is a need to develop novel selective GABA$_A$ ligands for various disorders.

2. Background

The continued research over the last decade resulted in a series of $\alpha_{2/3}$ subtype selective imidazodiazepine (IBZ) GABA$_A$R ligands (agonists), designed and synthesized based on the unified pharmacophore model.[13,227,239,265] Among the initial lead compounds which contained the "privileged" IBZ scaffold were XHe-II-053 **1**, Hz-166 **2**, and JY-XHe-053 **3**, (see Figure 1). They have been characterized for their selectivity towards $\alpha_{2/3}$ subtypes over α_1.[227,252] It has been illustrated that Hz-166 (ligand **2**) can evoke anxiolytic effects without causing sedation associated with non-selective PAMs such as diazepam.[246,253] It is evident that the presence of an acetylene function at the C(8) position of these ligands was the reason behind the diminished binding affinity and efficacy at the sedating $\alpha_1\beta_3\gamma_2$ ion channels.[13,239,265] Ligand Hz-166 **2** has shown antiseizure activity in mice and rats both from oral and i.p. administrations in a subcutaneous metrazole-

induced seizure (scMET) test.[266] Moreover it did not develop tolerance to the anticonvulsant effects; a very special Bz/GABAR ligand.[252] Furthemore, in primate studies with rhesus monkeys, Hz-166 **2** engendered non-sedating anxiolytic effects in the Geller-Seifter conflict assay at 1 mg/kg dose.[246] In addition, Hz-166 **2** showed a dose dependent antihyperalgesic effect in inflammation and neuropathic pain models without causing sedation, sensorimotor impairment nor tolerance unlike the commonly used antinociceptive molecules morphine, diazepam and gabapentin.[255] Ligand Hz-166 **2**, although stable enough on human liver microsomes (HLMs), was rapidly metabolized in mouse liver microsomes (MLMs). The labile nature of the ester function at C(3) in the presence of microsomal enzymes (especially in the liver) was responsible for the hydrolysis to the carboxylic acid which retarded the ability of the ligand to cross the blood brain barrier (BBB) and achieve the desired effects. The metabolite (the acid) was excreted to rapidly form the system.[267] Similar results were also observed for XHe-II-053 **1** and JY-XHe-053 **3**.[227] This limited the ADME toxicity studies in rodents and is a concern because poor pharmacokinetic profiles are one of the major reasons for the failure of promising drug candidates in the development process. As a result, strategies were undertaken to develop new ligands, which would retain the anxiolytic properties of Hz-166 **2** while achieving better stability on liver microsomes to increase plasma and brain exposure.[227] The prevention of the ester from being metabolized by blocking its metabolic site at C(3) was deemed necessary.

XHe-II-053, **1**   HZ-166, **2**   JY-XHe-053, **3**
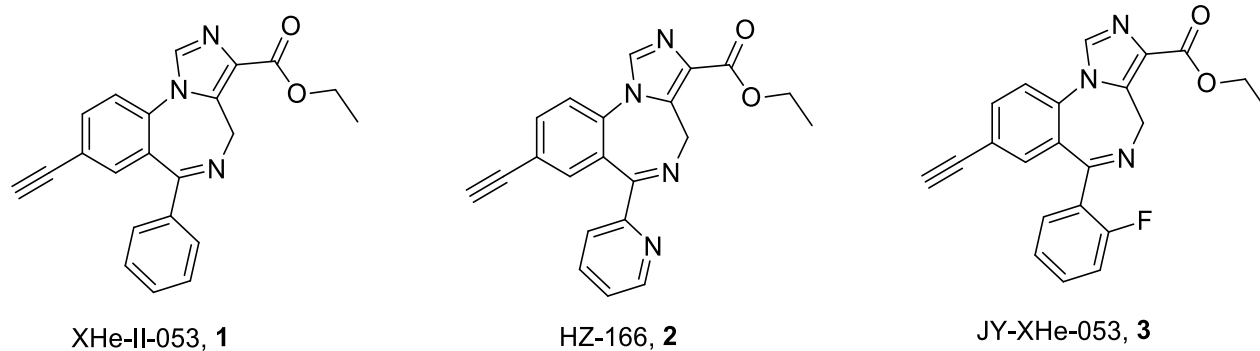
Figure 1. Initial lead compounds which contain the "privileged" IBZ scaffold

Bioisosteric alteration of labile functional groups has been key among the modern strategies for generating novel compounds that are similar in activity despite being different structures. They are, however, recognized similarly by the biological systems. It follows that a bioisostere should retain the biological properties, while being structurally different and devoid of activity toward the common metabolic pathways that motivated ligand Hz-166.[217] Accordingly, a bioisosteric replacement of the ester function, which is more stable under enzymatic metabolism would be a logical strategy. The 1,2,4-oxadiazole and 1,3-oxazole are known to be ester bioisosteres, which are more stable metabolically, although the latter is less-commonly used. As a result, conversion of the ester function at C(3) into an 1,2,4-oxadiazole or 1,3-oxazole would increase their stability and would increase plasma and brain exposure for the desired efficacy.[9,217] Moreover, the 1,3-oxazole is not a normal bioisostere for an ethyl ester and increased the strength of IP protection. Alternatively, incorporation of deuterium to block a primary site of oxidative metabolism of the ethyl esters (**1-3**) by replacing the -CH$_2$- function with a -CD$_2$- should also increase their stability through the kinetic isotopic effect.[227]

3. Aims of this Work

As indicated, from the in vitro and in vivo studies, bioisosteric replacement of the ester function is more likely to be a better strategy to design novel α_2/α_3 subtype selective ligands for the treatment of various CNS disorders. Further modification of the newly achieved lead compounds would result in ligands with even better drug like properties. A series of ester bioisosteres with suitable functional groups at different substituents on the heterocyclic ester bioisostere moiety, as well as incorporation of deuterium at the key metabolic sites should also be explored further. In addition, improvement of the current synthetic route to these ligands would also be highly desired.

4. Chemistry and Results

As discussed above, HZ-166 **2**, the initial lead ligand possessed all the desired biological properties except metabolic stability in rodents. Although it was stable on human liver microsomes (HLM), it was comparatively labile in mouse, and rat liver microsomes (MLM and RLM) due to the effect of enzymes which converted it into the carboxylic acid **4**.[239,267] Since the carboxylic acid was more hydrophilic, it was less able to cross the BBB, and effect the desired CNS effects in brain.[239] As a result, the potential ligand did have low plasma and brain exposure. Accordingly, it was felt that by increasing the metabolic stability of the ester function at C(3), while retaining its biological properties would be the key step in achieving the next generation of α_2/α_3 stable subtype selective ligands for CNS disorders.

In accordance with this hypothesis, several ester bioisosteres were synthesized and evaluated for their *in vitro* and *in vivo* metabolic stability, as well as general anxiolytic effects. Among the newly designed ligands, MP-III-80 **7** and KRM-II-81 **9** were found to possess superior drug stability,

166

pharmacokinetic profiles and anxiolytic efficacy, as well as the absence of significant sensorimotor impairment, which is indicative of CNS side-effects.[227] The 1,2,4-oxadiazoles (ligands **6**, **7**) were less potent (EC_{50} = 5.15 and 3.02 µM, respectively) than the corresponding 1,3-oxazoles (**8-10**, EC_{50} = 0.94 µM) towards $\alpha_3\beta_3\gamma_2$ $GABA_AR$ over $\alpha_1\beta_3\gamma_2$ (EC_{50} > 20 µM for all ligands) in the FLIPR assay.[227]

SR-II-54, **4**   MP-III-068, **5**

MP-III-085, **6**   MP-III-080, **7**

KRM-II-82, **8**   KRM-II-81, **9**   KRM-II-18B, **10**
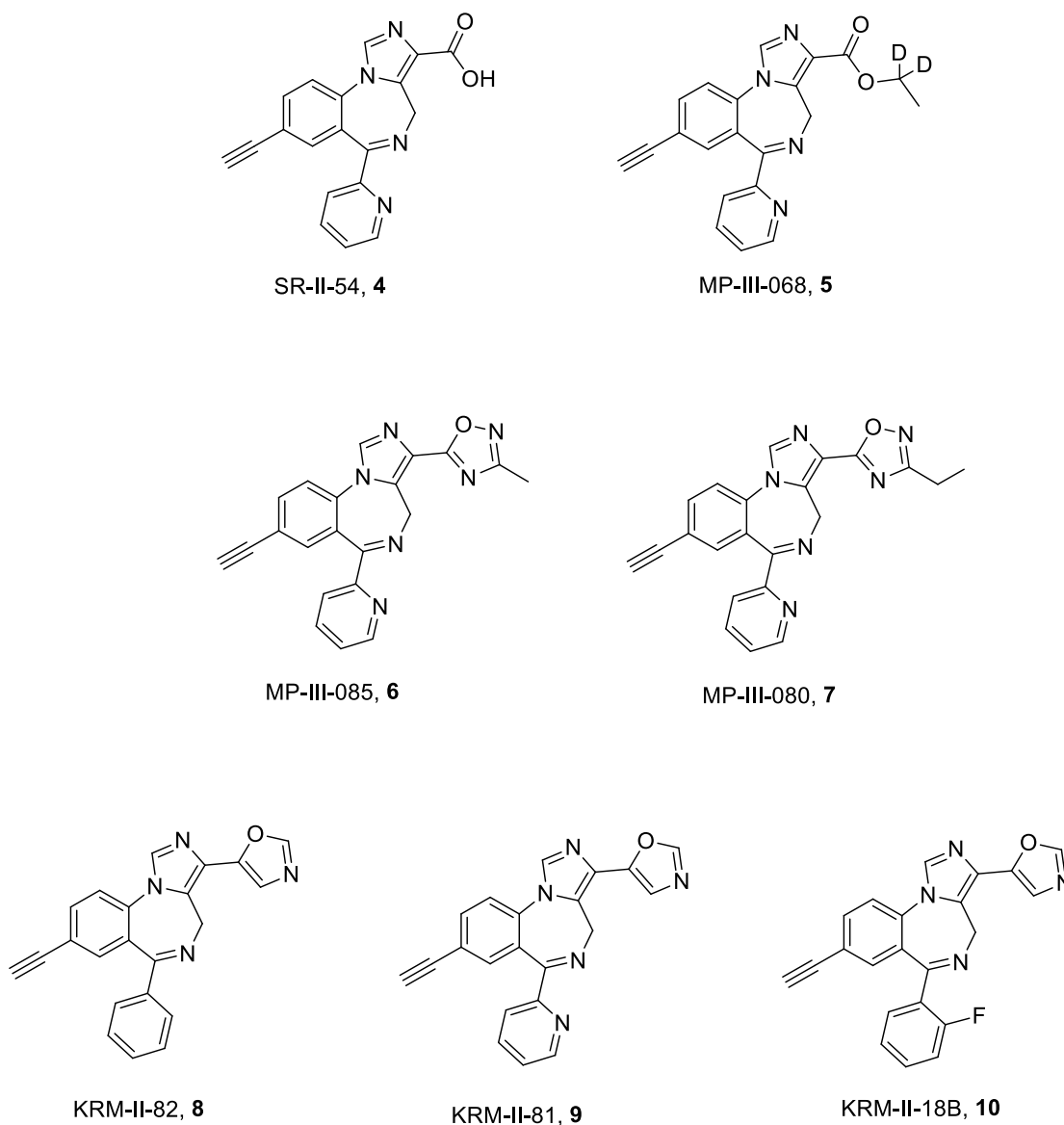
Figure 2. Representative examples of the new generation of α2/α3 subtype selective GABAAR ligands

The 2′-F (in the pendant phenyl ring) ligands **3** and **10** exhibited EC_{50}s in the nanomolar range (EC_{50} = 29 and 11 nM, respectively) while the deuterated ester **5** showed potency similar to the non-deuterated counterpart **2**.[227] Due to their lack of efficacy at the $\alpha_1\beta_3\gamma_2$ site, these compounds were expected to be devoid of tolerance and dependence.[257-259] As expected, the carboxylic acid **4** which was hydrophilic, did not travel across the BBB in appreciable amounts and thus was not detected in the brain in PK studies when administered as the acid **4** itself or as a metabolite of the esters **2** and **5**.
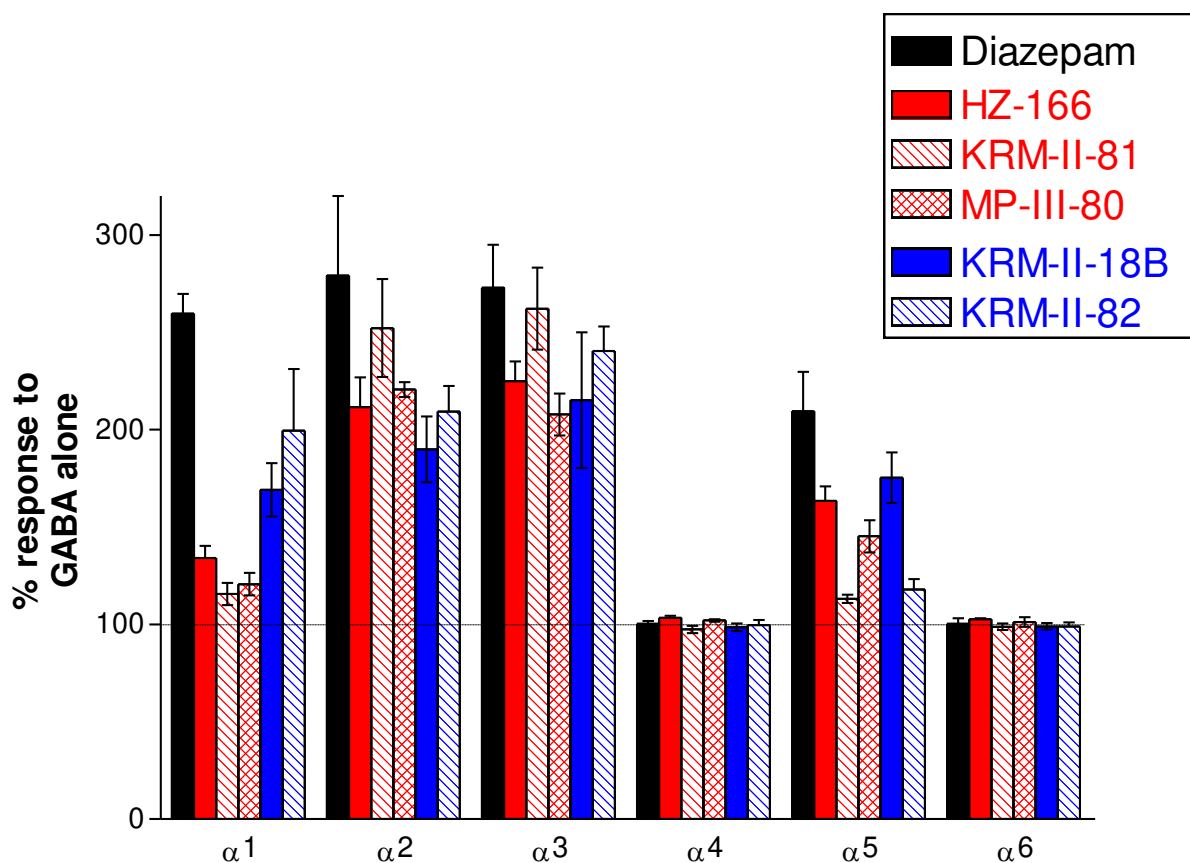
Figure 3. Comparison between the efficacies at various subtypes (α_1-α_6) GABA$_A$Rs determined in HEK cells by GABA induced EC$_3$ currents at 100 nM concentrations of ligands. This is work of Janet Fischer at the University of South Carolina. Presented at ASPET Annual Meeting at EB, Orlando, April 9, 2019.[268]

Illustrated in Figure 3, Hz-166 **2**, MP-III-80 **7** and KRM-II-81 **9** are more efficacious at α_2 and α_3 over α_1 subtypes ion channels while typical benzodiazepines such as diazepam elicit efficacy at α_1 (and α_5) subtypes, as well. While all three ligands show similar efficacy at α_2/α_3 subtypes, KRM-II-81 **9** exhibited the highest efficacy at these sites (Figure 3). Both MP-III-80 **7** and KRM-II-81 **9** exhibited lower efficacies at α_1 subtypes compared to diazepam and the parent ligand HZ-166 **2**. In addition, their efficacies at α_2/α_3 subtypes were higher (or similar to) than that of Hz-166 **2,** while the efficacy at α_5 subtypes was poorer than at HZ-166 **2**. This indicates MP-III-80 **7** and KRM-II-81 **9** are new generation GABA$_A$R PAMs with better or similar α_2/α_3 efficacies over α_1 (and α_5) efficacy, which is highly desired to avoid sedation, tolerance, dependence and related CNS side-effects.

In the evaluation of metabolic stability as expected, the incorporation of deuterium at the key metabolic sites indeed resulted in increased stability in HLM, MLM. In addition, the heterocyclic ester bioisosteres were more stable in liver microsomes, as well. The overall outcome of these studies was the identification of KRM-II-81 **9** as a unique and promising lead compound with desirable α_2/α_3 GABA$_A$R selectivity, low molecular weight (MW = 351), superior lipophilicity (clogP = 2.3), good solubility at pH 7, excellent plasma and brain exposure (26 and 18%, respectively), as well as in vivo anxiolytic activity in a rodent model.[227] It is hoped these ligands will soon be evaluated further in models of epilepsy and neuropathic pain. Likewise, MP-III-080 **7** exhibited marked improvement in pharmacokinetic properties over the parent compound HZ-166 **2**, as well.[227] In a mouse marble burying assay, which is a model of anxiety, MP-III-080 **7** at 10 mg/kg, significantly reduced marble burying activity, which indicated its potent anxiolytic activity (Figure 4). Ligand **7** also showed effective anticonvulsant effects versus GABA$_A$ NAM pentylenetetrazole (PTZ)-induced seizures with very mild sedation at 30 mg/kg i.p. dosage.[227] The

effect of these compounds on sensory motor ability via the rotarod assay was performed using the same mice used for the marble burying assay. At 30 mg/kg dosage all compounds showed minor motor impairment except for KRM-II-81 **9** (Figure 5).
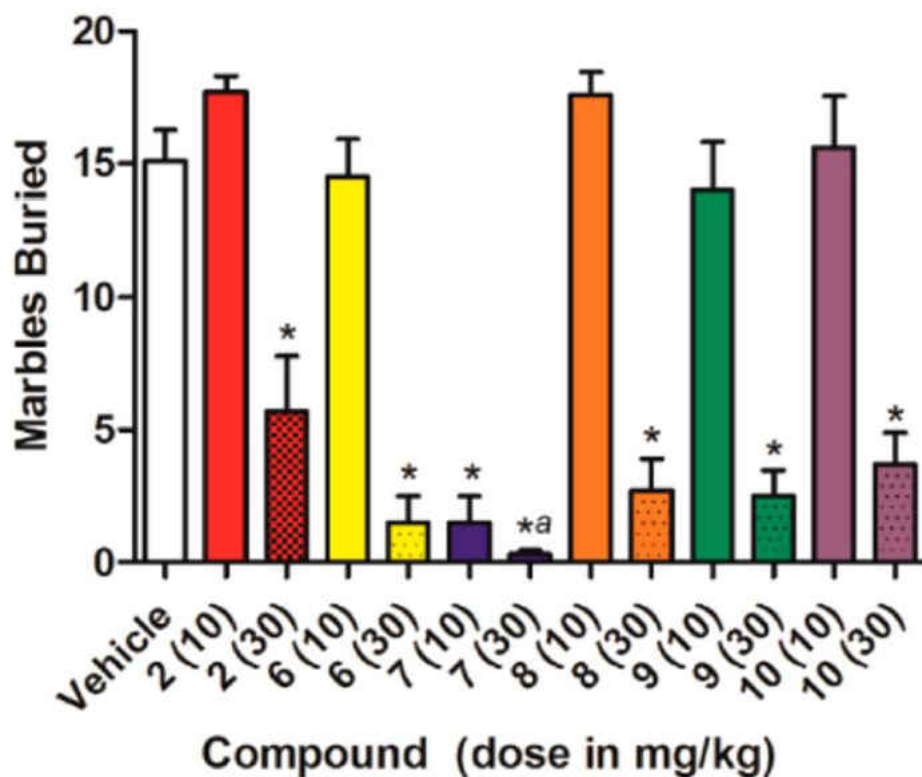
Figure 4. Assessment of anxiolytic-like activity of ligands 2 and 6−10 in the marble burying assay. Male NIH Swiss Webster mice (n = 10) were injected ip with vehicle or a test compound (10 or 30 mg/kg) 30 min prior to testing. Data were analyzed using ANOVA. Dunnett's test: (∗) P < 0.05 vs vehicle; (a) mild sedation-like behavior observed at 30 mg/kg. (modified from the Figures in Poe *et al.*)[227]
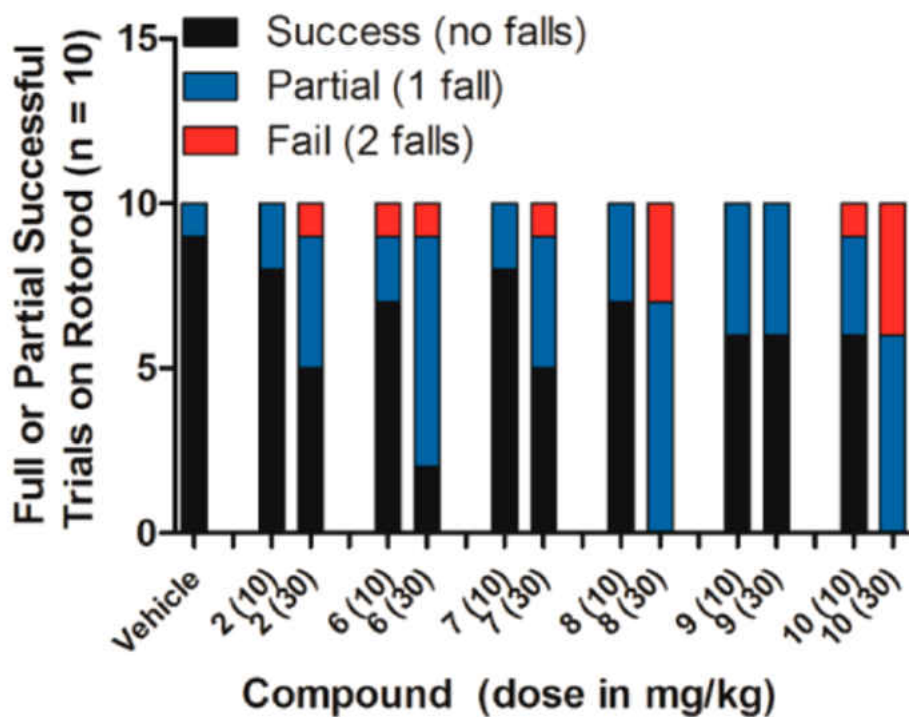
Figure 5. Assessment of ataxic effects of ligands 2 and 6−10 in the rotarod assay. Mice, as treated in the marble burying assay, were placed on a rotarod set at 4 rpm, and the testing time was 2 min. Mice not falling off during the test were given a "Success" designation, while mice that fell once were assigned a "Partial" designation. Mice falling twice during the 2 min time period failed the test (modified from the Figures in Poe *et al.*).[227]

In the Vogel conflict assay in rats, imidazo[1,5-a][1,4] diazepine esters were inactive due to their low bioavaiabilities.[251] This result is consistent with the previous observation by Poe et al.[227] Both oral and i.p. dosing resulted in low drug exposures,[227] which explained their inactivity in *in vivo* experiments. On the other hand, ligand **7** exhibited profound efficacy in this anxiolytic-detecting assay without affecting non-punished responding (Figure 6), i.e. no sedation.
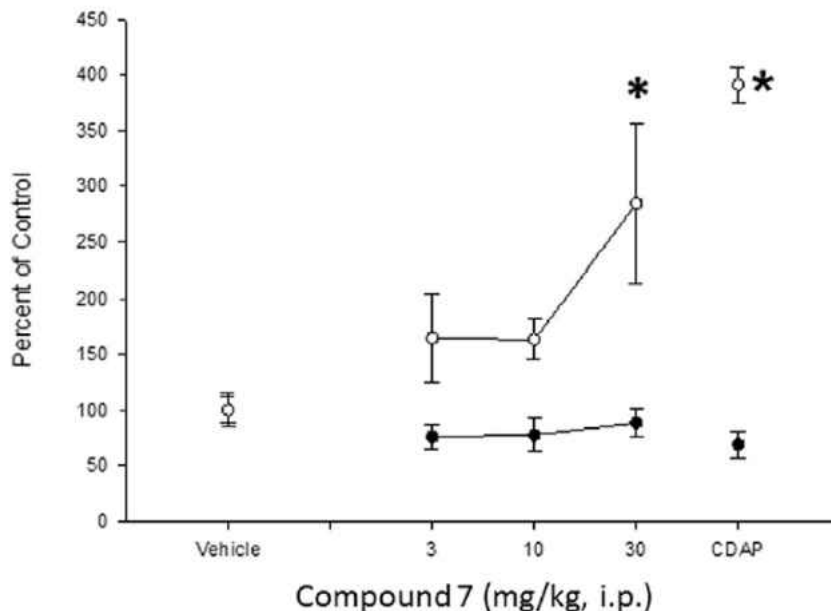
Figure 6. Effects of MP-III-080 (7) on punished (unfilled circles) and non-punished (filled circles) drinking of rats. Each point represents the mean ± S.E.M. of 8 rats/dose condition. Chlordiazepoxide (20 mg/kg, i.p.) was studied as a comparator. Data were analyzed by ANOVA followed by post-ho c Dunnett's test. *: p < 0.05. Non-punished responding: $F_{3,28} = 2.4$, p =0.1.1. Punished responding: $F_{3,2} = 8.7$, p < 0.001. *p < 0.05 by post-hoc Dunnett's test (modified from the Figures in Witkin *et al.*).[251]

It has been illustrated previously by Poe et al. that ester bioisosteres effected pronounced improvement in plasma and brain exposures as compared to the parent esters.[227] Although direct dose/exposure comparisons are not available, data document that both the MP-III-80 (**7**, anxiolytic active) and the oxazole KRM-II-82 (**8**, anxiolytic inactive) exhibited high exposure in both brain and plasma of rats after i.p. dosing.[251]

The distinctive nature of oxadiazole **7** and oxazole **8** in behavioral effects was deemed to be due to a yet to be determined ancillary action of oxadiazole **7** that supplemented its effects at GABA$_A$ $\alpha_{2/3}$ receptors. The oxazole **8** exhibited anti-depressant activity as compared to oxadiazole **7**, while oxazole **8** was safe but more cytotoxic than oxadiazole **7** in human embryonic kidney cells (HEK293T).[227,251]

Alcohol abuse and alcohol (ethanol) use disorder (AUD) have consequences on global public health. According to WHO, alcohol related health problems represent the 5th largest factor for premature death and disability.[269] Currently available treatment options are only partially effective and the global concern of alcohol abuse and use related complications are still prevalent even with decades of research.[270] As a result there is an unment demand for novel treatment options and further research for discovery and development of improved treatment options for alcohol abuse related behavioral effects, as well as understanding the neuropharmacological mechanisms involved in alcohol abuse.

It is known that ethanol induces its abuse-related effects, in part, by potentiating the activity of γ-aminobutyric acid at $GABA_A$ receptors.[271] Genetic studies in humans and preclinical studies with mutant mice indicated that $α_2$ and/or $α_3$ $GABA_A$ receptors play a role in the effects of ethanol. Consequetly, the design and synthesis of novel $GABA_A$R PAMs with $α_2$ and $α_3$ efficacies would permit evaluation of the effects of these subtypes in preclinical models of discriminative stimulus and reinforcing effects of ethanol use in primates by Platt *et al*.[269]

In a recent study by Berro et al, it has been illustrated that there is a key role for $α_2$ $GABA_A$ and/or $α_3$ $GABA_A$ receptors in the reinforcing effects of ethanol. Investigation on a series of functionally selective PAMs at $α_2$ and $α_3$ $GABA_A$ receptors (HZ-166 **2**, XHe-II-053 **3**, YT-III-31, YT-III-271) indicated the enhancement in ethanol intake at doses that did not alter sucrose intake (Figures 7 and 8).[269]
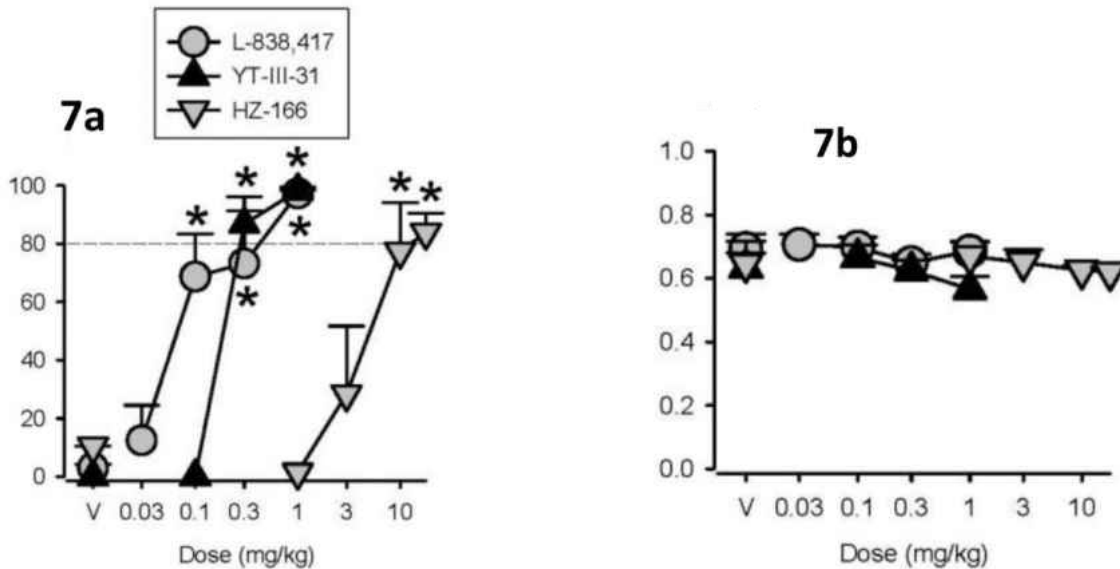
Figure 7. Effects of α₂GABA_A and α₃GABA_A Receptor-Preferring PAMs. All α₂/α₃ GABA_A receptor ligands reproduced the discriminative stimulus effects of ethanol (Figure 7a), engendering dose-dependent increases in ethanol-lever responding that were significantly different from that engendered by vehicle [L-838, 417: $F_{(4,12)}$ = 14.68, $p<0.001$; Bonferroni t-tests, $p<0.05$ vs. vehicle; HZ-166: $F_{(4,9)}$ = 14.47, $p<0.001$; Bonferroni t-tests, $p<0.05$ vs. vehicle; YT-III-31: $F_{(3,9)}$ = 120.45, $p<0.001$; Bonferroni t-tests, $p<0.05$ vs. vehicle]. L-838,417 (functionally selective PAM at α2GABA_A, α3GABA_A, and α5GABA_A receptors), HZ-166 (functionally selective PAM at α2GABA_A and α3GABA_A receptors) as well as YT-III-31 (functionally selective PAM at α3GABA_A receptors) induced almost exclusive responding on the ethanol-paired lever over the dose ranges tested, generating 97%, 84% and 99% ethanol-lever responding, respectively. None of these compounds significantly altered average rates of responding when compared to average rates following vehicle administration (Figure 7b). Modified from the Figures in Berro _et al._[269]

Figure 8. The effects of pretreatments with different doses of α_2GABA$_A$ and α_3GABA$_A$ receptor-preferring compounds on ethanol and sucrose intake. Daily pretreatment with the functionally selective PAMs at α_2GABA$_A$ and α_3GABA$_A$ receptors XHe-II-053 [group X dose: $F(3,24) = 7.20$, $p<0.005$] and HZ-166 [group X dose: $F(3,24) = 5.39$, $p<0.01$] resulted in significant increases in ethanol intake at 1 mg/kg without affecting sucrose intake (Bonferroni t-tests, $p<0.05$; Figure 8A and Figure 8B). Modified from the Figures in Berro *et al.*[269]

As suggested by these results, the parent lead compound Hz-166 **2** metabolized fast in rodents. Bioisosteric modification of the ester function in Hz-166 **2** into 1,3-oxazole **9** and 1,2,4-oxaidiazole **7** resulted in novel α_2/α_3 subtype selective positive allosteric modulators (PMAs) of GABA$_A$Rs and are stable in human, mouse, rat, and dog live microsomes.[227,239] These desired results suggest further evaluations of oxazole **9** and oxadiazole **7** in animal models of epilepsy, neuropathic pain, anxiety, and respiration in rodents, as well as in primates. These animal studies would require these ligands in gram quantities.

From a synthetic point of view, Hz-166 **2** is a key ligand which is not only a primary lead itself but also serves a as a key precursor for several potential drug candidates such as the 1,2,4-oxadiazoles and 1,3-oxazoles.[239] A sustainable supply of Hz-166 **2** is a prerequisite for availing gram quantities of the newly designed ligands MP-III-080 **7** and KRM-II-81 **9**. The ethyl

oxadiazole (MP-III-80 **7**) was previously synthesized in 40-71% yields from ester **2** (Hz-166).[227,252,253] More importantly, the oxazole **9** was available only in a mere 28% yield on a 3g scale process, which posed a major drawback in its synthesis.[227] In addition, very low overall yields toward Hz-166 (17% in a five step process) also posed a major hurdle in a robust supply of the desired ligands.[252,239] Consequently, an improved synthetic strategy was desired for accessing the ligands in deca-gram quantities for animal and pre-clinical studies.

An optimized route for the total synthesis of HZ-166 **2** is depicted in Scheme 1, as developed recently by Li et at.[239] After numerous modifications and fine-tuning in each of the five steps, the optimized route furnished the target compound Hz-166 **2** in a 56% overall yield from the beginning, while the previously available route provided Hz-166 **2** in a mere 17% overall yield.[239]

First, acylation of the aniline **11** with bromoacetyl bromide resulted in synthesis of the acylated aniline **12**, which could be used in the subsequent reaction without purification. The treatment of the crude **12** with dry methanol saturated with ammonia gas at 0 $^{\circ}$C was followed by gradual heating to reflux to furnish the 1,4-benzodiazepine **13** in 78% yield over two steps. Both of these steps could be performed on hundred-gram scales. The 1,4-benzodiazepine amide **13** could be purified by recrystallization instead of chromatographic purification. The imidazole top was attached via the modified procedure.[272] the amide **13** was stirred with potassium tert-butoxide and this was followed by diethylchlorophosphate at -50 $^{\circ}$C in THF for an hour. Afterwards, the mixture was allowed to warm to 0 $^{\circ}$C. After stirring for an additional couple of hours at 0 $^{\circ}$C, the reaction was cooled to -78 $^{\circ}$C and treated with ethyl isocyano acetate followed by another equivalent of potassium tert-butoxide to furnish the imidazodiazepine scaffold **14** in 81% yield. This step could be executed on 80 gram scales and the impurities were removed by washing with 10% EtOAc in hexanes. The Heck-type Sonogashira coupling of trimethylsilyl acetylene with the bromo-arene

176

incorporated the acetylene function into **14** in 92% yield. The Hz-166 **2** was furnished in 96%

yield simply by de-silylation of the protected acetylene **15** (TBAF×H$_2$O). The pure target

compound Hz-166 **2** could be obtained by recrystallization of the crude solid from hot methanol.

Scheme 1. Optimized synthetic Scheme for the synthesis of Hz-166 2 in 56% yield form

aniline 11 by Li *et al.*[239]
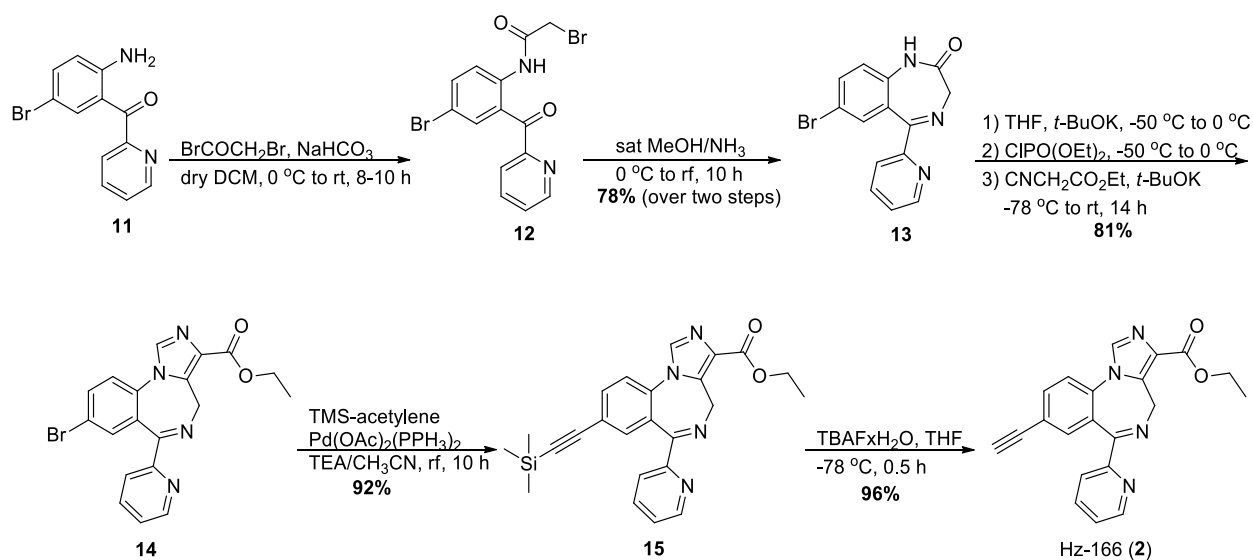
The 1,2,4-oxadiazole bioisostere, MP-III-80 **7** of the ethyl ester **2** is a promising anxiolytic,

anticonvulsant, as well as antinociceptive ligand. As a consequent, a steady supply of this ligand

is required for further pre-clinical studies. The previous method for preparing this 1,2,4-oxadiazole

7 from the ethyl ester **2** suffered from inconsistent yields, harsher conditions or extra steps.[273]

Consequently, the optimization of this process by Li et al. by treating the ethyl ester **2** with

amidoxime and sodium hydride at room temperature in the presence of 3Å molecular sieves to

push the reaction further by capturing the released water furnished the 3-ethyl-1,2,4-oxadiazole **7** in 88% yield.

Scheme 2. Synthesis of the 1,2,4-oxadizole 7 from ethyl ester 2[239]

ZJW-II-40 **16**
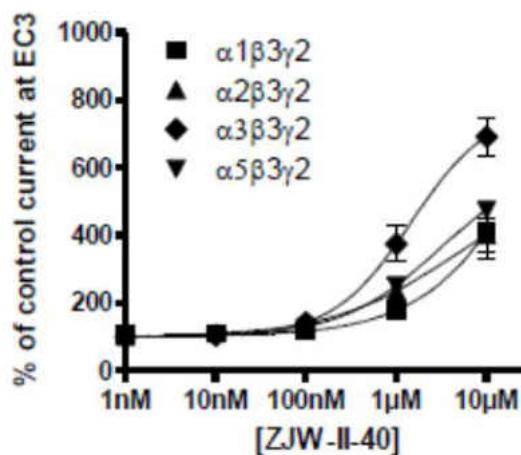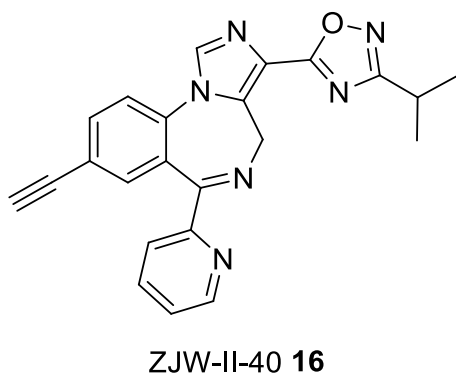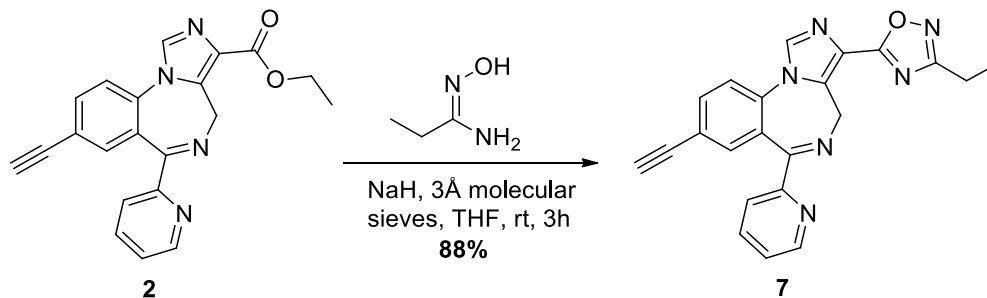
Figure 9. Structure and oocyte efficacy data of isopropyl oxadiazole 16. Concentration curve of oxadiazole 16 on GABA$_A$ receptors using an EC$_3$ GABA concentration (n = 3), as reported in Namjoshi, *et al.*[274]

It has been illustrated previously, that isopropyl oxadiazole **16** in Figure 9, could significantly increase metabolic stability as compared to Hz-166 **2**.[267] In contrast, isopropyl oxadiazole **16** lost efficacy at the α$_2$ subtype, while it remained potent at α$_3$ subtypes. This loss of efficacy at α$_2$

suggested that replacement of the ethyl function at C(3) with an isopropyl oxadiazole moiety had a negative impact on the efficacy profile.[267] Consequently, the corresponding cyclopropyl oxadiazole was synthesized, and awaits biological testing.

Scheme 3. Synthesis of the cyclopopyl 1,2,4-oxadizole 17 from ethyl ester 2
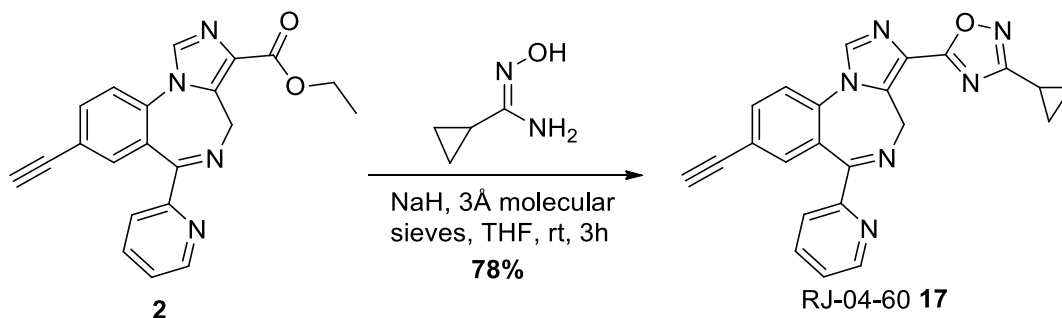
In addition, as hypothesized, incorporation of deuterium at a key metabolic site would increase the metabolic stability of a drug candidate. Consequently, the d3-version of MP-III-080 **18** was prepared. In addition, the d3-deuterated methyl ester version of the parent compound Hz-166 **20** was also prepared since metabolic instability of Hz-166 **2** was its only drawback. By refluxing MP-III-80 **7** in d4-methanol in the presence of potassium carbonate, this resulted in the incorporation of deuterium at four different positions in the IBZ scaffold (Scheme 4).[275] On stirring the d4-MP-III-80 **19** in methanol and this was followed by evaporation (5-6 cycles) of CH$_3$OH under reduced pressure the acetylene (C-D) proton was replaced back by C-H and this resulted in the desired d3-MP-III-80 **18** (>98% d). The extent of the deuterium incorporation was confirmed by NMR spectroscopic analysis (Figure 10). The same process on the ethyl ester Hz-166 effected the exchange of the same protons with deuterium. The ethyl ester was *trans*-esterified with the

solvent CD₃OD to furnished d3-Hz-166-OCD₃ ester **20** (Scheme 5). On the other hand, the carboxylic acid of Hz-166 **4** when reacted under the same conditions, gave the d5-version of **4** (**23**). The carboxylic acid deuterium proton was exchanged back to the acid proton by stirring it in CH₃OH to furnish the d3-HZ-166 acid **22** (Scheme 6). In all cases, the extent of deuterium incorporation was at least 98%.

Scheme 4. Synthesis of d3-MP-III-80 (18)[275]
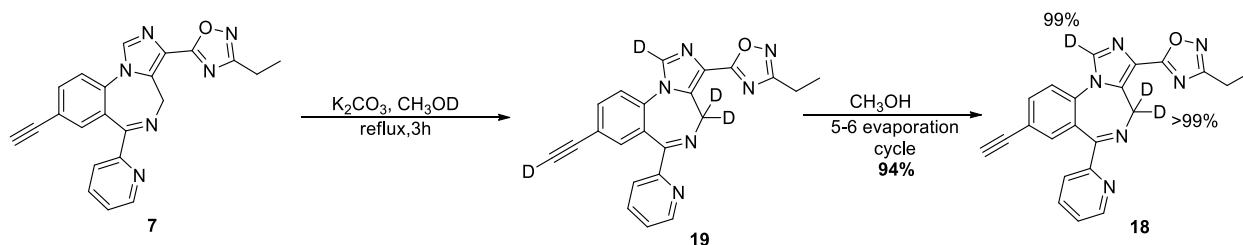
Scheme 5. Synthesis of d3-HZ-166-OCD₃ ester 20[275]
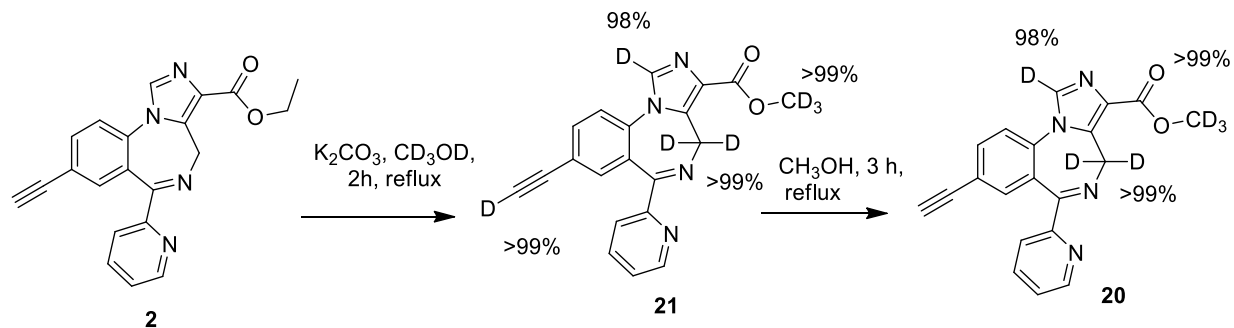
Scheme 6. Synthesis of d3-Hz-166 Acid 22[275]
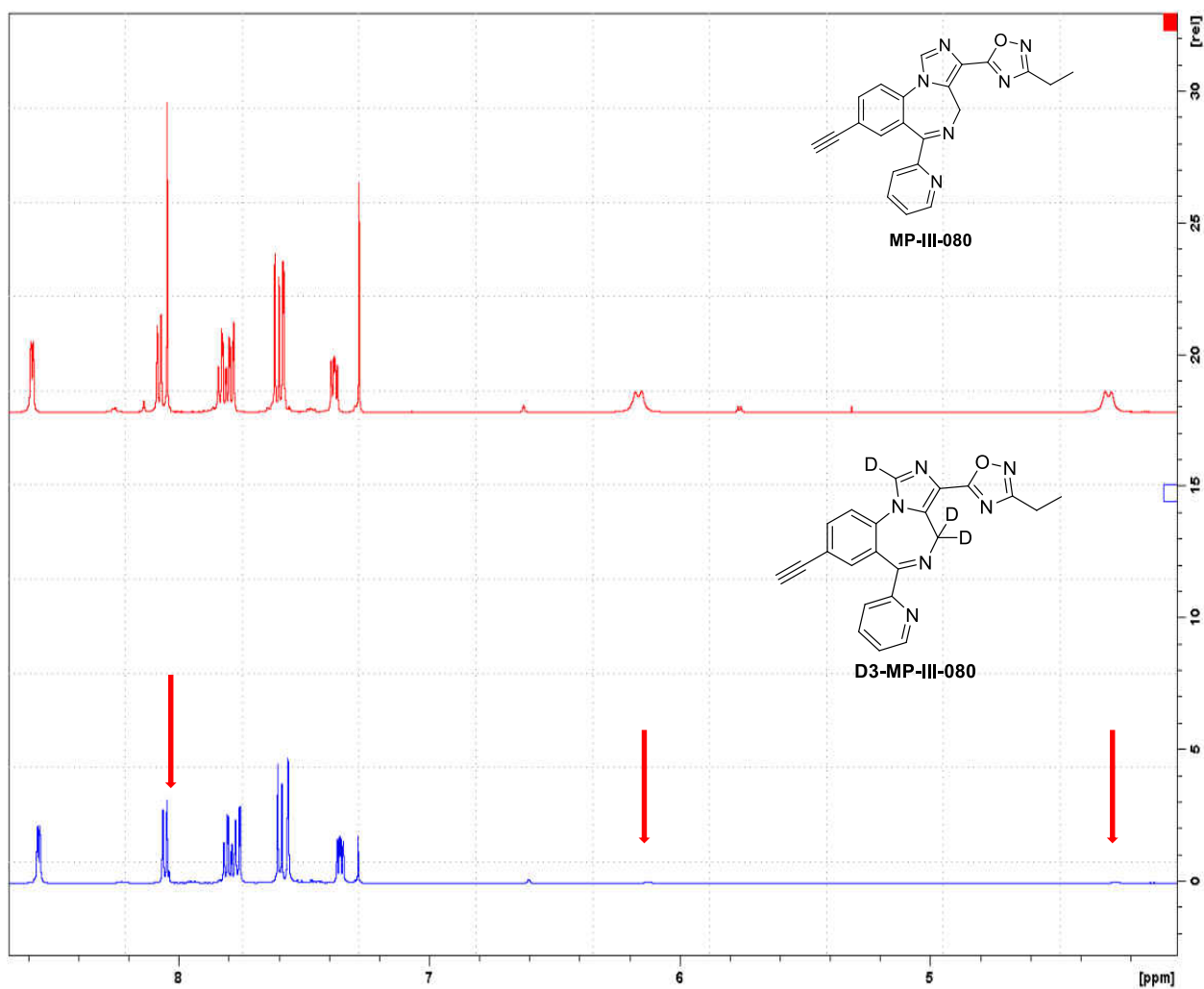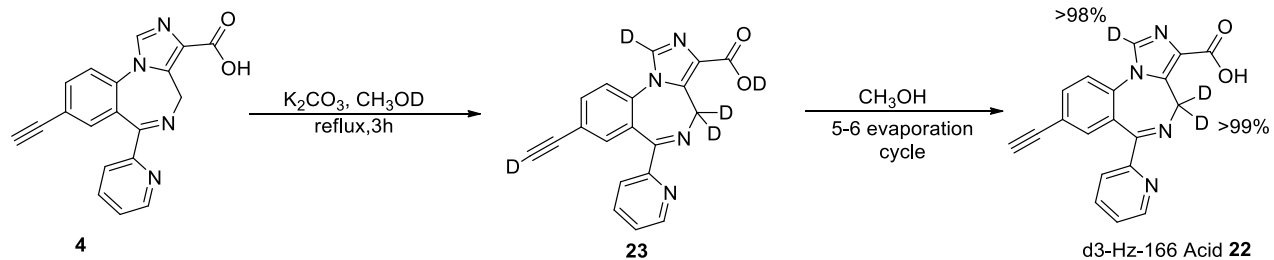
Figure 10. Typical ^{1}H NMR (CDCl$_3$) of deuterium exchange reaction of MP-III-80 (δ 8.7-4.0).

The d_3-MP-III-80 **18** was investigated for its stability in both acidic (near stomach pH) and alkaline (more than gut pH) pH and was found stable in both acidic and alkaline solutions (Tables 1 and 2). This is an important experiment to illustrate the applicability of d3-MP-III-80 **18** in oral dosage. Results indicated that d3-MP-III-80 **18** is stable enough in both stomach and gut pH, which infers that incorporation of deuterium would be beneficial towards improving metabolic stability in vivo.

Table 1. Stability of d_3-MP-III-080 (18) at the pH 2 of the stomach[275]

pH 2.2 buffer study:

The preparation of the pH 2.2 buffer solution: The buffer solution was prepared according to the previous procedure.

Procedure: 5 mg of d_3-MP-III-080 was dissolved in a minimum amount of methanol and 5 mL of above buffer solution was added. The solution was kept stirring at the desired temperature for 6 hours. At different time intervals 0.3 ml of the solution was collected, diluted with 0.3 ml H_2O and extracted with EtOAc (2x0.5 ml) and the combined organic layer were washed with brine and used for LC-MS analysis.

Results:

Compound	LC-MS m/z $[M + H]^+$ peaks			
MP-III-080 **7**	381 major			
Deuterated d_3-MP-III-080 **18**	384 (d_3)			
	At room temperature		At 37 °C	
	After 1 h	After 6 h	After 1 h	After 6 h
Deuterated d_3-MP-III-080 in pH 2.2 buffer solution	384 major (d_3)	384 major (d_3)	384 major (d_3)	384 major (d_3)

Inference: d_3-MP-III-080 is stable in acidic solution (pH near the stomach pH)

Table 2. Stability of d₃-MP-III-080 at pH 9.7-9.9; much more alkaline than gut (around 8.5-9)[275]

The pH 9.7-9.9 buffer solution preparation: buffer solution was prepared according to the previous procedure.

Procedure: 5 mg of d₃-MP-III-080 was dissolved in a minimum amount of methanol and 5 mL of the above buffer solution was added. The solution was stirred at the desired temperature for 6 hours. At different time intervals 0.3 ml of the solution was collected, diluted with 0.3 ml H_2O and extracted with EtOAc (2x0.5 ml) and the combined organic layer were washed with brine and used for LC-MS analysis.

Results:

Compound	LC-MS m/z [M + H]⁺ peaks			
MP-III-080	381 major			
Deuterated d₃-MP-III-080	384 (d₃)			
	At room temperature		At 37 °C	
	After 1 h	After 6 h	After 1 h	After 6 h
Deuterated d₃-MP-III-080 in pH 2.2 buffer solution	384 major (d₃)	384 major (d₃) (~10% of 383 peak present)	384 major (d₃)	384 major (d₃) (~10% of 383 peak present)

Inference: d₃-MP-III-080 was stable in this basic condition.

5. Conclusion

The strategic implication of the bioisosteric alteration of the ester functional group in the initial α_2/α_3 subtype selective GABA$_A$R PAM lead compound HZ-166 **2** resulted in a new better generation of lead compounds with 1,2,4-oxadilxole or 1,3-oxazole moieties at C(3). These novel ligands retaining the desired efficacies at α_2/α_3 receptor subtypes of GABA$_A$Rs, which avoided the CNS adverse effects associated with efficacies at α_1, as well as improved metabolic stability. Among the newly achieved lead compounds, the 3-ethyl-1,2,4-oxadiazole MP-III-80 **7** exhibited anxiolytic and antinociceptive properties. In recent investigations, it has been illustrated that α_2/α_3 subtype selective GABA$_A$R PAMs might have important applications in alcohol use and alcohol abuse disorders. Incorporation of deuterium at key metabolic sites of the lead compounds MP-III-80 **7**, HZ-166 2, and Hz-166-acid **4** furnished new derivatives of the PAMs, which would be more bioavailable due to better metabolic stability. Preliminary experiments have indicated the viability of this strategy. In addition, further derivatization of the lead compounds resulted in several newer ligands which are felt to be promising novel compounds. Although, most of the newly designed and synthesized ligands await full biological evaluation including pharmacokinetic profiles, this new set of GABA$_A$ PAMs with improved efficacies at the desired α_2/α_3 subtypes will add to the arsenal of imidazodiazepine drugs for the treatment of various CNS disorders. These ligands should meet the unmet need for better psychopharmaceutics which may be applicable in all patients including the elderly. These anxiolytic, anticonvulsant and antinociceptive ligands should be better for long term treatment and avoid adverse complications. It is hoped that the newly synthesized compounds will be evaluated by our collaborators in the near future. Especially d3-MP-III-080 **18**.

6. Methods

6.1 Marble Burying (CRO)[227]

Mice were tested in the marble burying assay using methods previously described (Li, et al., Life Sci., 2006, 78, 1933 – 1939). Mice were dosed i.p. with either vehicle (1% carboxymethyl cellulose) or a test compound 30 min prior to testing. Mice were placed in a 17 x 28 x 12 cm high plastic tub with 5 mm sawdust shavings (Harlan Sani-Chips, HarlanTeklad, Indianapolis, IN) on the floor that were covered with 20 blue marbles (1.5 cm diameter) placed in the center. Mice were left in the tub for 30 min. The number of marbles buried (2/3 covered with sawdust) were counted and recorded.

6.2 Rotarod (CRO)[227]

Male NIH Swiss mice (Harlan Sprague-Dawley, Indianapolis, IN) were tested in the rotarod assay in a dimly lit testing room according the general methods previously described (Li, et al., Life Sci., 2006, 78, 1933 – 1939). After being acclimated to the experimental room for one hour, the mice (n = 10 per group) were dosed i.p. 30 min prior to testing with either vehicle (1% CMC) or compound (10 or 30 mg/kg). Mice were placed on a rotarod (Ugo Basile 7650) operating at 4 rpm and observed for falling for 2 min. Mice that did not fall during the 2 min of testing were given a "Success" designation. Mice that fell once were given a "Partial" score, while the mice that fell twice failed the test. After rotarod testing, the mice were tested immediately in the marble-burying assay.

6.3 Vogel Conflict Behavior (CRO)[251]

Day 1, animals are moved from colony room into test room and put into operant chambers with water available, white noise, and houselight on (program title Vogel train). A timer starts when the first lick is made. For the first 3 min after the first lick, data is recorded as unpunished licks. After 3 min, the second component becomes active for 3 min. All licks in the second component are recorded as punished licks. At the end of the 6 min, the chamber goes dark. Animals are removed and returned to home cages. After all groups of animals have been exposed to the chambers, water is made available in the home cage for 30 min. After 30 min, water is removed and animals are transported back to colony room. Data for both components is recorded as the number of licks. Sometime data for day 1 and day 2 is not recorded due to operant chambers being used for other testing protocols. Data is always recorded for day 3.

Day 2 conditions were identical to day one training. On day 3, animals were randomly assigned to dose groups and drugged according to route and pre-treatment times recorded below. Animals are run on program Vogel FR20, which is identical to Vogel training with the exception of during the 2nd component (punished), every 20th lick is shocked. Data for both components is recorded as the number of licks. Shock intensity = 0.5 mA, duration = 100 ms. Shock is delivered through the water sipper tube. Chlordiazepoxide (CDAP) 20 mg/kg, i.p., 30 min pre-session is used as a positive control. Injection volume is 1 ml/kg unless otherwise noted.

6.4 Ethanol or Sucrose Self-Administration (Dr. Donna Platt at University of Mississippi Medical Center)[269]

Drinking sessions occurred 5 d/wk in the animal's home cage, as previously described (Sawyer et al., 2014). Each session lasted 3 hours. Animals were trained to drink either ethanol (2%, w/v; n=5) or sucrose solution (0.3 or 1%, w/v, depending on the animal; n=5) using an operant drinking panel mounted on the side of the home cage. The ethanol concentration was chosen because it maintained intake significantly above water levels and is on the ascending limb of the concentration-effect curve (see Ruedi-Bettschen et al., 2013), thus allowing us to detect either increases or decreases in drinking after pretreatment administration. The sucrose concentrations were chosen because they maintained approximately equivalent levels of intake to ethanol (EtOH) under baseline conditions (Ruedi-Bettschen et al., 2013; Sawyer et al., 2014).

The drinking panel contained two retractable sippers (Med Associates) connected with tygon tubing to stainless steel reservoirs mounted outside of the cage. A response lever (Med Associates) was positioned below each sipper, and a set of colored lights were positioned above. Each lever press resulted in an audible click and served as a response. In these experiments, only 1 side of the panel was active. Illumination of white lights signaled the start of the session and ethanol or sucrose availability. Every 10 responses (FR 10) resulted in a switch from illumination of the white light to illumination of a red light and extension of the drinking spout for 30 seconds. Depression of the spout during extension resulted in fluid delivery, continuing as long as the sipper was both depressed and extended. Thus, both the actual duration (up to 30 seconds) and volume of intake were controlled by the subject. A brief (1 second) timeout followed each spout extension, in which all stimulus lights were dark and responding had no programmed consequences. Responses were

recorded and outputs controlled by a software program (MedPC; Med Associates). At the end of each session, reservoirs were drained and the amount of liquid consumed (ml) measured.

XHe-II-053 (0.3-3 mg/kg), HZ-166 (0.3-3 mg/kg), YT-III-31 (0.1-3 mg/kg) or YT-III-271 (0.1-1 mg/kg) were administered intramuscularly 10 minutes before the start of a self-administration session. Each dose of each compound was studied for a minimum of 5 consecutive sessions and until intake was stable, which was defined as no upward or downward trend in amount consumed (ml) over 3 consecutive days (i.e., for each 3-day period, intake could not be consistently increasing or decreasing across the consecutive days). Following evaluation of each dose, monkeys were returned to baseline self-administration conditions (i.e., with no pretreatment injection) until intake stabilized again. Doses were randomized within each treatment condition, and all doses of a particular compound were generally completed before beginning a new compound.

7. Experimental Section

7.1 7-Bromo-5-(pyridin-2-yl)-1*H*-benzo[*e*][1,4]diazepin-2(3*H*)-one (13)

The 2'-pyridyl ketone **11** (120 g, 433.2 mmol) was dissolved in dry DCM (1.4 L) in a 3-neck round bottom flask and was stirred with an overhead mechanical stirrer for 15 min to obtain a homogenous solution. Then solid $NaHCO_3$ (72.8 g, 866.4 mmol) was added to the solution with vigorous stirring to avoid clogging of the stirrer, and the mixture was cooled to 0 °C using an ice bath. The bromoacetyl bromide (144.9 g, 714.8 mmol) was dissolved in dry DCM (200 mL) and was then added dropwise at 0 °C with an addition funnel. The reaction mixture was allowed to warm to rt and stirred overnight until the starting material was consumed as monitored on analysis by TLC (silica gel, EtOAc/hexane, 1:1). The reaction mixture was quenched with ice-water (500 mL) and stirred at rt for 30 min. The organic layer was then separated, and the aq layer was extracted with DCM (3 x 250 mL). The organic layers were combined, as well as washed (200 mL each) sequentially with a saturated aq solution of $NaHCO_3$, water, 10% HCl, brine and then dried (Na_2SO_4). The combined organic layer was then concentrated to 1/4th of its original volume under reduced pressure. The intermediate **12**, which was prepared, was used for the next step without further purification.

Methanol (1.4 L) was cooled to 0 °C using an ice-water cooling bath and saturated with anhydrous ammonia gas. The DCM solution of intermediate **12** was added to the solution of saturated MeOH/NH_3 at 0 °C. The mixture was allowed to warm to rt and slowly heated to **reflux with caution (mild exotherm observed)** until the starting material was consumed on analysis by TLC (silica gel) in 12 h. The reaction mixture was then cooled to rt and the solvent was removed under reduced pressure. The solid which remained was filtered and washed with water (3 x 150 mL), cold EtOAc (3 x 50 mL) and DCM (3 x 50 mL). The crude solid was dissolved in MeOH (600

mL) and DCM (100 mL) at 60 °C, and the solution was concentrated to 1/4th of its original volume. The amide **13** was recrystallized at rt and filtered, after which it was washed with DCM to obtain the majority of the pure amide **13** as white crystals. The filtrate was combined and concentrated under reduced pressure to an oily residue, which was further purified by flash chromatography on silica gel (EtOAc/hexane, 1:1 and 1% of TEA) to afford additional amide **13** (108.6 g, 78% yield over the two steps): M.p = 228-229 °C; R_f = 0.4 (EtOAc-hexane, 1:1 and 1% of TEA); ^{1}H NMR (300 MHz, DMSO-d_6) δ 10.63 (s, 1H), 8.55 (d, J = 4.1 Hz, 1H), 8.04 (d, J = 7.7 Hz, 1H), 7.93 (d, J = 7.4 Hz, 1H), 7.69 (d, J = 8.6 Hz, 1H), 7.54-7.44 (m, 1H), 7.42 (s, 1H), 7.18 (d, J = 8.7 Hz, 1H), 4.23 (s, 2H); ^{13}C NMR (75 MHz, DMSO-d_6) δ 170.34, 168.10, 156.30, 148.85, 139.28, 137.55, 134.40, 134.15, 127.92, 125.37, 123.91, 123.57, 114.51, 57.56. HRMS (ESI/IT-TOF) [M + H]$^+$ calcd for $C_{14}H_{11}BrN_3O$ 316.0080; found 316.0076.

7.2 Ethyl-8-bromo-6-(pyridin-2-yl)-4*H*-benzo[*f*]imidazo[1,5-*a*][1,4]diazepine-3-carboxylate (14)

The amide **13** (80 g, 253.2 mmol) was suspended in dry THF (1.5 L), and cooled to -35 °C using a dry ice bath, after which potassium *t*-butoxide (34.1 g, 303.8 mmol) was added in one portion. The reaction mixture was stirred until it reached 0° C and then stirred for 0.5 h at 0 °C. The mixture was then cooled to -50 °C, after which diethyl chlorophosphate (61.2 g, 354.5 mmol) was added dropwise with an addition funnel. The dry ice bath was removed to allow the temperature to rise to 0 °C, after which it was allowed to stir for 2 h with an ice-water bath. The solution was then cooled to -78 °C with a dry-ice bath and ethyl isocyanoacetate (40.1 g, 354.5 mmol) was added, immediately followed by a second portion of potassium *t*-butoxide (34.1 g, 303.8 mmol). This solution was allowed to stir overnight, during which period it was allowed to warm to rt. The

reaction was completed after 14 h on analysis by TLC (silica gel, EtOAc/hexanes/DCM, 2:2:1, and 1% TEA). The reaction mixture was quenched by addition of a cold saturated aq solution of $NaHCO_3$ (500 mL) and extracted with EtOAc. The organic layers were combined and washed with brine (2 x 200 mL), and dried (Na_2SO_4). The solvent was removed under reduced pressure to obtain a dark brown solid residue. The solid was washed with Et_2O/EtOAc (9:1) to remove most of the impurities and further recrystallized from EtOAc and hexane (1:4), followed by washing the solid with cold Et_2O to afford the majority of the pure ethyl ester **14**. The remaining filtrate was combined and purified by flash chromatography to obtain additional ethyl ester **14** (silica gel, EtOAc/ hexanes/DCM 2/2:1 and 1% TEA) as an off-white solid (84.2 g, 81% yield): M.p = 212-213 °C; R_f = 0.3 (EtOAc-hexane-DCM, 2:2:1 and 1% of TEA); ^{1}H NMR (300 MHz, $CDCl_3$) δ 8.60 (d, J = 4.4 Hz, 1H), 8.11 (d, J = 7.9 Hz, 1H), 8.00 (s, 1H), 7.86 (td, J = 8.0, 1.7 Hz, 1H), 7.80 (dd, J = 8.6, 2.2 Hz, 1H), 7.60 (d, J = 2.1 Hz, 1H), 7.51 (d, J = 8.6 Hz, 1H), 7.41 (dd, J = 7.1, 5.2 Hz, 1H), 6.13 (d, J = 10.4 Hz, 1H), 4.51 – 4.33 (m, 2H), 4.17 (d, J = 11.6 Hz, 1H), 1.44 (t, J = 7.1 Hz, 3H); ^{13}C NMR (75 MHz, $CDCl_3$) δ 167.04, 162.89, 156.17, 148.67, 138.39, 136.90, 135.27, 134.95, 134.53, 134.45, 129.33, 128.50, 124.86, 124.28, 123.94, 120.51, 60.75, 45.00, 14.42. HRMS (ESI/IT-TOF) [M + H][+] calcd for $C_{19}H_{16}BrN_4O_2$ 411.0451; found 411.0454.

7.3 Ethyl-6-(pyridin-2-yl)-8-((trimethylsilyl)ethynyl)-4*H*-benzo[*f*] imidazo[1,5*a*]-[1,4]diaze-pine-3-car boxylate (15)

The ethyl ester **14** (63.8 g, 155.1 mmol) was dissolved in TEA (400 mL) and dry CH_3CN (600 mL) in a 3-neck round bottom flask with a reflux column attached. The solution was then degassed three times under vacuum and argon. Trimethylsilylacetylene (22.9 g, 232.7 mmol) and bis(triphenyl phosphine)-palladium (II) acetate (6.4 g, 8.53 mmol) were added to the solution

under argon, and the mixture was degassed for four times (as above). The reaction mixture was then heated to reflux under argon and allow to stir overnight. The reaction process was completed in 15 h as monitored on analysis by TLC (silica gel, EtOAc/hexanes, 7:3, and 1% TEA). The reaction mixture was then cooled to 0 °C, and filtered through celite. This was followed by washing with EtOAc, and drying (Na$_2$SO$_4$). The filtrate was concentrated under reduced pressure. The black residue, which resulted, was loaded on a silica plug (4 g of silica/1 g of the product, EtOAc/hexanes, 1:1 with 1% TEA) to remove the baseline impurities and the material was recrystallized from EtOAc. The crystals were filtered and washed with Et$_2$O to afford pure trimethylsilyl ethyl ester **15**. The filtrate was purified by flash chromatography to afford additional ester **15** as an off-white solid (61.1 g, 92% yield): M.p = 203-204 °C; R_f = 0.5 (EtOAc-hexane, 1:1 and 1% of TEA); ^{1}H NMR (300 MHz, CDCl$_3$) δ 8.56 (d, J = 4.1 Hz, 1H), 8.02 (d, J = 7.8 Hz, 1H), 7.90 (s, 1H), 7.78 (t, J = 7.7 Hz, 1H), 7.70 (d, J = 8.3 Hz, 1H), 7.51 (d, J = 9.2 Hz, 2H), 7.34 (t, J = 5.9 Hz, 1H), 6.08 (d, J = 9.2 Hz, 1H), 4.47 – 4.31 (m, 2H), 4.10 (d, J = 6.9 Hz, 1H), 1.41 (t, J = 7.0 Hz, 3H), 0.21(s, 9H); ^{13}C NMR (75 MHz, CDCl$_3$) δ 167.80, 162.92, 156.55, 148.79, 138.47, 136.79, 135.67, 135.15, 135.05, 134.50, 129.26, 127.03, 124.71, 123.97, 122.72, 122.24, 102.79, 97.05, 60.71, 45.03, 14.42, -0.23. HRMS (ESI/IT-TOF) [M + H]$^+$ calcd for C$_{24}$H$_{25}$N$_4$O$_2$Si 429.1741; found 429.1747.

7.4   Ethyl-8-ethynyl-6-(pyridin-2-yl)-4*H*-benzo [*f*]imidazo [1,5-*a*][1,4] diazepine-3-car-boxylate (HZ-166, 2)

The trimethylsilyl ethyl ester **15** (50 g, 116.8 mmol) was dissolved in THF (1 L) and cooled to -78 °C. Tetrabutylammonium fluoride hydrate (1 M solution in THF, 175.1 mmol) was added to the solution, and this was followed by water (50 mL). The reaction mixture was stirred at -78 °C until

the starting material was consumed in 0.5 h, as analyzed by TLC (silica gel). The reaction mixture was allowed to warm to 0 °C and quenched by a slow addition of water (500 mL). The organic layer was separated and the aq layer was extracted EtOAc (5 x 300 mL). The combined organic layers were washed with brine (2 x 400 mL), and dried (Na$_2$SO$_4$). The solvent was removed under reduced pressure and the residue, which resulted, was dissolved in the mixture of DCM (100 mL) and MeOH (400 mL) at 50 °C and the solution was concentrated to 1/3rd of its original volume. The majority of the ethyl ester **2** was recrystallized at rt with a seed crystal added, and the solid was further washed with cold MeOH. The filtrate was combined and purified by a wash column (silica gel, EtOAc/hexane/DCM 8:1:2, and 1% TEA) to afford additional ethyl ester **2** as a white powder (37.8 g, 96% yield): M.p = 243-244 °C; R_f = 0.4 (EtOAc-hexane-DCM, 8:1:2 and 1% of TEA); ^{1}H NMR (300 MHz, CDCl$_3$) δ 8.59 (d, J = 4.6 Hz, 1H), 8.08 (d, J = 7.9 Hz, 1H), 7.96 (s, 1H), 7.83 (td, J = 7.8, 1.6 Hz, 1H), 7.77 (dd, J = 8.4, 1.7 Hz, 1H), 7.61 – 7.54 (m, 2H), 7.38 (dd, J = 7.0, 5.3 Hz, 1H), 6.12 (d, J = 10.6 Hz, 1H), 4.56 – 4.27 (m, 2H), 4.16 (d, J = 10.2 Hz, 1H), 3.17 (s, 1H), 1.44 (t, J = 7.1 Hz, 3H); ^{13}C NMR (75 MHz, CDCl$_3$) δ 167.59, 162.82, 156.17, 148.62, 138.38, 137.12, 136.18, 135.42, 135.38, 134.57, 129.23, 127.01, 124.92, 124.14, 122.92, 121.30, 81.64, 79.58, 60.86, 44.99, 14.43. HRMS (ESI/IT-TOF): [M + H]$^+$ calcd for C$_{21}$H$_{17}$N$_4$O$_2$ 357.1346; found 357.1344.

7.5 3-Ethyl-5-(8-ethynyl-6-(pyridin-2-yl)-4*H*-benzo[*f*]imidazo[1,5-*a*][1,4]diazepin-3-yl)-1,2-,4-oxadiazole (MP-III-080, 7)

The ethyl ester **2** (4.4 g, 12.4 mmol) was dissolved in dry THF (200 mL) at rt under argon. In a separate flask that contained 3Å molecular sieves, *N*-hydroxypropionimidamide (4.35 g, 19.4 mmol) was dissolved in dry THF (50 mL) under argon and then treated with sodium hydride (60%

dispersion in mineral oil, 360 mg, 14.8 mmol). The mixture was allowed to stir for 15 min and was then added dropwise to the solution of ethyl ester **2**. The reaction was completed in 3 h as analyzed by TLC (silica gel). The reaction mixture was quenched with a saturated aq NaHCO$_3$ solution (10 mL) extracted with EtOAc (3 x 250 mL). The organic layers were combined, washed with brine, and dried (Na$_2$SO$_4$) The solvent was removed under reduced pressure. The solid, which resulted, was purified by flash chromatography (silica gel, EtOAc/hexanes 4:1 and 1% TEA) to afford pure 1,2,4-oxadiazole **7** as a white powder (4.1 g, 88% yield): M.p = 204-205 °C; R_f = 0.6 (EtOAc-hexane, 4:1 and 1% of TEA); ^{1}H NMR (500 MHz, CDCl$_3$) δ 8.58 (d, J = 4.3 Hz, 1H), 8.07 (d, J = 8.0 Hz, 1H), 8.05 (s, 1H), 7.83 (dd, J = 11.8, 4.4 Hz, 1H), 7.78 (dd, J = 8.4, 1.3 Hz, 1H), 7.61 (d, J = 8.3 Hz, 1H), 7.57 (d, J = 1.0 Hz, 1H), 7.38 (dd, J = 6.7, 5.3 Hz, 1H), 6.16 (d, J = 11.4 Hz, 1H), 4.29 (d, J = 11.2 Hz, 1H), 3.19 (s, 1H), 2.85 (q, J = 7.6 Hz, 2H), 1.44 (t, J = 7.6 Hz, 3H); ^{13}C NMR (126 MHz, CDCl$_3$) δ 171.9, 170.7, 167.9, 156.3, 148.7, 137.1, 136.3, 136.1, 135.9, 135.5, 135.2, 127.1, 125.0, 124.8, 124.1, 122.9, 121.4, 81.6, 79.7, 44.9, 19.8, 11.6. HRMS (ESI/IT-TOF) [M + H]$^+$ calcd for C$_{22}$H$_{17}$N$_6$O 381.1458; found 381.1461.

7.6   3-Cyclopropyl-5-(8-ethynyl-6-(pyridin-2-yl)-4H-benzo[f]imidazo[1,5-a][1,4]diazepin-3-yl)-1,2,4-oxadiazole (17)

The ethyl ester **2** (0.5 g, 1.40 mmol) was dissolved in dry THF (50 mL) at rt under argon. In a separate flask that contained 3Å molecular sieves, *N*'-hydroxycyclopropanecarboximidamide (0.2 g, 2.10 mmol) was dissolved in dry THF (10 mL) under argon and then treated with sodium hydride (60% dispersion in mineral oil, 2.8 mg, 1.7 mmol). The mixture was allowed to stir for 15 min and was then added dropwise to the solution of ethyl ester **2**. The reaction was completed in 3 h as analyzed by TLC (silica gel). The reaction mixture was quenched with a saturated aq NaHCO$_3$

solution (2 mL) extracted with EtOAc (3 x 100 mL). The organic layers were combined, washed with brine, and dried (Na$_2$SO$_4$) The solvent was removed under reduced pressure. The solid, which resulted, was purified by flash chromatography (silica gel, EtOAc/hexanes 4:1 and 1% TEA) to afford pure 1,2,4-oxadiazole **17** as a white powder (0.43 g, 78% yield): ^{1}H NMR (300 MHz, CDCl$_3$) δ 8.59 (d, *J* = 4.8 Hz, 1H), 8.06 (d, *J* = 7.9 Hz, 1H), 8.03 (s, 1H), 7.84 (td, *J* = 7.8, 1.6 Hz, 1H), 7.78 (dd, *J* = 8.4, 1.7 Hz, 1H), 7.58 (dd, *J* = 7.2, 5.0 Hz, 2H), 7.43 – 7.34 (m, 1H), 6.10 (s, 1H), 4.28 (s, 1H), 3.18 (s, 1H), 2.28 – 2.03 (m, 1H), 1.10 (dd, *J* = 23.7, 15.5 Hz, 4H); ^{13}C NMR (126 MHz, CDCl$_3$) δ 172.7, 170.5, 167.7, 156.1, 148.6, 137.2, 136.3, 136.1, 135.9, 135.5, 135.3, 127.0, 124.8, 124.1, 122.9, 121.5, 81.6, 79.7, 44.9, 7.8, 6.9. HRMS (ESI/IT-TOF) [M + H]$^+$ calcd for C$_{23}$H$_{16}$N$_6$O 393.4127; found 393.1458.

Representative example: ethyl oxime "*N′*-hydroxypropionimidamide"

Hydroxylamine hydrochloride (9.73 g, 0.14 mol) and potassium carbonate (41.5 g, 0.3 mol) was added in methanol (400 mL) and water (80 mL). The suspension which resulted was stirred at rt for 15 min after which it was heated to reflux. Propionitrile (7.1 mL, 0.1 mol) was added dropwise and the reaction, which resulted, was stirred at reflux for 16 h. After that, the reaction mixture was cooled to 0 °C and the precipitate which formed was filtered. The solvent from the filtrate was removed under reduced pressure. The solid residue was dissolved in EtOAc and washed with water, brine, and dried (Na$_2$SO$_4$), after which the solvent was removed under reduced pressure to afford the ethyl oxime as a white solid (6.05 g, 69%): **HPLC-MS** (ESI) *m/z* (M+H) 89.06. This material was used for the next step without further characterization.

By following the same procedure with Cyclopropanecarbonitrile (6.49 mL, 72.3 mmol), this process furnished cyclopropyl oxime "*N*'-hydroxycyclopropanecarboximidamide" (5.54 g, 75%).

7.7 3-Ethyl-5-(1,4,4-deutero-8-ethynyl-6-(pyridin-2-yl)-4H-benzo[f]imidazo[1,5-a][1,4]diazepin-3-yl)-1,2,4-oxadiazole (18) [d₃-MP-III-80]

The 1,2,4-oxadiazole **7** (200 mg, 0.526 mmol) was taken in a clean and dry round bottom flask. K_2CO_3 (363 mg, 2.63 mmol) and CH_3OD (3 ml) were added to the above flask and the suspension which resulted was refluxed for 3 h. After that the reaction mixture was cooled to rt and the CH_3OD was evaporated under reduced pressure. Then 5 mL of distilled dry EtOAc was added to the white residue and it was sonicated for 5 min to dissolve the product completely. The suspension was then passed through a pad of celite to filter out the insoluble K_2CO_3 and the celite pad was washed with additional EtOAc (5x3 mL). The eluent was evaporated under reduced pressure. The residue was dissolve in dry CH_3OH and evaporated by rotary evaporator. This process was repeated 5-6 cycles to furnish completely protonated acetylene. The % deuterium incorporation was confirmed by NMR spectroscopy. Finally, the colored impurity was removed by re-crystallization to furnish the tri-deuterated MP-III-080 **18** (189 mg, 94%). ^{1}H NMR (300 MHz, CDCl₃) δ 8.57-8.55 (m, 1H), 8.07-8.04 (m, 1H), 7.80 (td, J = 7.8, 1.7 Hz, 1H), 7.76 (dd, J = 8.3, 1.8 Hz, 1H), 7.59 (brd, J = 8.3 Hz, 1H), 7.56 (d, J = 1.8 Hz, 1H), 7.37-7.34 (m, 1H), 3.18 (s, 1H), 2.84 (q, J = 7.6 Hz, 2H), 1.39 (t, J = 7.6 Hz, 3H); ^{13}C NMR (75 MHz, CDCl₃) δ 171.88, 170.73, 167.89, 156.38, 148.76, 136.88, 136.35, 136.06, 135.35, 135.19, 127.10, 124.85, 124.73, 123.96, 122.76, 121.39, 81.58, 79.62, 19.74, 11.50; HRMS (LCMS-IT-TOF) calc. for $C_{22}H_{14}D_3N_6O$ (M + H)+ 384.1647, found 384.1622.

7.8 Trideuteromethyl-1,4,4-trideutero-8-ethynyl-6-(pyridin-2-yl)-4H-benzo[f]imidazo[1,5-a][1,4]diazepine-3-carboxylate (20) [d₃-Hz-166-OCD₃ ester]

The ethyl ester **2** (100 mg, 0.28 mmol) and K_2CO_3 (38 mg, 0.28 mmol) were placed in a round bottom flask. Dry CD_3OD (5 mL) was added to the mixture under an argon atmosphere at rt. The reaction mixture was allowed to stir for 2 h under reflux. After 2 h TLC was taken. The excess solvent was removed under reduced pressure and the compound further purified by flash chromatography (silica gel, hexane and ethyl acetate) to afford compound **21** as a white solid (76 mg, 78% yield). The d7-ligand **21** was dissolved in dry CH_3OH (10 mL) and was added to the mixture under an argon atmosphere at rt. The reaction mixture was allowed to reflux for 3 h. The excess solvent was removed under reduced pressure to afford d6-methyl ester ligand **20** as a white solid (89 mg, 89% yield). d7-ligand **21**: ^{1}H NMR (300 MHz, CDCl₃) δ 8.59 (bs, 1H), 8.08 (d, J = 8 Hz, 1H), 7.83-7.76 (m, 2H), 7.58-7.55 (m, 2H), 7.38 (t, J = 6 Hz, 1H); LC-MS calcd for $C_{20}H_8D_7N_4O_2$ 350 found 350. d6-ligand **20** TLC; *Rf* = 0.35 (EtOAc:Hexane 3:1 and 1% of each MeOH and TEA) on silica gel plate; d6-ligand **20**: ^{1}H NMR (300 MHz, CDCl₃) δ 8.58 (bs, 1H), 8.07 (d, J = 8 Hz, 1H), 7.84-7.75 (m, 2H), 7.58-7.55 (m, 2H), 7.38 (t, J = 6 Hz, 1H), 3.17 (s, 1H); Compound **20** LC-MS calcd. for $C_{20}H_9D_6N_4O_2$ $(M + H)^+$ 349 found 349; HRMS (ESI) calcd. For $C_{20}H_9D_6N_4O_2$ $(M + H)^+$ 349.1572, found 349.1552.

7.9 1,4,4-Deuteroro-8-ethynyl-6-(pyridin-2-yl)-4H-benzo[f]imidazo[1,5-a][1,4]diazepine-3-carboxylic acid (22) [d₃-Hz-166-Acid]

The acid **4** (200 mg, 0.609 mmol) was placed in a clean and dry round bottom flask. Then K_2CO_3 (421 mg, 3.046 mmol) and CH_3OD (3 ml) was added to the above flask and the suspension that resulted was refluxed for 5 h under argon. After that, the reaction mixture was allowed cool to rt

and the solvent CH_3OD was removed under reduced pressure. The white solid which resulted was then dissolved in D_2O (3 ml) and cooled to 0°C in an ice bath. Then deuterium chloride (2M in D_2O) was added dropwise until the pH reached 4. The precipitate that formed was then filtered and washed with D_2O (2x1 mL). The white solid was dried at rt for 2 h and then at 45°C for 12h to furnish the tri-deuterated compound **22** (188 mg, 93%); ^{1}H NMR (300 MHz, $CDCl_3$): δ 8.62-8.52 (m, 1H), 8.11 (d, J = 7.7 Hz, 1H), 7.94-7.80 (m, 1H), 7.79-7.71 (m, 1H), 7.71-7.59 (m, 1H), 7.58-7.46 (m, 1H), 7.44-7.33 (m, 1H), 3.16 (s, 1 H); HRMS (ESI) calcd. for $C_{19}H_{10}D_3N_4O_2$ (M + H)$^+$ 332.1221, found 332.1201.

References

(1)   Townsend, E. A.; Emala Sr, C. W. *Am. J. Physiol. Lung Cell Mol. Physiol.* **2013**, *305*,
L396.

(2)   Yocum, G. T.; Gallos, G.; Zhang, Y.; Jahan, R.; Stephen, M. R.; Varagic, Z.;
Puthenkalam, R.; Ernst, M.; Cook, J. M.; Emala, C. W. *Am. J. Respir. Cell Mol. Biol.* **2016**, *54*,
546.

(3)   Jahan, R.; Stephen, M. R.; Forkuo, G. S.; Kodali, R.; Guthrie, M. L.; Nieman, A. N.;
Yuan, N. Y.; Zahn, N. M.; Poe, M. M.; Li, G. *Eur. J. Med. Chem.* **2017**, *126*, 550.

(4)   Forkuo, G. S.; Nieman, A. N.; Yuan, N. Y.; Kodali, R.; Yu, O. B.; Zahn, N. M.; Jahan,
R.; Li, G.; Stephen, M. R.; Guthrie, M. L. *Mol. Pharm.* **2017**, *14*, 2088.

(5)   Wardlaw, A.; Silverman, M.; Siva, R.; Pavord, I.; Green, R. *Clin. Exp. Allergy* **2005**, *35*,
1254.

(6)   Green, R. H.; Brightling, C. E.; Bradding, P. *Curr. Opin. Allergy Clin. Immunol.* **2007**, *7*,
43.

(7)   Clayton, T.; Chen, J. L.; Ernst, M.; Richter, L.; Cromer, B. A.; Morton, C. J.; Ng, H.;
Kaczorowski, C. C.; Helmstetter, F. J.; Furtmuller, R.; Ecker, G.; Parker, M. W.; Sieghart, W.;
Cook, J. M. *Curr. Med. Chem.* **2007**, *14*, 2755

(8)   Ernst, M.; Brauchart, D.; Boresch, S.; Sieghart, W. *Neuroscience* **2003**, *119*, 933

(9)   Poe, M. M. Ph.D. Thesis, University of Wisconsin-Milwaukee, **2016**.

(10)   Masiulis, S.; Desai, R.; Uchański, T.; Martin, I. S.; Laverty, D.; Karia, D.; Malinauskas, T.; Zivanov, J.; Pardon, E.; Kotecha, A. *Nature* **2019**, *565*, 454.

(11)   Liu, S.; Xu, L.; Guan, F.; Liu, Y.-T.; Cui, Y.; Zhang, Q.; Zheng, X.; Bi, G.-Q.; Zhou, Z. H.; Zhang, X. *Cell Res.* **2018**, *28*, 958.

(12)   Rallapalli, S. K. Ph.D. Thesis, University of Wisconsin-Milwaukee, **2012**.

(13)   Clayton, T.; Chen, J.; Ernst, M.; Richter, L.; Cromer, B.; Morton, C.; Ng, H.; Kaczorowski, C.; Helmstetter, F.; Furtmuller, R. *Curr. Med. Chem.* **2007**, *14*, 2755.

(14)   Huang, Q.; He, X.; Ma, C.; Liu, R.; Yu, S.; Dayer, C. A.; Wenger, G. R.; McKernan, R.; Cook, J. M. *J. Med. Chem.* **2000**, *43*, 71.

(15)   Forkuo, G. S.; Guthrie, M. L.; Yuan, N. Y.; Nieman, A. N.; Kodali, R.; Jahan, R.; Stephen, M. R.; Yocum, G. T.; Treven, M.; Poe, M. M. *Mol. Pharm.* **2016**, *13*, 2026.

(16)   Li, X.; Ma, C.; He, X.; Yu, J.; Han, D.; Zhang, C.; Atack, J. R.; Cook, J. M. *Med. Chem. Res.* **2002**, *11*, 504.

(17)   Stafford, D. C.; Cook, J. M.; Arnold, A. E.; Emala, C. W.; Gallos, G.; Stephen, M. R.; Novel GABAA Agonists and Methods of Using to Control Airway Hyperresponsiveness and Inflammation in Asthma, PCT WO 2014/0474113 A1, 2014.

(18)   Widmer, U. *Synthesis* **1983**, *1983*, 135.

(19)   Cook, J.M.; Witkin J.; Li, G., Improved Antiepileptic Profile with α2/3 Selective Receptor PAMs. In *ASPET Annual Meeting at EB* **2019**.

(20)   Saunders, K. *Thorax* **1993**, *48*, 647.

(21)   Nunes, C.; Pereira, A. M.; Morais-Almeida, M. *Asthma Res. Pract.* **2017**, *3*, 1.

(22)   Pascual, R. M.; Peters, S. P. *J. Allergy Clin. Immunol.* **2005**, *116*, 477.

(23)   American_Asthma_Foundation, Impact of Asthma, **2016**. Available at:

americanasthmafoundation.org/impact-asthma.

(24)   Barnett, S. B. L.; Nurmagambetov, T. A. *J. Allergy Clin. Immunol.* **2011**, *127*, 145.

(25)   https://www.who.int/news-room/fact-sheets/detail/asthma; Last visited: May 05, 2019.

(26)   https://www.who.int/news-room/fact-sheets/detail/asthma; Last Visited: May 05, 2019.

(27)   https://www.fda.gov/biologicsbloodvaccines/resourcesforyou/consumers/-ucm167471.htm; Last

visited: May 05, 2019.

(28)   Asher, M. I. *Thorax* **2011**, *66*, 1025.

(29)   Robinson, C. L.; Baumann, L. M.; Romero, K.; Combe, J. M.; Gomez, A.; Gilman, R. H.;

Cabrera, L.; Gonzalvez, G.; Hansel, N. N.; Wise, R. A. *Thorax* **2011**, *66*, 1051.

(30)   Guarnieri, M.; Balmes, J. R. *Lancet* **2014**, *383*, 1581.

(31)   Rackemann, F. M. *Am. J. Med. Sci.* **1921**, *12*, 802.

(32)   Turner-Warwick, M. *Br. J. Dos. Chest* **1977**, *71*, 73.

(33)   Global Initiative for Asthma. Global strategy for asthma management and prevention.

2005; www.ginasthma.com.

(34)   Wenzel, S. E.; Schwartz, L. B.; Langmack, E. L.; Halliday, J. L.; Trudeau, J. B.; Gibbs,

R. L.; Chu, H. W. Am *J. Respir. Crit. Care Med.* **1999**, *160*, 1001.

(35)   Wardlaw, A. J.; Silverman, M.; Siva R.; Green, R. *Clin. Exp. Allergy* **2005**, *35*, 1254.

(36)   https://doi.org/10.1016/S0140-6736(02)11679-5 Green, R. H.; Brightling, C. E.; McKenna, S.; Hargadon, B.; Parker, D.; Bradding, P.; Wardlaw, A. J.; Pavord, I. D. *Lancet* **2002**, *360*, 1715.

(37)   https://doi.org/10.1183/09031936.06.00137704 Jayaram, L.; Pizzichini, M. M.; Cook, R. J.; Boulet, L-P.; Lemiere, C.; Pizzichini, E.; Cartier, A.; Hussack, P.; Goldsmith, C. H.; Laviolette, M.; Parameswaran, K.; Hargreave, F. E. *Eur. Respir. J.* **2006**, *27*, 483.

(38)   Miranda, C.; Busacker, A.; Balzar, S.; Trudeau, J.; Wenzel. S. E. *J. Allergy Clin. Immunol.* **2004**, *113*, 101.

(39)   Pride, N. *Br. Med. Bull.* **1992**, *48*, 1.

(40)   Calhoun, W. J. *Drugs Today* **1999**, *35*, 595.

(41)   Bel, E. H. *Curr. Opin. Pulm. Med.* **2004**, *10*, 44.

(42)   Fuhlbrigge, A. L. *Curr. Opin. Pulm. Med.* **2004**, *10*, 1.

(43)   Wenzel, S. E. *Nat. Med.* **2012**, *18*, 716.

(44)   http://americanasthmafoundation.org/impact-asthma, Last visited: May 05, 2019.

(45)   Masoli, M.; Fabian, D.; Holt, S.; Beasley, R.; Program, *Allergy* **2004**, *59*, 469.

(46)   Schiller, J. S.; Lucas, J. W.; Peregoy, J. A. *Vital Health Stat.* **2012**, *252*, 1.

(47)   National Health Interview Survey (NHIS) 2012. Data, Statistics, and Surveillance. Available at http://www.cdc.gov/asthma/nhis/2012/data.htm.

(48)   CDC. 2015. NHIS Data; Table 5-1. www.cdc.gov/asthma/nhis/2015/table5-1.htm.

(49)   [World Health Organization. WHO factsheet 206: bronchial asthma. Available at:

www.who.int/mediacentre/factsheets/fs206/en]

(50)   www.cdc.gov/asthma/asthma_stats/missing_days.htm

(51)   National Hospital Ambulatory Medical Care Survey (NHAMCS), available at

http://www.cdc.gov/nchs/data/ahcd/nhamcs_emergency/2010.pdf

(52)   National Health Interview Survey (NHIS) 2012. Data, Statistics, and Surveillance.

Available at http://www.cdc.gov/asthma/nhis/2012/data.htm.

(53)   http://www.who.int/mediacentre/factsheets/fs206/en/.

(54)   Chowdhury, B. A.; Dal Pan, G. *N. Engl. J. Med.* **2010**, *362*, 1169.

(55)   Cates Christopher, J.; Cates Matthew, J.; Lasserson Toby, J. *Cochrane Database Syst.

Rev.* **2012**, *4*, 44. (CD CD006923).

(56)   Cates, C. J.; Cates, M. J. *Cochrane Database Syst. Rev.***2008**, *3*, CD006363.

(57)   Dahl, R. *Respir. Med.* **2006**, *100*, 1307.

(58)   Kelly, H. W.; Sternberg, A. L.; Lescher, R.; Fuhlbrigge, A. L.; Williams, P.; Zeiger, R.

S.; Raissy, H. H.; Van Natta, M. L.; Tonascia, J.; Strunk, R. C. *N. Engl. J. Med.* **2012**, *367*, 904.

(59)   Lipworth, B. J. *Arch. Intern. Med.* **1999**, *159*, 941.

(60)   Zhang, L.; Prietsch, S. O.; Ducharme, F. M. *Evid.-Based Child Health* 2014, 9, 829.

(61)   Barnes, P. J. *Trends Mol Med.* **2006**, *12*, 515.

(62)   Lima, J. J.; Zhang, S.; Grant, A.; Shao, L.; Tantisira, K. G.; Allayee, H.; Wang, J.;

Sylvester, J.; Holbrook, J.; Wise, R. *Am. J. Respir. Crit. Care Med.* **2006**, *173*, 379.

(63)   Holgate, S. T.; Polosa, R. *Lancet* **2006**, *368*, 780.

(64)   Unnerstall, J. R. In *Benzodiazepine/GABA receptors and chloride channels: Structural and functional properties*. Olsen, R. W.; Venter, J. C.; Eds: Alan R. Liss, Inc., New York, 1986.

(65)   Bowery, N.; Bittiger, H.; Olpe, H.-R. In *International GABA B Symposium* 1989: King's College; Wiley: 1990.

(66)   Egebjerg, J.; Schousboe, A.; Krogsgaard-Larsen, P. In *Glutamate and GABA receptors and transporters: structure, function and pharmacology*; CRC Press, 2001.

(67)   Krogsgaard-Larsen, P.; Fr, B.; Kristiansen, U.; Frydenvang, K.; Ebert, B. *Eur. J. Pharm. Sci.* **1997**, *5*, 355.

(68)   Martin, I. L. The GABAA/benzodiazepine receptor as a target for psychoactive drugs; Oxford Univ Press, 1996.

(69)   Wheal, H. V.; Thomson, A. M. Excitatory amino acids and synaptic transmission; Academic Press, 1995.

(70)   Monaghan, D.; Wenthold, R. The ionotropic glutamate receptors; Springer Science & Business Media, 2012.

(71)   Ong, J.; Kerr, D. I. *Life Sci.* **1990**, *46*, 1489.

(72)   Tanaka, C.; Bowery, N. G. GABA: receptors, transporters and metabolism; Birkhäuser, 2012.

(73)   Krogsgaard-Larsen, P.; Frølund, B.; Liljefors, T. *Chem. Rec.* **2002**, *2*, 419.

(74)   Caspary, D.; Raza, A.; Armour, B. L.; Pippin, J.; Arneric, S. *J. Neurosci.* **1990**, *10*, 2363.

(75)   Somogyi, P.; Tamas, G.; Lujan, R.; Buhl, E. H. *Brain Res. Rev.* **1998**, *26*, 113.

(76)   Sigel, E.; Buhr, A. *Trends Pharm. Sci.* **1997**, *18*, 425.

(77)   Fritschy, J.-M.; Kiener, T.; Bouilleret, V.; Loup, F. *Neurochem. Int.* **1999**, *34*, 435.

(78)   Olsen, R. W.; Avoli, M. *Epilepsia* **1997**, *38*, 399.

(79)   Pratt, J. A. *Pharmac. Ther.* **1992**, *55*, 149.

(80)   Nuit, D. J.; Que, P.; Iawson, C. *Prog. Neuropsychopharmacol. Biol. Psychiatry* **1990**, *14*, 737.

(81)   Berridge, K. C.; Peciña, S. *Neurosci. Biobehav. Rev.* **1995**, *19*, 121.

(82)   Cooper, S. J. *Hum. Psychopharm. Clin.* **1989**, *4*, 81.

(83)   Izquierdo, I.; Medina, J. H. *Trends Pharmacol. Sci.* **1991**, *12*, 260.

(84)   Sarter, M.; Schneider, H. H.; Stephens, D. N. *Trends Neurosci.* **1988**, *11*, 13.

(85)   Turek, F. W.; Van Reeth, O. *Trends Neurosci* **1988**, *11*, 535.

(86)   Wagner, S.; Castel, M.; Gainer, H.; Yarom, Y. *Nature* **1997**, *387*, 598.

(87)   Paulsen, O.; Moser, E. *Trends Neurosci.* **1998**, *21*, 273.

(88)   Nayeem, N.; Green, T.; Martin, I.; Barnard, E. *J. Neurochem.* **1994**, *62*, 815.

(89)   Schofield, P. R.; Darlison, M. G.; Fujita, N.; Burt, D. R.; Stephenson, F. A.; Rodriguez, H.; Rhee, L. M.; Ramachandran, J.; Reale, V.; Glencorse, T. A. *Nature* **1987**, *328*, 221.

(90)   Tretter, V.; Ehya, N.; Fuchs, K.; Sieghart, W. *J. Neurosci.* **1997**, *17*, 2728.

(91)   Burt, D. R.; Kamatchi, G. L. *FASEB J.* **1991**, *5*, 2916

(92)   Keramidas, A.; Moorhouse, A.; Schofield, P. C.; Barry, P. *Prog. Biophys. Mol. Biol.* **2004**, *86*, 161

(93)   Barnard, E.; Skolnick, P.; Olsen, R.; Mohler, H.; Sieghart, W.; Biggio, G.; Braestrup, C.; Bateson, A.; Langer, S. *Pharmacol. Rev.* **1998**, *50*, 291.

(94)   Sieghart, W.; Sperk, G. *Curr. Opin. Med. Chem.* **2002**, *2*, 795.

(95)   Simon, J.; Wakimoto, H.; Fujita, N.; Lalande, M.; Barnard, E. A. *J. Biol. Chem.* **2004**, *279*, 41422.

(96)   Hosie, A.; Sattelle, D.; Aronstein, K. *Trends Neurosci.* **1997**, *20*, 578.

(97)   Schuske, K.; Beg, A. A.; Jorgensen, E. M. *Trends Neurosci.* **2004**, *27*, 407.

(98)   Burt, D. R.; Kamatchi, G. L. *FASEB J.* **1991**, *5*, 2916.

(99)   Baumann, S. W.; Baur, R.; Sigel, E. *J. Biol. Chem.* **2002**, *277*, 46020.

(100)   Chang, Y.; Wang, R.; Barot, S.; Weiss, D. S. *J. Neurosci.* **1996**, *16*, 5415.

(101)   Ernst, M.; Brauchart, D.; Boresch, S.; Sieghart, W. *Neuroscience* **2003**, *119*, 933.

(102)   Farrar, S. J.; Whiting, P. J.; Bonnert, T. P.; McKernan, R. M. *J. Biol. Chem.* **1999**, *274*, 10100.

(103)   Im, H. K.; Im, W. B.; Carter, D. B.; McKinley, D. D. *Br. J. Pharmacol.* **1995**, *114*, 1040.

(104)   Sieghart, W. *Adv. Pharmacol.* **2006**, *54*, 231.

(105)   Sieghart, W. *Pharmacol. Rev.* **1995**, *47*, 181

(106)   MacDonald, R. L. In *Antiepileptic Drugs*; Levy, R. H., Mattson, R. H., Meldrum, B. S., Perucca, E., Eds.; Lippincott Williams and Wilkins: Philadelphia, 2002, p 179

(107)   Sieghart, W.; Ernst, M. *Curr. Med. Chem.* - Central Nervous System Agents **2005**, *5*, 217

(108)   Sigel, E.; Luscher, B. P. *Curr. Topics Med. Chem.* **2011**, *11*, 241

(109)   Ramerstorfer, J.; Furtmüller, R.; Sarto-Jackson, I.; Varagic, Z.; Sieghart, W.; Ernst, M. *J. Neurosci.* **2011**, *31*, 870.

(110)   Varagic, Z.; Ramerstorfer, J.; Huang, S.; Rallapalli, S.; Sarto-Jackson, I.; Cook, J.; Sieghart, W.; Ernst, M. *Br. J. Pharmacol.* **2013**, *169*, 384.

(111)   Sigel, E. *Curr. Topics Med. Chem.* **2002**, *2*, 833.

(112)   Harris, R. A. *Alcohol. Clin. Exp. Res.* **1999**, *23*, 1563.

(113)   Lobo, I. A.; Harris, R. A. *Pharmacol. Biochem. Behave.* **2008**, *90*, 90.

(114)   Belelli, D.; Lambert, J. J. *Nat. Rev. Neurosci.* **2005**, *6*, 565

(115)   Olsen, R. W.; Hanchar, H. J.; Meera, P.; Wallner, M. Alcohol 2007, 41, 201

(116)   Sawyer, E.; Moran, C.; Sirbu, M. H.; Szafir, M.; Van Linn, M.; Namjoshi, O.; Tiruveedhula, V. V. N. P. B.; Cook, J. M.; Platt, D. M. *Alcohol Clin. Exp. Res.* **2014**, *38*, 1108

(117)   Haefely, W. *J. Psychoactive Drugs* **1983**, *15*, 19

(118)   Haefely, W.; Facklam, M.; Schoch, P.; Martin, J. R.; Bonetti, E. P.; Moreau, J. L.; Jenck, F.; Richards, J. G. *Adv. Biochem. Psychopharmacol.* **1992**, *47*, 379

(119)   Gorman, J. M. *CNS Spectr.* **2005**, *10*, 14

(120) Garattini, S.; Mussini, E.; Marucci, F.; Guaitani, A. In The Benzodiazepines; Garattini, S., Mussini, E., Randall, L. O., Eds.; Raven Press: New York, 1973, p 75

(121) Rutherford, D. M.; Okoko, A.; Tyrer, P. J. *Br. J. Clin. Pharmacol.* **1978**, *6*, 69.

(122) Bond, A. J.; Hailey, D. M.; Lader, M. H. *Br. J. Clin. Pharmacol.* **1977**, *4*, 51

(123) Killam, E. K.; Suria, A. In *Antiepileptic Drugs: Mechanisms of Action*; Glaser, G. H., Penry, J. K., Woodbury, D. M., Eds.; Raven Press: New York, 1980, p 597

(124) Rogawski, M. A. In *Antiepileptic Drugs;* 5th ed.; Levy, R. H., Mattson, R. H., Meldrum, B. S., Perucca, E., Eds.; Lippincott Williams and Wilkins: Philadelphia, 2002, p 3

(125) Wieland, H. A.; Lüddens, H.; Seeburg, P. H. *J. Biol. Chem.* **1992**, *267*, 1426.

(126) Sternfeld, F.; Carling, R. W.; Jelley, R. A.; Ladduwahetty, T.; Merchant, K. J.; Moore, K. W.; Reeve, A. J.; Street, L. J.; O'Connor, D.; Sohal, B. *J. Med. Chem.* **2004**, *47*, 2176.

(127) Khom, S.; Baburin, I.; Timin, E. N.; Hohaus, A.; Sieghart, W.; Hering, S. *Mol. Pharmacol.* **2006**, *69*, 640.

(128) Sieghart, W.; Sperk, G. *Curr. Topics Med. Chem.* **2002**, *2*, 785

(129) Rudolph, U.; Mohler, H. *Annu. Rev. Pharmacol. Toxicol.* **2004**, *44*, 475

(130) Rudolph, U.; Crestani, F.; Benke, D.; Brunig, I.; Benson, J. A.; Fritschy, J.-M.; Martin, J. R.; Bluethmann, H.; Mohler, H. *Nature* **1999**, *401*, 796

(131) McKernan, R. M.; Rosahl, T. W.; Reynolds, D. S.; Sur, C.; Wafford, K. A.; Atack, J. R.; Farrar, S.; Myers, J.; Cook, G.; Ferris, P.; Garrett, L.; Bristow, L.; Marshall, G.; Macaulay, A.;

Brown, N.; Howell, O.; Moore, K. W.; Carling, R. W.; Street, L. J.; Castro, J. L.; Ragan, C. I.; Dawson, G. R.; Whiting, P. J. *Nat. Neurosci.* **2000**, *3*, 587

(132)   Löw, K.; Crestani, F.; Keist, R.; Benke, D.; Brünig, I.; Benson, J. A.; Fritschy, J.-M.; Rülicke, T.; Bluethmann, H.; Möhler, H. *Science* **2000**, *290*, 131.

(133)   Morris, H.; Dawson, G.; Reynolds, D.; Atack, J.; Stephens, D. *Eur. J. Neurosci.* **2006**, *23*, 2495.

(134)   Dias, R.; Sheppard, W. F.; Fradley, R. L.; Garrett, E. M.; Stanley, J. L.; Tye, S. J.; Goodacre, S.; Lincoln, R. J.; Cook, S. M.; Conley, R. *J. Neurosci.* **2005**, *25*, 10682.

(135)   Yee, B. K.; Keist, R.; Von Boehmer, L.; Studer, R.; Benke, D.; Hagenbuch, N.; Dong, Y.; Malenka, R.; Fritschy, J.-M.; Bluethmann, H. *Proc. Natl. Acad. Sci. U.S.A.* **2005**, *102*, 17154.

(136)   Crestani, F.; Keist, R.; Fritschy, J.-M.; Benke, D.; Vogt, K.; Prut, L.; Bluthmann, H.; Mohler, H.; Rudolph, U. *Proc. Natl. Acad. Sci. U.S.A.* **2002**, *99*, 8980

(137)   Sur, C.; Wafford, K. A.; Reynolds, D. S.; Hadingham, K. L.; Bromidge, F.; Macaulay, A.; Collinson, N.; O'Meara, G.; Howell, O.; Newman, R. *J. Neurosci.* **2001**, *21*, 3409.

(138)   Vicini, S.; Ferguson, C.; Prybylowski, K.; Kralic, J.; Morrow, A. L.; Homanics, G. E. *J. Neurosci.* **2001**, *21*, 3009.

(139)   Fritschy, J. M.; Mohler, H. *J. Comp. Neurol.* **1995**, *359*, 154

(140)   Collinson, N.; Kuenzi, F. M.; Jarolimek, W.; Maubach, K. A.; Cothliff, R.; Sur, C.; Smith, A.; Otu, F. M.; Howell, O.; Atack, J. R.; McKernan, R. M.; Seabrook, G. R.; Dawson, G. R.; Whiting, P. J.; Rosahl, T. W. *J. Neurosci.* **2002**, *22*, 5572

(141)   Bohlhalter, S.; Weinmann, O.; Mohler, H.; Fritschy, J. M. *J. Neurosci.* **1996**, *16*, 283

(142)   Bencsits, E.; Ebert, V.; Tretter, V.; Sieghart, W. *J. Biol. Chem.* **1999**, *274*, 19613

(143)   Tanaka, C.; Taniyama, K. In *GABA Outside the CNS*; Erdo, S. L., Ed.; Springer: 1992, p 3

(144)   Magnaghi, V.; Ballabio, M.; Consoli, A.; Lambert, J. J.; Roglio, I.; Melcangi, R. C. *J. Mol. Neurosci.* **2006**, *28*, 89

(145)   Gallos, G.; Yim, P.; Chang, S.; Zhang, Y.; Xu, D.; Cook, J. M.; Gerhoffer, W. T.; Emala Sr., C. W. *Am. J. Physiol. Lung Cell Mol. Physiol.* **2012**, *302*, L248

(146)   Gallos, G.; Yocum, G. T.; Siviski, M. E.; Yim, P. D.; Fu, X. W.; Poe, M. M.; Cook, J. M.; Harrison, N.; Perez-Zoghbi, J.; Emala Sr., C. W. *Am. J. Physiol. Lung Cell Mol. Physiol.* **2015**, *308*, L931

(147)   Mizuta, K.; Xu, D.; Pan, Y.; Comas, G.; Sonett, J. R.; Zhang, Y.; Panettieri Jr., R. A.; Yang, J.; Emala Sr., C. W. *Am. J. Physiol. Lung Cell Mol. Physiol.* **2008**, *294*, L1206

(148)   Bergeret, M.; Khrestchatisky, M.; Tremblay, E.; Bernard, A.; Gregoire, A.; Chany, C. *Biomed. Pharmacother.* **1998**, *52*, 214

(149)   Labonte, D.; Thies, E.; Kneussel, M. *Eur. J. Cell Biol.* **2014**, *93*, 338

(150)   Knutson, D. E.; Kodali, R.; Divović, B.; Treven, M.; Stephen, M. R.; Zahn, N. M.; Dobričić, V.; Huber, A. T.; Meirelles, M. A.; Verma, R. S. *J. Med. Chem.* **2018**, *61*, 2422.

(151)   Mizuta, K.; Xu, D.; Pan, Y.; Comas, G.; Sonett, J. R.; Zhang, Y.; Panettieri Jr., R. A.; Yang, J.; Emala Sr., C. W. *Am. J. Physiol. Lung Cell Mol. Physiol.* **2008**, *294*, L1206

(152)   Cook, J.M.; Witkin J.; Li, G., Improved Antiepileptic Profile with α2/3 Selective Receptor PAMs. In *ASPET Annual Meeting at EB* **2019**.

(153)   Gallos, G.; Yim, P.; Chang, S.; Zhang, Y.; Xu, D.; Cook, J. M.; Gerthoffer, W. T.; Emala Sr, C. W. *Am. J. Physiol. Lung Cell Mol. Physiol.* **2012**, *302*, L248.

(154)   Alam, S.; Laughton, D. L.; Walding, A.; Wolstenholme, A. *J. Mol. Immunol.* **2006**, *43*, 1432.

(155)   Gallos, G.; Townsend, E.; Yim, P.; Virag, L.; Zhang, Y.; Xu, D.; Bacchetta, M.; Emala, C. W. *Am. J. Physiol. Lung Cell Mol. Physiol.* **2012**, *304*, L191.

(156)   Issazadeh-Navikas, S.; Birnir, B. J. *Neuroimmunol.* **2008**, *205*, 44.

(157)   Reyes-García, M. G.; Hernández-Hernández, F.; Hernández-Téllez, B.; García-Tamayo, F. *J. Neuroimmunol.* **2007**, *188*, 64.

(158)   Xiang, Y.-Y.; Wang, S.; Liu, M.; Hirota, J. A.; Li, J.; Ju, W.; Fan, Y.; Kelly, M. M.; Ye, B.; Orser, B. *Nat. Med.* **2007**, *13*, 862.

(159)   Tian, J.; Chau, C.; Hales, T. G.; Kaufman, D. L. *J. Neuroimmunol.* **1999**, *96*, 21.

(160)   Munroe, M. E.; Businga, T. R.; Kline, J. N.; Bishop, G. A. *J. Immunol.* **2010**, *185*, 5586.

(161)   Whiting, P. J. *Drug Discov. Today* **2003**, *8*, 445.

(162)   Fu, X. W.; Wood, K.; Spindel, E. R. *Am. J. Respir. Cell Mol. Biol.* **2011**, *44*, 222.

(163)   Gundavarapu, S.; Wilder, J. A.; Mishra, N. C.; Langley, R. J.; Singh, S. P.; Saeed, A. I.; Jaramillo, R. J.; Gott, K. M.; Peña-Philippides, J. C.; Harrod, K. S. *J. Allergy Clin. Immunol.* **2012**, *130*, 770.

(164)   Richetto, J.; Labouesse, M. A.; Poe, M. M.; Cook, J. M.; Grace, A. A.; Riva, M. A.; Meyer, U. *Int. J. Neuropsychopharmacol.* **2015**, 18, 1.

(165)   Zurek, A. A.; Yu, J.; Wang, D.-S.; Haffey, S. C.; Bridgwater, E. M.; Penna, A.; Lecker, I.; Lei, G.; Chang, T.; Salter, E. W. *J. Clin. Invest.* **2014**, *124*, 5437.

(166)   Sharma, R.; Strelevitz, T. J.; Gao, H.; Clark, A. J.; Schildknegt, K.; Obach, R. S.; Ripp, S. L.; Spracklin, D. K.; Tremaine, L. M.; Vaz, A. D. *Drug Metab. Dispos.* **2012**, *40*, 625.

(167)   Scheiner, S.; Čuma, M. *J. Am. Chem. Soc.***1996**, *118*, 1511.

(168)   Wuts, P. G. M.; Greene, T. W. Protective Groups in Organic Synthesis, 4th ed.; Wiley & Sons: Hoboken, NJ, 2007

(169)   Ranu, B. C.; Bhar, S. *Org. Prep. Proced. Int.* **1996**, *28*, 371.

(170)   Weissman, S. A.; Zewge, D. *Tetrahedron* **2005**, *61*, 7833.

(171)   Bernard, A. M.; Ghiani, M. R.; Piras, P. P.; Rivoldini, A. Synthesis 1989, 1989, 287.

(172)   Fang, Z.; Zhou, G.-C.; Zheng, S.-L.; He, G.-L.; Li, J.-L.; He, L.; Bei, D. *J. Mol. Catal. A: Chem.* **2007**, *274*, 16.

(173)   Soni, A.; Dutt, A.; Sattigeri, V.; Cliffe, I. A. *Synth. Commun.* **2011**, *41*, 1852.

(174)   Kraft, P.; Eichenberger, W. *Eur. J. Org. Chem.* **2003**, *2003*, 3735.

(175)   Benton, F.; Dillon, T. E. *J. Am. Chem. Soc.* **1942**, *64*, 1128.

(176)   McOmie, J.; Watts, M.; West, D. *Tetrahedron* **1968**, *24*, 2289.

(177)   Punna, S.; Meunier, S.; Finn, M. *Org. Lett.* **2004**, *6*, 2777.

(178)   Taub, D.; Girotra, N.; Hoffsommer, R.; Kuo, C.; Slates, H.; Weber, S.; Wendler, N. *Tetrahedron* **1968**, *24*, 2443.

(179) Vlattas, I.; Harrison, I. T.; Tokes, L.; Fried, J. H.; Cross, A. D. *J. Org. Chem.* **1968**, *33*, 4176.

(180) Wehrmeister, H. L.; Robertson, D. E. *J. Org. Chem.* **1968**, *33*, 4173.

(181) Grieco, P. A.; Hiroi, K.; Reap, J. J.; Noguez, J. A. *J. Org. Chem.* **1975**, *40*, 1450.

(182) Grieco, P. A.; Nishizawa, M.; Oguri, T.; Burke, S. D.; Marinovic, N. *J. Am. Chem. Soc.* **1977**, *99*, 5773.

(183) Matsumoto, T.; Usui, S. *Bull. Chem. Soc. Jpn.* **1979**, *52*, 212.

(184) Stevens, R. V.; Bisacchi, G. S. *J. Org. Chem.* **1982**, *47*, 2396.

(185) Demyttenaere, J.; Van Syngel, K.; Markusse, A. P.; Vervisch, S.; Debenedetti, S.; De Kimpe, N. *Tetrahedron* **2002**, *58*, 2163.

(186) Learmonth, D. A.; Alves, P. C. *Synth. Commun.* **2002**, *32*, 641.

(187) Mateeva, N. N.; Kode, R. N.; Redda, K. K. *J. Heterocyl. Chem.* **2002**, *39*, 1251.

(188) Negi, A. S.; Chattopadhyay, S. K.; Srivastava, S.; Bhattacharya, A. K. *Synth. Commun.* **2005**, *35*, 15.

(189) Asnawi, A.; Kartasasmita, R. E.; Ibrahim, S.*J. Math. Fundam. Sci.* **2011**, *43*, 43.

(190) Akiyama, T.; Shima, H.; Ozaki, S. *Tetrahedron Lett.* **1991**, *32*, 5593.

(191) Du, Z.-T.; Lu, J.; Yu, H.-R.; Xu, Y.; Li, A.-P. *J. Chem. Res.* **2010**, *34*, 222.

(192) Mechoulam, R.; Gaoni, Y. *J. Am. Chem. Soc.* **1965**, *87*, 3273.

(193) Carnduff, J.; Miller, J. *Chem. Commun.* **1967**, *0*, 606b.

(194)   Esumi, T.; Yamamoto, C.; Fukuyama, Y. *Synlett* **2013**, *24*, 1845.

(195)   Zuo, L.; Yao, S.; Wang, W.; Duan, W. *Tetrahedron Lett.* **2008**, *49*, 4054.

(196)   Node, M.; Nishide, K.; Fuji, K.; Fujita, E. *J. Org. Chem.* **1980**, *45*, 4275.

(197)   Canonica, L.; Rindone, B.; Santaniello, E.; Scolastico, C. *Tetrahedron* **1972**, *28*, 4395.

(198)   Hanna, R. *Tetrahedron Lett.* **1968**, *9*, 2105.

(199)   Monson, R. S. *J. Chem. Soc. D. Chem. Commun.* **1971**, 113.

(200)   Hutchins, R. O.; Hutchins, M. G.; Milewsi, C. A. *J. Org. Chem.* **1972**, *37*, 4190.

(201)   Matsubara, S.; Matsuda, H.; Hamatani, T.; Schlosser, M. *Tetrahedron* **1988**, *44*, 2855.

(202)   Pettit, G. R.; Hoffmann, H.; Herald, D. L.; McNulty, J.; Murphy, A.; Higgs, K. C.;

Hamel, E.; Lewin, N. E.; Pearce, L. V.; Blumberg, P. M. *J. Org. Chem.* **2004**, *69*, 2251.

(203)   Feutrill, G.; Mirrington, R. *Tetrahedron Lett.* **1970**, *11*, 1327.

(204)   Feutrill, G.; Mirrington, R. *Aust. J. Chem.* **1972**, *25*, 1719.

(205)   Node, M.; Ohta, K.; Kajimoto, T.; Nishide, K.; Fujita, E.; Fuji, K. *Chem. Pharm. Bull.*
1983, *31*, 4178.

(206)   Node, M.; Kumar, K.; Nishide, K.; Ohsugi, S.-i.; Miyamoto, T. *Tetrahedron Lett.* **2001**,
42, 9207.

(207)   Saeed, A.; Rafique, H.; Arshad, M. *J. Asian Nat. Prod. Res.* **2013**, *15*, 1112.

(208)   Namba, T.; Hirota, T.; Hayakawa, S. *J. Lipid Res.* **1988**, *29*, 809.

(209)   Ramerstorfer, J.; Furtmüller, R.; Vogel, E.; Huck, S.; Sieghart, W. *Eur. J. Pharmacol.* **2010**, *636*, 18.

(210)   Henderson, W. R.; Lewis, D. B.; Albert, R. K.; Zhang, Y.; Lamm, W. J.; Chiang, G. K.; Jones, F.; Eriksen, P.; Tien, Y.; Jonas, M. *J. Exp. Med.* **1996**, *184*, 1483.

(211)   Eum, S.-Y.; Maghni, K.; Hamid, Q.; Eidelman, D. H.; Campbell, H.; Isogai, S.; Martin, J. G. *J. Allergy Clin. Immunol.* **2003**, *111*, 1049.

(212)   Pawelec, G.; Borowitz, A.; Krammer, P. H.; Wernet, P. *Eur. J. Immunol.* **1982**, *12*, 387.

(213)   Weiss, A.; Imboden, J.; Shoback, D.; Stobo, J. *Proc. Natl. Acad. Sci. U.S.A.* **1984**, *81*, 4169.

(214)   Lee, J. J.; McGarry, M. P.; Farmer, S. C.; Denzler, K. L.; Larson, K. A.; Carrigan, P. E.; Brenneise, I. E.; Horton, M. A.; Haczku, A.; Gelfand, E. W. *J. Exp. Med.* **1997**, *185*, 2143.

(215)   Burger, A. Isosterism and Bioisosterism in Drug Design. *Prog. Drug Res.* **1991**, *37*, 287.

(216)   Patani, G. A.; LaVoie, E. J. *Chem. Rev.* **1996**, *96*, 3147.

(217)   Meanwell, N. A. *J. Med. Chem.* **2011**, *54*, 2529.

(218)   Langmuir, I. *J. Am. Chem. Soc.* **1919**, *41*, 1543.

(219)   Erlenmeyer, H.; Berger, E. *Biochem. Z.* **1932**, *252*, 22.

(220)   Friedman, H. L. Influence of Isosteric Replacements upon Biological Activity. NAS-NRS Publication No. 206; NAS-NRS: Washington, DC, 1951, Vol. 206, p 295.

(221)   Lipinski, C. A. In *Annual Reports in Medicinal Chemistry*; Elsevier: 1986; Vol. 21, p 283.

(222)   Lima, L. M.; Barreiro, E. J. *Curr. Med. Chem.* **2005**, *12*, 23.

(223)   Olesen, P. H. *Curr. Opin. Drug Discov. Devel.* **2001**, *4*, 471.

(224)   MacMillan, D. W. *Nature* **2008**, *455*, 304.

(225)   Wu, W.-L.; Burnett, D. A.; Spring, R.; Greenlee, W. J.; Smith, M.; Favreau, L.; Fawzi, A.; Zhang, H.; Lachowicz, J. E. *J. Med. Chem.* **2005**, *48*, 680.

(226)   Carini, D. J.; Christ, D. D.; Duncia, J. V.; Pierce, M. E. In *Integration of Pharmaceutical Discovery and Development*; Springer: 2002, p 29.

(227)   Poe, M. M.; Methuku, K. R.; Li, G.; Verma, A. R.; Teske, K. A.; Stafford, D. C.; Arnold, L. A.; Cramer, J. W.; Jones, T. M.; Cerne, R. *J. Med. Chem.* **2016**, *59*, 10800.

(228)   Suzuki, Y.; Moriyama, K.; Togo, H. *Tetrahedron* **2011**, *67*, 7956.

(229)   Arnold;, A. E.; Stafford;, D. C.; Cook; J. M.; Emala; C. W.; Forkuo; G.; Jahan; R.; Kodali;, R.; Li; G.; Stephen, M. R. PCT/US2017/047185, 22.02.2018.

(230)   Shie, J.-J.; Fang, J.-M. *J. Org. Chem.* **2003**, *68*, 1158.

(231)   Ducharme, F. M.; Lasserson, T. J.; Cates, C. J. *Cochrane Database Syst. Rev.* **2011**, 5:CD003137

(232)   Nelson, H.; Nathan, R.; Kalberg, C.; Yancey, S.; Rickard, K. *Med. Gen. Med.* **2001**, *3*, 3.

(233)   Cohn, R. C. *Curr. Ther. Res. Clin. Exp.* **2003**, *64*, 34.

(234)   Fabbri, L. M.; Piattella, M.; Caramori, G.; Ciaccia, A. *Drugs* **1996**, *52*, 20.

(235)   McKernan, R.; Rosahl, T.; Reynolds, D.; Sur, C.; Wafford, K.; Atack, J.; Farrar, S.; Myers, J.; Cook, G.; Ferris, P. *Nat. Neurosci.* **2000**, *3*, 587.

(236)   Houser, R.; Harrison, N.; Homanics, G. *Proc. Nat. Acad. Sci. U.S.A.* **2006**, *103*, 15230.

(237)   Townsend, E. A.; Siviski, M. E.; Zhang, Y.; Xu, C.; Hoonjan, B.; Emala, C. W. *Am. J. Respir. Cell Mol. Biol.* **2013**, *48*, 157.

(238)   Townsend, E. A.; Zhang, Y.; Xu, C.; Wakita, R.; Emala, C. W. *Am. J. Respir. Cell Mol. Biol.* **2014**, *50*, 115.

(239)   Li, G.; Golani, L. K.; Jahan, R.; Rashid, F.; Cook, J. M. *Synthesis* **2018**, *50*, 4124.

(240)   Sieghart, W.; Ernst, M. *Curr. Med. Chem.* **2005**, *5*, 217.

(241)   Mendelson, W.; Owen, C.; Skolnick, P.; Paul, S.; Martin, J.; Ko, G.; Wagner, R. *Sleep* **1984**, *7*, 64.

(242)   Ninan, P. T.; Insel, T. M.; Cohen, R. M.; Cook, J. M.; Skolnick, P.; Paul, S. M. *Science* **1982**, *218*, 1332.

(243)   Rudolph, U.; Crestani, F.; Benke, D.; Brünig, I.; Benson, J. A.; Fritschy, J.-M.; Martin, J. R.; Bluethmann, H.; Möhler, H. *Nature* **2000**, *404*, 629.

(244)   Atack, J.; Wafford, K.; Street, L.; Dawson, G.; Tye, S.; Van Laere, K.; Bormans, G.; Sanabria-Bohórquez, S.; De Lepeleire, I.; de Hoon, J. *J. Psychopharmacol.* **2011**, *25*, 314.

(245)   Da Settimo, F.; Taliani, S.; Trincavelli, M. L.; Montali, M.; Martini, C. *Curr. Med. Chem.* **2007**, *14*, 2680.

(246)   Fischer, B. D.; Licata, S. C.; Edwankar, R. V.; Wang, Z.-J.; Huang, S.; He, X.; Yu, J.; Zhou, H.; Johnson Jr, E. M.; Cook, J. M. *Neuropharmacology* **2010**, *59*, 612.

(247)   Fischer, B. D.; Schlitt, R. J.; Hamade, B. Z.; Rehman, S.; Ernst, M.; Poe, M. M.; Li, G.; Kodali, R.; Arnold, L. A.; Cook, J. M. *Brain Res. Bull.* **2017**, *131*, 62.

(248)   Mirza, N.; Larsen, J.; Mathiasen, C.; Jacobsen, T.; Munro, G.; Erichsen, H.; Nielsen, A.; Troelsen, K.; Nielsen, E.; Ahring, P. *J. Pharmacol. Exp. Ther.* **2008**, *327*, 954.

(249)   Munro, G.; Lopez-Garcia, J.; Rivera-Arconada, I.; Erichsen, H.; Nielsen, E.; Larsen, J.; Ahring, P.; Mirza, N. *J. Pharmacol. Exp. Ther.* **2008**, *327*, 969.

(250)   R Atack, J. *Curr. Top. Med. Chem.* **2011**, *11*, 1176.

(251)   Witkin, J.; Cerne, R.; Wakulchik, M.; Gleason, S.; Jones, T.; Li, G.; Arnold, L.; Li, J.-X.; Schkeryantz, J.; Methuku, K. *Pharmacol. Biochem. Behav.* **2017**, *157*, 35.

(252)   Cook, J. M.; Zhou, H.; Huang, S.; Sarma, P. V. V. S.; Zhang, C. US Patent US 7,618,958 B2, Pub. Date Nov. 17, 2009.

(253)   Cook, J. M.; Huang, Q.; He, X.; Li, X.; Yu, J.; Han, D.; Lelas, S.; McElroy, J. F. US Patent US 7,119,196 B2, Pub. Date Oct. 10, 2006.

(254)   Rudolf, U.; Crestani, F.; Benke, J.; Brünig, I.; Benson, J.; Fritschy, J.; Martin, J.; Bluethmann, H.; Mohler, H. *Nature* **1999**, *401*, 796.

(255)   Di Lio, A.; Benke, D.; Besson, M.; Desmeules, J.; Daali, Y.; Wang, Z.-j.; Edwankar, R.; Cook, J. M.; Zeilhofer, H. U. *Neuropharmacology* **2011**, *60*, 626.

(256)   Knabl, J.; Witschi, R.; Hösl, K.; Reinold, H.; Zeilhofer, U. B.; Ahmadi, S.; Brockhaus, J.; Sergejeva, M.; Hess, A.; Brune, K. *Nature* **2008**, *451*, 330.

(257)   Licata, S. C.; Platt, D. M.; Cook, J. M.; Van Linn, M. L.; Rowlett, J. K. *Psychopharmacology* **2009**, *203*, 539.

(258)   Tan, K. R.; Brown, M.; Labouèbe, G.; Yvon, C.; Creton, C.; Fritschy, J.-M.; Rudolph, U.; Lüscher, C. *Nature* **2010**, *463*, 769.

(259)   van Rijnsoever, C.; Täuber, M.; Choulli, M. K.; Keist, R.; Rudolph, U.; Mohler, H.; Fritschy, J. M.; Crestani, F. *J. Neurosci.* **2004**, *24*, 6785.

(260)   Atack, J.; Hallett, D. J.; Tye, S.; Wafford, K. A.; Ryan, C.; Sanabria-Bohórquez, S.; Eng, W.-s.; Gibson, R. E.; Burns, H. D.; Dawson, G. R. *J. Psychopharmacol.* **2011**, *25*, 329.

(261)   Zuiker, R. G.; Chen, X.; Østerberg, O.; Mirza, N. R.; Muglia, P.; de Kam, M.; Klaassen, E. S.; van Gerven, J. M. *J. Psychopharmacol.* **2016**, *30*, 253.

(262)   Scott-Stevens, P.; Atack, J.; Sohal, B.; Worboys, P. *Biopharm. Drug Dispos.* **2005**, *26*, 13.

(263)   Hofmann, M.; Kordás, K. S.; Gravius, A.; Bölcskei, K.; Parsons, C. G.; Dekundy, A.; Danysz, W.; Dézsi, L.; Wittko-Schneider, I. M.; Sághy, K. *Behav. Pharmacol.* **2012**, *23*, 790.

(264)   Möhler, H. *Neuropharmacology* **2011**, *60*, 1042.

(265)   Clayton, T.; Poe, M. M.; Rallapalli, S.; Biawat, P.; Savić, M. M.; Rowlett, J. K.; Gallos, G.; Emala, C. W.; Kaczorowski, C. C.; Stafford, D. C. *Int. J. Med. Chem.* **2015**, 2015, Article ID 43024, 54 pages.

(266)   Rivas, F. M.; Stables, J. P.; Murphree, L.; Edwankar, R. V.; Edwankar, C. R.; Huang, S.; Jain, H. D.; Zhou, H.; Majumder, S.; Sankar, S. *J. Med. Chem.* **2009**, *52*, 1795.

(267)   Namjoshi, O. A.; Wang, Z.-j.; Rallapalli, S. K.; Johnson Jr, E. M.; Johnson, Y.-T.; Ng, H.; Ramerstorfer, J.; Varagic, Z.; Sieghart, W.; Majumder, S. *Bioorg. Med. Chem.* **2013**, *21*, 93.

(268)   Cook, J.M.; Witkin J.; Li, G., Improved Antiepileptic Profile with α2/3 Selective Receptor PAMs. In *ASPET Annual Meeting at EB* 2019.

(269)   Berro, L. F.; Rüedi-Bettschen, D.; Cook, J. E.; Golani, L. K.; Li, G.; Jahan, R.; Rashid, F.; Cook, J. M.; Rowlett, J. K.; Platt, D. M. *Alcohol. Clin. Exp. Res.* **2019**, (DOI: 10.1111/acer.14000)

(270)   Mason, B. J. *Neuropharmacology* **2017**, *122*, 244.

(271)   Stephens, D.; King, S.; Lambert, J.; Belelli, D.; Duka, T. *Genes Brain Behav.* **2017**, *16*, 149.

(272)   Aguilar, A.; Zhou, H.; Chen, J.; Liu, L.; Bai, L.; McEachern, D.; Yang, C.-Y.; Meagher, J.; Stuckey, J.; Wang, S. *J. Med. Chem.* **2013**, *56*, 3048.

(273)   Kayukova, L. *Pharm. Chem. J.* **2005**, *39*, 539.

(274)   Namjoshi, O. A.; Wang, Z.-j.; Rallapalli, S. K.; Jr., E. M. J.; Johnson, Y.-T.; Ng, H.; Ramerstorfer, J.; Varagic, Z.; Sieghart, W.; Majumder, S.; Roth, B. L.; Rowlett, J. K.; Cook, J. M. *Bioorg. Med. Chem.* **2013**, *21*, 93

(275)   GABA(A)ergic Subtype Selective Ligands as Anxiolytic, Antinociceptive, Anticonvulsant and Antidepressant Agents via Deuterium Exchange, Filed Jan 2019.

APPENDIX

III. Appendix (Part I)

Basket Test: The Basket test is useful in assessing motor coordination and sensorimotor deficits in rodent models of CNS disorders. An animal is placed in the center of the basket and the basket is inverted. The animal is allowed to climb down the walls of the wire basket into its home cage. The time it takes for the animal to complete the task is scored. This test is used to evaluate novel chemical entities for their effect on motor performance.

I. BASKET TEST

Study: pilot   _____

Group: C57BL/6 mice, male   _____TAPE #:

Age: 6 months   _____   DATE: April 1, 2015

Table A1

MOUSE #	GROUP	Trial 1 (s)	Trial 2 (s)	Trial 3 (s)	Mean (s)
1	10 mg/kg DZP	4	14	3	7,0
2		23	55	28	35,3
3		13	12	10	11,7
4	30 mg/kg CMD-45	180	180	30	130,0
5		16	44	49	36,3
6		106	180	178	154,7
7	30 mg/kg XHE-III-74	61	180	168	136,3
8		60	22	10	30,7
9		17	33	8	19,3
10		25	22	10	19,0

Comments:

Men values per group:

10 mg/kg DZP: 15,0 s (highly incapacitating)

30 mg/kg CMD-45: 107,0 s (moderately incapacitating)

30 mg/kg XHE-III-74: 51,3 s (clearly incapacitating)

Hence, when administered at high doses of 30 mg/kg, both alpha4-selective ligands diminished the capability of male C57BL/6 mice to perform the basket test, pointing to the effect of motor impairment, possibly connected with neuromuscular strength and/or motor coordination. The effect was more pronounced with XHE-III-74.

Step-down Test: The Passive Avoidance step-down cage, for mice or immature rats, is based on the stepdown scheme in which the animal is dropped on an elevated platform. The grid surrounding the base will start vibrating and the latency (time on the platform) will be measured. Animals will be trained for this study. This test is used to evaluate novel chemical entities for their effect on anti-anxiety behavior.

II. STEP-DOWN TEST

Study: pilot   _____

Group: C57BL/6 mice_____TAPE #:

Age: 6 months   _____   DATE: April 1, 2015

Table A2

MOUSE #	GROUP	LATENCY TO STEP DOWN (s)
1	10 mg/kg DZP	2
2		180
3		2
4	30 mg/kg CMD-45	180
5		180
6		180
7	30 mg/kg XHE-III-74	180
8		180
9		180
10		180

223

Comments:

The experiment was performed under bright light, which promotes anxious reaction and helps reveal anti-anxiety potential of a treatment.

Mice dosed with 10 mg/kg DZP showed a clear tendency of decreased anxiety, while two alpha4-preferring ligands were devoid of any hint of anti-anxiety action.

Rotarod: At least two weeks of training are needed to ensure that all subjects have learned the task to the same degree. In the fixed rotation protocol, the animals are placed on a rod which constantly rotates at 20 rpm. A trial is complete when the animal falls or the time period ends (180 s); This test is used to evaluate novel chemical entities for their effect on motor performance.

III. ROTAROD TEST

Study: pilot   _____

Group: Wistar rats, male   _____TAPE #:

Age: 10 weeks   _____   DATE: April 1-3, 2015

Table A3

RAT #	GROUP	Time until fall (s)
1	SOL	163
2	DZP (5mg/kg)	1
3	CMD-45 (15 mg/kg)	31
4	XHE-III-74 (15 mg/kg)	2
5	CMD-45 (10 mg/kg)	15
6	CMD-45 (10 mg/kg)	180
7	XHE-III-74 (10 mg/kg)	7
8	XHE-III-74 (10 mg/kg)	52
9	CMD-45 (5 mg/kg)	180

Comments:

During two consecutive days, 16 rats were trained to keep balance while on the rotating rod (20 rpm, fixed velocity). On the third day, 9 of 6 animals satisfied the cut-off criterion of balancing without any fall during 180 s.

During testing (20 min after i.p. administration), diazepam at 5 mg/kg and XHE-III-74 at 15 mg/kg were exceptionally incapacitating. XHE-III-74 dosed at 10 mg/kg was still incapacitating

and we did not find the no-observed-effect-level of XHE-III-74. On the other hand, CMD-45 was incapacitating at 15 mg/kg and less so at 10 mg/kg, while 5 mg/kg appeared to be the dose close to the no-observed effect level of CMD-45.

Hence, ataxia is a dose-dependent effect of both alpha4-preferring ligands. Nonetheless, the ataxic potential of XHE-III-74 is more pronounced.

Table A4 LOCOMOTOR ACTIVITY TEST in adult male Wistar rats 2 months old (Any-maze software)

The animals were recorded during 45 min, beginning 20 min after i.p. administration of treatment

Total distance travelled (m)

Treatment	N	Mean	SD	SE	Data
sol	6	22.6427	±3.0003	±1.2248	25.712, 22.019, 23.710, 23.290, 17.028, 24.097
XHe III 74 10 mg/kg			6	12.0625	±2.8401 ±1.1595 10.088, 15.450, 9.999, 10.566, 15.978, 10.294
CMD 45 10 mg/kg	6	12.1652	±5.6081	±2.2895	7.570, 6.207, 15.374, 9.883, 12.574, 21.383

ANOVA : $F_{(2,15)} = 13.7099$ p = 0.000
Tukey test
  sol vs. XHe III 74 10 mg/kg $q_{(15,3)} = 6.4443$ p = 0.001
  sol vs. CMD 45 10 mg/kg $q_{(15,3)} = 6.3817$ p = 0.001
  XHe III 74 10 mg/kg vs. CMD 45 10 mg/kg $q_{(15,3)} = 0.0625$ p = 0.999

Total time mobile (s)

Treatment	N	Mean	SD	SE	Data
sol	6	1878.10	±375.37	±153.24	1587.2, 1999.2, 2251.4, 1913.5, 2225.6, 1291.7
XHe III 74 10 mg/kg			6	1096.38	±252.38 ±103.03 755.4, 1506.5, 949.8, 1074.5, 1086.4, 1205.7
CMD 45 10 mg/kg	6	1104.83	±294.22	±120.11	709.8, 873.4, 1521.8, 1023.1, 1261.8, 1239.1

ANOVA: $F_{(2,15)} = 12.4579$ p = 0.001
Tukey test
  sol vs. XHe III 74 10 mg/kg $q_{(15,3)} = 6.1464$ p = 0.002

sol vs. CMD 45 10 mg/kg   q(15,3) = 6.0799 p = 0.002
XHe III 74 10 mg/kg vs. CMD 45 10 mg/kg   q(15,3) = 0.0664   p = 0.999

Total distance travelled (m)
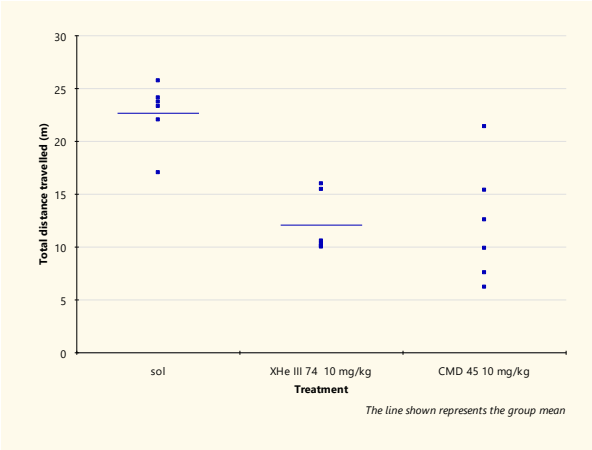
Figure 1. Total distance travelled. The data analysed has been limited in the following way: Treatment = sol, XHe III 74 10 mg/kg or CMD 45 10 mg/kg.
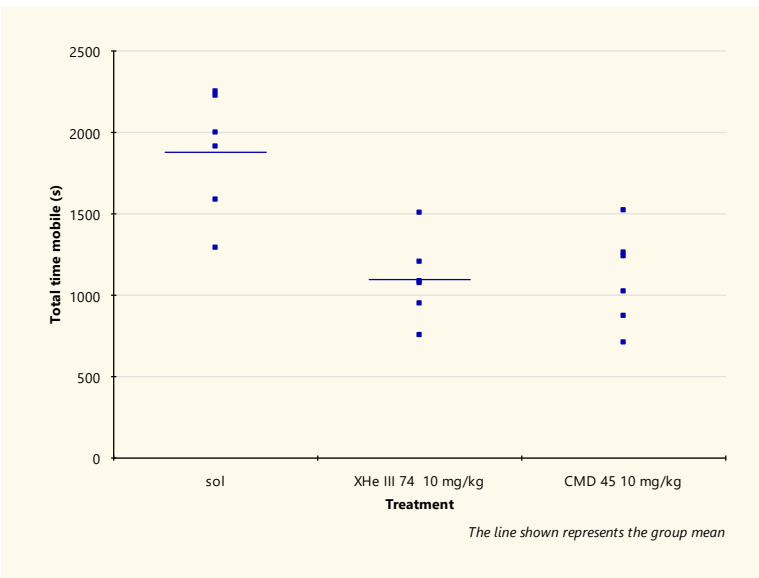
Total time mobile (s)

Figure 2. Total time mobile. The data analysed has been limited in the following way: Treatment = sol, XHe III 74 10 mg/kg or CMD 45 10 mg/kg.

Total distance travelled (m)
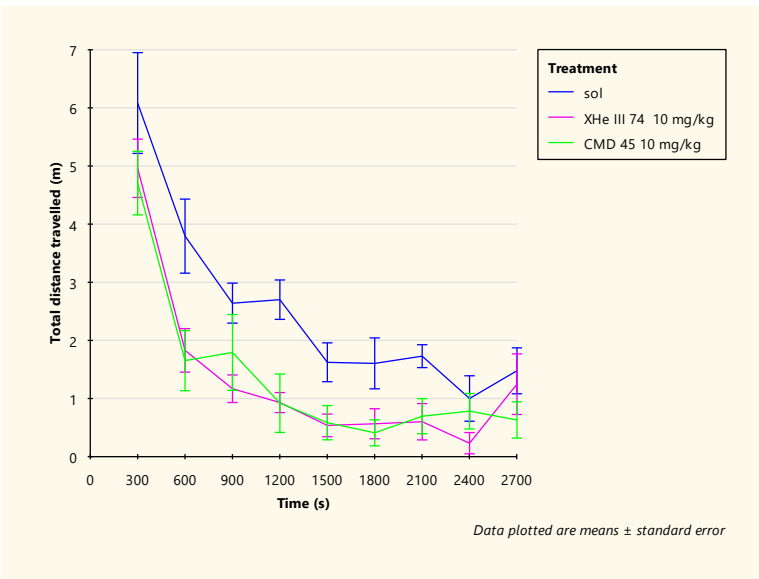
Figure 1. Total distance travelled. The data analysed has been limited in the following way: Treatment = sol, XHe III 74 10 mg/kg or CMD 45 10 mg/kg
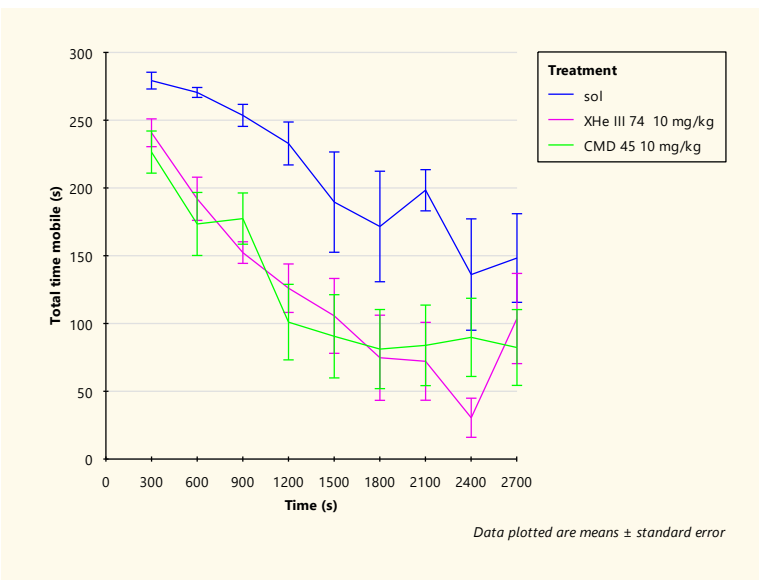
Total time mobile (s)

Figure 2. Total time mobile. The data analysed has been limited in the following way: Treatment = sol, XHe III 74 10 mg/kg or CMD 45 10 mg/kg

Comment: Both, XHe III 74 and CMD 45 dosed at 10 mg/kg were **clearly sedative in locomotor activity test**. The effect appeared to be robust and replicable without any doubt.

V. LOCOMOTOR ACTIVITY TEST in adult female Wistar rats 4 month old, weighing 350 g and more (Any-maze software)
     -Pilot experiment-

The animals were recorded during 30 min, beginning 20 min after i.p. administration of treatment

Total distance travelled (m), female Wistar rat

Treatment	N	Mean	SD	Data	
CMD 45 30 mg/kg	2	0.1010	±0.0665	0.054, 0.148	
XHe III 74 30 mg/kg		2	0.0000	±0.0000	0.000, 0.000
SOL	2	1.5775	±1.1391	2.383, 0.772	
DZP 10 mg/kg	2	0.3090	±0.3550	0.560, 0.058	

ANOVA: $F_{(3,4)} = 3.0001$ $p = 0.158$

Total time mobile (s), female Wistar rat

Treatment	N	Mean	SD	Data	
CMD 45 30 mg/kg	2	32.55	±10.54	40.0, 25.1	
XHe III 74 30 mg/kg		2	0.35	±0.07	0.4, 0.3
SOL	2	308.75	±168.64	428.0, 189.5	
DZP 10 mg/kg	2	50.65	±55.79	90.1, 11.2	

ANOVA : $F_{(3,4)} = 5.0931$ $p = 0.075$

Comment:

When dosed at 30 mg/kg, both, **XHe III 74 and CMD 45 were exceptionally sedative in locomotor activity test in adult female rats**. The effect may be even more pronounced than that obtainable with diazepam dosed at 10 mg/kg. Notably, the effect of XHe III 74 dosed at 30 mg/kg was so pronounced that it cannot be distinguished – by the used method – from possible anesthetic action of this ligand.

From all this CNS study it is obvious that both ligands are sedative and some test shows that XHe-III-74 is somewhat more sedative than CMD-45. But for better activity, potency and selectivity towards alpha 4 GABAA receptor, it was chosen as the lead compound.

In the meanwhile, Dr. Savic's group have done the pk study on XHe-III-74.

Pharmacokinetic studies
Experiment I
In order to determine pharmacokinetic profile of XHe-III-4 rats were divided in two groups, each containing 18 animals i.e. three animals per one time point. The rats from group I received XHe-III-74 nanoemulsion and rats from group II received XHe-III-74 solution into the tail vein, via

infusion pump, both at doses of **2 mg/kg**. At predetermined time intervals, that is, 10, 20, 40, 60, 180 and 720 min after dosing, rats were sacrificed to collect blood samples and brains.
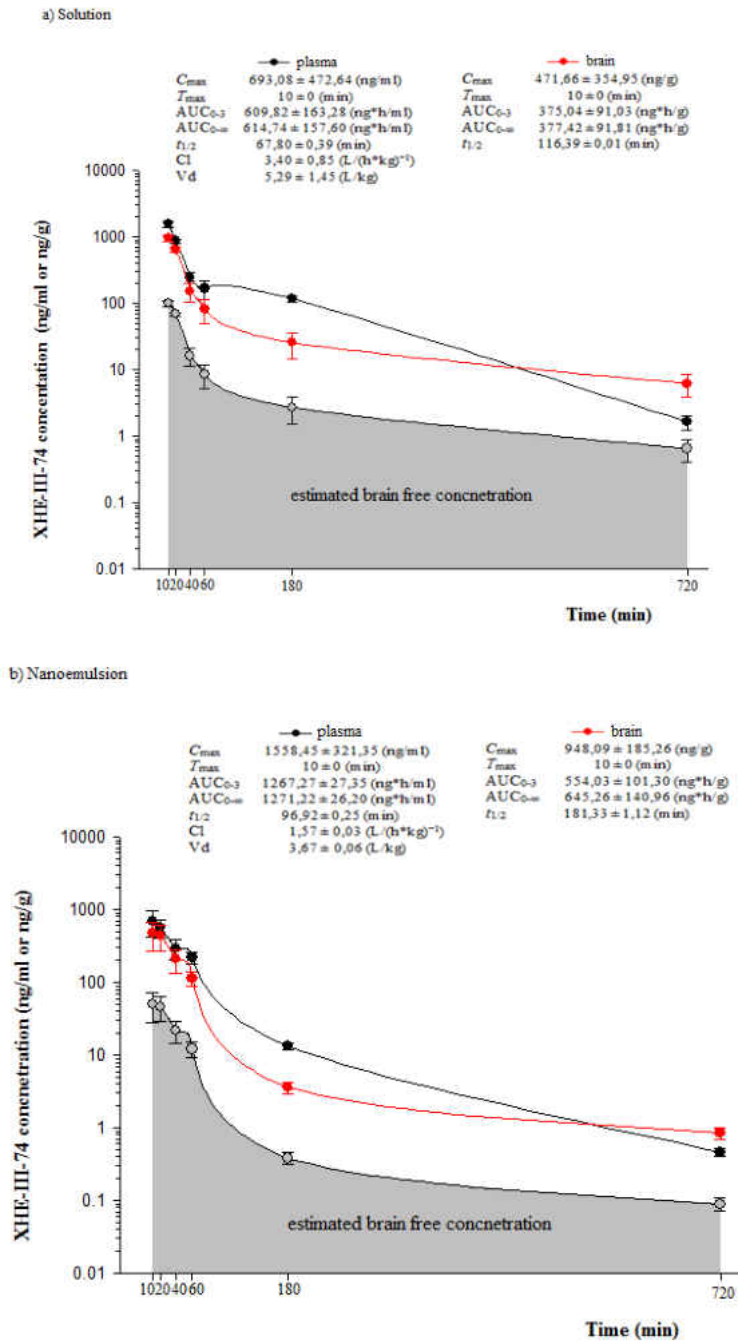
Figure A1. Plasma and brain concentration–time profiles of XHe-III-74 after intravenous administration of solution (a) and nanoemulsion (b) ($n = 3$, mean ± SEM).

Table 4.
Plasma and brain concentrations of XHe-III-74 after intravenous administration of solution and nanoemulsion ($n = 3$, mean ± SEM).

Time (min)	Nanoemulsion (2 mg/kg)		Solution (2 mg/kg)	
	Plasma (nmol/L)	Brain (nmol/kg)	Plasma (nmol/L)	Brain (nmol/kg)
5	1876.19 ± 738.68	1276.79 ± 554.75	4218.76 ± 502.24	12364.14 ± 2664.42
20	1537.01 ± 449.72	1180.64 ± 444.06	2338.58 ±215.26	1745.17 ± 128.02
40	791.06 ± 251.02	561.91 ± 193.30	656.30± 120.39	412.24 ± 125.15
60	599.22 ± 110.53	310.77 ± 71.32	453.15 ± 150.90	220.84 ± 88.29
180	35.90 ± 3.99	9.79 ± 1.77	325.24 ± 26.73	69.17 ± 29.92
720	107.27 ± 106.02	2.30 ± 0.44	4.41 ± 1.05	16.65 ± 6.05

Experiment II
Additional pharmacokinetic experiment was performed in order to determine brain and plasma concentration, as well as to calculate free brain and plasma levels of XHe-III-74 dosed at **10 mg/kg**, 20 min after intravenous infusion.

		Total conc.	Free conc.
Plasma (nmol/l)	Nanoemulsion	6530.84±854.12	756.27±98.90635
	Solution	13752.82±2375.53	1586.27±275.09
Brain (nmol/l)	Nanoemulsion	5608.33±953.93	590.00±100.35
	Solution	12364.14±2664.42	1300.71±280.30

Table 5. Total and estimated free concentrations of XHe-III-74 (dosed at 10 mg/kg) in plasma and brain samples after 20 min ($n = 3$, mean±SEM)

Experiment III
XHe-III-74 nanoemulsion (concentration 2 mg/ml) was injected into the tail vein at dose of **20 mg/kg** (the dose used in LOOR experiment). At predetermined time intervals, that is, 5, 10, 20, 40, 180 and 720 min after dosing rats were sacrificed to collect blood samples and brains.

Time (min)	Plasma concentration		Brain concentration	
	nmol/l	ng/ml	nmol/kg	ng/g
5	73904.63 ± 3777.95	27301.11 ± 1395.61	69041.67 ± 3898.48	25504.68 ± 1440.14
10	52424.80 ± 3134.74	19366.25 ± 1158.00	52375.26 ± 6423.55	19347.94 ± 2372.92
20	40393.56 ± 2681.59	14921.76 ± 990.61	34335.14 ± 1471.47	12683.74 ± 543.58
40	23889.09 ± 4652.03	8824.87 ± 1718.506	19638.77 ± 3552.36	7254.76 ± 1312.28

60	16311.87 ± 1811.01	6025.77 ± 669.00	25361.54 ± 2486.93	9368.81 ± 918.70
180	3623.02 ± 344.13	1338.38 ± 127.12	3589.57 ±595.43	1326.02 ± 219.6
720	28.69 ± 11.54	10.60 ± 4.26	799.76 ± 75.71	295.44 ± 27.97

Table 6. Plasma and brain concentration of XHe-III-74 after intravenous administration of nanoemulsion (n = 3, mean±SEM)

Anticonvulsant Screening Program
Test 7 Results - Anticonvulsant Evaluation (6Hz, Mice)

ASP ID: 482011 U Screen ID: 1

Solvent Code: MC Solvent Prep: M&P,SB Route Code: IP
Animal Weight: - g Current(mA): 44
Date Started: 20-Apr-2015 Date Completed: 23-Apr-2015
Reference: 513:228-231.

ED50 Biological Response

Test	Time (hr)	Dose (mg/kg)	Dths	N/F	C
6HZ	2.0	50		0/8	
6HZ	2.0	75		1/8	
6HZ	2.0	100		4/8	
6HZ	2.0	180	3	1/1	1
TOX	0.25	50		0/8	
TOX	0.25	75		1/8	
TOX	0.25	100		8/8	*
TOX	0.25	180		4/4	*

Note: Presence of an asterisk (*) indicates that there are multiple comment codes.

ED50 Biological Response Comments

Test	Dose (mg/kg)	Time (Hrs)	Code	Comment
6HZ	180	2	1	Death
TOX	100	0.25	14	Unable to grasp rotorod
TOX	100	0.25	34	Muscle spasms
TOX	180	0.25	14	Unable to grasp rotorod
TOX	180	0.25	34	Muscle spasms

Time to Peak Effect

Test	Dose	Dths	0.25 N/F	C	0.5 N/F	C	1.0 N/F	C	2.0 N/F	C	4.0 N/F	C	6.0 N/F	C	8.0 N/F	C	24 N/F	C	3.0 N/F	C
6HZ	100		1/4		1/4		2/4		3/4		0/4		/		/		/		/	
6HZ	180	11	0/4		0/1	1	2/2	1	1/1	1	0/1	3	/		/		/		/	

232

Anticonvulsant Screening Program
Test 7 Results - Anticonvulsant Evaluation (6Hz, Mice)

ASP ID: 482011   U   Screen ID: 1

TOX	50			0/8		0/8		0/8		0/8		/		/		/	/	/
TOX	75			1/8		1/8		0/8		0/8		/		/		/	/	/
TOX	100			4/4	*	4/4	*	0/4		0/4		0/4		/		/	/	/
TOX	180		11	4/4	*	4/4	1	4/4	*	3/4	1	3/4	1	/		/	/	/

Note: N/F = number of animals active or toxic over the number tested.

C= Comment code. Presence of an asterisk (*) indicates that there are multiple comment codes.

Response Comments

Test	Dose (mg/kg)	Time	Code	Comments
6 HZ	180	0.5	1	Death
6 HZ	180	1	1	Death
6 HZ	180	2	1	Death
6 HZ	180	4	3	Death following continuous seizure
TOX	100	0.25	14	Unable to grasp rotorod
TOX	100	0.25	34	Muscle spasms
TOX	100	0.5	14	Unable to grasp rotorod
TOX	100	0.5	34	Muscle spasms
TOX	180	0.25	14	Unable to grasp rotorod
TOX	180	0.25	34	Muscle spasms
TOX	180	0.5	1	Death
TOX	180	1	1	Death
TOX	180	1	14	Unable to grasp rotorod
TOX	180	1	34	Muscle spasms
TOX	180	2	1	Death
TOX	180	4	1	Death

Anticonvulsant Screening Program
Test 7 Results - Anticonvulsant Evaluation (6Hz, Mice)

ASP ID: 482011   U   Screen ID: 1

Comments to Supplier: Insufficient material to continue further tests.Not a good compd as lot of death is seen.See Time-course done below at dose 180m/kg,11/20 mice died.

233

Anticonvulsant Screening Program
Test 31 Results - Mice MES & 6Hz Identification

ASP ID: 486001   **U**   **Screen ID: 1**

Solvent Code:	**MC**	**Solvent Prep:**	**M&P,SB**
Animal Weight:	**20.0 - 28.0 g**		
Date Started:	**02-Jul-2015**	**Date Completed:**	**06-Jul-2015**

Route Code: IP

6Hz Current(mA): 32

Reference: **511: pg 215-216**

Response

Time (Hours)				0.5		2.0		0.25		1.0		4.0		6.0		3.0		8.0		24	
Test	Dose	Form	Dths	N/F	C	N/F	C	N/F	C	N/F	C	N/F	C	N/F	C	N/F	C	N/F	C	N/F	C
6HZ	30	SUS		0/4		0/4		/		/		/		/		/		/		/	
6HZ	100	SUS		0/4		0/4		/		/		/		/		/		/		/	
6HZ	300	SUS		0/4		0/4		/		/		/		/		/		/		/	
MES	30	SUS		0/4		0/4		/		/		/		/		/		/		/	
MES	100	SUS		0/4		0/4		/		/		/		/		/		/		/	
MES	300	SUS		0/4		0/4		/		/		/		/		/		/		/	
TOX	30	SUS		0/8		0/8		/		/		/		/		/		/		/	
TOX	100	SUS		0/8		0/8		/		/		/		/		/		/		/	
TOX	300	SUS		3/8		0/8		/		/		/		/		/		/		/	

Note: N/F = number of animals active or toxic over the number tested.

C = Comment code. Presence of an asterisk (*) indicates that there are multiple comment codes.

Comments to Supplier:

XHe-III-74 Ethyl ester

Anticonvulsant Screening Program
Test 31 Results - Mice MES & 6Hz Identification

Response

Time (Hours)				0.5		2.0		0.25		1.0		4.0		6.0		3.0		8.0		24	
Test	Dose	Form	Dths	N/F	C	N/F	C	N/F	C	N/F	C	N/F	C	N/F	C	N/F	C	N/F	C	N/F	C
6HZ	30	SUS		0/4		0/4		/		/		/		/		/		/		/	
6HZ	100	SUS		0/4		0/4		/		/		/		/		/		/		/	
6HZ	300	SUS		1/4		0/4		/		/		/		/		/		/		/	
MES	30	SUS		0/4		0/4		/		/		/		/		/		/		/	
MES	100	SUS		0/4		0/4		/		/		/		/		/		/		/	
MES	300	SUS		1/4		0/4		/		/		/		/		/		/		/	
TOX	30	SUS		0/8		0/8		/		/		/		/		/		/		/	
TOX	100	SUS		0/8		0/8		/		/		/		/		/		/		/	
TOX	300	SUS		0/8		0/8		/		/		/		/		/		/		/	

Note: N/F = number of animals active or toxic over the number tested.

C = Comment code. Presence of an asterisk (*) indicates that there are multiple comment codes.

Comments to Supplier:
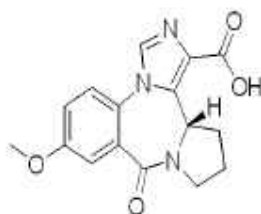
XHe-III-74 acid
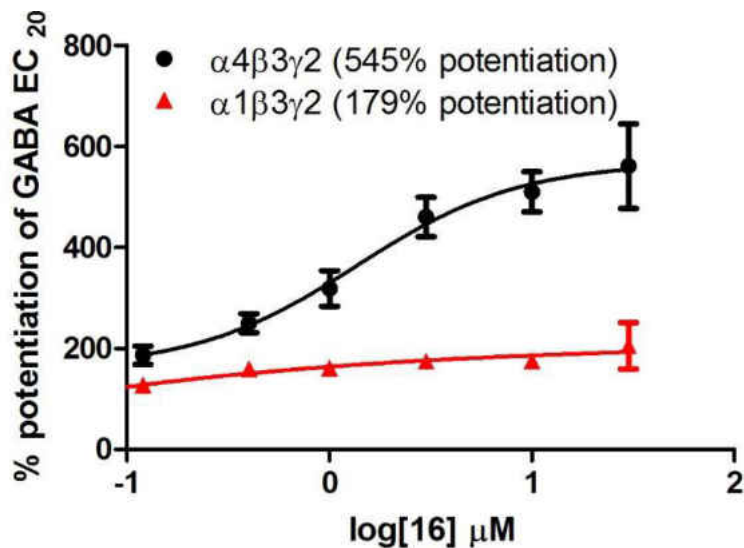
Figure A2. The $\alpha_4\beta_3\gamma_2$ GABA$_A$R subtype selectivity of **16** was confirmed by comparison of its GABA induced current potentiation with the $\alpha_1\beta_3\gamma_2$ GABA$_A$R
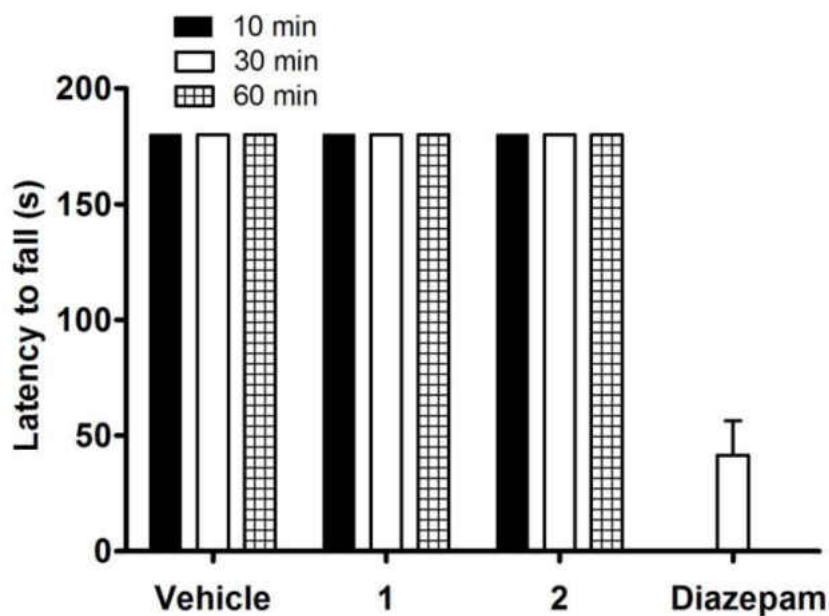
Figure A3 (related to Figure 34). Effect of 1 and 2 on sensorimotor coordination. Swiss Webster mice received a single intra-gastric gavage of test compound (100 mg/kg) or diazepam (5 mg/kg ip) and placed on a rotarod at 15rpm for 3 minutes after 10, 30 and 60 minutes of drug administration. A fail was assigned to a mouse having fallen twice prior to 3 minutes. The latency to fall is expressed as mean ± SEM from 9 mice in each group. Vehicle and diazepam was used as negative and positive control respectively.
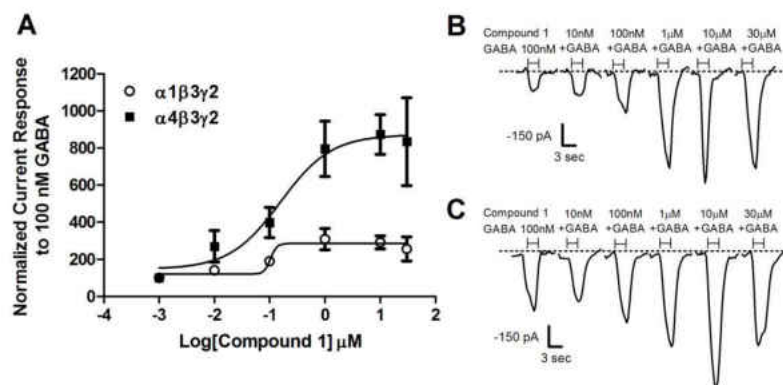
Figure A4 (related to Figure 34). Automated patch clamp with compound 1 (phenol **6**). A) Concentration-dependent negative current responses in the presence of EC20 concentration of GABA and increasing concentration of compound 1 applied together for 3 seconds using α1β3γ2 or α4β3γ2 GABAAR expressing HEK293T cells. Negative current readings were normalized to EC20 concentration of GABA response set as 100% (n = 16). B) Current recordings in the presence of EC20 concentration of GABA and increasing concentrations of compound 1 applied together for 3 seconds using α4β3γ2 expressing HEK293T cells. C) Current recordings in the presence of EC20 concentration of GABA and increasing concentrations of compound 1 applied together for 3 seconds using α1β3γ2 expressing HEK293T cells.
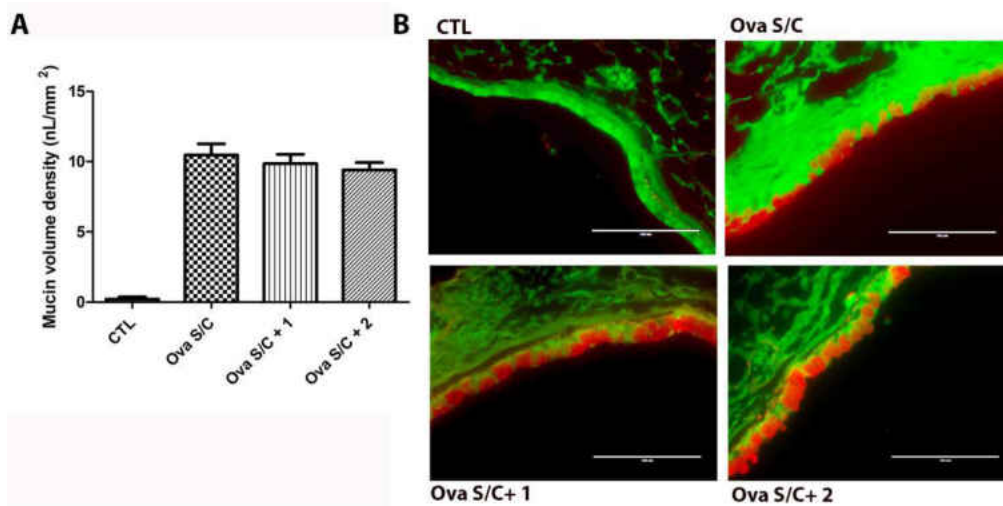
Figure A5. Effect of 1 and 2 on mucous production Morphometric quantification of mucin volume density and B) representative images of mucin (red) in the airway epithelium (green) with periodic acid fluorescent Schiff's stain. Ova s/c BALB/c mice were administered 1 via oral gavage, 100 mg/kg twice daily for 5 days or 2 via oral gavage, 100 mg/kg twice daily for 5 days. Data represent mean ± SEM mucin volume density from 6 mice in each group. Scale bar represents 100 μm.

Table A5. Cytotoxicity of oxadiazoles (24,25,26) determined in the presence of human kidney, liver and lung cells

Compound	Toxicity in HEK293 (Kidney) LD_{50}	Toxicity in HEP2 (Liver) LD_{50}	Toxicity in BEAS 2B (Lung) LD_{50}
RJ-03-12	>100 μM	>200 μM	>100 μM
RJ-03-13	>200 μM	>400 μM	>200 μM
RJ-03-14	>200 μM	>400 μM	>400 μM

Table A6. Cytotoxicity of oxazole **28** determined in the presence of human kidney, liver and lung cells

Compound	Toxicity in HEK293 (Kidney) LD_{50}	Toxicity in HEP2 (Liver) LD_{50}	Toxicity in BEAS 2B (Lung) LD_{50}
KRM-II-68	>400 μM	>400 μM	>400 μM
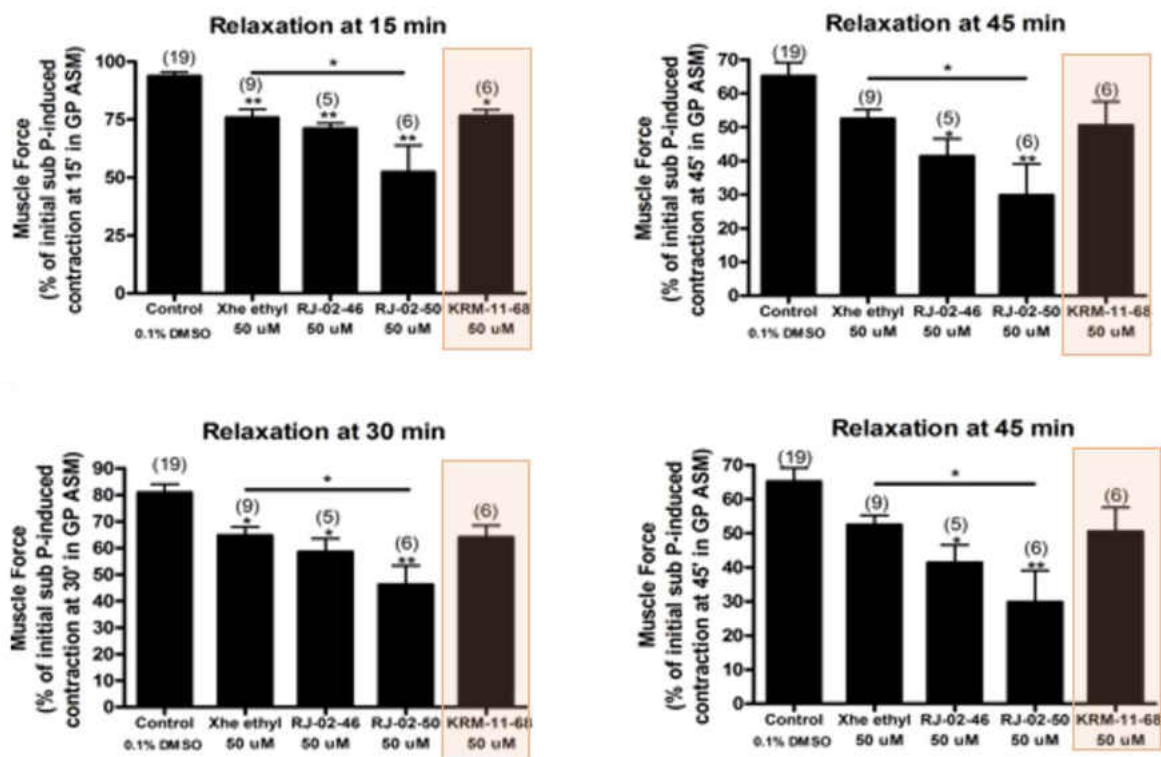
Figure A6. Airway smooth muscle relaxation in guinea pig tracheal ring by oxazole **28**
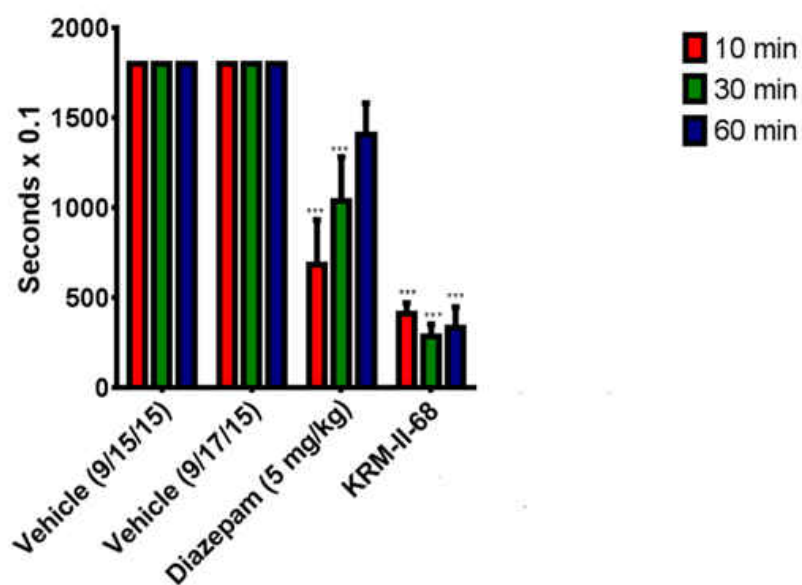
Figure A7. Sensorimotor impairment of **28**

Table A7. Microsomal stability of compounds was tested with human and mouse liver microsomes.

Compound	HLM % remaining after 60 min	MLM % remaining after 60 min
RJ-03-57, 31	94.3 ± 0.1	98.3 ± 0.2
RJ-02-67	90.6 ± 0.2	46.6 ± 0.3
RJ-03-30, 29	91.8 ± 0.2	80.0 ± 0.3

Table A8. Cytotoxicity of compounds determined in the presence of human kidney and liver cells. None of the investigated compounds induced cytotoxicity up to a concentration of 100 µM. For the majority of compounds no toxicity was observed at a concentration of 400 µM.

Compound	LD_{50} HEK293 (µM) (Kidney)	LD_{50} HEPG2 (µM) (Liver)
RJ-03-57, 31	>200	>200
RJ-02-50	>400	>400
RJ-02-67	>400	>400
RJ-03-30, 29	>400	>400
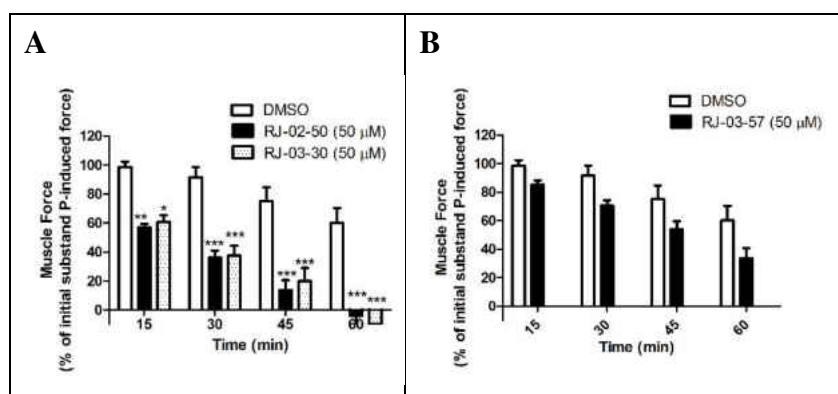
Figure A8. Airway smooth muscle contractile force in guinea pig tracheal rings. Tracheal rings were contracted with 1 mM substance P and then treated with 50 mM of compounds or vehicle control (0.1% DMSO). The percent of remaining contractile force was measured at various time

points and expressed as a percent of the initial substance P induced contractile force. (N > 6) A 2way ANOVA was used to calculate significance with *(p <0.05), ** (p < 0.01) or *** (p < 0.001) p-values are given for each condition. All investigated compounds except RJ-03-57 reduced the constriction of airway smooth muscle after 15 minutes for a period of at least 60 minutes.
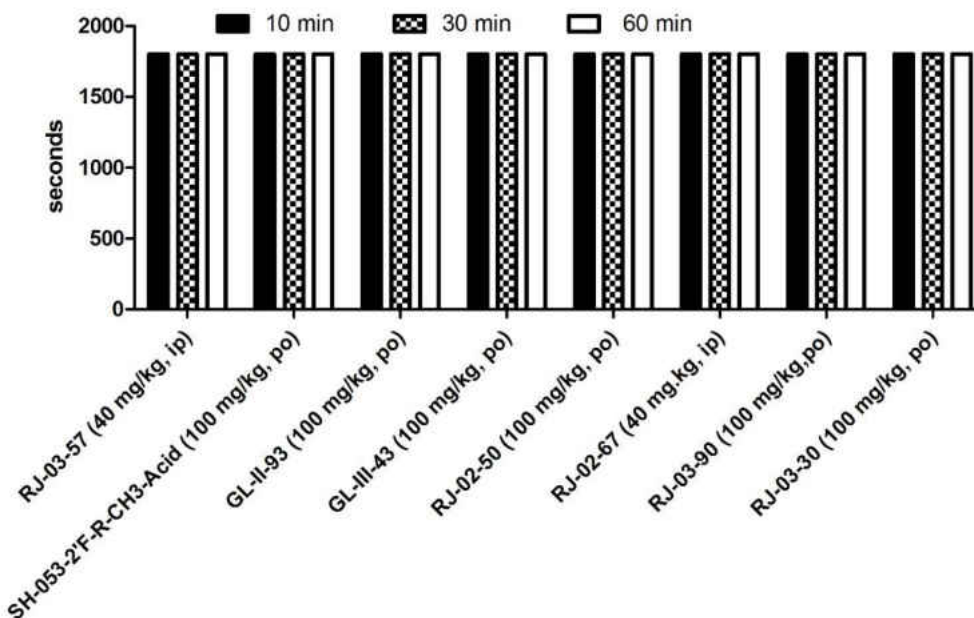
Figure A9. Effect of compounds on sensorimotor coordination. Swiss Webster mice were tested on a rotarod at 15 rpm for 3 min at 10, 30, and 60 min following compound exposure. Mice (N = 10) received a single injection (i.p. or p.o.) of test compound. The time of fall was recorded if it occurred prior to 3 min. Data are expressed as mean ± SEM (N = 10). Student t-test was used to calculate significance: *(p <0.05), ** (p < 0.01) or *** (p < 0.001) significance compared to vehicle-treated mice. None of the investigated compounds induced any sensorimotor impairments at the concentration tested.
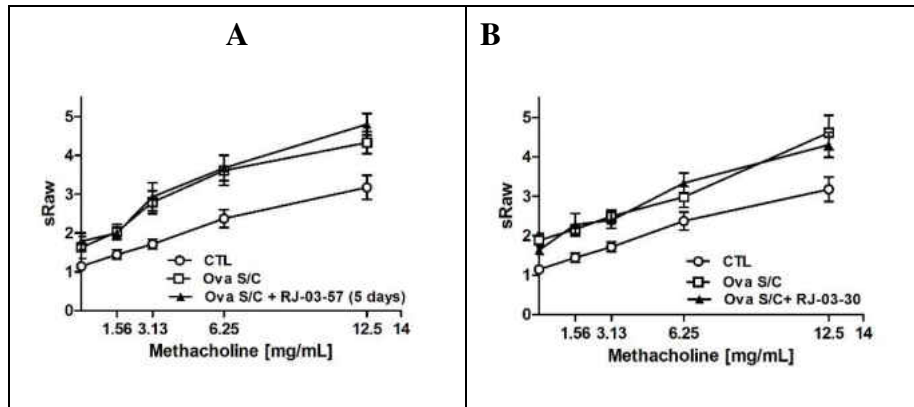
Figure A10. Compound effects on airway hyperresponsiveness Specific airway resistance (sRaw) was measured at increasing dosages of methacholine by a DSI's Buxco FinePointe non-invasive airway mechanics instrument. Ova s/c BALB/c mice were administered all compounds via oral gavage, 100 mg/kg twice daily for 5 days. Data represent mean ± SEM from 10 mice in each group. ∗, ∗∗, and ∗∗∗ indicate $p < 0.05$, $p < 0.01$, $p < 0.001$ significance, respectively, compared to vehicle treated ova s/c BALB/c mice. Compounds RJ-03-57, RJ-03-30 were not able to alleviated airway hyperresponsiveness.
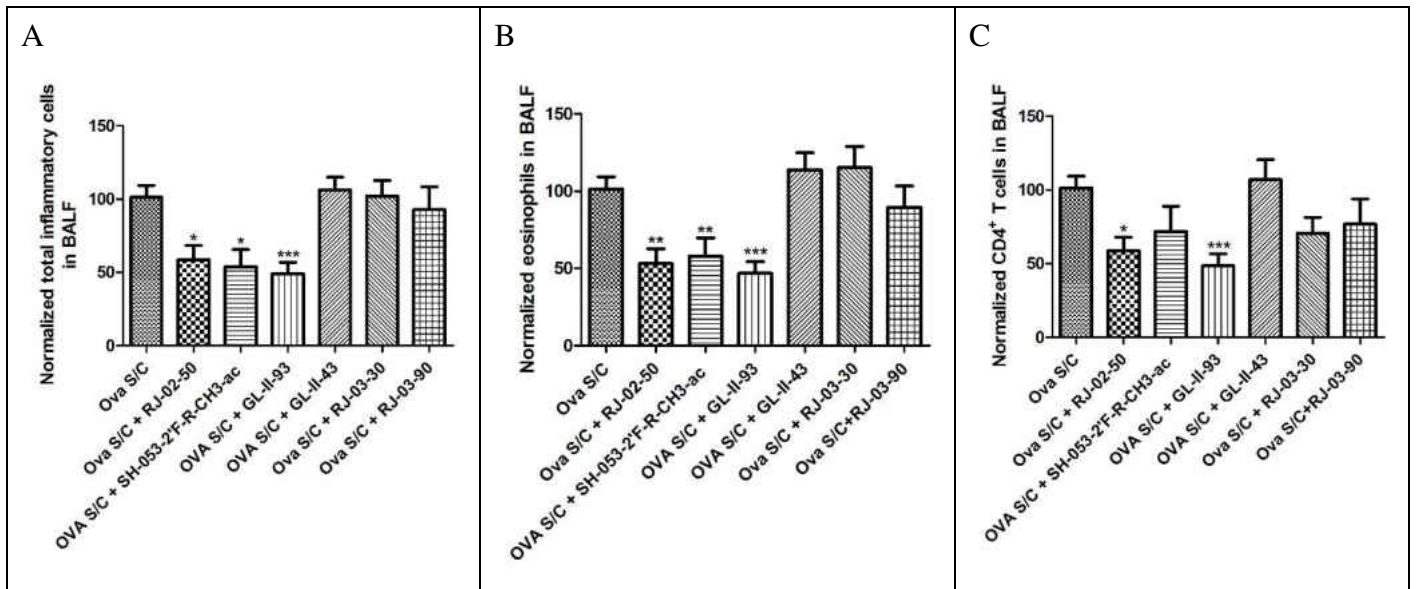
Figure A11. Effect of compounds on inflammatory cells. Groups of 10 ova s/c BALB/c mice were administered compounds at 100 mg/kg twice daily for 5 days. BALF was harvested from each animal and used for (A) quantification of total inflammatory cells; (B) eosinophils; (C) CD4$^+$ T cells. Cells were stained with mouse CD45$^+$ APC antibody, and samples were analyzed with BD FACS Calibur on high flow rate (60 μl/min) for 180 s. The gated positive events in the fourth

channel (FL4) were used to calculate the total inflammatory cell count as cells/ml. Quantification of specific leukocyte population (B) eosinophils (C) CD4$^+$ T cell populations were stained with specific antibodies and detected by flow cytometry. Data represent mean ± SEM from 10 mice in each group. *, **, and *** indicate $p < 0.05$, $p < 0.01$, and $p < 0.001$ significance, respectively, compared to vehicle treated ova s/c BALB/c mice. Compounds GL-II-43, RJ-03-30, RJ-03-90 did not modulated the numbers of inflammatory cells. However, RJ-02-50 and GL-II-93 did reduce the numbers of eosinophils and CD4$^+$ T cells in the asthmatic mouse lung. SH-053-2F'F-R-CH3-Acid reduced the numbers of eosinophils but not CD4$^+$ T cells.
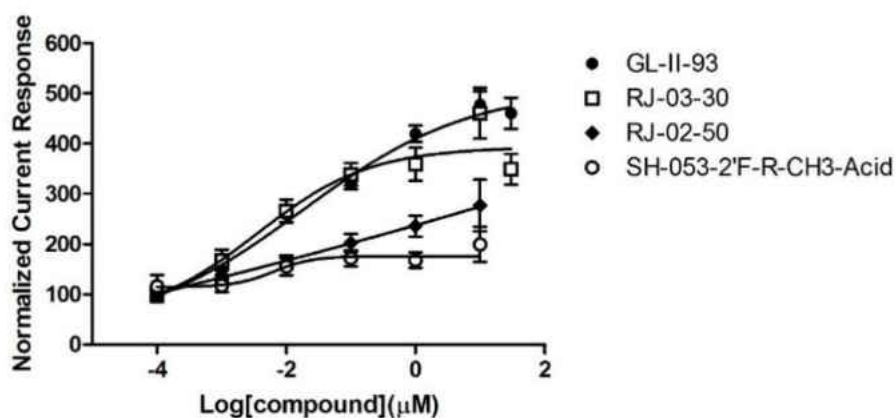
Figure A12. Current recordings in the presence of 600 nM GABA and increasing concentrations of compounds applied together for 3 s using CD4+ T-cells isolated from ova s/c BALB/c mice spleen. The concentration-dependent current responses of CD4+ T-cells in the presence of 600 nM GABA and increasing concentration of compounds were carried out with an N of 16 and normalized to the current response of 600 nM GABA. Compound RJ-02-50 potentiated the GABA-induced membrane current more than SH-053-2F'F-R-CH3-Acid. Importantly, GL-II-93 and RJ-03-30 evoked a very pronounced GABA-induced transmembrane current.
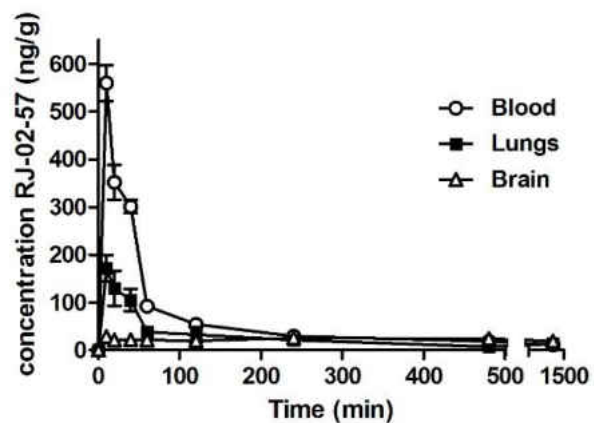
	Blood	Lung	Brain
t_{max} (min)	10	10	-
C_{max} (ng/g)	559.8	171.6	-
E_{rate} (min^{-1})	0.019	0.012	-
$t_{1/2}$ (min)	37.4	59.0	-
A_{rate} (min^{-1})	0.147	0.063	-
AUC$_{0-t}$ (ng*min/g)	47344	24584	-

Figure A13. Pharmacokinetic profile of tetrazole **31** in mice blood lungs, and brain. Time-dependent systemic distribution of compounds administered at 25 mg/kg via oral gavage. RJ-03-57 has a moderate absorption and fast clearance.
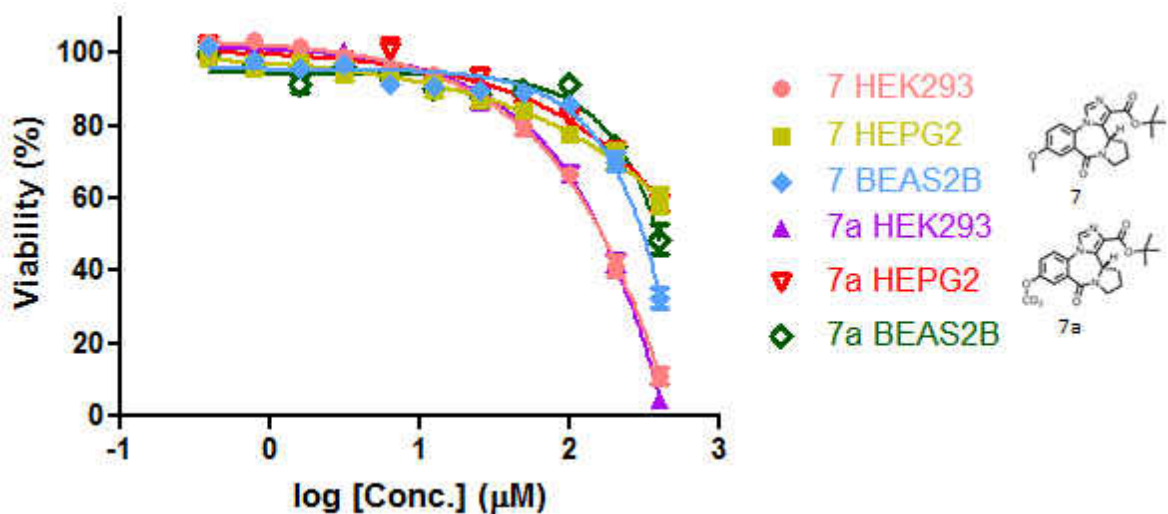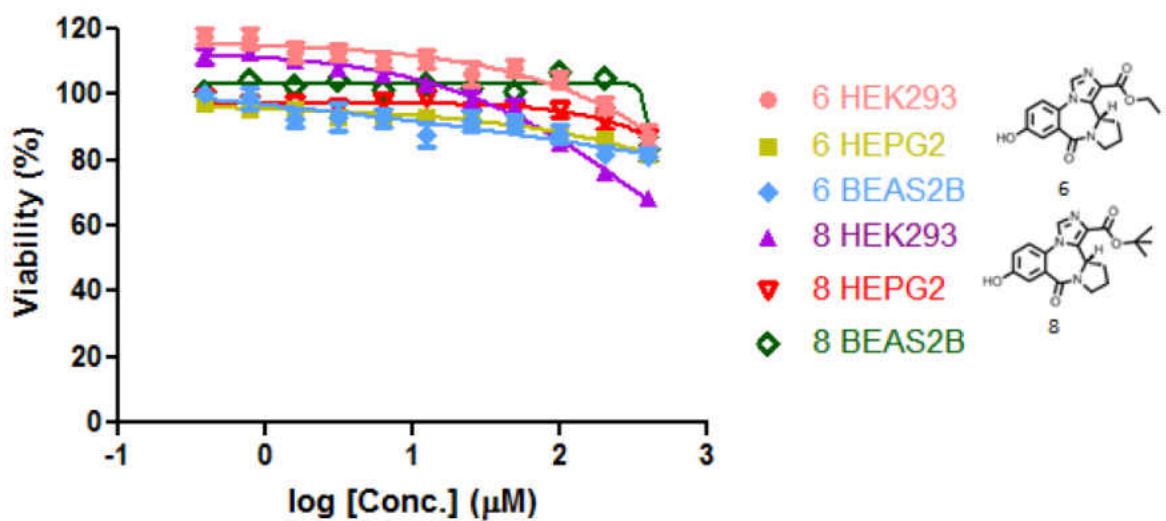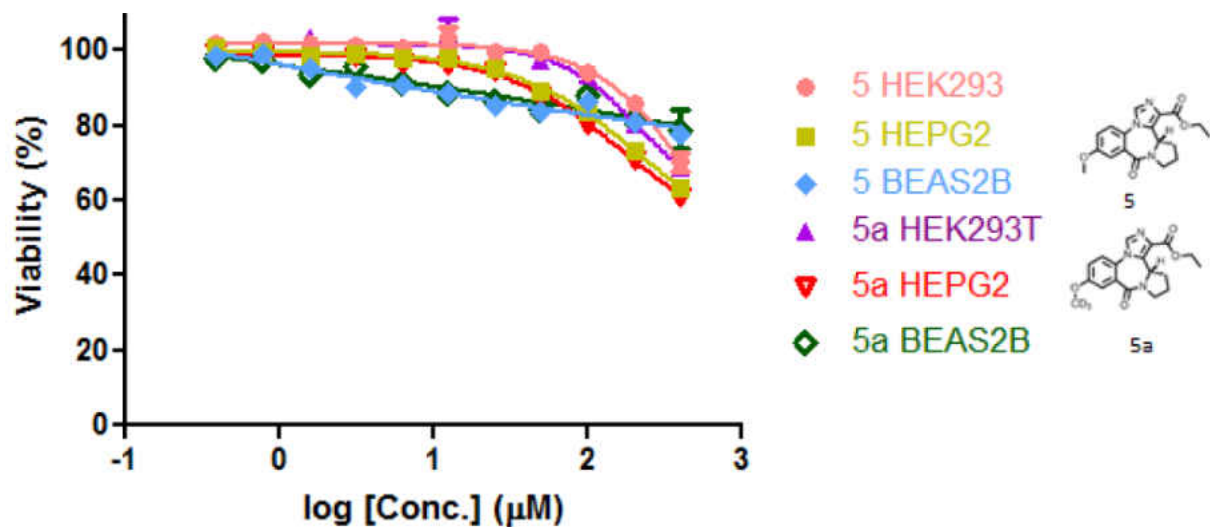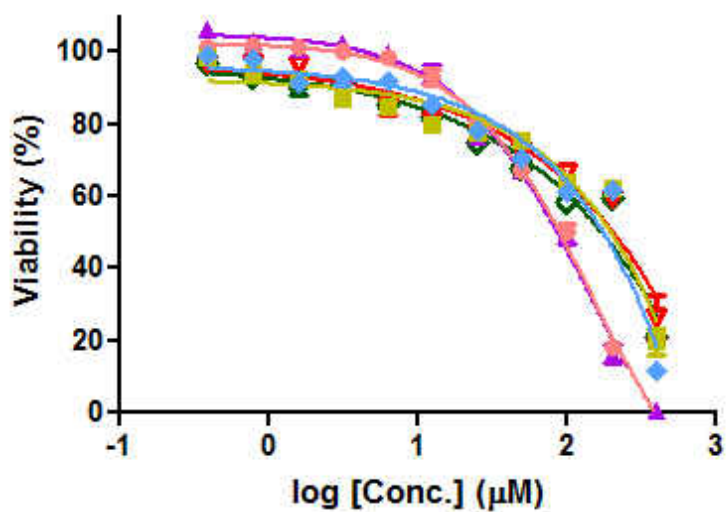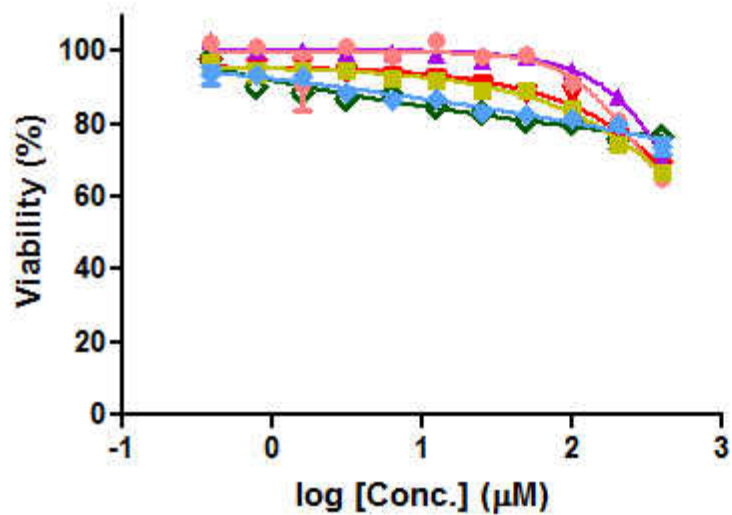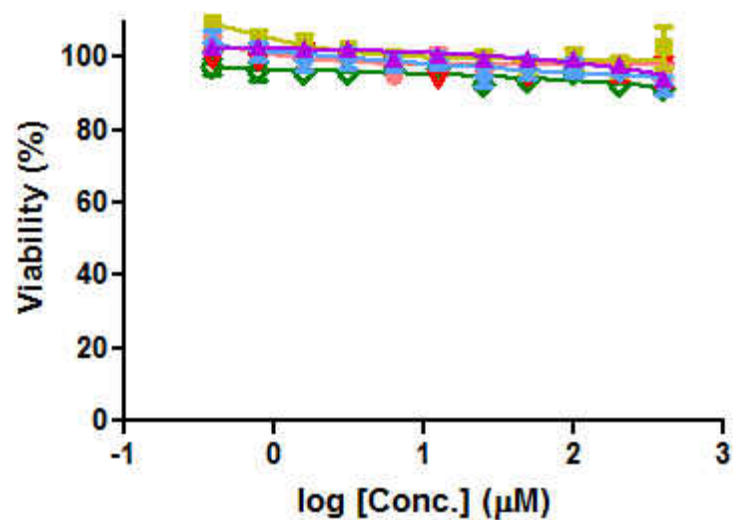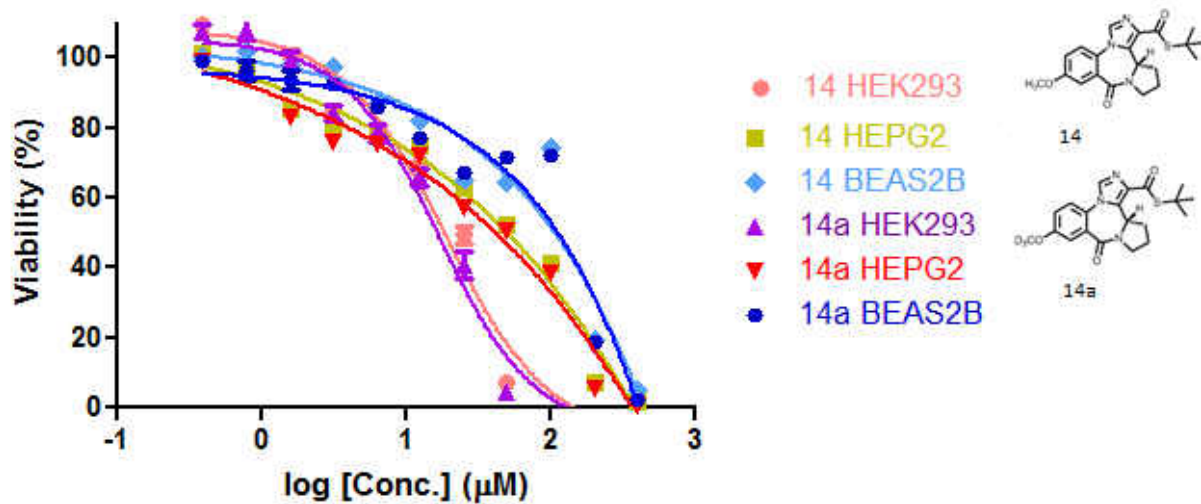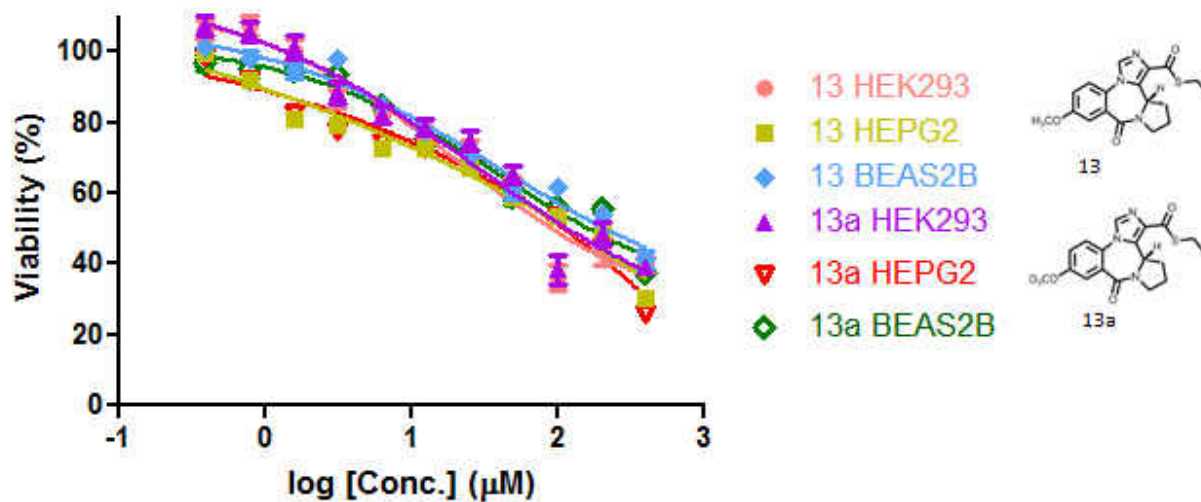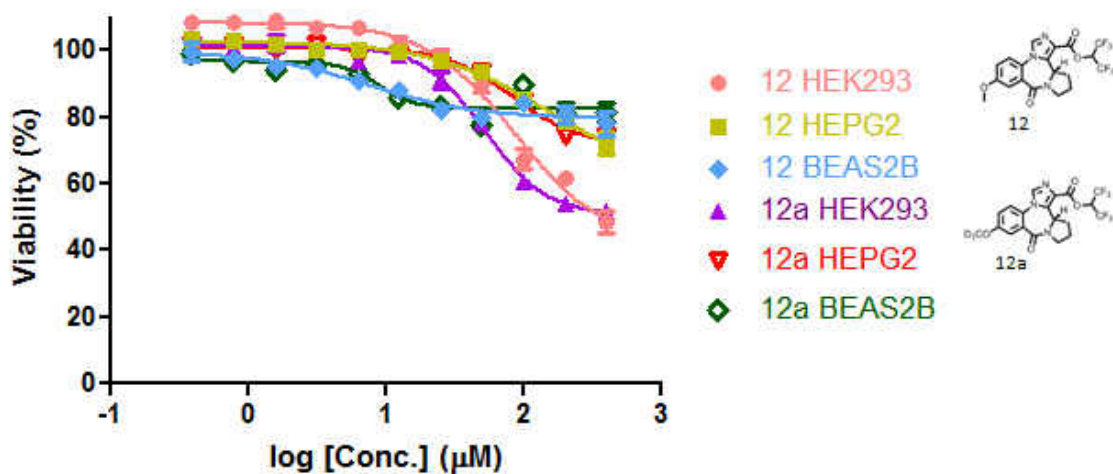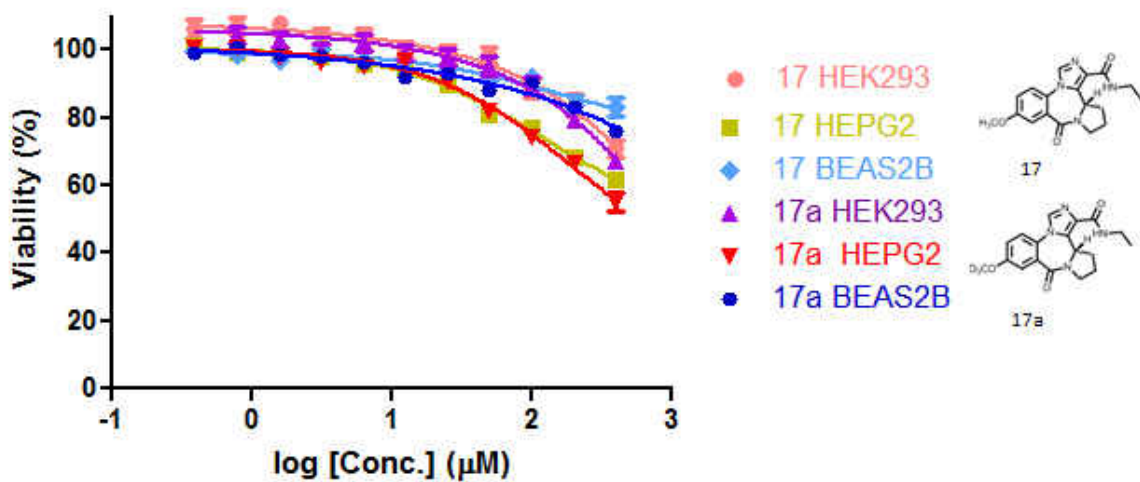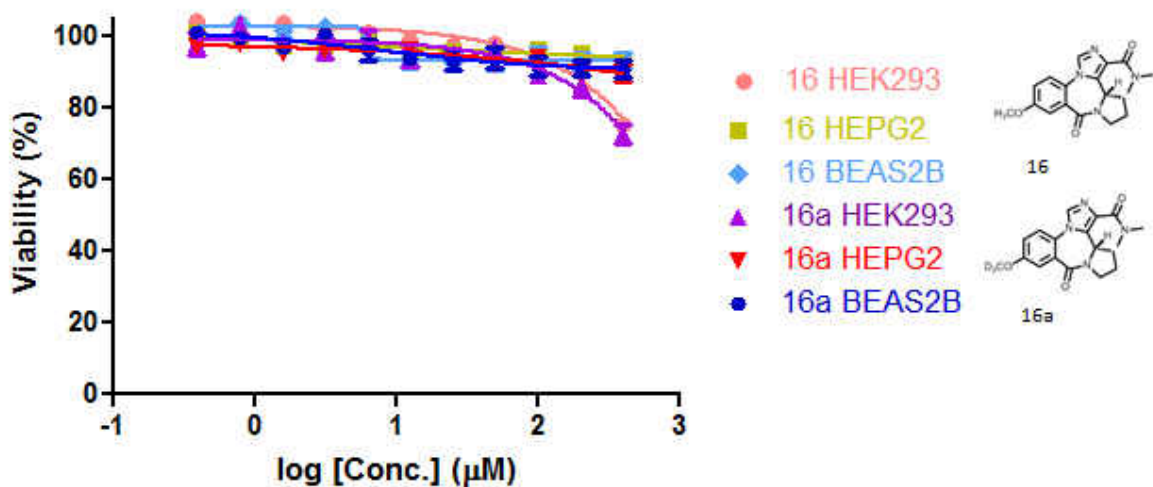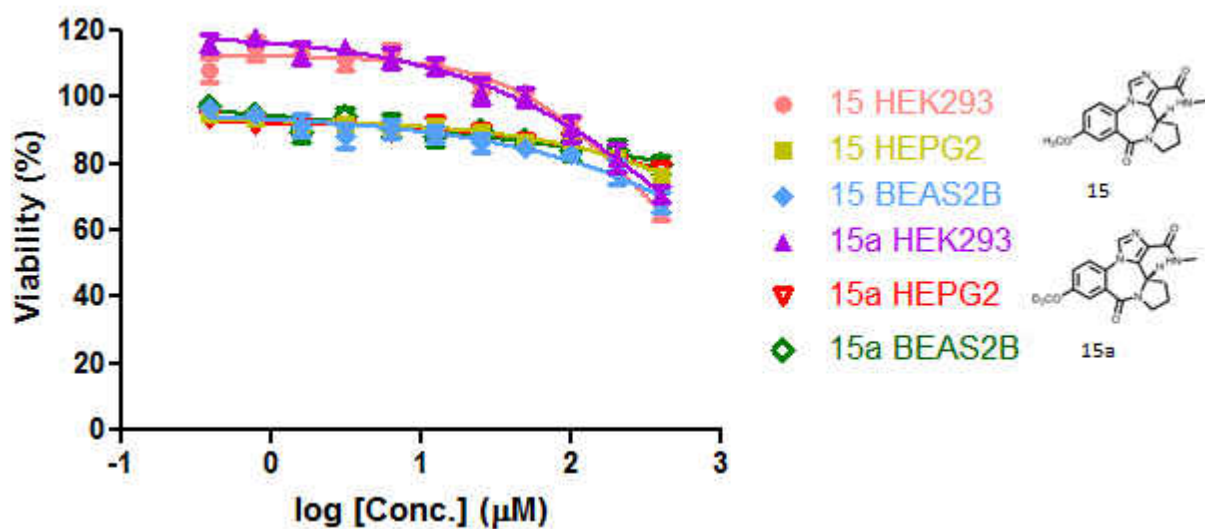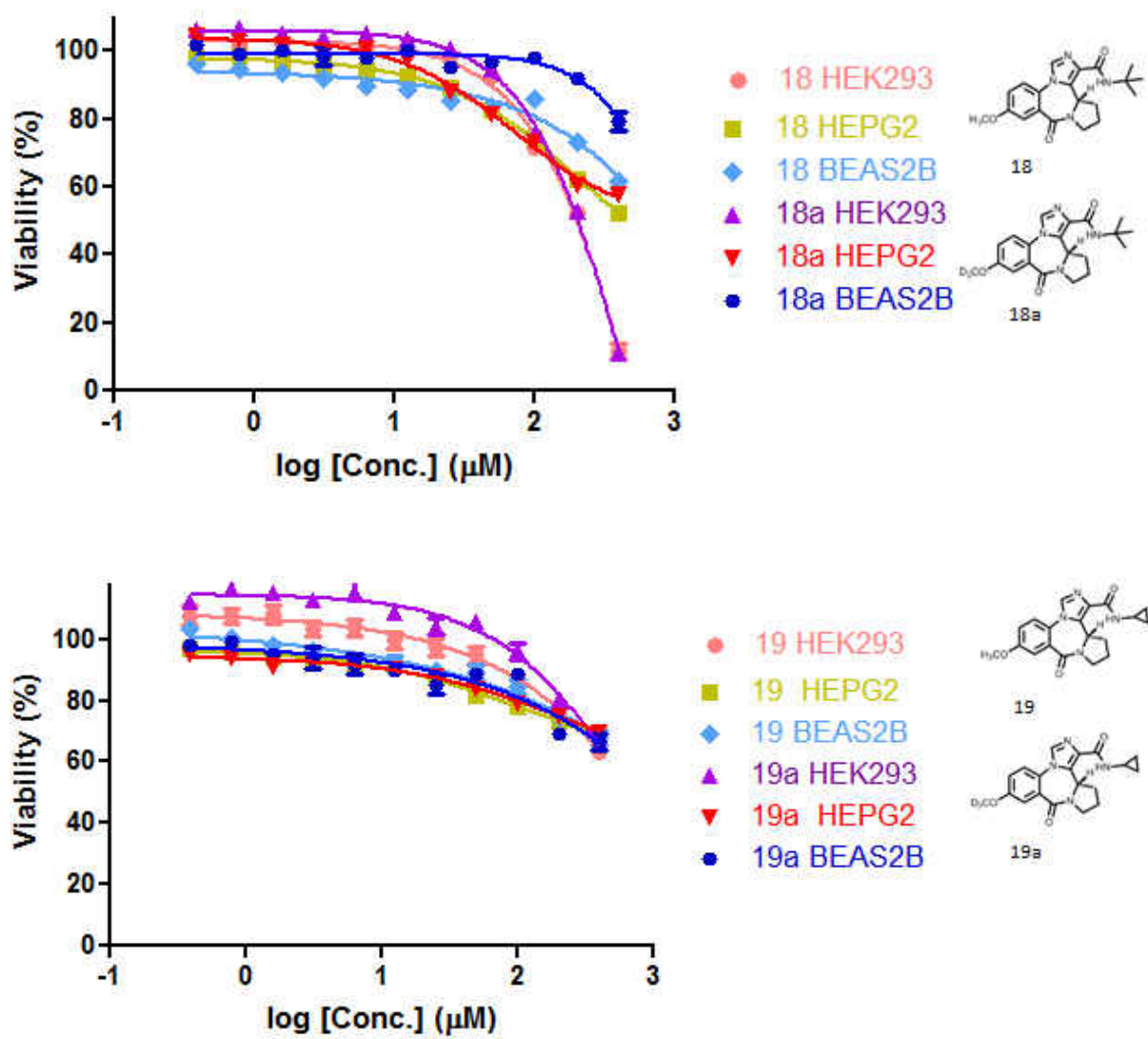
Figure A14. Cytotoxicity assay results of XHE-III-74 analogs on human liver hepatocellular carcinoma (HEPG2), human embryonic kidney 293T (HEK293T) and human bronchial epithelial (BEAS 2B) cell lines.

X-ray Crystal Data for XHE-III-74EE (*S* isomer), 5

Table A9. Crystal data and structure refinement for XHe-III-74EE **5**.

Identification code	cook115x
Empirical formula	$C_{18}H_{19}N_3O_4$
Formula weight	341.36
Temperature	150(2) K
Wavelength	1.54178 Å
Crystal system	Orthorhombic
Space group	$P2_12_12_1$
Unit cell dimensions	a = 8.8015(3) Å $\alpha = 90°$.
	b = 12.3627(5) Å $\beta = 90°$.
	c = 14.6328(5) Å $\gamma = 90°$.
Volume	1592.20(10) Å^3
Z	4
Density (-123ºC)	1.424 Mg/m^3
Absorption coefficient	0.846 mm^{-1}
F(000)	720
Crystal size	0.639 x 0.537 x 0.372 mm^3
θ range for data collection	4.682 to 68.183°.
Index ranges	-9<=h<=10, -14<=k<=14, -16<=l<=17
Reflections collected	9325
Independent reflections	2738 [R(int) = 0.2000]
Completeness to θ = 67.679°	98.1 %
Absorption correction	Semi-empirical from equivalents
Max. and min. transmission	0.7438 and 0.6141
Refinement method	Full-matrix least-squares on F^2
Data / restraints / parameters	2738 / 0 / 229
Goodness-of-fit on F^2	1.085
Final R indices [I>2σ(I)]	R1 = 0.0507, wR2 = 0.1390
R indices (all data)	R1 = 0.0508, wR2 = 0.1392
Absolute structure parameter	-0.1(3)
Extinction coefficient	0.022(2)
Largest diff. peak and hole	0.375 and -0.315 e.Å^{-3}

Table A10. Atomic coordinates (x 10^4) and equivalent isotropic displacement parameters (Å^2x 10^3) for **5**. U(eq) is defined as one third of the trace of the orthogonalized U^{ij} tensor.

	x	y	z	U(eq)
N(1)	9167(3)	5590(2)	4986(2)	21(1)
C(2)	8942(3)	5685(2)	5865(2)	21(1)
N(3)	8473(3)	6697(2)	6104(2)	19(1)
C(4)	8043(3)	7014(2)	7014(2)	20(1)
C(5)	7231(3)	6282(2)	7532(2)	20(1)
C(6)	6814(3)	6521(2)	8427(2)	22(1)
C(7)	7204(3)	7528(2)	8786(2)	21(1)
O(7)	6819(2)	7870(2)	9650(1)	28(1)
C(7A)	5844(4)	7188(3)	10161(2)	34(1)
C(8)	8046(3)	8252(2)	8271(2)	22(1)
C(9)	8479(3)	8008(2)	7382(2)	19(1)
C(10)	9481(3)	8813(2)	6907(2)	20(1)
O(10)	10460(2)	9317(2)	7336(1)	26(1)
N(11)	9259(2)	8968(2)	6009(2)	20(1)
C(12)	10175(3)	9740(2)	5477(2)	24(1)
C(13)	9608(3)	9573(3)	4507(2)	25(1)
C(14)	7944(3)	9253(2)	4650(2)	22(1)
C(15)	8008(3)	8489(2)	5463(2)	19(1)
C(16)	8381(3)	7301(2)	5310(2)	20(1)
C(17)	8810(3)	6598(2)	4624(2)	20(1)
C(18)	8915(3)	6674(2)	3612(2)	21(1)
O(18)	9603(3)	6028(2)	3153(1)	31(1)
O(19)	8143(2)	7511(2)	3267(1)	26(1)
C(20)	8162(4)	7610(3)	2279(2)	28(1)
C(21)	7671(4)	8745(3)	2049(2)	36(1)

Table A11. Bond lengths [Å] and angles [°] for **5**.

_____

N(1)-C(2)	1.306(4)	N(1)-C(17)	1.391(4)
C(2)-N(3)	1.363(4)	C(2)-H(2A)	0.9500
N(3)-C(16)	1.384(4)	N(3)-C(4)	1.440(4)
C(4)-C(5)	1.380(4)	C(4)-C(9)	1.395(4)
C(5)-C(6)	1.392(4)	C(5)-H(5A)	0.9500
C(6)-C(7)	1.394(4)	C(6)-H(6A)	0.9500
C(7)-O(7)	1.375(3)	C(7)-C(8)	1.385(4)
O(7)-C(7A)	1.417(4)	C(7A)-H(7AA)	0.9800
C(7A)-H(7AB)	0.9800	C(7A)-H(7AC)	0.9800
C(8)-C(9)	1.389(4)	C(8)-H(8A)	0.9500
C(9)-C(10)	1.500(4)	C(10)-O(10)	1.235(3)
C(10)-N(11)	1.341(4)	N(11)-C(12)	1.472(4)
N(11)-C(15)	1.484(3)	C(12)-C(13)	1.519(4)
C(12)-H(12A)	0.9900	C(12)-H(12B)	0.9900
C(13)-C(14)	1.532(4)	C(13)-H(13A)	0.9900
C(13)-H(13B)	0.9900	C(14)-C(15)	1.521(4)
C(14)-H(14A)	0.9900	C(14)-H(14B)	0.9900
C(15)-C(16)	1.521(4)	C(15)-H(15A)	1.0000
C(16)-C(17)	1.381(4)	C(17)-C(18)	1.487(4)
C(18)-O(18)	1.206(4)	C(18)-O(19)	1.336(4)
O(19)-C(20)	1.450(3)	C(20)-C(21)	1.506(5)
C(20)-H(20A)	0.9900	C(20)-H(20B)	0.9900
C(21)-H(21A)	0.9800	C(21)-H(21B)	0.9800
C(21)-H(21C)	0.9800		
C(2)-N(1)-C(17)	105.1(2)	N(1)-C(2)-N(3)	112.4(3)
N(1)-C(2)-H(2A)	123.8	N(3)-C(2)-H(2A)	123.8
C(2)-N(3)-C(16)	107.4(2)	C(2)-N(3)-C(4)	124.5(2)
C(16)-N(3)-C(4)	127.9(2)	C(5)-C(4)-C(9)	120.6(3)
C(5)-C(4)-N(3)	117.8(3)	C(9)-C(4)-N(3)	121.6(2)
C(4)-C(5)-C(6)	120.9(3)	C(4)-C(5)-H(5A)	119.5
C(6)-C(5)-H(5A)	119.5	C(5)-C(6)-C(7)	118.6(3)
C(5)-C(6)-H(6A)	120.7	C(7)-C(6)-H(6A)	120.7
O(7)-C(7)-C(8)	115.6(3)	O(7)-C(7)-C(6)	124.1(3)
C(8)-C(7)-C(6)	120.3(3)	C(7)-O(7)-C(7A)	116.8(2)
O(7)-C(7A)-H(7AA)	109.5	O(7)-C(7A)-H(7AB)	109.5
H(7AA)-C(7A)-H(7AB)	109.5	O(7)-C(7A)-H(7AC)	109.5
H(7AA)-C(7A)-H(7AC)	109.5	H(7AB)-C(7A)-H(7AC)	109.5
C(7)-C(8)-C(9)	121.0(3)	C(7)-C(8)-H(8A)	119.5
C(9)-C(8)-H(8A)	119.5	C(8)-C(9)-C(4)	118.5(3)
C(8)-C(9)-C(10)	116.8(2)	C(4)-C(9)-C(10)	124.6(3)
O(10)-C(10)-N(11)	121.8(3)	O(10)-C(10)-C(9)	120.6(2)
N(11)-C(10)-C(9)	117.6(2)	C(10)-N(11)-C(12)	122.1(2)
C(10)-N(11)-C(15)	125.3(2)	C(12)-N(11)-C(15)	112.4(2)
N(11)-C(12)-C(13)	103.1(2)	N(11)-C(12)-H(12A)	111.1
C(13)-C(12)-H(12A)	111.1	N(11)-C(12)-H(12B)	111.1
C(13)-C(12)-H(12B)	111.1	H(12A)-C(12)-H(12B)	109.1
C(12)-C(13)-C(14)	102.8(2)	C(12)-C(13)-H(13A)	111.2
C(14)-C(13)-H(13A)	111.2	C(12)-C(13)-H(13B)	111.2
C(14)-C(13)-H(13B)	111.2	H(13A)-C(13)-H(13B)	109.1
C(15)-C(14)-C(13)	103.4(2)	C(15)-C(14)-H(14A)	111.1
C(13)-C(14)-H(14A)	111.1	C(15)-C(14)-H(14B)	111.1
C(13)-C(14)-H(14B)	111.1	H(14A)-C(14)-H(14B)	109.0
N(11)-C(15)-C(14)	101.6(2)	N(11)-C(15)-C(16)	107.7(2)

Table A11. (continued).

_____

C(14)-C(15)-C(16)	119.5(2)	N(11)-C(15)-H(15A)	109.2
C(14)-C(15)-H(15A)	109.2	C(16)-C(15)-H(15A)	109.2
C(17)-C(16)-N(3)	104.7(2)	C(17)-C(16)-C(15)	140.7(3)
N(3)-C(16)-C(15)	114.2(2)	C(16)-C(17)-N(1)	110.4(2)
C(16)-C(17)-C(18)	134.6(3)	N(1)-C(17)-C(18)	115.0(3)
O(18)-C(18)-O(19)	123.9(2)	O(18)-C(18)-C(17)	122.9(3)
O(19)-C(18)-C(17)	113.2(2)	C(18)-O(19)-C(20)	115.9(2)
O(19)-C(20)-C(21)	107.4(3)	O(19)-C(20)-H(20A)	110.2
C(21)-C(20)-H(20A)	110.2	O(19)-C(20)-H(20B)	110.2
C(21)-C(20)-H(20B)	110.2	H(20A)-C(20)-H(20B)	108.5
C(20)-C(21)-H(21A)	109.5	C(20)-C(21)-H(21B)	109.5
H(21A)-C(21)-H(21B)	109.5	C(20)-C(21)-H(21C)	109.5
H(21A)-C(21)-H(21C)	109.5	H(21B)-C(21)-H(21C)	109.5

_____

Table A12. Anisotropic displacement parameters (Å^2x 10^3) for **5**. The anisotropic displacement factor exponent takes the form: $-2\pi^2[h^2a^{*2}U^{11} + ... + 2\,h\,k\,a^*\,b^*\,U^{12}]$

	U^{11}	U^{22}	U^{33}	U^{23}	U^{13}	U^{12}
N(1)	23(1)	14(1)	27(1)	-2(1)	-2(1)	2(1)
C(2)	25(1)	10(1)	27(1)	2(1)	-3(1)	2(1)
N(3)	21(1)	13(1)	22(1)	-1(1)	-2(1)	1(1)
C(4)	20(1)	16(1)	23(1)	3(1)	-2(1)	3(1)
C(5)	22(1)	12(1)	26(1)	1(1)	-4(1)	-2(1)
C(6)	22(1)	17(2)	26(1)	7(1)	0(1)	-2(1)
C(7)	23(1)	19(1)	23(1)	3(1)	1(1)	3(1)
O(7)	36(1)	21(1)	26(1)	-2(1)	8(1)	-4(1)
C(7A)	45(2)	24(2)	31(2)	-1(1)	8(1)	-9(1)
C(8)	24(1)	15(1)	26(1)	-2(1)	0(1)	1(1)
C(9)	19(1)	14(1)	24(1)	0(1)	-4(1)	0(1)
C(10)	20(1)	13(1)	26(1)	-7(1)	1(1)	2(1)
O(10)	27(1)	21(1)	29(1)	-1(1)	-3(1)	-9(1)
N(11)	20(1)	13(1)	27(1)	-1(1)	0(1)	-2(1)
C(12)	22(1)	16(1)	34(2)	4(1)	3(1)	-2(1)
C(13)	28(1)	17(1)	31(1)	5(1)	7(1)	1(1)
C(14)	24(1)	14(1)	28(1)	-2(1)	1(1)	4(1)
C(15)	17(1)	14(1)	27(1)	-2(1)	-1(1)	0(1)
C(16)	17(1)	17(1)	25(1)	0(1)	-2(1)	-1(1)
C(17)	17(1)	18(1)	25(1)	1(1)	-2(1)	-1(1)
C(18)	22(1)	14(1)	27(1)	-3(1)	-1(1)	-2(1)
O(18)	39(1)	27(1)	27(1)	-2(1)	4(1)	10(1)
O(19)	36(1)	21(1)	23(1)	-1(1)	-1(1)	6(1)
C(20)	33(2)	27(2)	24(1)	1(1)	0(1)	-2(1)
C(21)	45(2)	30(2)	32(2)	6(2)	-4(1)	1(2)

Table A13. Hydrogen coordinates (x 10^4) and isotropic displacement parameters ($Å^2$x 10^3) for **5**

	x	y	z	U(eq)
H(2A)	9089	5113	6289	25
H(5A)	6953	5605	7274	24
H(6A)	6274	6009	8786	26
H(7AA)	5649	7515	10760	50
H(7AB)	6327	6481	10243	50
H(7AC)	4882	7097	9833	50
H(8A)	8332	8927	8530	26
H(12A)	11272	9573	5527	29
H(12B)	9998	10492	5683	29
H(13A)	10181	8990	4195	31
H(13B)	9692	10246	4144	31
H(14A)	7310	9894	4787	27
H(14B)	7531	8883	4103	27
H(15A)	7037	8545	5815	23
H(20A)	7458	7079	2001	34
H(20B)	9197	7472	2041	34
H(21A)	7713	8849	1385	54
H(21B)	8352	9263	2348	54
H(21C)	6629	8861	2263	54

Table A14. Torsion angles [°] for **5**.

_____

C(17)-N(1)-C(2)-N(3)	-0.6(3)	N(1)-C(2)-N(3)-C(16)	0.4(3)
N(1)-C(2)-N(3)-C(4)	175.7(2)	C(2)-N(3)-C(4)-C(5)	-38.7(4)
C(16)-N(3)-C(4)-C(5)	135.6(3)	C(2)-N(3)-C(4)-C(9)	138.7(3)
C(16)-N(3)-C(4)-C(9)	-47.0(4)	C(9)-C(4)-C(5)-C(6)	0.7(4)
N(3)-C(4)-C(5)-C(6)	178.2(2)	C(4)-C(5)-C(6)-C(7)	1.4(4)
C(5)-C(6)-C(7)-O(7)	178.1(3)	C(5)-C(6)-C(7)-C(8)	-2.7(4)
C(8)-C(7)-O(7)-C(7A)	174.5(3)	C(6)-C(7)-O(7)-C(7A)	-6.3(4)
O(7)-C(7)-C(8)-C(9)	-178.8(2)	C(6)-C(7)-C(8)-C(9)	2.0(4)
C(7)-C(8)-C(9)-C(4)	0.2(4)	C(7)-C(8)-C(9)-C(10)	-175.8(2)
C(5)-C(4)-C(9)-C(8)	-1.5(4)	N(3)-C(4)-C(9)-C(8)	-178.9(2)
C(5)-C(4)-C(9)-C(10)	174.1(2)	N(3)-C(4)-C(9)-C(10)	-3.2(4)
C(8)-C(9)-C(10)-O(10)	35.6(4)	C(4)-C(9)-C(10)-O(10)	-140.1(3)
C(8)-C(9)-C(10)-N(11)	-143.6(2)	C(4)-C(9)-C(10)-N(11)	40.7(4)
O(10)-C(10)-N(11)-C(12)	0.6(4)	C(9)-C(10)-N(11)-C(12)	179.9(2)
O(10)-C(10)-N(11)-C(15)	-173.0(2)	C(9)-C(10)-N(11)-C(15)	6.2(4)
C(10)-N(11)-C(12)-C(13)	175.7(3)	C(15)-N(11)-C(12)-C(13)	-9.9(3)
N(11)-C(12)-C(13)-C(14)	31.0(3)	C(12)-C(13)-C(14)-C(15)	-41.5(3)
C(10)-N(11)-C(15)-C(14)	158.6(3)	C(12)-N(11)-C(15)-C(14)	-15.6(3)
C(10)-N(11)-C(15)-C(16)	-75.0(3)	C(12)-N(11)-C(15)-C(16)	110.8(3)
C(13)-C(14)-C(15)-N(11)	34.4(3)	C(13)-C(14)-C(15)-C(16)	-83.8(3)
C(2)-N(3)-C(16)-C(17)	0.1(3)	C(4)-N(3)-C(16)-C(17)	-175.1(3)
C(2)-N(3)-C(16)-C(15)	-174.7(2)	C(4)-N(3)-C(16)-C(15)	10.1(4)
N(11)-C(15)-C(16)-C(17)	-109.8(4)	C(14)-C(15)-C(16)-C(17)	5.2(5)
N(11)-C(15)-C(16)-N(3)	62.2(3)	C(14)-C(15)-C(16)-N(3)	177.3(2)
N(3)-C(16)-C(17)-N(1)	-0.4(3)	C(15)-C(16)-C(17)-N(1)	172.1(3)
N(3)-C(16)-C(17)-C(18)	177.0(3)	C(15)-C(16)-C(17)-C(18)	-10.5(6)
C(2)-N(1)-C(17)-C(16)	0.6(3)	C(2)-N(1)-C(17)-C(18)	-177.3(2)
C(16)-C(17)-C(18)-O(18)	164.8(3)	N(1)-C(17)-C(18)-O(18)	-17.9(4)
C(16)-C(17)-C(18)-O(19)	-16.6(4)	N(1)-C(17)-C(18)-O(19)	160.7(2)
O(18)-C(18)-O(19)-C(20)	0.4(4)	C(17)-C(18)-O(19)-C(20)	-178.2(2)
C(18)-O(19)-C(20)-C(21)	-163.0(2)		

_____

Table A15. Hydrogen bonds for **5** [Å and °].

_____

D-H...A	d(D-H)	d(H...A)	d(D...A)	<(DHA)
C(2)-H(2A)...O(10)#1	0.95	2.27	3.173(3)	157.5
C(6)-H(6A)...N(1)#2	0.95	2.67	3.573(4)	158.3
C(7A)-H(7AB)...N(1)#2	0.98	2.62	3.445(4)	141.3
C(12)-H(12A)...N(1)#3	0.99	2.66	3.602(4)	158.1
C(14)-H(14B)...O(19)	0.99	2.16	2.960(4)	136.7
C(20)-H(20A)...O(10)#4	0.99	2.65	3.413(4)	134.2

_____

Symmetry transformations used to generate equivalent atoms:
#1 -x+2,y-1/2,-z+3/2   #2 -x+3/2,-y+1,z+1/2   #3 x+1/2,-y+3/2,-z+1
#4 x-1/2,-y+3/2,-z+1

X-ray Crystal Data for XHE-III-74EE (*R* isomer), 5′

Table A16. Crystal data and structure refinement for **5′** (RJ-01-17).

Identification code	cook129
Empirical formula	$C_{18}H_{19}N_3O_4$
Formula weight	341.36
Temperature	150(2) K
Wavelength	0.71073 Å
Crystal system	Orthorhombic
Space group	$P2_12_12_1$
Unit cell dimensions	a = 8.8045(5) Å $\alpha = 90°$.
	b = 12.3701(9) Å $\beta = 90°$.
	c = 14.6254(10) Å $\gamma = 90°$.
Volume	1592.89(18) $Å^3$
Z	4
Density (-123ºC)	1.423 Mg/m^3
Absorption coefficient	0.102 mm^{-1}
F(000)	720
Crystal size	0.465 x 0.279 x 0.156 mm^3
θ range for data collection	2.156 to 29.131°.
Index ranges	-10<=h<=12, -16<=k<=16, -20<=l<=18
Reflections collected	14196
Independent reflections	4250 [R(int) = 0.0327]
Completeness to θ = 25.000°	99.9 %
Refinement method	Full-matrix least-squares on F^2
Data / restraints / parameters	4250 / 0 / 228
Goodness-of-fit on F^2	0.997
Final R indices [I>2σ(I)]	R1 = 0.0314, wR2 = 0.0729
R indices (all data)	R1 = 0.0355, wR2 = 0.0749
Absolute structure parameter	0.3(3)
Largest diff. peak and hole	0.255 and -0.199 e.$Å^{-3}$

Table A17. Atomic coordinates (x 10^4) and equivalent isotropic displacement parameters (Å^2x 10^3) for **5′**. U(eq) is defined as one third of the trace of the orthogonalized U^{ij} tensor.

	x	y	z	U(eq)
N(1)	1523(2)	3304(1)	8896(1)	15(1)
C(2)	1052(2)	4319(1)	9134(1)	17(1)
N(3)	831(2)	4410(1)	10014(1)	18(1)
C(4)	1185(2)	3401(1)	10378(1)	16(1)
C(5)	1616(2)	2696(1)	9693(1)	14(1)
C(6)	1993(2)	1514(1)	9537(1)	15(1)
C(7)	2054(2)	745(1)	10353(1)	18(1)
C(8)	395(2)	429(1)	10500(1)	22(1)
C(9)	-175(2)	261(1)	9524(1)	20(1)
N(10)	741(2)	1033(1)	8993(1)	16(1)
C(11)	518(2)	1185(1)	8094(1)	16(1)
O(11)	-458(1)	681(1)	7665(1)	22(1)
C(12)	1518(2)	1988(1)	7618(1)	15(1)
C(13)	1953(2)	1746(1)	6730(1)	18(1)
C(14)	2796(2)	2471(1)	6213(1)	17(1)
O(14)	3181(2)	2130(1)	5351(1)	24(1)
C(14A)	4155(2)	2814(1)	4840(1)	31(1)
C(15)	3185(2)	3478(1)	6572(1)	18(1)
C(16)	2769(2)	3720(1)	7464(1)	16(1)
C(17)	1955(2)	2988(1)	7990(1)	15(1)
O(18)	400(2)	3971(1)	11848(1)	28(1)
C(18)	1085(2)	3324(1)	11386(1)	17(1)
O(19)	1856(2)	2490(1)	11733(1)	23(1)
C(20)	1839(2)	2388(1)	12722(1)	24(1)
C(21)	2337(3)	1252(2)	12953(1)	32(1)

Table A18. Bond lengths [Å] and angles [°] for **5′**.

_____

N(1)-C(2)	1.3676(18)	N(1)-C(5)	1.3888(18)
N(1)-C(17)	1.4330(19)	C(2)-N(3)	1.306(2)
C(2)-H(2A)	0.9500	N(3)-C(4)	1.3924(19)
C(4)-C(5)	1.382(2)	C(4)-C(18)	1.480(2)
C(5)-C(6)	1.5158(19)	C(6)-N(10)	1.4843(19)
C(6)-C(7)	1.528(2)	C(6)-H(6A)	1.0000
C(7)-C(8)	1.527(2)	C(7)-H(7A)	0.9900
C(7)-H(7B)	0.9900	C(8)-C(9)	1.527(2)
C(8)-H(8A)	0.9900	C(8)-H(8B)	0.9900
C(9)-N(10)	1.4713(19)	C(9)-H(9A)	0.9900
C(9)-H(9B)	0.9900	N(10)-C(11)	1.3416(19)
C(11)-O(11)	1.2333(18)	C(11)-C(12)	1.499(2)
C(12)-C(13)	1.387(2)	C(12)-C(17)	1.4045(19)
C(13)-C(14)	1.389(2)	C(13)-H(13A)	0.9500
C(14)-O(14)	1.3707(18)	C(14)-C(15)	1.394(2)
O(14)-C(14A)	1.417(2)	C(14A)-H(14A)	0.9800
C(14A)-H(14B)	0.9800	C(14A)-H(14C)	0.9800
C(15)-C(16)	1.387(2)	C(15)-H(15A)	0.9500
C(16)-C(17)	1.388(2)	C(16)-H(16A)	0.9500
O(18)-C(18)	1.2089(19)	C(18)-O(19)	1.3350(19)
O(19)-C(20)	1.4513(17)	C(20)-C(21)	1.510(2)
C(20)-H(20A)	0.9900	C(20)-H(20B)	0.9900
C(21)-H(21A)	0.9800	C(21)-H(21B)	0.9800
C(21)-H(21C)	0.9800		
C(2)-N(1)-C(5)	107.60(12)	C(2)-N(1)-C(17)	124.48(12)
C(5)-N(1)-C(17)	127.72(12)	N(3)-C(2)-N(1)	111.98(13)
N(3)-C(2)-H(2A)	124.0	N(1)-C(2)-H(2A)	124.0
C(2)-N(3)-C(4)	105.45(12)	C(5)-C(4)-N(3)	110.50(13)
C(5)-C(4)-C(18)	134.28(14)	N(3)-C(4)-C(18)	115.16(13)
C(4)-C(5)-N(1)	104.47(12)	C(4)-C(5)-C(6)	141.07(14)
N(1)-C(5)-C(6)	114.14(12)	N(10)-C(6)-C(5)	107.74(12)
N(10)-C(6)-C(7)	101.26(11)	C(5)-C(6)-C(7)	119.38(12)
N(10)-C(6)-H(6A)	109.3	C(5)-C(6)-H(6A)	109.3
C(7)-C(6)-H(6A)	109.3	C(8)-C(7)-C(6)	103.63(12)
C(8)-C(7)-H(7A)	111.0	C(6)-C(7)-H(7A)	111.0
C(8)-C(7)-H(7B)	111.0	C(6)-C(7)-H(7B)	111.0
H(7A)-C(7)-H(7B)	109.0	C(9)-C(8)-C(7)	102.58(13)
C(9)-C(8)-H(8A)	111.3	C(7)-C(8)-H(8A)	111.3
C(9)-C(8)-H(8B)	111.3	C(7)-C(8)-H(8B)	111.3
H(8A)-C(8)-H(8B)	109.2	N(10)-C(9)-C(8)	103.04(13)
N(10)-C(9)-H(9A)	111.2	C(8)-C(9)-H(9A)	111.2
N(10)-C(9)-H(9B)	111.2	C(8)-C(9)-H(9B)	111.2
H(9A)-C(9)-H(9B)	109.1	C(11)-N(10)-C(9)	121.85(13)
C(11)-N(10)-C(6)	125.27(13)	C(9)-N(10)-C(6)	112.59(12)
O(11)-C(11)-N(10)	122.02(14)	O(11)-C(11)-C(12)	120.50(14)
N(10)-C(11)-C(12)	117.48(13)	C(13)-C(12)-C(17)	118.49(14)
C(13)-C(12)-C(11)	116.99(13)	C(17)-C(12)-C(11)	124.39(14)
C(12)-C(13)-C(14)	121.24(13)	C(12)-C(13)-H(13A)	119.4
C(14)-C(13)-H(13A)	119.4	O(14)-C(14)-C(13)	115.75(13)
O(14)-C(14)-C(15)	124.09(14)	C(13)-C(14)-C(15)	120.16(14)
C(14)-O(14)-C(14A)	116.83(12)	O(14)-C(14A)-H(14A)	109.5
O(14)-C(14A)-H(14B)	109.5	H(14A)-C(14A)-H(14B)	109.5
O(14)-C(14A)-H(14C)	109.5	H(14A)-C(14A)-H(14C)	109.5

Table A18. (continued).

_____

H(14B)-C(14A)-H(14C)	109.5	C(16)-C(15)-C(14)	118.88(14)
C(16)-C(15)-H(15A)	120.6	C(14)-C(15)-H(15A)	120.6
C(15)-C(16)-C(17)	121.09(13)	C(15)-C(16)-H(16A)	119.5
C(17)-C(16)-H(16A)	119.5	C(16)-C(17)-C(12)	120.08(14)
C(16)-C(17)-N(1)	118.14(12)	C(12)-C(17)-N(1)	121.72(13)
O(18)-C(18)-O(19)	123.49(14)	O(18)-C(18)-C(4)	122.99(14)
O(19)-C(18)-C(4)	113.50(13)	C(18)-O(19)-C(20)	116.18(12)
O(19)-C(20)-C(21)	107.53(13)	O(19)-C(20)-H(20A)	110.2
C(21)-C(20)-H(20A)	110.2	O(19)-C(20)-H(20B)	110.2
C(21)-C(20)-H(20B)	110.2	H(20A)-C(20)-H(20B)	108.5
C(20)-C(21)-H(21A)	109.5	C(20)-C(21)-H(21B)	109.5
H(21A)-C(21)-H(21B)	109.5	C(20)-C(21)-H(21C)	109.5
H(21A)-C(21)-H(21C)	109.5	H(21B)-C(21)-H(21C)	109.5

_____

Table A19. Anisotropic displacement parameters ($\text{Å}^2 \times 10^3$) for **5′**. The anisotropic displacement factor exponent takes the form: $-2\pi^2[h^2a^{*2}U^{11} + ... + 2\,h\,k\,a^*\,b^*\,U^{12}]$

	U^{11}	U^{22}	U^{33}	U^{23}	U^{13}	U^{12}
N(1)	19(1)	13(1)	13(1)	0(1)	-2(1)	1(1)
C(2)	21(1)	14(1)	17(1)	0(1)	-3(1)	1(1)
N(3)	22(1)	15(1)	17(1)	-1(1)	-3(1)	2(1)
C(4)	16(1)	15(1)	16(1)	0(1)	-3(1)	-1(1)
C(5)	14(1)	14(1)	14(1)	2(1)	-2(1)	-1(1)
C(6)	15(1)	14(1)	15(1)	0(1)	-1(1)	1(1)
C(7)	24(1)	14(1)	16(1)	2(1)	0(1)	3(1)
C(8)	27(1)	18(1)	20(1)	4(1)	6(1)	2(1)
C(9)	19(1)	17(1)	23(1)	2(1)	5(1)	-1(1)
N(10)	17(1)	14(1)	16(1)	1(1)	0(1)	-3(1)
C(11)	17(1)	13(1)	17(1)	-3(1)	1(1)	1(1)
O(11)	24(1)	22(1)	20(1)	-4(1)	-3(1)	-7(1)
C(12)	16(1)	14(1)	15(1)	1(1)	-3(1)	0(1)
C(13)	20(1)	16(1)	18(1)	-2(1)	-2(1)	1(1)
C(14)	21(1)	17(1)	13(1)	0(1)	0(1)	2(1)
O(14)	34(1)	21(1)	16(1)	-3(1)	8(1)	-3(1)
C(14A)	43(1)	27(1)	21(1)	0(1)	10(1)	-9(1)
C(15)	21(1)	16(1)	16(1)	4(1)	-1(1)	0(1)
C(16)	20(1)	13(1)	17(1)	1(1)	-3(1)	-1(1)
C(17)	17(1)	15(1)	13(1)	-1(1)	-2(1)	1(1)
O(18)	36(1)	28(1)	19(1)	-2(1)	3(1)	10(1)
C(18)	18(1)	17(1)	17(1)	-1(1)	-1(1)	-3(1)
O(19)	33(1)	23(1)	13(1)	1(1)	-1(1)	6(1)
C(20)	31(1)	26(1)	13(1)	2(1)	-1(1)	-2(1)
C(21)	44(1)	30(1)	22(1)	7(1)	-4(1)	3(1)

Table A20. Hydrogen coordinates (x 10^4) and isotropic displacement parameters (Å^2x 10^3) for **5′**.

	x	y	z	U(eq)
H(2A)	902	4890	8709	21
H(6A)	2963	1459	9184	18
H(7A)	2684	103	10214	22
H(7B)	2472	1111	10900	22
H(8A)	311	-245	10862	26
H(8B)	-174	1012	10811	26
H(9A)	3	-490	9317	24
H(9B)	-1272	428	9474	24
H(13A)	1668	1072	6471	21
H(14A)	4407	2465	4258	46
H(14B)	5088	2946	5187	46
H(14C)	3641	3502	4721	46
H(15A)	3725	3989	6212	21
H(16A)	3047	4398	7718	20
H(20A)	803	2523	12960	28
H(20B)	2539	2920	13000	28
H(21A)	2338	1158	13619	48
H(21B)	3363	1128	12715	48
H(21C)	1633	733	12676	48

Table A21. Torsion angles [°] for **5′**.

C(5)-N(1)-C(2)-N(3)	-0.17(18)	C(17)-N(1)-C(2)-N(3)	-175.44(14)
N(1)-C(2)-N(3)-C(4)	0.34(19)	C(2)-N(3)-C(4)-C(5)	-0.39(19)
C(2)-N(3)-C(4)-C(18)	177.28(13)	N(3)-C(4)-C(5)-N(1)	0.28(17)
C(18)-C(4)-C(5)-N(1)	-176.76(16)	N(3)-C(4)-C(5)-C(6)	-172.35(18)
C(18)-C(4)-C(5)-C(6)	10.6(3)	C(2)-N(1)-C(5)-C(4)	-0.07(16)
C(17)-N(1)-C(5)-C(4)	175.00(15)	C(2)-N(1)-C(5)-C(6)	174.86(13)
C(17)-N(1)-C(5)-C(6)	-10.1(2)	C(4)-C(5)-C(6)-N(10)	109.6(2)
N(1)-C(5)-C(6)-N(10)	-62.57(16)	C(4)-C(5)-C(6)-C(7)	-4.9(3)
N(1)-C(5)-C(6)-C(7)	-177.11(13)	N(10)-C(6)-C(7)-C(8)	-34.66(14)
C(5)-C(6)-C(7)-C(8)	83.28(15)	C(6)-C(7)-C(8)-C(9)	41.62(14)
C(7)-C(8)-C(9)-N(10)	-31.17(14)	C(8)-C(9)-N(10)-C(11)	-175.94(13)
C(8)-C(9)-N(10)-C(6)	9.86(16)	C(5)-C(6)-N(10)-C(11)	75.46(17)
C(7)-C(6)-N(10)-C(11)	-158.45(13)	C(5)-C(6)-N(10)-C(9)	-110.57(13)
C(7)-C(6)-N(10)-C(9)	15.51(15)	C(9)-N(10)-C(11)-O(11)	-0.4(2)
C(6)-N(10)-C(11)-O(11)	173.00(14)	C(9)-N(10)-C(11)-C(12)	-179.81(13)
C(6)-N(10)-C(11)-C(12)	-6.4(2)	O(11)-C(11)-C(12)-C(13)	-35.6(2)
N(10)-C(11)-C(12)-C(13)	143.75(14)	O(11)-C(11)-C(12)-C(17)	140.14(16)
N(10)-C(11)-C(12)-C(17)	-40.5(2)	C(17)-C(12)-C(13)-C(14)	-0.2(2)
C(11)-C(12)-C(13)-C(14)	175.81(14)	C(12)-C(13)-C(14)-O(14)	178.75(14)
C(12)-C(13)-C(14)-C(15)	-2.0(2)	C(13)-C(14)-O(14)-C(14A)	-174.56(15)
C(15)-C(14)-O(14)-C(14A)	6.2(2)	O(14)-C(14)-C(15)-C(16)	-178.11(14)
C(13)-C(14)-C(15)-C(16)	2.7(2)	C(14)-C(15)-C(16)-C(17)	-1.2(2)
C(15)-C(16)-C(17)-C(12)	-0.9(2)	C(15)-C(16)-C(17)-N(1)	-178.11(14)
C(13)-C(12)-C(17)-C(16)	1.7(2)	C(11)-C(12)-C(17)-C(16)	-174.05(15)
C(13)-C(12)-C(17)-N(1)	178.72(14)	C(11)-C(12)-C(17)-N(1)	3.0(2)
C(2)-N(1)-C(17)-C(16)	38.5(2)	C(5)-N(1)-C(17)-C(16)	-135.76(16)
C(2)-N(1)-C(17)-C(12)	-138.58(16)	C(5)-N(1)-C(17)-C(12)	47.1(2)
C(5)-C(4)-C(18)-O(18)	-165.19(17)	N(3)-C(4)-C(18)-O(18)	17.9(2)
C(5)-C(4)-C(18)-O(19)	16.5(3)	N(3)-C(4)-C(18)-O(19)	-160.49(14)
O(18)-C(18)-O(19)-C(20)	0.0(2)	C(4)-C(18)-O(19)-C(20)	178.31(13)
C(18)-O(19)-C(20)-C(21)	163.09(15)		

Table A22. Hydrogen bonds for **5′** [Å and °].

D-H...A	d(D-H)	d(H...A)	d(D...A)	<(DHA)
C(2)-H(2A)...O(11)#1	0.95	2.27	3.1672(19)	157.5
C(7)-H(7B)...O(19)	0.99	2.17	2.9608(18)	136.3
C(9)-H(9B)...N(3)#2	0.99	2.67	3.604(2)	158.2
C(14A)-H(14C)...N(3)#3	0.98	2.66	3.444(2)	137.3
C(15)-H(15A)...N(3)#3	0.95	2.67	3.5742(19)	158.3
C(20)-H(20B)...O(11)#4	0.99	2.65	3.419(2)	134.2

Symmetry transformations used to generate equivalent atoms:
#1 -x,y+1/2,-z+3/2   #2 x-1/2,-y+1/2,-z+2   #3 -x+1/2,-y+1,z-1/2
#4 x+1/2,-y+1/2,-z+2

X-ray Crystal Data for oxadiazole (RJ-03-13), 25

Table A23. Crystal data and structure refinement for oxadiazole **25** (RJ-03-13).

Identification code	cook157
Empirical formula	$C_{19}H_{19}N_5O_3$
Formula weight	365.39
Temperature	150(2) K
Wavelength	0.71073 Å
Crystal system	Orthorhombic
Space group	$P2_12_12_1$
Unit cell dimensions	a = 8.7093(7) Å $\alpha = 90°$.
	b = 12.3887(9) Å $\beta = 90°$.
	c = 15.9890(13) Å $\gamma = 90°$.
Volume	1725.2(2) Å^3
Z	4
Density (-123ºC)	1.407 Mg/m^3
Absorption coefficient	0.099 mm^{-1}
F(000)	768
Crystal size	0.788 x 0.639 x 0.611 mm^3
θ range for data collection	2.548 to 29.128°.
Index ranges	-11<=h<=11, -16<=k<=16, -21<=l<=21
Reflections collected	15536
Independent reflections	4595 [R(int) = 0.0245]
Completeness to $\theta = 25.000°$	99.8 %
Refinement method	Full-matrix least-squares on F^2
Data / restraints / parameters	4595 / 0 / 244
Goodness-of-fit on F^2	1.107
Final R indices [I>2σ(I)]	R1 = 0.0326, wR2 = 0.0841
R indices (all data)	R1 = 0.0332, wR2 = 0.0849
Absolute structure parameter	-0.12(15)
Largest diff. peak and hole	0.260 and -0.366 e.Å^{-3}

Table A24. Atomic coordinates (x 10^4) and equivalent isotropic displacement parameters ($\mathring{A}^2$x 10^3) for **25**. U(eq) is defined as one third of the trace of the orthogonalized U^{ij} tensor.

	x	y	z	U(eq)
O(1)	4484(1)	9376(1)	7665(1)	24(1)
C(1)	5460(2)	8857(1)	8056(1)	17(1)
N(2)	5665(1)	8991(1)	8884(1)	17(1)
C(3)	4724(2)	9757(1)	9367(1)	21(1)
C(4)	5229(2)	9551(1)	10268(1)	24(1)
C(5)	6920(2)	9233(1)	10168(1)	21(1)
C(6)	6922(1)	8514(1)	9389(1)	16(1)
C(7)	6587(1)	7330(1)	9499(1)	16(1)
C(8)	6229(2)	6608(1)	10128(1)	17(1)
N(9)	5914(1)	5592(1)	9802(1)	20(1)
C(10)	6092(2)	5693(1)	8992(1)	20(1)
N(11)	6500(1)	6725(1)	8772(1)	16(1)
C(12)	6924(2)	7059(1)	7948(1)	16(1)
C(13)	7767(2)	6340(1)	7463(1)	19(1)
C(14)	8168(2)	6590(1)	6642(1)	20(1)
C(15)	7744(2)	7591(1)	6312(1)	19(1)
O(15)	8124(1)	7930(1)	5523(1)	27(1)
C(15A)	9051(2)	7225(1)	5033(1)	28(1)
C(16)	6884(2)	8307(1)	6791(1)	20(1)
C(17)	6466(2)	8056(1)	7611(1)	17(1)
C(18)	6231(2)	6721(1)	11033(1)	18(1)
O(19)	5415(1)	5984(1)	11468(1)	22(1)
N(20)	5640(2)	6239(1)	12328(1)	24(1)
C(21)	6553(2)	7067(1)	12302(1)	21(1)
N(22)	6962(2)	7400(1)	11508(1)	22(1)
C(22)	7165(2)	7593(1)	13073(1)	30(1)
C(23)	7247(2)	8816(2)	12996(1)	39(1)

Table A25. Bond lengths [Å] and angles [°] for **25**.

_____

O(1)-C(1)	1.2351(16)	C(1)-N(2)	1.3458(16)
C(1)-C(17)	1.5037(17)	N(2)-C(3)	1.4717(16)
N(2)-C(6)	1.4830(16)	C(3)-C(4)	1.5277(19)
C(3)-H(3A)	0.9900	C(3)-H(3B)	0.9900
C(4)-C(5)	1.533(2)	C(4)-H(4A)	0.9900
C(4)-H(4B)	0.9900	C(5)-C(6)	1.5318(17)
C(5)-H(5A)	0.9900	C(5)-H(5B)	0.9900
C(6)-C(7)	1.5053(16)	C(6)-H(6A)	1.0000
C(7)-C(8)	1.3827(17)	C(7)-N(11)	1.3851(15)
C(8)-N(9)	1.3896(16)	C(8)-C(18)	1.4536(17)
N(9)-C(10)	1.3104(17)	C(10)-N(11)	1.3722(16)
C(10)-H(10A)	0.9500	N(11)-C(12)	1.4296(16)
C(12)-C(13)	1.3903(18)	C(12)-C(17)	1.4060(16)
C(13)-C(14)	1.3926(18)	C(13)-H(13A)	0.9500
C(14)-C(15)	1.3971(17)	C(14)-H(14A)	0.9500
C(15)-O(15)	1.3697(15)	C(15)-C(16)	1.3916(18)
O(15)-C(15A)	1.4256(18)	C(15A)-H(15A)	0.9800
C(15A)-H(15B)	0.9800	C(15A)-H(15C)	0.9800
C(16)-C(17)	1.3949(17)	C(16)-H(16A)	0.9500
C(18)-N(22)	1.3004(18)	C(18)-O(19)	1.3497(16)
O(19)-N(20)	1.4252(15)	N(20)-C(21)	1.2989(19)
C(21)-N(22)	1.3808(17)	C(21)-C(22)	1.4926(19)
C(22)-C(23)	1.522(2)	C(22)-H(22A)	0.9900
C(22)-H(22B)	0.9900	C(23)-H(23A)	0.9800
C(23)-H(23B)	0.9800	C(23)-H(23C)	0.9800
O(1)-C(1)-N(2)	121.66(12)	O(1)-C(1)-C(17)	120.29(11)
N(2)-C(1)-C(17)	118.05(11)	C(1)-N(2)-C(3)	121.43(11)
C(1)-N(2)-C(6)	125.70(11)	C(3)-N(2)-C(6)	112.50(10)
N(2)-C(3)-C(4)	103.12(10)	N(2)-C(3)-H(3A)	111.1
C(4)-C(3)-H(3A)	111.1	N(2)-C(3)-H(3B)	111.1
C(4)-C(3)-H(3B)	111.1	H(3A)-C(3)-H(3B)	109.1
C(3)-C(4)-C(5)	102.78(11)	C(3)-C(4)-H(4A)	111.2
C(5)-C(4)-H(4A)	111.2	C(3)-C(4)-H(4B)	111.2
C(5)-C(4)-H(4B)	111.2	H(4A)-C(4)-H(4B)	109.1
C(6)-C(5)-C(4)	103.61(11)	C(6)-C(5)-H(5A)	111.0
C(4)-C(5)-H(5A)	111.0	C(6)-C(5)-H(5B)	111.0
C(4)-C(5)-H(5B)	111.0	H(5A)-C(5)-H(5B)	109.0
N(2)-C(6)-C(7)	107.99(10)	N(2)-C(6)-C(5)	102.12(10)
C(7)-C(6)-C(5)	118.10(10)	N(2)-C(6)-H(6A)	109.4
C(7)-C(6)-H(6A)	109.4	C(5)-C(6)-H(6A)	109.4
C(8)-C(7)-N(11)	104.33(10)	C(8)-C(7)-C(6)	139.44(11)
N(11)-C(7)-C(6)	116.10(10)	C(7)-C(8)-N(9)	110.94(11)
C(7)-C(8)-C(18)	131.42(12)	N(9)-C(8)-C(18)	117.50(11)
C(10)-N(9)-C(8)	105.15(11)	N(9)-C(10)-N(11)	111.87(11)
N(9)-C(10)-H(10A)	124.1	N(11)-C(10)-H(10A)	124.1
C(10)-N(11)-C(7)	107.70(10)	C(10)-N(11)-C(12)	124.87(10)
C(7)-N(11)-C(12)	127.06(10)	C(13)-C(12)-C(17)	119.93(11)
C(13)-C(12)-N(11)	117.73(10)	C(17)-C(12)-N(11)	122.29(11)
C(12)-C(13)-C(14)	121.01(12)	C(12)-C(13)-H(13A)	119.5
C(14)-C(13)-H(13A)	119.5	C(13)-C(14)-C(15)	119.17(12)
C(13)-C(14)-H(14A)	120.4	C(15)-C(14)-H(14A)	120.4
O(15)-C(15)-C(16)	116.16(11)	O(15)-C(15)-C(14)	123.83(12)
C(16)-C(15)-C(14)	120.01(12)	C(15)-O(15)-C(15A)	117.07(11)

O(15)-C(15A)-H(15A)	109.5	O(15)-C(15A)-H(15B)	109.5
H(15A)-C(15A)-H(15B)	109.5	O(15)-C(15A)-H(15C)	109.5
H(15A)-C(15A)-H(15C)	109.5	H(15B)-C(15A)-H(15C)	109.5
C(15)-C(16)-C(17)	121.02(12)	C(15)-C(16)-H(16A)	119.5
C(17)-C(16)-H(16A)	119.5	C(16)-C(17)-C(12)	118.83(12)
C(16)-C(17)-C(1)	116.75(11)	C(12)-C(17)-C(1)	124.31(11)
N(22)-C(18)-O(19)	113.23(12)	N(22)-C(18)-C(8)	130.16(12)
O(19)-C(18)-C(8)	116.52(11)	C(18)-O(19)-N(20)	105.96(10)
C(21)-N(20)-O(19)	103.16(11)	N(20)-C(21)-N(22)	115.08(12)
N(20)-C(21)-C(22)	122.46(13)	N(22)-C(21)-C(22)	122.41(13)
C(18)-N(22)-C(21)	102.55(11)	C(21)-C(22)-C(23)	112.58(14)
C(21)-C(22)-H(22A)	109.1	C(23)-C(22)-H(22A)	109.1
C(21)-C(22)-H(22B)	109.1	C(23)-C(22)-H(22B)	109.1
H(22A)-C(22)-H(22B)	107.8	C(22)-C(23)-H(23A)	109.5
C(22)-C(23)-H(23B)	109.5	H(23A)-C(23)-H(23B)	109.5
C(22)-C(23)-H(23C)	109.5	H(23A)-C(23)-H(23C)	109.5
H(23B)-C(23)-H(23C)	109.5		

_____

Table A26. Anisotropic displacement parameters ($\text{Å}^2\text{x }10^3$) for **25**. The anisotropic displacement factor exponent takes the form: $-2\pi^2[h^2a^{*2}U^{11} + ... + 2\,h\,k\,a^*\,b^*\,U^{12}]$

	U^{11}	U^{22}	U^{33}	U^{23}	U^{13}	U^{12}
O(1)	23(1)	23(1)	25(1)	5(1)	-3(1)	6(1)
C(1)	17(1)	14(1)	21(1)	3(1)	0(1)	0(1)
N(2)	17(1)	14(1)	20(1)	1(1)	-1(1)	2(1)
C(3)	20(1)	16(1)	26(1)	-1(1)	4(1)	2(1)
C(4)	28(1)	19(1)	24(1)	-3(1)	4(1)	-1(1)
C(5)	26(1)	14(1)	22(1)	-2(1)	-3(1)	-4(1)
C(6)	16(1)	13(1)	18(1)	1(1)	-2(1)	-2(1)
C(7)	15(1)	14(1)	17(1)	0(1)	-3(1)	0(1)
C(8)	20(1)	15(1)	18(1)	0(1)	-3(1)	0(1)
N(9)	27(1)	14(1)	20(1)	1(1)	-4(1)	-3(1)
C(10)	26(1)	14(1)	20(1)	1(1)	-4(1)	-3(1)
N(11)	21(1)	12(1)	16(1)	1(1)	-3(1)	-1(1)
C(12)	19(1)	14(1)	16(1)	1(1)	-3(1)	-1(1)
C(13)	24(1)	14(1)	21(1)	1(1)	-2(1)	1(1)
C(14)	23(1)	16(1)	20(1)	-1(1)	-1(1)	0(1)
C(15)	23(1)	19(1)	16(1)	1(1)	-1(1)	-2(1)
O(15)	40(1)	22(1)	18(1)	3(1)	6(1)	2(1)
C(15A)	39(1)	28(1)	18(1)	-2(1)	2(1)	2(1)
C(16)	24(1)	16(1)	19(1)	2(1)	-2(1)	1(1)
C(17)	18(1)	14(1)	18(1)	1(1)	-3(1)	1(1)
C(18)	18(1)	15(1)	20(1)	2(1)	-1(1)	2(1)
O(19)	24(1)	22(1)	19(1)	3(1)	-1(1)	-2(1)
N(20)	27(1)	27(1)	17(1)	2(1)	1(1)	3(1)
C(21)	25(1)	21(1)	18(1)	-1(1)	0(1)	6(1)
N(22)	28(1)	21(1)	16(1)	-1(1)	-2(1)	-1(1)
C(22)	33(1)	38(1)	20(1)	-8(1)	-2(1)	5(1)
C(23)	39(1)	38(1)	39(1)	-16(1)	-1(1)	-8(1)

Table A27. Hydrogen coordinates (x 10^4) and isotropic displacement parameters (Å^2x 10^3) for **25**.

	x	y	z	U(eq)
H(3A)	3616	9608	9294	25
H(3B)	4938	10511	9198	25
H(4A)	4627	8960	10525	28
H(4B)	5121	10210	10614	28
H(5A)	7574	9878	10085	25
H(5B)	7291	8831	10664	25
H(6A)	7917	8603	9085	19
H(10A)	5956	5121	8603	24
H(13A)	8076	5668	7695	23
H(14A)	8722	6086	6311	24
H(15A)	9244	7554	4485	42
H(15B)	10031	7100	5319	42
H(15C)	8517	6535	4957	42
H(16A)	6577	8978	6557	23
H(22A)	8206	7308	13189	36
H(22B)	6500	7403	13553	36
H(23A)	7654	9122	13515	58
H(23B)	7922	9009	12529	58
H(23C)	6216	9103	12893	58

Table A28. Torsion angles [°] for **25**.

_____

O(1)-C(1)-N(2)-C(3)	0.55(19)	C(17)-C(1)-N(2)-C(3)	-179.83(11)
O(1)-C(1)-N(2)-C(6)	-171.93(12)	C(17)-C(1)-N(2)-C(6)	7.69(18)
C(1)-N(2)-C(3)-C(4)	174.18(11)	C(6)-N(2)-C(3)-C(4)	-12.42(14)
N(2)-C(3)-C(4)-C(5)	32.02(13)	C(3)-C(4)-C(5)-C(6)	-40.37(12)
C(1)-N(2)-C(6)-C(7)	-74.14(15)	C(3)-N(2)-C(6)-C(7)	112.80(11)
C(1)-N(2)-C(6)-C(5)	160.67(12)	C(3)-N(2)-C(6)-C(5)	-12.39(13)
C(4)-C(5)-C(6)-N(2)	32.12(12)	C(4)-C(5)-C(6)-C(7)	-86.09(13)
N(2)-C(6)-C(7)-C(8)	-114.16(18)	C(5)-C(6)-C(7)-C(8)	0.9(2)
N(2)-C(6)-C(7)-N(11)	60.81(14)	C(5)-C(6)-C(7)-N(11)	175.87(11)
N(11)-C(7)-C(8)-N(9)	-0.69(15)	C(6)-C(7)-C(8)-N(9)	174.65(14)
N(11)-C(7)-C(8)-C(18)	174.87(14)	C(6)-C(7)-C(8)-C(18)	-9.8(3)
C(7)-C(8)-N(9)-C(10)	0.66(16)	C(18)-C(8)-N(9)-C(10)	-175.60(12)
C(8)-N(9)-C(10)-N(11)	-0.35(16)	N(9)-C(10)-N(11)-C(7)	-0.07(16)
N(9)-C(10)-N(11)-C(12)	173.42(12)	C(8)-C(7)-N(11)-C(10)	0.46(14)
C(6)-C(7)-N(11)-C(10)	-176.17(11)	C(8)-C(7)-N(11)-C(12)	-172.85(13)
C(6)-C(7)-N(11)-C(12)	10.52(18)	C(10)-N(11)-C(12)-C(13)	-36.60(19)
C(7)-N(11)-C(12)-C(13)	135.63(13)	C(10)-N(11)-C(12)-C(17)	140.87(13)
C(7)-N(11)-C(12)-C(17)	-46.90(19)	C(17)-C(12)-C(13)-C(14)	-0.19(19)
N(11)-C(12)-C(13)-C(14)	177.34(12)	C(12)-C(13)-C(14)-C(15)	1.6(2)
C(13)-C(14)-C(15)-O(15)	177.77(13)	C(13)-C(14)-C(15)-C(16)	-2.4(2)
C(16)-C(15)-O(15)-C(15A)	177.80(13)	C(14)-C(15)-O(15)-C(15A)	-2.3(2)
O(15)-C(15)-C(16)-C(17)	-178.41(12)	C(14)-C(15)-C(16)-C(17)	1.7(2)
C(15)-C(16)-C(17)-C(12)	-0.3(2)	C(15)-C(16)-C(17)-C(1)	-176.54(12)
C(13)-C(12)-C(17)-C(16)	-0.49(19)	N(11)-C(12)-C(17)-C(16)	-177.91(12)
C(13)-C(12)-C(17)-C(1)	175.48(12)	N(11)-C(12)-C(17)-C(1)	-1.93(19)
O(1)-C(1)-C(17)-C(16)	34.08(17)	N(2)-C(1)-C(17)-C(16)	-145.55(12)
O(1)-C(1)-C(17)-C(12)	-141.97(14)	N(2)-C(1)-C(17)-C(12)	38.40(18)
C(7)-C(8)-C(18)-N(22)	-22.2(2)	N(9)-C(8)-C(18)-N(22)	153.11(14)
C(7)-C(8)-C(18)-O(19)	161.44(14)	N(9)-C(8)-C(18)-O(19)	-23.23(18)
N(22)-C(18)-O(19)-N(20)	0.93(15)	C(8)-C(18)-O(19)-N(20)	177.89(11)
C(18)-O(19)-N(20)-C(21)	-0.68(14)	O(19)-N(20)-C(21)-N(22)	0.26(16)
O(19)-N(20)-C(21)-C(22)	-177.36(13)	O(19)-C(18)-N(22)-C(21)	-0.74(15)
C(8)-C(18)-N(22)-C(21)	-177.19(13)	N(20)-C(21)-N(22)-C(18)	0.27(17)
C(22)-C(21)-N(22)-C(18)	177.90(13)	N(20)-C(21)-C(22)-C(23)	-141.74(16)
N(22)-C(21)-C(22)-C(23)	40.8(2)		

_____

Table A29. Hydrogen bonds for **25** [Å and °].

_____

D-H...A	d(D-H)	d(H...A)	d(D...A)	<(DHA)
C(5)-H(5B)...N(22)	0.99	2.25	3.1223(17)	146.7
C(6)-H(6A)...O(19)#1	1.00	2.40	3.3934(17)	170.7
C(10)-H(10A)...O(1)#2	0.95	2.26	3.1520(16)	155.9
C(13)-H(13A)...N(20)#3	0.95	2.68	3.4894(18)	143.6
C(15A)-H(15C)...N(9)#3	0.98	2.69	3.5091(19)	141.0

_____

Symmetry transformations used to generate equivalent atoms:
#1 x+1/2,-y+3/2,-z+2   #2 -x+1,y-1/2,-z+3/2   #3 -x+3/2,-y+1,z-1/2

X-ray Crystal Data for oxadiazole (RJ-03-14), 26

Table A30. Crystal data and structure refinement for **26**.

Identification code	cook156
Empirical formula	$C_{18}H_{19}N_{15}O_4$
Formula weight	509.48
Temperature	150(2) K
Wavelength	1.54178 Å
Crystal system	Orthorhombic
Space group	$P2_12_12_1$
Unit cell dimensions	a = 4.4720(2) Å $\alpha = 90°$.
	b = 18.7822(7) Å $\beta = 90°$.
	c = 20.5765(7) Å $\gamma = 90°$.
Volume	1728.30(12) $Å^3$
Z	4
Density (-123ºC)	1.958 Mg/m^3
Absorption coefficient	1.259 mm^{-1}
F(000)	1056
Crystal size	0.543 x 0.216 x 0.172 mm^3
θ range for data collection	3.186 to 68.149°.
Index ranges	-5<=h<=4, -22<=k<=21, -24<=l<=22
Reflections collected	9038
Independent reflections	3041 [R(int) = 0.0443]
Completeness to θ = 67.679°	99.1 %
Absorption correction	Semi-empirical from equivalents
Max. and min. transmission	0.7530 and 0.6333
Refinement method	Full-matrix least-squares on F^2
Data / restraints / parameters	3041 / 3 / 253
Goodness-of-fit on F^2	1.070
Final R indices [I>2σ(I)]	R1 = 0.0335, wR2 = 0.0899
R indices (all data)	R1 = 0.0337, wR2 = 0.0900
Absolute structure parameter	0.12(6)
Extinction coefficient	0.0143(10)
Largest diff. peak and hole	0.276 and -0.233 e.$Å^{-3}$

Table A31. Atomic coordinates (x 10^4) and equivalent isotropic displacement parameters (Å^2 x 10^3) for **26**. U(eq) is defined as one third of the trace of the orthogonalized U^{ij} tensor.

	x	y	z	U(eq)
C(1)	7331(4)	-289(1)	5776(1)	20(1)
O(1)	8428(4)	-889(1)	5830(1)	28(1)
N(2)	6606(4)	105(1)	6296(1)	19(1)
C(3)	6815(5)	-180(1)	6962(1)	22(1)
C(4)	5925(5)	453(1)	7382(1)	23(1)
C(5)	3772(5)	871(1)	6956(1)	22(1)
C(6)	5047(4)	797(1)	6267(1)	19(1)
C(7)	7182(4)	1352(1)	6024(1)	18(1)
C(8)	8576(5)	1967(1)	6228(1)	20(1)
N(9)	10402(4)	2238(1)	5742(1)	23(1)
C(10)	10108(5)	1802(1)	5255(1)	22(1)
N(11)	8197(4)	1255(1)	5394(1)	19(1)
C(12)	7147(4)	731(1)	4940(1)	20(1)
C(13)	6624(5)	951(1)	4302(1)	24(1)
C(14)	5587(5)	473(1)	3849(1)	26(1)
C(15)	5019(5)	-232(1)	4025(1)	23(1)
O(15)	3929(4)	-658(1)	3546(1)	30(1)
C(15A)	2955(6)	-1351(1)	3721(1)	34(1)
C(16)	5598(5)	-457(1)	4655(1)	22(1)
C(17)	6687(4)	20(1)	5118(1)	20(1)
C(18)	8416(5)	2369(1)	6836(1)	21(1)
O(19)	10023(5)	2969(1)	6845(1)	45(1)
N(20)	9516(7)	3279(1)	7466(1)	45(1)
C(21)	7715(5)	2838(1)	7745(1)	24(1)
C(22)	6558(6)	2966(1)	8413(1)	29(1)
N(22)	6998(4)	2254(1)	7373(1)	26(1)
O(1S)	8556(4)	-2087(1)	4992(1)	37(1)

Table A32. Bond lengths [Å] and angles [°] for **26**.

_____

C(1)-O(1)	1.233(2)	C(1)-N(2)	1.341(3)
C(1)-C(17)	1.500(3)	N(2)-C(3)	1.476(2)
N(2)-C(6)	1.476(2)	C(3)-C(4)	1.521(3)
C(3)-H(3A)	0.9900	C(3)-H(3B)	0.9900
C(4)-C(5)	1.520(3)	C(4)-H(4A)	0.9900
C(4)-H(4B)	0.9900	C(5)-C(6)	1.533(3)
C(5)-H(5A)	0.9900	C(5)-H(5B)	0.9900
C(6)-C(7)	1.499(3)	C(6)-H(6A)	1.0000
C(7)-C(8)	1.378(3)	C(7)-N(11)	1.386(2)
C(8)-N(9)	1.388(3)	C(8)-C(18)	1.463(3)
N(9)-C(10)	1.300(3)	C(10)-N(11)	1.367(3)
C(10)-H(10A)	0.9500	N(11)-C(12)	1.435(2)
C(12)-C(13)	1.396(3)	C(12)-C(17)	1.401(3)
C(13)-C(14)	1.375(3)	C(13)-H(13A)	0.9500
C(14)-C(15)	1.395(3)	C(14)-H(14A)	0.9500
C(15)-O(15)	1.360(2)	C(15)-C(16)	1.388(3)
O(15)-C(15A)	1.420(3)	C(15A)-H(15A)	0.9800
C(15A)-H(15B)	0.9800	C(15A)-H(15C)	0.9800
C(16)-C(17)	1.396(3)	C(16)-H(16A)	0.9500
C(18)-N(22)	1.293(3)	C(18)-O(19)	1.336(3)
O(19)-N(20)	1.421(2)	N(20)-C(21)	1.290(3)
C(21)-N(22)	1.375(3)	C(21)-C(22)	1.487(3)
C(22)-H(22A)	0.9800	C(22)-H(22B)	0.9800
C(22)-H(22C)	0.9800	O(1S)-H(1SA)	0.869(12)
O(1S)-H(1SB)	0.865(12)		
O(1)-C(1)-N(2)	121.93(18)	O(1)-C(1)-C(17)	120.75(18)
N(2)-C(1)-C(17)	117.30(16)	C(1)-N(2)-C(3)	121.72(15)
C(1)-N(2)-C(6)	124.72(16)	C(3)-N(2)-C(6)	112.69(15)
N(2)-C(3)-C(4)	103.15(15)	N(2)-C(3)-H(3A)	111.1
C(4)-C(3)-H(3A)	111.1	N(2)-C(3)-H(3B)	111.1
C(4)-C(3)-H(3B)	111.1	H(3A)-C(3)-H(3B)	109.1
C(5)-C(4)-C(3)	103.98(16)	C(5)-C(4)-H(4A)	111.0
C(3)-C(4)-H(4A)	111.0	C(5)-C(4)-H(4B)	111.0
C(3)-C(4)-H(4B)	111.0	H(4A)-C(4)-H(4B)	109.0
C(4)-C(5)-C(6)	104.53(16)	C(4)-C(5)-H(5A)	110.8
C(6)-C(5)-H(5A)	110.8	C(4)-C(5)-H(5B)	110.8
C(6)-C(5)-H(5B)	110.8	H(5A)-C(5)-H(5B)	108.9
N(2)-C(6)-C(7)	108.93(16)	N(2)-C(6)-C(5)	102.62(15)
C(7)-C(6)-C(5)	118.87(16)	N(2)-C(6)-H(6A)	108.7
C(7)-C(6)-H(6A)	108.7	C(5)-C(6)-H(6A)	108.7
C(8)-C(7)-N(11)	104.31(17)	C(8)-C(7)-C(6)	140.27(18)
N(11)-C(7)-C(6)	115.42(16)	C(7)-C(8)-N(9)	110.77(17)
C(7)-C(8)-C(18)	132.15(19)	N(9)-C(8)-C(18)	117.07(17)
C(10)-N(9)-C(8)	105.30(17)	N(9)-C(10)-N(11)	112.15(18)
N(9)-C(10)-H(10A)	123.9	N(11)-C(10)-H(10A)	123.9
C(10)-N(11)-C(7)	107.48(16)	C(10)-N(11)-C(12)	125.80(17)
C(7)-N(11)-C(12)	126.27(16)	C(13)-C(12)-C(17)	120.20(18)
C(13)-C(12)-N(11)	117.65(17)	C(17)-C(12)-N(11)	122.14(17)
C(14)-C(13)-C(12)	120.09(18)	C(14)-C(13)-H(13A)	120.0
C(12)-C(13)-H(13A)	120.0	C(13)-C(14)-C(15)	120.33(18)
C(13)-C(14)-H(14A)	119.8	C(15)-C(14)-H(14A)	119.8
O(15)-C(15)-C(16)	124.38(19)	O(15)-C(15)-C(14)	115.81(18)
C(16)-C(15)-C(14)	119.80(19)	C(15)-O(15)-C(15A)	117.75(16)

Table A32. (continued).

_____

O(15)-C(15A)-H(15A)	109.5	O(15)-C(15A)-H(15B)	109.5
H(15A)-C(15A)-H(15B)	109.5	O(15)-C(15A)-H(15C)	109.5
H(15A)-C(15A)-H(15C)	109.5	H(15B)-C(15A)-H(15C)	109.5
C(15)-C(16)-C(17)	120.55(18)	C(15)-C(16)-H(16A)	119.7
C(17)-C(16)-H(16A)	119.7	C(16)-C(17)-C(12)	118.96(18)
C(16)-C(17)-C(1)	115.78(17)	C(12)-C(17)-C(1)	125.24(18)
N(22)-C(18)-O(19)	113.07(18)	N(22)-C(18)-C(8)	131.98(19)
O(19)-C(18)-C(8)	114.95(18)	C(18)-O(19)-N(20)	105.81(17)
C(21)-N(20)-O(19)	103.75(17)	N(20)-C(21)-N(22)	114.12(19)
N(20)-C(21)-C(22)	121.70(19)	N(22)-C(21)-C(22)	124.17(19)
C(21)-C(22)-H(22A)	109.5	C(21)-C(22)-H(22B)	109.5
H(22A)-C(22)-H(22B)	109.5	C(21)-C(22)-H(22C)	109.5
H(22A)-C(22)-H(22C)	109.5	H(22B)-C(22)-H(22C)	109.5
C(18)-N(22)-C(21)	103.23(17)	H(1SA)-O(1S)-H(1SB)	107.3(19)

_____

Table A33. Anisotropic displacement parameters (Å^2x 10^3) for **26**. The anisotropic displacement factor exponent takes the form: $-2\pi^2[h^2a^{*2}U^{11} + ... + 2\,h\,k\,a^*\,b^*\,U^{12}]$

	U^{11}	U^{22}	U^{33}	U^{23}	U^{13}	U^{12}
C(1)	24(1)	17(1)	20(1)	1(1)	-4(1)	-1(1)
O(1)	46(1)	16(1)	22(1)	0(1)	-4(1)	7(1)
N(2)	25(1)	14(1)	17(1)	2(1)	-3(1)	0(1)
C(3)	29(1)	20(1)	18(1)	4(1)	-2(1)	-3(1)
C(4)	25(1)	25(1)	20(1)	0(1)	5(1)	-2(1)
C(5)	20(1)	23(1)	24(1)	-2(1)	4(1)	-3(1)
C(6)	18(1)	16(1)	22(1)	-2(1)	-2(1)	1(1)
C(7)	20(1)	16(1)	17(1)	2(1)	-2(1)	5(1)
C(8)	24(1)	16(1)	20(1)	2(1)	-2(1)	2(1)
N(9)	29(1)	18(1)	22(1)	3(1)	-2(1)	-1(1)
C(10)	26(1)	18(1)	21(1)	3(1)	0(1)	1(1)
N(11)	24(1)	15(1)	16(1)	-1(1)	-1(1)	1(1)
C(12)	24(1)	16(1)	18(1)	-1(1)	-2(1)	1(1)
C(13)	34(1)	16(1)	21(1)	2(1)	0(1)	1(1)
C(14)	38(1)	23(1)	17(1)	3(1)	-4(1)	1(1)
C(15)	29(1)	22(1)	19(1)	-3(1)	-2(1)	0(1)
O(15)	46(1)	24(1)	19(1)	-2(1)	-6(1)	-8(1)
C(15A)	52(1)	25(1)	26(1)	-2(1)	-7(1)	-8(1)
C(16)	30(1)	16(1)	21(1)	0(1)	-1(1)	0(1)
C(17)	25(1)	17(1)	19(1)	1(1)	-1(1)	3(1)
C(18)	28(1)	13(1)	23(1)	1(1)	-5(1)	-1(1)
O(19)	78(1)	32(1)	24(1)	-9(1)	12(1)	-31(1)
N(20)	84(2)	32(1)	21(1)	-11(1)	6(1)	-26(1)
C(21)	32(1)	17(1)	22(1)	0(1)	-6(1)	-1(1)
C(22)	41(1)	23(1)	25(1)	-6(1)	0(1)	-2(1)
N(22)	35(1)	19(1)	24(1)	-4(1)	1(1)	-3(1)
O(1S)	37(1)	27(1)	46(1)	-13(1)	-5(1)	2(1)

Table A34. Hydrogen coordinates (x 10^4) and isotropic displacement parameters (Å^2x 10^3) for **26**.

	x	y	z	U(eq)
H(3A)	8877	-338	7062	27
H(3B)	5426	-584	7026	27
H(4A)	4933	293	7786	28
H(4B)	7693	744	7496	28
H(5A)	3698	1377	7090	27
H(5B)	1731	668	6980	27
H(6A)	3346	758	5954	23
H(10A)	11107	1857	4851	26
H(13A)	6985	1431	4181	29
H(14A)	5256	623	3414	31
H(15A)	2191	-1597	3335	52
H(15B)	1364	-1315	4047	52
H(15C)	4639	-1620	3902	52
H(16A)	5251	-939	4771	27
H(22A)	7615	3370	8607	44
H(22B)	6883	2540	8679	44
H(22C)	4413	3071	8393	44
H(1SA)	10210(50)	-2330(13)	5009(16)	55
H(1SB)	8750(70)	-1730(11)	5254(13)	55

Table A35. Torsion angles [°] for **26**.

_____

O(1)-C(1)-N(2)-C(3)	-5.8(3)	C(17)-C(1)-N(2)-C(3)	172.78(18)
O(1)-C(1)-N(2)-C(6)	-174.34(18)	C(17)-C(1)-N(2)-C(6)	4.2(3)
C(1)-N(2)-C(3)-C(4)	177.59(18)	C(6)-N(2)-C(3)-C(4)	-12.6(2)
N(2)-C(3)-C(4)-C(5)	30.0(2)	C(3)-C(4)-C(5)-C(6)	-36.80(19)
C(1)-N(2)-C(6)-C(7)	-73.5(2)	C(3)-N(2)-C(6)-C(7)	117.05(18)
C(1)-N(2)-C(6)-C(5)	159.64(18)	C(3)-N(2)-C(6)-C(5)	-9.8(2)
C(4)-C(5)-C(6)-N(2)	28.39(18)	C(4)-C(5)-C(6)-C(7)	-91.8(2)
N(2)-C(6)-C(7)-C(8)	-115.8(3)	C(5)-C(6)-C(7)-C(8)	1.2(3)
N(2)-C(6)-C(7)-N(11)	64.1(2)	C(5)-C(6)-C(7)-N(11)	-178.98(16)
N(11)-C(7)-C(8)-N(9)	-0.3(2)	C(6)-C(7)-C(8)-N(9)	179.6(2)
N(11)-C(7)-C(8)-C(18)	178.3(2)	C(6)-C(7)-C(8)-C(18)	-1.8(4)
C(7)-C(8)-N(9)-C(10)	0.3(2)	C(18)-C(8)-N(9)-C(10)	-178.51(17)
C(8)-N(9)-C(10)-N(11)	-0.2(2)	N(9)-C(10)-N(11)-C(7)	0.1(2)
N(9)-C(10)-N(11)-C(12)	172.76(18)	C(8)-C(7)-N(11)-C(10)	0.1(2)
C(6)-C(7)-N(11)-C(10)	-179.75(17)	C(8)-C(7)-N(11)-C(12)	-172.51(17)
C(6)-C(7)-N(11)-C(12)	7.6(3)	C(10)-N(11)-C(12)-C(13)	-35.6(3)
C(7)-N(11)-C(12)-C(13)	135.8(2)	C(10)-N(11)-C(12)-C(17)	143.6(2)
C(7)-N(11)-C(12)-C(17)	-45.1(3)	C(17)-C(12)-C(13)-C(14)	1.5(3)
N(11)-C(12)-C(13)-C(14)	-179.33(19)	C(12)-C(13)-C(14)-C(15)	0.7(3)
C(13)-C(14)-C(15)-O(15)	178.4(2)	C(13)-C(14)-C(15)-C(16)	-2.2(3)
C(16)-C(15)-O(15)-C(15A)	8.6(3)	C(14)-C(15)-O(15)-C(15A)	-172.0(2)
O(15)-C(15)-C(16)-C(17)	-179.3(2)	C(14)-C(15)-C(16)-C(17)	1.3(3)
C(15)-C(16)-C(17)-C(12)	0.9(3)	C(15)-C(16)-C(17)-C(1)	-177.93(19)
C(13)-C(12)-C(17)-C(16)	-2.3(3)	N(11)-C(12)-C(17)-C(16)	178.59(18)
C(13)-C(12)-C(17)-C(1)	176.37(19)	N(11)-C(12)-C(17)-C(1)	-2.7(3)
O(1)-C(1)-C(17)-C(16)	38.3(3)	N(2)-C(1)-C(17)-C(16)	-140.3(2)
O(1)-C(1)-C(17)-C(12)	-140.4(2)	N(2)-C(1)-C(17)-C(12)	41.0(3)
C(7)-C(8)-C(18)-N(22)	2.9(4)	N(9)-C(8)-C(18)-N(22)	-178.5(2)
C(7)-C(8)-C(18)-O(19)	-177.1(2)	N(9)-C(8)-C(18)-O(19)	1.4(3)
N(22)-C(18)-O(19)-N(20)	-1.0(3)	C(8)-C(18)-O(19)-N(20)	179.0(2)
C(18)-O(19)-N(20)-C(21)	0.0(3)	O(19)-N(20)-C(21)-N(22)	0.9(3)
O(19)-N(20)-C(21)-C(22)	-179.1(2)	O(19)-C(18)-N(22)-C(21)	1.5(2)
C(8)-C(18)-N(22)-C(21)	-178.5(2)	N(20)-C(21)-N(22)-C(18)	-1.6(3)
C(22)-C(21)-N(22)-C(18)	178.5(2)		

_____

276

Table A36. Hydrogen bonds for **26** [Å and °].

D-H...A	d(D-H)	d(H...A)	d(D...A)	<(DHA)
C(4)-H(4A)...O(15)#1	0.99	2.43	3.255(3)	140.8
C(4)-H(4B)...O(15)#2	0.99	2.64	3.344(3)	128.1
C(5)-H(5A)...N(22)	0.99	2.29	3.094(3)	137.8
C(13)-H(13A)...N(9)#3	0.95	2.60	3.446(3)	148.2
C(13)-H(13A)...O(19)#3	0.95	2.55	3.194(3)	125.4
C(16)-H(16A)...O(1S)	0.95	2.65	3.407(3)	136.6
C(22)-H(22A)...O(1)#4	0.98	2.53	3.477(3)	161.8
O(1S)-H(1SA)...O(1S)#5	0.869(12)	1.855(12)	2.7223(18)	175(3)
O(1S)-H(1SB)...O(1)	0.865(12)	1.980(12)	2.836(2)	170(3)
C(13)-H(13A)...N(9)#3	0.95	2.60	3.446(3)	148.2
C(13)-H(13A)...O(19)#3	0.95	2.55	3.194(3)	125.4
C(16)-H(16A)...O(1S)	0.95	2.65	3.407(3)	136.6
O(1S)-H(1SA)...O(1S)#5	0.869(12)	1.855(12)	2.7223(18)	175(3)
O(1S)-H(1SB)...O(1)	0.865(12)	1.980(12)	2.836(2)	170(3)

Symmetry transformations used to generate equivalent atoms:
#1 -x+1/2,-y,z+1/2   #2 -x+3/2,-y,z+1/2   #3 x-1/2,-y+1/2,-z+1
#4 -x+2,y+1/2,-z+3/2   #5 x+1/2,-y-1/2,-z+1

X-ray Crystal Data for oxazole (KRM-II-68), 28

Table A37. Crystal data and structure refinement for **28** (KRM-II-68).

Identification code	cook136
Empirical formula	$C_{18}H_{16}N_4O_3$
Formula weight	336.35
Temperature	150(2) K
Wavelength	1.54178 Å
Crystal system	Orthorhombic
Space group	$P2_12_12_1$
Unit cell dimensions	a = 10.8051(3) Å $\qquad$ α= 90°.
	b = 20.3413(8) Å $\qquad$ β= 90°.
	c = 7.0384(3) Å $\qquad$ γ = 90°.
Volume	1546.97(10) Å^3
Z	4
Density (-123ºC)	1.444 Mg/m^3
Absorption coefficient	0.836 mm^{-1}
F(000)	704
Crystal size	0.493 x 0.399 x 0.207 mm^3
θ range for data collection	4.347 to 68.135°.
Index ranges	-12<=h<=12, -23<=k<=24, -7<=l<=8
Reflections collected	8881
Independent reflections	2708 [R(int) = 0.0603]
Completeness to θ = 67.679°	97.2 %
Absorption correction	Semi-empirical from equivalents
Max. and min. transmission	0.7530 and 0.5955
Refinement method	Full-matrix least-squares on F^2
Data / restraints / parameters	2708 / 0 / 228
Goodness-of-fit on F^2	1.101
Final R indices [I>σ(I)]	R1 = 0.0431, wR2 = 0.1196
R indices (all data)	R1 = 0.0432, wR2 = 0.1197
Absolute structure parameter	0.05(11)
Extinction coefficient	0.0039(8)
Largest diff. peak and hole	0.580 and -0.259 e.Å^{-3}

Table A38. Atomic coordinates (x 10^4) and equivalent isotropic displacement parameters (Å^2x 10^3) for **28**. U(eq) is defined as one third of the trace of the orthogonalized U^{ij} tensor.

	x	y	z	U(eq)
N(1)	2313(2)	563(1)	11013(4)	28(1)
C(2)	1313(3)	228(1)	10607(5)	25(1)
N(3)	906(2)	349(1)	8803(4)	21(1)
C(4)	-137(2)	50(1)	7911(4)	19(1)
C(5)	-316(3)	-618(1)	8160(4)	23(1)
C(6)	-1392(3)	-925(1)	7530(4)	23(1)
C(7)	-2301(3)	-547(1)	6665(4)	24(1)
O(7)	-3429(2)	-771(1)	6121(4)	37(1)
C(7A)	-3672(3)	-1458(2)	6351(5)	35(1)
C(8)	-2092(3)	120(1)	6345(4)	24(1)
C(9)	-1014(3)	424(1)	6917(4)	20(1)
C(10)	-913(3)	1150(1)	6519(4)	21(1)
O(10)	-1851(2)	1498(1)	6501(3)	29(1)
N(11)	206(2)	1404(1)	6132(3)	20(1)
C(12)	373(3)	2111(1)	5750(5)	25(1)
C(13)	1753(3)	2208(2)	5918(5)	34(1)
C(14)	2284(3)	1556(1)	5227(4)	26(1)
C(15)	1399(2)	1040(1)	6060(4)	20(1)
C(16)	1700(2)	800(1)	8010(4)	20(1)
C(17)	2571(3)	920(1)	9384(4)	22(1)
C(18)	3663(3)	1349(1)	9311(4)	23(1)
O(19)	4670(2)	1139(1)	8255(3)	30(1)
C(20)	5524(3)	1625(2)	8479(5)	31(1)
N(21)	5171(3)	2101(1)	9524(4)	33(1)
C(22)	3970(3)	1926(1)	10083(5)	29(1)

Table A39. Bond lengths [Å] and angles [°] for **28**.

_____

N(1)-C(2)	1.309(4)	N(1)-C(17)	1.386(4)
C(2)-N(3)	1.366(4)	C(2)-H(2A)	0.9500
N(3)-C(16)	1.374(4)	N(3)-C(4)	1.426(4)
C(4)-C(5)	1.383(4)	C(4)-C(9)	1.402(4)
C(5)-C(6)	1.392(4)	C(5)-H(5A)	0.9500
C(6)-C(7)	1.388(4)	C(6)-H(6A)	0.9500
C(7)-O(7)	1.357(4)	C(7)-C(8)	1.395(4)
O(7)-C(7A)	1.430(4)	C(7A)-H(7AA)	0.9800
C(7A)-H(7AB)	0.9800	C(7A)-H(7AC)	0.9800
C(8)-C(9)	1.378(4)	C(8)-H(8A)	0.9500
C(9)-C(10)	1.507(3)	C(10)-O(10)	1.238(3)
C(10)-N(11)	1.343(4)	N(11)-C(12)	1.475(3)
N(11)-C(15)	1.487(3)	C(12)-C(13)	1.509(4)
C(12)-H(12A)	0.9900	C(12)-H(12B)	0.9900
C(13)-C(14)	1.525(4)	C(13)-H(13A)	0.9900
C(13)-H(13B)	0.9900	C(14)-C(15)	1.536(4)
C(14)-H(14A)	0.9900	C(14)-H(14B)	0.9900
C(15)-C(16)	1.493(4)	C(15)-H(15A)	1.0000
C(16)-C(17)	1.372(4)	C(17)-C(18)	1.467(4)
C(18)-C(22)	1.336(4)	C(18)-O(19)	1.385(3)
O(19)-C(20)	1.361(4)	C(20)-N(21)	1.275(4)
C(20)-H(20A)	0.9500	N(21)-C(22)	1.402(4)
C(22)-H(22A)	0.9500		
C(2)-N(1)-C(17)	104.9(3)	N(1)-C(2)-N(3)	112.1(3)
N(1)-C(2)-H(2A)	124.0	N(3)-C(2)-H(2A)	124.0
C(2)-N(3)-C(16)	107.2(2)	C(2)-N(3)-C(4)	125.9(2)
C(16)-N(3)-C(4)	126.8(2)	C(5)-C(4)-C(9)	120.1(3)
C(5)-C(4)-N(3)	118.3(2)	C(9)-C(4)-N(3)	121.5(2)
C(4)-C(5)-C(6)	121.2(3)	C(4)-C(5)-H(5A)	119.4
C(6)-C(5)-H(5A)	119.4	C(7)-C(6)-C(5)	118.8(3)
C(7)-C(6)-H(6A)	120.6	C(5)-C(6)-H(6A)	120.6
O(7)-C(7)-C(6)	125.0(3)	O(7)-C(7)-C(8)	115.3(3)
C(6)-C(7)-C(8)	119.7(3)	C(7)-O(7)-C(7A)	117.4(2)
O(7)-C(7A)-H(7AA)	109.5	O(7)-C(7A)-H(7AB)	109.5
H(7AA)-C(7A)-H(7AB)	109.5	O(7)-C(7A)-H(7AC)	109.5
H(7AA)-C(7A)-H(7AC)	109.5	H(7AB)-C(7A)-H(7AC)	109.5
C(9)-C(8)-C(7)	121.7(3)	C(9)-C(8)-H(8A)	119.1
C(7)-C(8)-H(8A)	119.1	C(8)-C(9)-C(4)	118.3(3)
C(8)-C(9)-C(10)	116.5(3)	C(4)-C(9)-C(10)	125.1(2)
O(10)-C(10)-N(11)	121.0(2)	O(10)-C(10)-C(9)	120.2(2)
N(11)-C(10)-C(9)	118.7(2)	C(10)-N(11)-C(12)	121.5(2)
C(10)-N(11)-C(15)	126.5(2)	C(12)-N(11)-C(15)	111.9(2)
N(11)-C(12)-C(13)	103.5(2)	N(11)-C(12)-H(12A)	111.1
C(13)-C(12)-H(12A)	111.1	N(11)-C(12)-H(12B)	111.1
C(13)-C(12)-H(12B)	111.1	H(12A)-C(12)-H(12B)	109.0
C(12)-C(13)-C(14)	103.5(2)	C(12)-C(13)-H(13A)	111.1
C(14)-C(13)-H(13A)	111.1	C(12)-C(13)-H(13B)	111.1
C(14)-C(13)-H(13B)	111.1	H(13A)-C(13)-H(13B)	109.0
C(13)-C(14)-C(15)	103.8(2)	C(13)-C(14)-H(14A)	111.0
C(15)-C(14)-H(14A)	111.0	C(13)-C(14)-H(14B)	111.0
C(15)-C(14)-H(14B)	111.0	H(14A)-C(14)-H(14B)	109.0
N(11)-C(15)-C(16)	108.7(2)	N(11)-C(15)-C(14)	102.3(2)
C(16)-C(15)-C(14)	116.0(2)	N(11)-C(15)-H(15A)	109.9

Table A39. (continued).

_____

C(16)-C(15)-H(15A)	109.9		C(14)-C(15)-H(15A)	109.9
C(17)-C(16)-N(3)	105.2(2)		C(17)-C(16)-C(15)	137.7(3)
N(3)-C(16)-C(15)	117.1(2)		C(16)-C(17)-N(1)	110.6(2)
C(16)-C(17)-C(18)	129.3(3)		N(1)-C(17)-C(18)	120.1(3)
C(22)-C(18)-O(19)	107.1(3)		C(22)-C(18)-C(17)	135.0(3)
O(19)-C(18)-C(17)	117.9(2)		C(20)-O(19)-C(18)	104.3(2)
N(21)-C(20)-O(19)	114.6(3)		N(21)-C(20)-H(20A)	122.7
O(19)-C(20)-H(20A)	122.7		C(20)-N(21)-C(22)	104.2(3)
C(18)-C(22)-N(21)	109.8(3)		C(18)-C(22)-H(22A)	125.1
N(21)-C(22)-H(22A)	125.1			

_____

Table A40. Anisotropic displacement parameters (Å^2x 10^3) for **28**. The anisotropic displacement factor exponent takes the form: $-2\pi^2[h^2a^{*2}U^{11} + ... + 2\,h\,k\,a^*\,b^*\,U^{12}]$

_____

	U^{11}	U^{22}	U^{33}	U^{23}	U^{13}	U^{12}
N(1)	26(1)	29(1)	28(1)	2(1)	-4(1)	-2(1)
C(2)	22(1)	27(1)	26(2)	7(1)	-2(1)	1(1)
N(3)	16(1)	22(1)	24(1)	2(1)	-2(1)	2(1)
C(4)	18(1)	21(1)	20(1)	0(1)	1(1)	2(1)
C(5)	21(1)	23(1)	25(1)	0(1)	0(1)	4(1)
C(6)	27(2)	21(1)	23(1)	-1(1)	2(1)	-2(1)
C(7)	23(1)	28(1)	22(1)	1(1)	-1(1)	-5(1)
O(7)	33(1)	33(1)	45(2)	11(1)	-16(1)	-16(1)
C(7A)	40(2)	33(2)	32(2)	3(1)	-4(2)	-17(1)
C(8)	23(1)	28(1)	22(1)	5(1)	-3(1)	-1(1)
C(9)	19(1)	22(1)	19(1)	2(1)	3(1)	-1(1)
C(10)	21(1)	21(1)	21(1)	4(1)	0(1)	1(1)
O(10)	21(1)	27(1)	39(1)	8(1)	-1(1)	3(1)
N(11)	21(1)	18(1)	22(1)	3(1)	1(1)	1(1)
C(12)	31(2)	17(1)	28(2)	2(1)	-1(1)	-2(1)
C(13)	37(2)	30(2)	35(2)	1(1)	0(2)	-7(1)
C(14)	23(1)	29(1)	26(2)	1(1)	2(1)	-4(1)
C(15)	18(1)	22(1)	21(1)	-2(1)	2(1)	1(1)
C(16)	16(1)	20(1)	25(1)	-1(1)	3(1)	1(1)
C(17)	20(1)	22(1)	24(1)	-1(1)	-1(1)	1(1)
C(18)	17(1)	28(1)	24(1)	-1(1)	-4(1)	3(1)
O(19)	21(1)	35(1)	34(1)	-8(1)	0(1)	-3(1)
C(20)	22(2)	38(2)	33(2)	4(1)	-4(1)	-5(1)
N(21)	29(1)	31(1)	40(2)	5(1)	-5(1)	-6(1)
C(22)	25(1)	27(1)	33(2)	0(1)	-4(1)	0(1)

_____

Table A41. Hydrogen coordinates (x 10^4) and isotropic displacement parameters (Å^2x 10^3) for **28**.

	x	y	z	U(eq)
H(2A)	917	-64	11465	30
H(5A)	306	-871	8771	28
H(6A)	-1502	-1385	7690	28
H(7AA)	-4515	-1555	5923	53
H(7AB)	-3587	-1577	7694	53
H(7AC)	-3080	-1712	5593	53
H(8A)	-2709	372	5717	29
H(12A)	-76	2382	6695	30
H(12B)	78	2227	4461	30
H(13A)	1996	2296	7251	41
H(13B)	2037	2577	5109	41
H(14A)	3137	1490	5706	31
H(14B)	2292	1535	3822	31
H(15A)	1326	659	5169	24
H(20A)	6318	1610	7903	37
H(22A)	3453	2180	10891	34

Table A42. Torsion angles [°] for **28**.

_____

C(17)-N(1)-C(2)-N(3)	-0.1(3)	N(1)-C(2)-N(3)-C(16)	-0.7(3)
N(1)-C(2)-N(3)-C(4)	178.2(2)	C(2)-N(3)-C(4)-C(5)	-42.3(4)
C(16)-N(3)-C(4)-C(5)	136.3(3)	C(2)-N(3)-C(4)-C(9)	133.2(3)
C(16)-N(3)-C(4)-C(9)	-48.2(4)	C(9)-C(4)-C(5)-C(6)	-3.6(4)
N(3)-C(4)-C(5)-C(6)	172.0(2)	C(4)-C(5)-C(6)-C(7)	-1.0(4)
C(5)-C(6)-C(7)-O(7)	-174.6(3)	C(5)-C(6)-C(7)-C(8)	3.7(4)
C(6)-C(7)-O(7)-C(7A)	-4.0(4)	C(8)-C(7)-O(7)-C(7A)	177.6(3)
O(7)-C(7)-C(8)-C(9)	176.5(3)	C(6)-C(7)-C(8)-C(9)	-1.9(4)
C(7)-C(8)-C(9)-C(4)	-2.6(4)	C(7)-C(8)-C(9)-C(10)	-178.9(3)
C(5)-C(4)-C(9)-C(8)	5.3(4)	N(3)-C(4)-C(9)-C(8)	-170.1(3)
C(5)-C(4)-C(9)-C(10)	-178.7(3)	N(3)-C(4)-C(9)-C(10)	5.9(4)
C(8)-C(9)-C(10)-O(10)	30.9(4)	C(4)-C(9)-C(10)-O(10)	-145.2(3)
C(8)-C(9)-C(10)-N(11)	-147.2(3)	C(4)-C(9)-C(10)-N(11)	36.8(4)
O(10)-C(10)-N(11)-C(12)	2.6(4)	C(9)-C(10)-N(11)-C(12)	-179.3(3)
O(10)-C(10)-N(11)-C(15)	-178.5(3)	C(9)-C(10)-N(11)-C(15)	-0.4(4)
C(10)-N(11)-C(12)-C(13)	165.4(3)	C(15)-N(11)-C(12)-C(13)	-13.7(3)
N(11)-C(12)-C(13)-C(14)	32.3(3)	C(12)-C(13)-C(14)-C(15)	-39.3(3)
C(10)-N(11)-C(15)-C(16)	-66.2(3)	C(12)-N(11)-C(15)-C(16)	112.8(3)
C(10)-N(11)-C(15)-C(14)	170.6(3)	C(12)-N(11)-C(15)-C(14)	-10.4(3)
C(13)-C(14)-C(15)-N(11)	30.1(3)	C(13)-C(14)-C(15)-C(16)	-88.0(3)
C(2)-N(3)-C(16)-C(17)	1.1(3)	C(4)-N(3)-C(16)-C(17)	-177.8(2)
C(2)-N(3)-C(16)-C(15)	-176.6(2)	C(4)-N(3)-C(16)-C(15)	4.6(4)
N(11)-C(15)-C(16)-C(17)	-112.5(4)	C(14)-C(15)-C(16)-C(17)	1.9(5)
N(11)-C(15)-C(16)-N(3)	64.1(3)	C(14)-C(15)-C(16)-N(3)	178.6(2)
N(3)-C(16)-C(17)-N(1)	-1.2(3)	C(15)-C(16)-C(17)-N(1)	175.7(3)
N(3)-C(16)-C(17)-C(18)	178.3(3)	C(15)-C(16)-C(17)-C(18)	-4.8(6)
C(2)-N(1)-C(17)-C(16)	0.8(3)	C(2)-N(1)-C(17)-C(18)	-178.8(3)
C(16)-C(17)-C(18)-C(22)	107.7(4)	N(1)-C(17)-C(18)-C(22)	-72.8(4)
C(16)-C(17)-C(18)-O(19)	-73.8(4)	N(1)-C(17)-C(18)-O(19)	105.6(3)
C(22)-C(18)-O(19)-C(20)	-0.3(3)	C(17)-C(18)-O(19)-C(20)	-179.2(3)
C(18)-O(19)-C(20)-N(21)	-0.1(4)	O(19)-C(20)-N(21)-C(22)	0.5(4)
O(19)-C(18)-C(22)-N(21)	0.6(3)	C(17)-C(18)-C(22)-N(21)	179.2(3)
C(20)-N(21)-C(22)-C(18)	-0.7(4)		

_____

Table A43. Hydrogen bonds for **28** [Å and °].

_____

D-H...A	d(D-H)	d(H...A)	d(D...A)	<(DHA)
C(2)-H(2A)...O(19)#1	0.95	2.60	3.513(4)	160.8
C(13)-H(13B)...O(10)#2	0.99	2.50	3.478(4)	168.0
C(14)-H(14A)...O(19)	0.99	2.54	3.451(4)	152.1
C(20)-H(20A)...O(10)#3	0.95	2.22	3.170(4)	175.7

_____

Symmetry transformations used to generate equivalent atoms:
#1 -x+1/2,-y,z+1/2   #2 x+1/2,-y+1/2,-z+1   #3 x+1,y,z

IV. CURRICULUM VITAE

Rajwana Jahan

Place of Birth: Narayanganj, Bangladesh

EDUCATION

- **PhD Candidate, Organic Chemistry**, University of Wisconsin-Milwaukee (UWM),

  Milwaukee, WI,   May, 2019

  Advisor: Professor Dr. James M. Cook; CGPA: 3.82 (out of 4.0).

  Dissertation Title: "Design and Synthesis of Subtype Selective Ligands to Treat

  Asthma Targeting the GABAA Receptors Expressed in the Airway Smooth Muscle

  (ASM) of the Lung"

  MS, Organic Chemistry, University of Dhaka (DU), Dhaka, Bangladesh

  2011

  Result: First Class

- **B.Sc (Honors), Chemistry**, DU, Dhaka, Bangladesh

  2009

  Result: First Class

RESEARCH EXPERIENCE

- University of Wisconsin-Milwaukee, Milwaukee, WI: Graduate Research/Teaching
  Assistant,

  2012-present
- Undergraduate Research (B. Sc. Hon's) & Graduate Research (M.S.), University of

  Dhaka, Dhaka-Bangladesh.

  2008-2011

TEACHING EXPERIENCE

- University of Wisconsin-Milwaukee: Teaching Assistant: Fall 2012 (Gen. Chem.), Spring 2013 (Gen Chem.), Fall 2013 (Organic Laboratory), Spring 2014 (Intro. Biochemistry), Spring 2015 (Intro. Biochemistry), Fall 2017 (Gen. Chem.), and Spring 2018 (Intro. Biochemistry)

PROFESSIONAL AFFILIATIONS

- American Chemical Society (ACS)   2015 present

- Division of Medicinal Chemistry (ACS)   2015-Present

- International Chemical Biology Society (ICBS)   2016-2017

- Milwaukee Institute for Drug Discovery (MIDD)   present

AWARDS & GRANTS

- 1st Prize, 8th Yao Yuan Biotech-Pharma Symposium, Chicago, IL, 2016

- Sweden Bangladesh Trust Fund (Ministry of Education, Bangladesh, **2013**)

- Chemistry and Biochemistry Graduate Students Council @UWM Travel Grant, **Spring 2016**

- UWM Graduate School Travel Grant (**Spring 2015**, **Spring 2016**)

- UWM Department of Chemistry and Biochemistry Travel Grant (**Spring 2016**)

- ACS-Milwaukee Travel Grant (**Spring 2016**)

- Chancellor's Graduate Student Fellowship received every semester employed as a TA since Fall-2012

PUBLICATIONS
PAPERS

1. "Optimization of substituted imidazobenzodiazepines as novel asthma treatments", <u>Jahan, Rajwana</u>; Stephen, Michael Rajesh; Forkuo, Gloria S.; Kodali, Revathi; Guthrie, Margaret L.; Nieman, Amanda N.; Yuan, Nina Y.; Zahn, Nicolas M.; Poe, Michael M.; Li, Guanguan; et al, *European Journal of Medicinal Chemistry* (2017), 126, 550-560.

2. "Alleviation of Multiple Asthmatic Pathologic Features with Orally Available and Subtype Selective GABAA Receptor Modulators", Forkuo, Gloria S.; Nieman, Amanda N.; Yuan, Nina Y.; Kodali, Revathi; Yu, Olivia B.; Zahn, Nicolas M.; Jahan, Rajwana; Li, Guanguan; Stephen, Michael Rajesh; Guthrie, Margaret L.; et al, *Molecular Pharmaceutics* (2017), 14(6), 2088-2098.

3. "Targeting the g-aminobutyric acid A receptor a4 subunit in airway smooth muscle to alleviate bronchoconstriction", Yocum, Gene T.; Gallos, George; Zhang, Yi; Jahan, Rajwana; Stephen, Michael Rajesh; Varagic, Zdravko; Puthenkalam, Roshan; Ernst, Margot; Cook, James M.; Emala, Charles W., *American Journal of Respiratory Cell and Molecular Biology* (2016), 54(4), 546-553.

4. "Development of GABAA Receptor Subtype-Selective Imidazobenzodiazepines as Novel Asthma Treatments", Forkuo, Gloria S.; Guthrie, Margaret L.; Yuan, Nina Y.; Nieman, Amanda N.; Kodali, Revathi; Jahan, Rajwana; Stephen, Michael R.; Yocum, Gene T.; Treven, Marco; Poe, Michael M.; et al, *Molecular Pharmaceutics* (2016), 13(6), 2026-2038.

5. "Metabolic Studies of Drug Candidates for Neurological Disorders and Asthma Based on GABAA Receptor Subtype Selective Ligands using Mass Spectrometry", Revathi Kodali, Margaret L , Michael M. Poe, Michael R. Stephen , Rajwana Jahan, Charles W. Emala ,

James M. Cook, Douglas Stafford, Leggy A. Arnold, *Shimadzu Journal*, Vol.3, Issue3-Dec 2015.

6. "A novel orally available asthma drug candidate that reduces smooth muscle constriction and inflammation by targeting GABA(A) receptors in the lung" Forkuo, Gloria; Nieman, Amanda; Kodali, Revathi; Zahn, Nicolas; Li, Guanguan; Rashid Roni, Shadiqur; Stephen, Michael Rajesh; Harris, Ted; Jahan, Rajwana; Guthrie, Margaret; Yu, Olivia; Fisher, Janet; Yocum, Gene ; Emala, Charles; Steeber, Douglas; Stafford, Douglas; Cook, James; Arnold, Leggy, Submitted to *Molecular Pharmaceutics*, Manuscript ID: mp-2017-010139.R1.

7. "Improved Synthesis of Anxiolytic, Anticonvulsant and Antinociceptive α2/α3-GABA(A)ergic Receptor Subtype Selective Ligands as Promising Agents to Treat Anxiety, Epilepsy, as well as Neuropathic Pain", Li, G.; Golani, L. K.; Jahan, R.; Rashid, F.; Cook, J. M, Synthesis, 2018, 50(20): 4124-4132, DOI: 10.1055/s-0037-1610211.

8. "The a2,3-selective potentiator of GABAA receptors, KRM-II-81, reduces nociceptive-associated behaviors induced by formalin and spinal nerve ligation in rats", Witkin, J.M.; Cerne, R; Davis P.G.; Freeman, K.b.; Carmo, J.M.; Rowlett, J.; Methuku, K.R.; Okun, A.; Gleason, S.D.; Li, X.; Poe, R.M.; Li, G.; Schkeryantz, J.M.; Jahan, R.; Yang, L.; Guo1, W.; Anderson, W.H.; Catlow, J.T.; Jones, T/M.; Porreca, F.; Smith, J.l.; Knopp, K.L.; Cook, J.M., Pharmacol. Biochem. Behav. doi.org/10.1016/j.pbb.2019.02.013, Feb 2019.

9. "The value of human epileptic tissue in the discovery of novel antiepileptic drugs: The example of CERC-611 and KRM-II-81", Witkin JM, Ping X, Mouser C, Jin X, Hobbs J, Tiruveedhula VVNPB, Li G, Jahan R, Rashid F, Golani L, Cook JM, Smith JL, Brain. Res. Rev, submitted.

10. "GABAA α2/α3 receptor subtypes and the abuse-related effects of ethanol in rhesus monkeys: Experiments with selective positive allosteric modulators", Berro, L.F.; Rüedi-Bettschen, D.; Cook, J.E.; Golani, L.K.; Li, G.; Jahan, R.; Rashid, F.; Cook, J.M.; Rowlett, J.K.; Platt, D.M., Alcohol. Clin. Exp. Res., doi.org/10.1111/acer.14000, March, 2019.

11. Several manuscripts are in the process of publication.

CONFERENCE PROCEEDINGS AND POSTERS PRESENTATIONS (selected)

1. Oral presentation at 8th Yao Yuan Biotech-Pharma Symposium, Chicago, IL, April 23, 2016. "Novel Strategy for The Treatment of Asthma by Targeting the α4 Subunit of GABAA Receptors in Airway Smooth Muscle" <u>Rajwana Jahan</u>, Michael Stephen, Gene T. Yocum, George Gallos, Yi Zhang, Revathi Kodali ,Zdravko Varagic, Roshan Puthenkalam4, Margot Ernst4, Leggy A. Arnold, Douglas Stafford, Charles Emala, James M. Cook.

2. "Novel strategy for the treatment of asthma by targeting the a4 subunit of GABAA receptors in airway smooth muscle", <u>Jahan, Rajwana</u>; Stephen, Michael; Yocum, Gene T.; Gallos, George; Zhang, Yi; Varagic, Zdravko; Puthenkalam, Roshan; Ernst, Margot; Arnold, Alexander; Stafford, Douglas; et al, 251st ACS National Meeting & Exposition, San Diego, CA, United States, March 13-17, 2016 (2016), MEDI-167.

3. "Metabolic studies of drug candidates for neurological disorders and asthma based on GABAA receptor subtype selective ligands using mass spectrometry", Kodali, Revathi; Guthrie, Margaret L.; Poe, Michael M.; Stephen, Michael Rajesh; Jahan, Rajwana; Emala, Charles W.; Cook, James M.; Stafford, Douglas; Arnold, Alexander, From Abstracts of

Papers, 250th ACS National Meeting & Exposition, Boston, MA, United States, August 16-20, 2015 (2015), MEDI-432.

4. "Selective targeting of a4b3g2 GABAA receptors on airway smooth muscle as a novel strategy to treat asthma", Stephen, Michael Rajesh; Jahan, Rajwana; Gallos, George; Emala, Charles W.; Ernst, Margot; Sieghart, Werner; Cook, James M., From Abstracts of Papers, 250th ACS National Meeting & Exposition, Boston, MA, United States, August 16-20, 2015 (2015), MEDI-121.

5. "First enantiospecific total synthesis of macrosalhine chloride (4) and progress toward the synthesis of macroline-related indole alkaloids macrocarpine A, B, and C", Rahman, Md Toufiqur; Jahan, Rajwana; Edwankar, Rahul V.; Deschamps, Jaffrey R.; Cook, James M. From Abstracts of Papers, 249th ACS National Meeting & Exposition, Denver, CO, United States, March 22-26, 2015 (2015), ORGN-164.

6. "Novel strategy for the treatment of asthma by targeting GABAA receptors in the lung", Jahan, Rajwana; Stephen, Michael R.; Gallos, George; Emala, Charles W.; Cook, James M. From Abstracts of Papers, 249th ACS National Meeting & Exposition, Denver, CO, United States, March 22-26, 2015 (2015), MEDI-101.

7. "Inducing airway smooth muscle relaxation by targeting the restricted a-subunit repertoire of GABAA receptors using CMD-45", Stephen, Michael Rajesh; Jahan, Rajwana; Gallos, George; Emala, Charles W.; Cook, James M., From Abstracts of Papers, 248th ACS National Meeting & Exposition, San Francisco, CA, United States, August 10-14, 2014 (2014), MEDI-57.

8. "New Oral Treatments for Asthma through Tissue-Specific Modulation of the GABAA Receptor", Leggy Arnold, Gloria Forkuo, Amanda Nieman, Olivia B. Yu, Margaret L.

Guthrie, Revathi Kodali, Nina Yuan, Rajwana Jahan, Michael S. Stephen, Charles W. Emala, Gene T. Yocum, James M. Cook, Mitchell H. Grayson, MD, FAAAAI.

Major: Organic Chemistry
Minor: Biochemistry